Photosynthetic characterisation of tropical and temperate rainforest species

Nur Hazwani Abdul Bahar

A thesis submitted for the degree of

Doctor of Philosophy

of

The Australian National University

Australian National University

Declaration

The research presented in this thesis was my own work with the following exceptions:

Chapter 2: Field measurements in Peru were conducted by F. Yoko Ishida, Lasantha K. Weerasinghe, Rossella Guerrieri and Tomas Domingues; soil data was collected by Carlos A. Quesada. Leaf nutrient analysis was carried out by F. Yoko Ishida and leaf chlorophyll contents were provided by Roberta E. Martin and Gregory P. Asner. Keith J. Bloomfield performed mixed-effects linear models. Lastly, Benedict M. Long provided advice on troubleshooting protein assays. The optimisation of protein assays, quantification of Rubisco and data analysis (with the exception of mixed-effects linear models) and interpretation were carried out by me.

This chapter has been recently published in the *New Phytologist*:

Leaf-level photosynthetic capacity in lowland Amazonian and high-elevation Andean tropical moist forests of Peru

Bahar N.H.A., Ishida F.Y., Weerasinghe L.K., Guerrieri R., O'Sullivan O.S., Bloomfield K.J., Asner G.P., Martin R.E., Lloyd J., Malhi Y., Phillips O.L., Meir P., Salinas N., Cosio E.G., Domingues T.F., Quesada C.A., Sinca F., Escudero Vega A., Zuloaga Ccorimanya P.P., del Aguila-Pasquel J., Quispe Huaypar K., Cuba Torres I., Butrón Loayza R., Pelaez Tapia Y., Huaman Ovalle J., Long B.M., Evans J.R. & Atkin O.K.

Chapters 3 and 4: John R. Evans and Soumi Bala were involved in operating the tuneable diode laser (TDL) system at the early stage of data collection and assisted with the interpretation of TDL outputs. Leaf nutrient analysis was carried out by Lucy Hayes.

I certify that the contents of this thesis were not previously submitted for a degree in any university.

Nur H.A. Bahar

19 September 2016

Acknowledgement

I am wholeheartedly thankful to my primary supervisor, Professor Owen Atkin, for his excellent guidance, expertise and support from the beginning to the completion of my project. Thanks for keeping me on track Owen!

My sincere gratitude to Professor John Evans for his immense knowledge and patience which helped me develop a thorough understanding and appreciation of my research subject. Thanks for your generosity John!

I would like to thank my advisory committees Professor Patrick Meir and Professor Hans Lambers for their insightful comments and encouragement, especially during early stage of my PhD candidature. To Professor Marilyn Ball, I cannot thank you enough for being a source of knowledge, wisdom and comfort!

I would also like to thank the team of experts and staffs who were involved in field campaign in the Amazon-Andes regions. Special thanks to Dr Keith Bloomfield for his amazing work on mixed effects modelling (and countless model re-runs), Dr Benedict Long for his expert advice on biochemistry and protein work, and Dr Lasantha Weerasinghe for helping me navigate through impressive field datasets.

I have been aided in running equipment by Soumi Bala (TDL), Daryl Webb (confocal microscopy), Dr Tim Brown (leaf imaging system) and Dr Ian Wallis (tannin analysis) - and also Jack Egerton (Atkin/Ball lab maintenance). Many thanks to all of you for transferring your valuable skills and experience to me!

I am indebted to my colleagues at the Research School of Biology, ANU particularly in the Atkin, Ball, Evans and (Adrienne) Nicotra lab, whom assistance, encouragement and support helped me to enjoy (and endure) my PhD journey.

Thanks to Dr Ana Clarissa Alves for being my PhD sparring partner, Dr Andrew Scafaro for being a fantastic post-doc (you have set the bar high for me), Dr Mary Heskel for sharing your insights and stories from the other side of the world, Dr Veronica Briceño and Associate Prof Rafael Coopman for warm companion and strict mentoring, Dr Viridiana Silva-Pérez and Ross Deans for intellectual, cultural and personal exchanges, Fatimah Azzahra Rashid and Jasmin Ghazalli for honest, critical comments and conversation. Thanks to Lucy Hayes, Stephanie McCaffery and Josephine Tucker for your help in sample analysis.

Many thanks to friends and colleagues I met during my PhD journey; particularly the staffs at University of Minnesota's Hubachek Wilderness Research Center (Prof Peter Reich & Anne Reich, Karen Rice, Dr Kerrie Sendall), staffs and friends of Parque Katalapi-University of Concepción (Prof Luis Corcuera, Anita Corcuera, Meli Santana, Dr León Bravo, Dra Sandra Durán, Karina Acuña, Yadira Andrea Rojas Ramirez, Dra Claudia Rabert Pinilla & Carolina Hernández, Briceno-Rodriguez family) and the vibrant inhabitants of Cutipay, Valdivia (Roke Rojas & family, Claudia Kalleg Jerez & family). To the Canberrans (past and present): Anne-Sophie Dielen & family, Abdeljalil Elhabti, Annisa Satyanti & family, Connie Loh, Emma McIntosh & family, Deborah Veliz, Sashika Richards, Zohara Lucas & family, Sarah Zainal & family, Phillipa Beale, Jacinta Watkins, Marjorie Chamberlain, Callum Bryant, Zuraida Shelmerdine & family, Heidi Congdon, Fatin Atiqah, Fatin Shahirah, Husna Othman, Roselind Wan, Michelle Liong, Natasya Makhtar, Omar Hashmi, Asyikin Othman, Sara Chica Latorre, Sarini Azizan & family, Vivienne Seedsman, Widiastuti Karim, Rémi Branco and Paul Kriedemann; thank you very much for your friendship (and mentoring) and support.

I owe my deepest gratitude to my parents, Mom, Jaliah Md Yatim who always looks forward to hear new exciting findings from my research. Dad, Abdul Bahar Ma'arof motivates me to strive for excellence. I am equally thankful to my siblings (Hakim & Mariam, Hafiz & Ani, Huda, Aqilah and Hisyamuddin), whom over time have grown an understanding of my passion in research. I offer my regards and blessings to all of you who supported me in any respect during my PhD candidature. They say it takes a whole village to raise a child - I would say it takes a whole village to keep a PhD student sane, healthy and happy.

This PhD thesis would not have been possible without financial support from the Malaysian government postgraduate scholarship.

"Education is an ornament in prosperity and a refuge in adversity."

Aristotle

Abstract

Rubisco catalyses a rate-limiting step in photosynthesis and is the largest nitrogen sink in leaves. The maximum rate of carboxylation of Rubisco, V_{cmax}, is routinely estimated from gas exchange using the Farquhar, von Caemmerer & Berry 1980 model of photosynthesis. As V_{cmax} allows mechanistic representation of photosynthesis, it has been incorporated into terrestrial biosphere models to estimate global primary productivity. However, doubts remain about previous estimates of V_{cmax} for globally important biomes, such as moist forests, both in tropical and temperate regions.

In my thesis, I present a survey of V_{cmax} values – calculated assuming infinite mesophyll conductance - along a 3,300-meter elevation gradient from lowland western Amazon to the Andean tree line in Peru; this region is home to the largest moist forest on Earth. Large variations in V_{cmax} were found within and across the 18 field sites. As hypothesised, when estimated at a common measuring temperature (25°C), average V_{cmax} values of lowland Amazon trees were significantly lower than that of Andean trees. When data for the lowland Amazon and upland Andean trees were combined, the resultant mean tropical V_{cmax} value was lower than that of temperate trees reported in past studies. My analysis points to low V_{cmax} of Peruvian tropical trees being linked to limitations in phosphorus supply, and to a high proportion of Rubisco being inactive.

The second part of my thesis investigated how mesophyll conductance influences the estimation of V_{cmax} for several Australian tropical (i.e. warm-adapted) and temperate (i.e. cool-adapted) moist-forest trees. Consistent with previous glasshouse studies, the selected tropical tree species exhibited significantly lower V_{cmax} values than their temperate counterparts. Importantly, I showed, for the first time, that the V_{cmax} estimated on the basis of intercellular CO_2 partial pressure was equivalent to that on the basis of chloroplastic CO_2 partial pressure, when using appropriate Michaelis-Menten constants for CO_2 and O_2. Thus, low mesophyll conductance in tropical moist forest is unlikely to account for the low estimates of V_{cmax} found in the Peruvian field work study.

Finally, mechanisms underpinning development of photosynthesis in tropical moist forest trees, which include ontogenetic changes in leaf anatomy, and mesophyll and stomatal conductances, were examined. Key components of photosynthesis such as V_{cmax}, maximum electron transport rate and chlorophyll content increased synchronously during expansion, accompanied by development of leaf internal structures such as intercellular air spaces and mesophyll cells. The balance between

photosynthetic carbon uptake and respiratory release changed dramatically during leaf development, reflecting a two-fold decline in area-based rates of respiration in expanding leaves as photosynthesis became fully functional.

The dataset presented in my PhD thesis adds to the growing number of empirical estimates highly needed by the photosynthetic modelling communities, and validates the accuracy of V_{cmax} estimation using biochemical approaches. Collectively, my study is expected to contribute towards better understanding and representation of V_{cmax} in tropical forests.

Table of Contents

List of Figures

List of Tables

Chapter 1: General Introduction

Vegetation is a major driver of the terrestrial global carbon (C) cycle (Fig. 1.1). Globally, gross primary production (GPP) takes up ~120 Gt C per year but ~60 Gt C is returned back into the atmosphere via respiration, giving a net primary production (NPP) of ~60 Gt C (Prentice *et al.*, 2001; Canadell *et al.*, 2007; IPCC, 2013). Such fluxes greatly obscure anthropogenic emission of CO_2 (~6 Gt C per year) (Steffen *et al.*, 1998; Beer *et al.*, 2010). The world's forests contribute hugely to C fluxes and storage (Fig. 1.2) despite covering only 30% of land surface, with much of the terrestrial C sink being accounted for by forests (Bonan, 2008; Pan *et al.*, 2011). Since the global C cycle is central to climate simulation by terrestrial biosphere models (TBMs), future climate projections are heavily influenced by how forests behave under both current and future climates (Bonan, 2008).

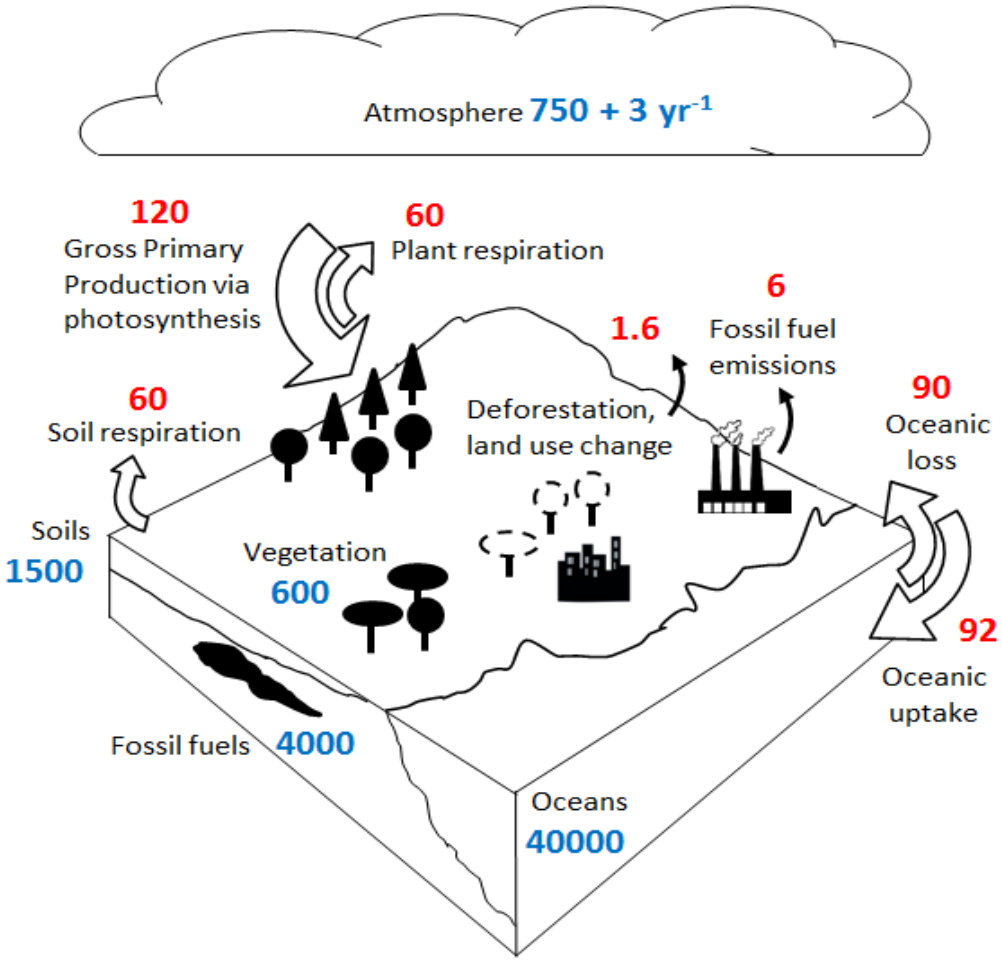

Figure 1.1. The global carbon cycle illustrates the movement of carbon between the atmosphere, land and oceans. The main annual fluxes (Gt C per year) are shown in red and cumulative storages are shown in blue. Adapted from Grace (2004) and Houghton (2007).

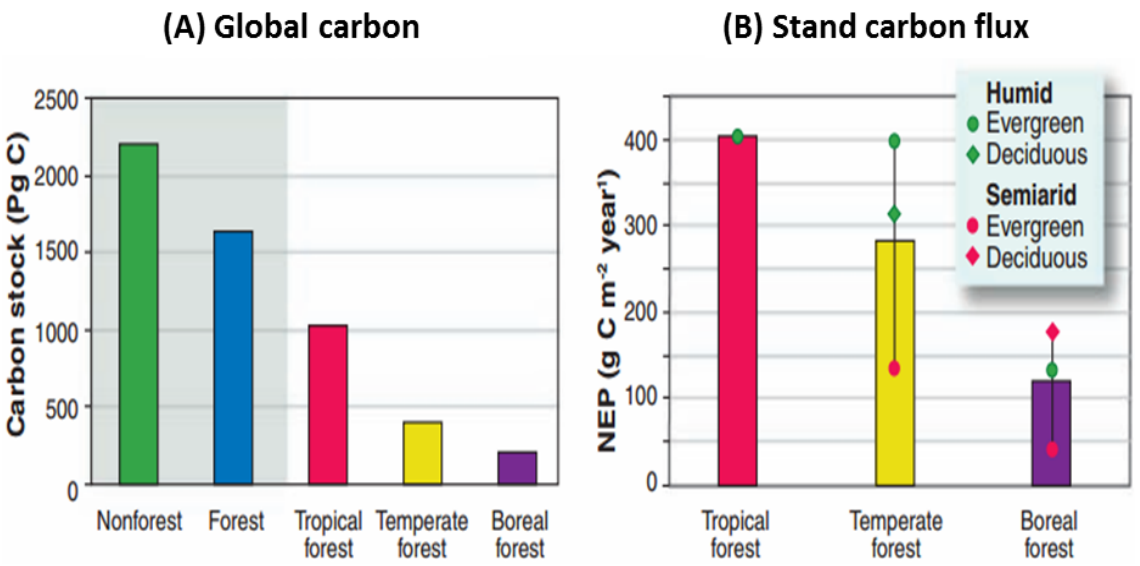

Figure 1.2. (A) Total (plant and soil) carbon stock of non-forest and forest biomes. Individual forest biomes are also shown and sum to the forest total. (B) Net ecosystem production (NEP) for tropical, temperate, and boreal forest. Individual symbols shown mean NEP for humid/moist evergreen tropical forest, three types of temperate and boreal forest. Vertical bars show NEP averaged across forest types. Figures adapted from Bonan (2008).

Tropical forests account for one-third of global GPP (Beer *et al.*, 2010; Malhi, 2010). They also account for 25% of terrestrial C stocks and have the potential to sequester large amounts of C per year, with average NEP (net ecosystem productivity – the net accumulation of carbon by an ecosystem that includes carbon accumulation in plants and soils) being near ~400 g m^{-2} yr^{-1} in tropical forests [Fig. 1.2; Bonan (2008)]. Tropical forests of South/Central America, Africa and South/South East Asia make up a total area of 18.5 × 10^6 km^2, being larger than any other forest biome (Malhi, 2010; Pan *et al.*, 2011). In each continent, the contribution of tropical forest types to overall land cover varies, with tropical Central/South America being dominated by moist forests (47%), whereas tropical Africa is often drier and covered mostly by shrublands/ grasslands and bare land (~28% each), while tropical Asia is evenly covered by moist forests, agricultural land and herbaceous vegetation (~23% each) (Bartholomé & Belward, 2005; Malhi, 2010). Thus, the contribution of moist forests to tropical ecosystems varies depending on the continent, with tropical moist forests contributing to land cover to the greatest extent in Central and South America. The amount of each forest type, combined with the rate of forest conversion or land-use change have direct impacts on the rate of C uptake and C release in each tropical continent (Malhi, 2010; Pan *et al.*, 2011). 1.3 ± 0.7 Pg C is released annually from tropical deforestation/land-use change, which is partially compensated by C uptake of 1.2 ± 0.4 Pg C yr^{-1} by intact tropical forest (Pan *et al.*, 2011). Importantly, the largest uncertainties in these estimates

of C fluxes are associated with C flows in tropical forests, with the degree of uncertainty being less in temperate/boreal forests [0.4-0.7 vs. 0.08 Pg C yr^{-1}, respectively; (Pan *et al.*, 2011)] suggesting that understanding C cycling and its underlying components in tropics should be a high priority in future.

An accurate estimation of GPP in the global TBMs requires robust representation of photosynthesis at leaf, canopy and ecosystem levels (Luyssaert *et al.*, 2007; Kattge *et al.*, 2009; Ito, 2011; Rogers, 2014). Leaf photosynthesis is represented in many global TBMs by either biochemical models (Farquhar *et al.*, 1980; Haxeltine & Prentice, 1996) or light use-efficiency models [Table 1.1; Hikosaka et al. (2015)]. Leaf-level photosynthesis is then scaled up to the canopy level using several methods, including: 1) a big-leaf model which treats the canopy as single-layer leaf (Amthor, 1994; Lloyd *et al.*, 1995); 2) a sun/shade model which calculates the sum of photosynthetic CO_2 uptake of sunlit and shade leaves (de Pury & Farquhar, 1997); and, 3) optimal leaf nitrogen (N) distribution which accounts for leaf N and its distribution among leaf layers (Anten *et al.*, 1995). Canopy photosynthesis schemes such as those above have been tested against eddy covariance systems (which measure ecosystem carbon exchange and which are used to estimate GPP) - in many cases, the predicted rates of carbon uptake from models were found to be consistent with GPP estimated from eddy covariance (e.g. Lloyd *et al.*, 1995; Ito *et al.*, 2005; Krinner *et al.*, 2005).

Table 1.1. Summary of canopy photosynthesis schemes in several global terrestrial biosphere models, taken from Hikosaka *et al*. (2015)

Model	**CASA**	**CLM ver. 4**	**LPJ**	**ORCHIDEE**	**VISIT**
References	Potter et al. (1993)	Bonan et al. (2011)	Sitch et al. (2003)	Krinner et al. (2005)	Ito et al. (2005)
Canopy structure	Mono-layer	Mono-layer (tree/grass)	Mono-layer (tree/grass)	Mono-layer (tree/grass)	Overstory/ understory
Leaf photosynthesis	Light-use efficiency	Biochemical model (Farquhar)	Biochemical model (Haxeltin and Prentice)	Biochemical model (Farquhar)	Biochemical model (Farquhar)
Scaling-up method	Big-leaf	Sun/ shade, N distribution	Optimal leaf N distribution	Optimal leaf N distribution	Sun/ shade, N distribution
C3/C4 plants	No	Yes	Yes	Yes	Yes
Stomata	No	Ball et al.	Haxeltin and Prentice	Ball et al.	Leuning

Nevertheless, differences in model structure, complexity and assumptions can result in different simulation outputs (Cramer *et al.*, 1999; Hikosaka *et al.*, 2015); such discrepancies contribute to large uncertainties in current C estimates and future climate-vegetation projections. Increasing information on plant traits such as leaf biochemical characteristics, leaf area index, variation in leaf traits through canopies, and eddy covariance flux measurements are expected to reduce uncertainties in our prediction of future changes in atmospheric C and climate.

In a majority of TBMs, leaf photosynthesis is represented by the biochemical model of Farquhar-von Caemmerer-Berry (1980). By fitting the Farquhar *et al.* model to $A \leftrightarrow C_i$ curves (i.e. the photosynthetic response to CO_2 partial pressure in leaf sub-stomatal cavity), a number of important parameters related to leaf biochemistry can be derived (Sharkey *et al.*, 2007). One of the key parameters obtained from $A \leftrightarrow C_i$ curve is the V_{cmax}, which denotes maximum Rubisco carboxylation capacity, is employed in at least eleven TBMs to model global C fluxes and to simulate future global change (Rogers, 2014). In these TBMs, empirical estimates of V_{cmax} are usually compiled from past studies; alternatively V_{cmax} could be inferred from leaf N content or from optimising photosynthesis and respiration (e.g. Cox, 2001; Krinner *et al.*, 2005; Kattge *et al.*, 2009; Friend, 2010). The range of V_{cmax} values reported in the models is large, even within a plant functional type (PFT[1]) (-46 to +77% of the PFT mean) due to limited datasets and poorly defined coefficients (Beerling & Quick, 1995; Kattge *et al.*, 2009; Rogers, 2014). Uncertainty associated with V_{cmax} values accounts for 30 Pg C yr^{-1} variation in the estimates of GPP (Bonan *et al.*, 2011) and also for substantial variations in NPP (-22 to +28% of the PFT mean) (Friend, 2010). Given the critical role of V_{cmax} in modelling global C fluxes, there is a need to expand data coverage especially in the under-represented tropical biome (where the biggest uncertainty lies) to allow better parameterisation of V_{cmax} in global TBMs (Friend, 2010; Bonan *et al.*, 2011; Verheijen *et al.*, 2013; Rogers, 2014).

The V_{cmax} of tropical forests remain under-characterised despite the dominant role of tropical forests in regulating C fluxes between land surfaces and the atmosphere. For example, the analysis of Kattge *et al.* (2009) was based on a compilation of a relatively small number of V_{cmax} estimates (n = 66) from tropical ecosystems, which contrasts with the greater availability of data from temperate broadleaved and

[1] Groupings of plant species that share similar roles (e.g. photosynthetic pathway) and characteristics (e.g. growth form) in ecosystem function.

coniferous trees (358 and 136 individual plants, respectively). Subsequently, additional studies on tropical forests (Domingues *et al.*, 2010; Cernusak *et al.*, 2011; van de Weg *et al.*, 2012) have broadened V_{cmax} estimates (Walker *et al.*, 2014; Ali *et al.*, 2015). In addition, the highly heterogeneous nature of tropical forests could further complicate representation and parameterisation of V_{cmax} in global TBMs. As tropical forests are found from sea level to the alpine tree line (at around 4000m above sea level in the tropics), adjustments in major physiological functions, including V_{cmax}, occur in response to changing abiotic (soil nutrient, temperature, atmospheric pressure, cloud cover) and biotic conditions (species competition, herbivory) (Fyllas *et al.*, 2009; Mercado *et al.*, 2011; Marthews *et al.*, 2012; Asner *et al.*, 2016). Most of these aspects are under- or unexplored relative to temperate/boreal forests. Clearly, tropical forests present us fertile ground of opportunities for research and discovery.

V_{cmax} scales positively with leaf N, reflecting the considerable investment of N in Rubisco and other components in photosynthetic metabolism (electron transport proteins, pigment-protein complexes, Calvin cycle enzymes) (Field & Mooney, 1986; Evans, 1989; Evans & Seemann, 1989; Schulze *et al.*, 1994). These strong correlations form the basis of deriving PFT-specific V_{cmax} from leaf N in many TBMs, with numerous models calculating V_{cmax} as a function of leaf N, whereas others estimate V_{cmax} from the fraction of N invested in Rubisco (Cox, 2001; Kattge *et al.*, 2009; Friend, 2010; Bonan *et al.*, 2011). The parameterisation of V_{cmax}↔N on a PFT basis (e.g. tropical evergreen/ deciduous trees, temperate evergreen/ needle trees, boreal deciduous trees, grass) reflects inherent genotypic and physiological differences among PFTs (Wullschleger *et al.*, 2014) and has been shown to reduce uncertainties in model outputs (Kattge *et al.*, 2009; Alton, 2011). For the PFT tropical trees, the response of V_{cmax} to leaf N is thought to be constrained by leaf phosphorus (P) (Meir *et al.*, 2002; Kattge *et al.*, 2009; Domingues *et al.*, 2010; Mercado *et al.*, 2011; Walker *et al.*, 2014), which has the effect of reducing the GPP estimate of tropical trees (Kattge *et al.*, 2009). Phosphorus, rather than N, has been identified as a dominant driver of productivity in tropical forests (Mercado *et al.*, 2011; Quesada *et al.*, 2012) since older, more impoverished soils of tropical regions are generally P-limited (Hedin, 2004; Townsend *et al.*, 2007). Nevertheless, there is considerable heterogeneity across the tropical forests such that other nutrients, including N, can also be limiting (Fyllas *et al.*, 2009; Mercado *et al.*, 2011; Marthews *et al.*, 2012). Hence, establishing V_{cmax} responses to leaf N and P across a wide range of soil nutrient availabilities in tropical ecosystems will enable us to

identify key drivers of photosynthesis in this globally important biome and provide further empirical evidence for representation of photosynthesis in TBMs.

Estimation of V_{cmax} value by fitting the Farquhar *et al.* model to $A \leftrightarrow C_i$ curves relies on the assumption that the diffusional resistance between the sub-stomatal cavity (C_i) and carboxylation sites (C_c) is insignificant and can be ignored. In other words, mesophyll conductance (g_m, diffusion conductance to CO_2 in the mesophyll) is assumed to be infinite and hence no drawdown occurs from C_i to C_c (i.e. C_i equals C_c). However, estimating V_{cmax} on a C_i basis potentially underestimates the 'true' V_{cmax} by 60 - 75%, if appropriate kinetic constants are not used (Fig. 1.3A) (Epron *et al.*, 1995; Manter & Kerrigan, 2004; Warren, 2008; Sun *et al.*, 2014b). Almost all TBMs assume infinite g_m and calculate V_{cmax} on a C_i basis; however, a recent model demonstrates that accounting for limitations in g_m can yield substantial increases in the modelled cumulative CO_2 fertilization effect on GPP from 915 to 1057 Pg C (for 1901 - 2010) (Sun *et al.*, 2014a).

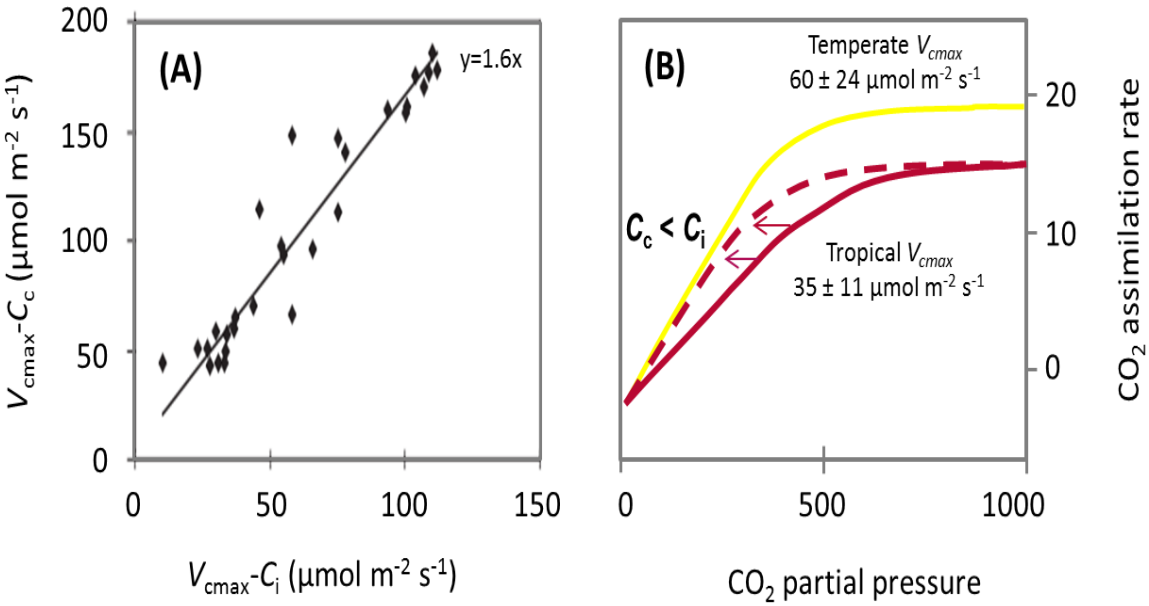

Figure 1.3. (A) The relationship between V_{cmax} calculated on a C_i basis with V_{cmax} calculated on a C_c basis, using the same kinetic constants, taken from Warren (2008). (B) Example of $A \leftrightarrow C_i$ curves for temperate and tropical species (solid lines). Dashed line denotes hypothetical shift in the initial slope of $A \leftrightarrow C_i$ curve when factoring reduction in CO_2 concentration from C_i to C_c, resulting higher V_{cmax} on C_c basis than V_{cmax} on C_i basis.

Moreover, there is evidence of greater mesophyll resistance (inverse of g_m) for leaves with lower photosynthetic capacity, which results in a larger drawdown of CO_2 concentration from C_i to C_c (Warren & Adams, 2006; Niinemets *et al.*, 2009; Tosens *et al.*, 2012). Given these observations, lower V_{cmax} (calculated assuming infinite g_m) of tropical trees compared to temperate trees [35 ± 11 vs. 60 ± 24 μmol m^{-2} s^{-1}, respectively (Kattge *et al.*, 2009)] might be explained by greater mesophyll resistance. If so, then tropical trees exhibiting low photosynthetic rates might exhibit low g_m, with the result that estimates of V_{cmax} being lower than actual V_{cmax} values, when ignoring the large CO_2 drawdown from C_i to C_c. If this is the case, accounting for g_m might yield a higher V_{cmax} on a C_c basis than that on a C_i basis in tropical trees (Fig. 1.3B). Further, the above scenario raises the possibility that V_{cmax} (on C_c basis) per unit N might be higher than previously assumed. Past studies, using C_i-based estimates of $V_{cmax,}$ have reported lower V_{cmax} per unit N of tropical than temperate trees [22 vs. 34 μmol CO_2 gN^{-1} s^{-1}, respectively (Kattge *et al.*, 2009)]. To our knowledge, the possibility of tropical leaves being more limited by mesophyll resistance than temperate leaves has not yet been investigated.

THESIS OUTLINES

This thesis is divided into three stand-alone chapters to address some of the gaps in knowledge highlighted in the previous section. Chapter 2 greatly increases coverage of V_{cmax} values for tropical moist forests (TMFs), a forest-type that represents 47% of the tropical Central/South America and 23% of tropical Asia. The V_{cmax} variations of TMFs were characterised at 18 sites distributed along a 3,300-meter elevation gradient from lowland western Amazon to the Andean tree line in Peru. The site selection enabled an assessment of the potential role of P-availability on photosynthetic performance across Amazonian-Andean regions differing >40-fold in total soil P. In addition, the influence of growth temperature on photosynthesis and key leaf traits was examined via comparison of lowland TMFs (~200 m above sea level; ~25ºC of mean annual temperature) and upland TMFs (1500 - 3380 m a.s.l.; 8 - 19ºC of MAT). Taking advantage of wide variations of leaf traits collected from the 18 sites, the relationships between photosynthetic capacity (V_{cmax} and J_{max}, maximum rate of electron transport) and leaf nutrient (leaf N and P) and structure (leaf mass per area) were assessed.

To further explore factors explaining variations in photosynthesis and photosynthetic N-use efficiency (Fig. 1.4), N-partitioning in photosynthetic metabolism and *in vitro* Rubisco levels were quantified.

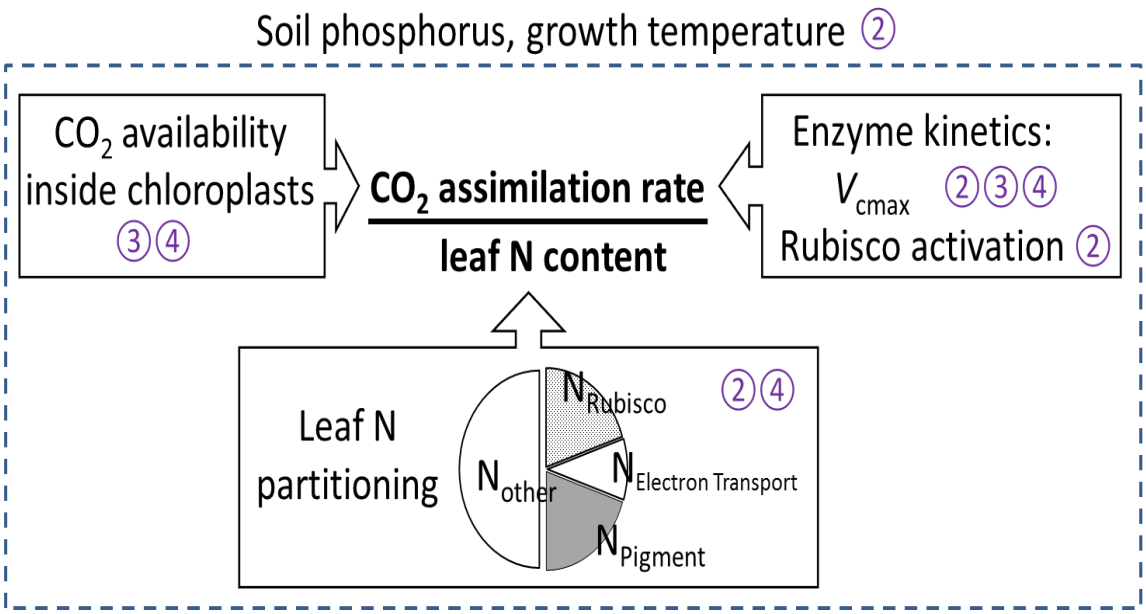

Figure 1.4. Conceptual diagram depicts several factors influencing photosynthetic N-use efficiency. Underpinning efficient use of N for carbon gain is the availability of CO_2 inside chloroplasts i.e. the sites of carboxylation, the kinetics of Rubisco and the amount and partitioning of leaf N to photosynthetic metabolism and non-photosynthetic pools (e.g. cell walls). Soil phosphorus and/or growth temperature are hypothesised to drive differences in photosynthetic N-use efficiency between different types of forests e.g. lowland vs. upland tropical moist forests and tropical vs. temperate moist forests. Number in circles denotes topics being covered in Chapters 2, 3 and 4.

Chapter 3 investigates how mesophyll conductance - estimated using a combination of leaf gas exchange and carbon isotope discrimination - influenced the estimation of V_{cmax} for several Australian tropical and temperate moist forest trees. This study used broadleaved evergreen species from thermally contrasting environments which are moist and non-freezing in order to minimise the potential impacts of co-variation in moisture stress and special adaptations needed to cope with freezing conditions (Xiang *et al.*, 2013). Warm-adapted tropical and cold-adapted temperate trees were grown in common, temperature-controlled environment to test whether greater mesophyll resistance contributes to lower rates of photosynthesis in tropical moist forest trees, in contrast to temperate moist forest trees. V_{cmax} estimated on a C_c basis were compared with V_{cmax} estimated on a C_i basis, using appropriate Michaelis-Menten constants for CO_2 and O_2, to confirm whether correction of CO_2 availability inside chloroplasts yielded higher photosynthetic N-use efficiency for tropical trees.

Chapter 4 seeks to explore mechanisms underpinning photosynthetic development in expanding tropical canopy leaves, which currently are not very well known. Changes in photosynthetic capacity, respiratory rates, leaf anatomy and partitioning of leaf N in developing leaves of tropical evergreen tree seedlings were monitored at 65 to 100% expansion and a few weeks after full leaf expansion. Here, particular focus was placed on establishing whether photosynthetic capacity (V_{cmax} and J_{max}) and diffusion conductances (stomata and mesophyll) develop in synchrony, and whether changes in leaf anatomy reflect photosynthetic development. Given the importance of tropical forests in global C flux, this chapter examines how the balance between photosynthesis and leaf respiration varies as leaves mature.

Chapter 2: Leaf-level photosynthetic capacity in lowland Amazonian and high-elevation, Andean tropical moist forests of Peru

2.1 Introduction

Tropical moist forests (TMFs) play a significant role in the terrestrial carbon cycle, contributing one-third of global gross primary productivity (Beer *et al.*, 2010; Malhi, 2010). Understanding the factors that regulate leaf photosynthesis (*A*) in TMFs is a prerequisite for modelling carbon storage in tropical ecosystems, with *A* being influenced *inter alia* by nutrient supply [particularly nitrogen (N) and phosphorus (P)], elevation and growth temperature.

Early studies in lowland TMFs implicated low foliar P concentrations as a major influence on light-saturated net photosynthesis (A_{sat}) (Reich & Walters, 1994; Raaimakers *et al.*, 1995), with soil P being a major factor limiting Amazon productivity (Quesada *et al.*, 2012). Foliar P is crucial to the fine-tuning A_{sat} (Fredeen *et al.*, 1989; Jacob & Lawlor, 1993) via regulation of key intermediates in carbon metabolism (e.g. ATP, NADPH and sugar phosphates including ribulose 1,5-bisphosphate - RuBP). While the direct effect of P-limitation is primarily on RuBP regeneration, reductions in Rubisco activity also occur (Brooks, 1986; Jacob & Lawlor, 1992; Loustau *et al.*, 1999). Although Meir *et al.* (2002; 2007) and Reich *et al.* (2009) showed that A_{sat} at a given leaf N concentration ([N]) was less in lowland tropical trees than their temperate counterparts, the extent to which P limitations *per se* alter $A_{sat}\leftrightarrow$[N] relations within TMFs is uncertain (Bloomfield *et al.*, 2014a; Domingues *et al.*, 2015). A further unknown is the extent to which large elevation gradients affect $A_{sat}\leftrightarrow$[N] relations in the tropics. Upland TMFs are more likely to be limited by N than their lowland counterparts (Tanner *et al.*, 1998). Upland TMFs also experience lower temperatures and atmospheric CO_2 partial pressures, more frequent cloud cover and experience greater leaf wetness (Grubb, 1977; Vitousek, 1984; Girardin *et al.*, 2010; Bruijnzeel *et al.*, 2011). Such factors can limit A_{sat} (Terashima *et al.*, 1995; Bruijnzeel & Veneklaas, 1998; Letts & Mulligan, 2005), leading to declines in productivity (Girardin *et al.*, 2010). A_{sat} in upland TMFs have been documented (e.g. Quilici & Medina, 1998; Cordell *et al.*, 1999; Hikosaka *et al.*, 2002; Letts & Mulligan, 2005; Rada *et al.*, 2009), showing A_{sat} being constant with increasing elevation (Cordell *et al.*, 1999), or declining with increasing elevation (Hikosaka *et al.*, 2002; Wittich *et al.*, 2012).

Rates of A_{sat} are subject to variations in stomatal conductance (g_s) and the partial pressure of internal leaf CO_2 (C_i) (Santiago & Mulkey, 2003). As variations in C_i alter both CO_2 uptake and photorespiratory CO_2 release, variations in C_i could potentially confound our understanding of how environmental gradients alter N investment in *A*. By contrast, variations in g_s have less impact on the fundamental, biochemical parameter of photosynthetic capacity – that being the maximum rate of carboxylation by Rubisco (i.e. V_{cmax}). Positive correlations between V_{cmax} and leaf [N] have been reported for some tropical species (Carswell *et al.*, 2000; Meir *et al.*, 2002; Domingues *et al.*, 2005; Kumagai *et al.*, 2006; Meir *et al.*, 2007) – whereas in others no strong V_{cmax}↔[N] relationship was observed (Coste *et al.*, 2005; van de Weg *et al.*, 2012; Dusenge *et al.*, 2015). Although reports on V_{cmax} are less widespread in the tropics than A_{sat}, the available data suggest that V_{cmax} values, as well as V_{cmax} per unit N (herein termed '$V_{cmax,N}$'), are lower in lowland TMFs than their non-tropical counterparts (Carswell *et al.*, 2000; Meir *et al.*, 2002; Domingues *et al.*, 2007; Meir *et al.*, 2007; Domingues *et al.*, 2010). Kattge *et al.* (2009) re-analysed data to show that V_{cmax} per unit N in TMFs growing on young, relatively high nutrient status soils was higher compared to their older, Ferralsol and Acrisol soil counterparts that are characterised by very low soil P availability (Quesada *et al.*, 2010). These observations are consistent with laboratory studies showing reduced V_{cmax} (Lauer *et al.*, 1989; Loustau *et al.*, 1999) and reduced N allocation to Rubisco (Warren & Adams, 2002) under P-limited conditions. Increased allocation of N to non-photosynthetic components may also play a role (Domingues *et al.*, 2010; Lloyd *et al.*, 2013), as might inactivation of Rubisco (Stitt & Schulze, 1994). Yet, doubt remains regarding the general V_{cmax}↔[N] relationship in TMFs due to the scarcity of data, both in lowland and upland TMFs. Comprehensive surveys of V_{cmax} (and J_{max} - maximum rate of electron transport) across lowland and upland TMFs are required to establish whether there are generalized patterns of photosynthetic capacity in relation to environmental conditions and/or other leaf traits.

TMF species with higher leaf nutrient concentrations and lower leaf mass per unit leaf area (M_a) values are often found in more fertile soils (Fyllas *et al.*, 2009), and M_a tends to increase with increasing elevation (Hikosaka *et al.*, 2002; van de Weg *et al.*, 2009; Almeida *et al.*, 2012; Asner *et al.*, 2014b); leaf chemistry also systematically shifts along elevation gradients in the tropics (Asner *et al.*, 2014b). Large variations in leaf traits have also been observed among co-occurring species, reflecting the importance of phylogenetic relationships in determining trait values in TMFs

(Townsend *et al.*, 2007; Kraft *et al.*, 2008; Fyllas *et al.*, 2009). Whether similar patterns hold for estimates of V_{cmax} in lowland and upland TMFs, is, however, not known.

Variations in $V_{cmax,N}$ underlie variations in photosynthetic N use efficiency. Further insights can be gained by quantifying the proportion of N allocated to the pigment-protein complexes (n_P), electron transport (n_E) and Rubisco (n_R) (Evans & Seemann, 1989; Pons *et al.*, 1994; Hikosaka, 2004). Quantification of V_{cmax}, J_{max}, leaf chlorophyll and [N] can be used to estimate n_P, n_E and n_R (Evans & Seemann, 1989; Niinemets & Tenhunen, 1997). In non-tropical plants, lower A_{sat} at a given N (A_N) are associated with reduced allocation of N to photosynthesis and increased allocation to non-photosynthetic components (Poorter & Evans, 1998; Westbeek *et al.*, 1999; Warren & Adams, 2001; Takashima *et al.*, 2004; Hikosaka & Shigeno, 2009). Similarly, variations in A_N were associated with differences in N allocation to and within the photosynthetic apparatus in greenhouse-grown tropical tree seedlings (Coste *et al.*, 2005) and in high elevation TMFs of Rwanda (Dusenge *et al.*, 2015). To our knowledge, no study has quantified N allocation patterns in field-grown tropical trees, and not with respect to field sites in upland and lowland TMFs.

We examined variations in photosynthetic capacity and leaf traits across TMF canopies located at 18 sites along a 3,300-m elevation gradient stretching from lowland western Amazonia to the Andean tree line in Peru. The study included 11 lowland sites in northern and southern Peru (elevation 117-223 m a.s.l.), and seven upland sites at elevations of 1527-3379 m a.s.l. in southern Peru. Our site selection enabled an assessment of the potential role of P-availability on photosynthetic performance across Amazonian-Andean TMF sites differing >40-fold in total soil P. The upland sites were characterised by a floristically distinct assemblage of montane forest species, with the transition from lowland moist forests to upland montane forests coinciding with an increase in cloud cover (van de Weg *et al.*, 2009; Bruijnzeel *et al.*, 2011). In conjunction with the recent findings of the key role of P in modulating carbon investment (Quesada *et al.*, 2012) and photosynthesis (Bloomfield *et al.*, 2014b) of tropical trees, and that leaf P varies predictably along soil P and elevation gradients (Asner *et al.*, 2014b), we addressed the following questions:

(1) Do tropical TMF species growing on low-P soils exhibit lower photosynthetic capacity and photosynthetic N use efficiency than TMF trees growing on sites with higher P availability?

(2) Are there marked differences in V_{cmax}, J_{max} and $V_{cmax,N}$ between lowland Amazonian and upland Andean TMFs?
(3) Are differences in V_{cmax}, J_{max} and $V_{cmax,N}$ linked to concomitant variations in other leaf traits and/or environmental variables?

2.2 Materials and Methods

2.2.1 Study sites

Field work was carried out in 18 one-hectare long-term monitoring plots in Peru which contribute to the ABERG and RAINFOR networks of permanent sample plots. The plots are arrayed along gradients of elevation (117 to 3379 m above sea level) and soil nutrient status (Table 2.1). Four of the lowland sites (TAM-09, TAM-06, TAM-05 and CUZ-03) were located in the Tambopata watersheds of SE Peru, while seven additional lowland sites (ALP-01, ALP-30, ALP-40, JEN-11, JEN-12, SUC-01, and SUC-05) were located in the Ucayali watershed in NE Peru. Seven upland sites (SPD-01, SPD-02, ESP-01, WAQ-01, TRU-01, TRU-03, and TRU-08) were distributed along SE slopes of the Andes in the Kosñipata valley. The 18 plots used in this study are part of the ABERG Kosñipata study transect (www.andesconservation.org/), Amazon Forest Inventory Network (RAINFOR; http://www.rainfor.org/) and the Carnegie Spectranomics Project (http://spectranomics.ciw.edu/). For each site, climate data were obtained from Asner *et al.* (2014a) and Y. Malhi *et al.* (unpublished).

Marked changes in species richness, canopy cover and tree height occur along the elevation gradient (Asner *et al.*, 2014a; Girardin *et al.*, 2014b; Silman, 2014), reflecting local geological substrates, as well as changes in growth temperature, cloud cover and light environment. The lowland sites lie on a mosaic of young to old soil substrates, whereas upland forests exist primarily on young geologic substrates (van de Weg *et al.*, 2009; Quesada *et al.*, 2010; Fisher *et al.*, 2013). Data on soil type, as well as total N and P concentrations in soils, were obtained from Dr Carlos Alberto Quesada (Instituto Nacional de Pesquisas da Amazônia), using a combination of unpublished and published (Quesada *et al.*, 2010) data. In addition to marked inter-site differences in total soil [N] (0.6 - 15.5 g N kg^{-1}), substantial variation in total soil [P] occurs across both the lowland (38 - 727 mg P kg^{-1}) and upland sites (496 - 1631 mg P kg^{-1}) (Table 2.1). Soils at three of the lowland sites in northern Peru (JEN-12, ALP-30 and ALP-40) are notable for being low nutrient status arenosols/podzols (‘white sands’).

Table 2.1. Description of the sampled Peruvian field sites.

Category	Site Code	Latitude	Longitude	Elevation (m a.s.l.)	No. of species	MAT (°C)	MAP (m)	Atm. Pressure (kPa)	Soil classification	Total soil		Leaf chemistry			
										[N] ($g\ kg^{-1}$)	[P] ($mg\ kg^{-1}$)	Leaf N_a ($g\ m^{-2}$)	Leaf P_a ($g\ m^{-2}$)	Leaf N:P	M_a ($g\ m^{-2}$)
Lowland	SUC-05	-3.2558	-72.8942	132	20	26.2	2.75	100	Alisols	1.9	276	1.94 ± 0.61	0.06 ± 0.04	30.1 ± 7.03	129 ± 31
	TAM-05	-12.8309	-69.2705	223	8	24.4	1.90	99	Cambisols	1.6	256	2.14 ± 0.27	0.08 ± 0.02	28.6 ± 9.49	119 ± 27
	JEN-11	-4.8781	-73.6295	131	18	26.6	2.70	100	Acrisols	1.8	141	2.12 ± 0.52	0.06 ± 0.02	27.9 ± 10.4	144 ± 37
	ALP-01	-3.9500	-73.4333	120	18	25.2	2.69	100	Gleysols	0.6	110	1.90 ± 0.40	0.08 ± 0.03	26.2 ± 8.62	119 ± 24
	SUC-01	-3.2519	-72.9078	117	17	26.2	2.75	100	Plinthosols	1.7	305	1.81 ± 0.63	0.09 ± 0.03	22.1 ± 4.99	123 ± 27
	JEN-12	-4.8990	-73.6276	135	19	26.6	2.70	100	Podzols	6.9	133	1.97 ± 0.52	0.09 ± 0.05	21.9 ± 10.42	156 ± 31
	ALP-30	-3.9543	-73.4267	150	21	25.2	2.69	100	Arenosols	0.8	38	1.67 ± 0.47	0.09 ± 0.04	20.8 ± 6.85	145 ± 46
	CUZ-03	-12.5344	-69.0539	205	12	24.4	1.90	99	Cambisols	2.4	727	1.88 ± 0.47	0.10 ± 0.04	17.2 ± 5.97	109 ± 18
	ALP-40	-3.9410	-73.4400	142	12	26.3	2.76	100	Podzols	2.1	59	1.84 ± 0.36	0.10 ± 0.02	16.8 ± 5.00	171 ± 50
	TAM-09	-12.8309	-69.2843	219	13	24.4	1.90	99	Alisols	1.1	326	2.19 ± 0.45	0.14 ± 0.03	16.4 ± 3.77	105 ± 21
	TAM-06	-12.8385	-69.2960	215	13	24.4	1.90	99	Alisols	1.7	529	2.56 ± 0.34	0.17 ± 0.04	15.3 ± 2.84	126 ± 26
Upland	SPD-02	-13.0491	-71.5365	1527	19	18.8	5.30	83	Cambisols	8.8	1631	2.23 ± 0.45	0.16 ± 0.05	15.4 ± 4.05	126 ± 36
	SPD-01	-13.0475	-71.5423	1776	21	17.4	5.30	85	Cambisols	11.9	1071	2.25 ± 0.35	0.16 ± 0.04	14.3 ± 3.34	124 ± 29
	TRU-08	-13.0702	-71.5559	1885	20	18.0	2.47	82	Cambisols	8.1	496	1.99 ± 0.36	0.12 ± 0.05	16.9 ± 3.54	165 ± 38
	ESP-01	-13.1751	-71.5948	2863	17	13.1	1.56	72	Umbrisols	14.8	981	2.39 ± 0.50	0.19 ± 0.05	12.7 ± 1.78	140 ± 32
	TRU-03	-13.1097	-71.5995	3044	13	11.8	1.78	71	Umbrisols	15.5	787	2.24 ± 0.44	0.21 ± 0.04	10.5 ± 2.35	164 ± 40
	WAQ-01	-13.1908	-71.5874	3045	13	11.8	1.56	72	Umbrisols	8.8	1414	2.68 ± 0.42	0.24 ± 0.05	11.5 ± 2.16	149 ± 46
	TRU-01	-13.1136	-71.6069	3379	16	8.0	1.98	67	Umbrisols	15.0	856	2.53 ± 0.31	0.21 ± 0.04	11.2 ± 3.10	151 ± 49

Lowland sites are listed in order of decreasing leaf N:P ratios, while upland sites are listed in order of increasing elevation. Extremely low soil P did not necessarily produce low leaf P as in the case of ALP-03 and ALP-04, therefore lowland sites were ranked according to leaf N to P ratio which provides better indication of nutrient limitation (Aerts & Chapin, 2000). Atmospheric pressure was obtained from a Licor 6400 gas exchange system. For each site name, a site code is shown as designated by the JACARE (the Joint Amazon Carnegie RAINFOR Expedition); values of total soil nitrogen and phosphorus are shown (expressed per unit soil dry mass). Also shown are average leaf area-based concentrations of total nitrogen (N_a) and phosphorus (P_a), as well as the ratio of leaf N:P and leaf mass per unit area, M_a, all shown with SD. Soil classification follows World Reference Base (WRB). Abbreviations: MAP = mean annual precipitation, MAT = mean annual temperature. Source Asner *et al.* (2014a), Quesada (*et al.* 2010; pers. comm. 2014) and Y. Malhi *et al.* (unpublished)

Among the lowland and upland sites, mean annual precipitation (MAP) values range from 1560 to 5300 mm yr^{-1}. Mean annual temperature ranged from 8.0 to 18.8 °C across the upland sites, and 24.4 to 26.6 °C among the lowland sites.

At each site, tree climbers collected from upper canopy branches (supporting leaves considered to typically be exposed to full sunlight for much of the day) from dominant tree species. There was little replication of individual species possible at any site. Each tree was initially identified to the genus-level and, whenever possible, to the species-level. A total of 353 individual trees drawn from 210 species were sampled across the 18 sites. For each tree, voucher specimens were collected and matched to herbarium collections at the National Agrarian University La Molina Herbarium in Peru and the Missouri Botanical Garden for full taxonomic verification by Carnegie Institution taxonomists.

2.2.2 Leaf gas exchange measurements

Measurements of leaf gas exchange were made during July to September 2011, using portable photosynthesis systems (Licor 6400XT infrared gas analyser, Li-Cor BioSciences, Lincoln, NE, USA). Measurements were made on the most recently fully expanded leaves attached to the cut branches (which had been re-cut under water immediately after harvesting to preserve xylem water continuity).

CO_2 response curves of light-saturated photosynthesis (i.e. $A \leftrightarrow C_i$ curves) were quantified within 30–60 minutes after branch detachment, with CO_2 concentrations inside the reference chamber ranging from 35 to 2000 µmol mol^{-1}; initial measurements were made at 400 µmol mol^{-1}, followed by decreases in CO_2 to 300, 200, 150, 125, 100, 75, 50 and 35 µmol mol^{-1}; thereafter, CO_2 concentrations were increased back to 400 µmol mol^{-1}, and then to 600, 900, 1250, 1500, 1750 and finally 2000 µmol mol^{-1}. Block temperatures within the chamber were set to the prevailing day-time air temperature at each site (from 25-28 °C). A photosynthetic active radiation (PAR) flux density of 1800 µmol m^{-2} s^{-1}, generated from an artificial light source (6400-02B Red/Blue LED Light Source, Li-Cor, Inc.), was used for all measurements. The resultant $A \leftrightarrow C_i$ curves (examples shown in Fig. 2.1) were fitted following the model described by Farquhar *et al.* (1980) in order to calculate V_{cmax} and J_{max} on a leaf area basis. V_{cmax} and J_{max} values at the prevailing leaf temperature were determined via minimizing the sum of squares of modelled vs observed estimates of net CO_2 exchange at given C_i values. This was done

for both the CO_2-limited and CO_2-saturated regions of $A \leftrightarrow C_i$ curves (using C_i values expressed on a partial pressure basis, corrected for altitudinal changes in air pressure), with these regions being defined individually for each replicate. V_{cmax} at the prevailing leaf temperature was calculated under the assumption that at C_i values below 15-20 Pa (depending on site altitude) photosynthesis was limited by Rubisco only. Rates of A at these low CO_2 values were fitted to the Rubisco-limited equation of photosynthesis:

$$A = \left[\frac{V_{cmax}(C_i - \Gamma_*)}{\left(C_i + K_c\left(1 + {}^{O}/_{K_o}\right)\right)}\right] - R_{light} \qquad \text{(Eqn 2.1)}$$

where R_{light} is respiration in the light, Γ* is the CO_2 compensation point in the absence of photorespiration [3.69 Pa at 25ºC; von Caemmerer *et al.* (1994)], K_c and K_o are the effective Michaelis-Menten constants for CO_2 and O_2 at 25˚C [40.4 Pa and 24.8 kPa, respectively, von Caemmerer *et al.* (1994)] and O is partial pressure of O_2, corrected for atmospheric pressure at each altitude, according to:

$$O_2 \text{ partial pressure at site } = O_2 \text{ partial pressure at sea level} \times \frac{\text{air pressure at site}}{\text{air pressure at sea level}}$$

The resultant O_2 partial pressures at each site were then used to modify estimates of Γ* and K'. C_i values were corrected for air pressure in the same manner. Rates of J_{max} were calculated using the electron-transport-limited equation of CO_2 assimilation:

$$A = \left[\frac{J_{max}(C_i - \Gamma_*)}{(4C_i + 8\Gamma_*)}\right] - R_{light} \qquad \text{(Eqn 2.2)}$$

assuming that A is limited by RuBP regeneration at higher concentrations of atmospheric CO_2 (Fig. 2.1).

Rates of CO_2 exchange were corrected for diffusion through the gasket of the LI-6400 leaf chamber (Bruhn *et al.*, 2002) prior to calculation of V_{cmax} and J_{max}. Assuming infinite internal diffusion conductance (g_m), Michaelis constants of Rubisco for CO_2 (K_c) and O_2 (K_o) at a reference temperature 25°C were assumed to be 40.4 Pa and 24.8 kPa, respectively (von Caemmerer *et al.*, 1994); these values were adjusted to actual leaf temperatures assuming activation energies of 59.4 and 36 kJ mol^{-1} for K_c and K_o, respectively (Farquhar *et al.*, 1980). Fitted parameters were then scaled to a reference temperature of 25°C using activation energies of 64.8 and 37.0 kJ mol^{-1} for V_{cmax} and J_{max}, respectively (Farquhar *et al.*, 1980). Γ* at each leaf temperature was assumed to follow the temperature dependency reported by Brooks and Farquhar (1985).

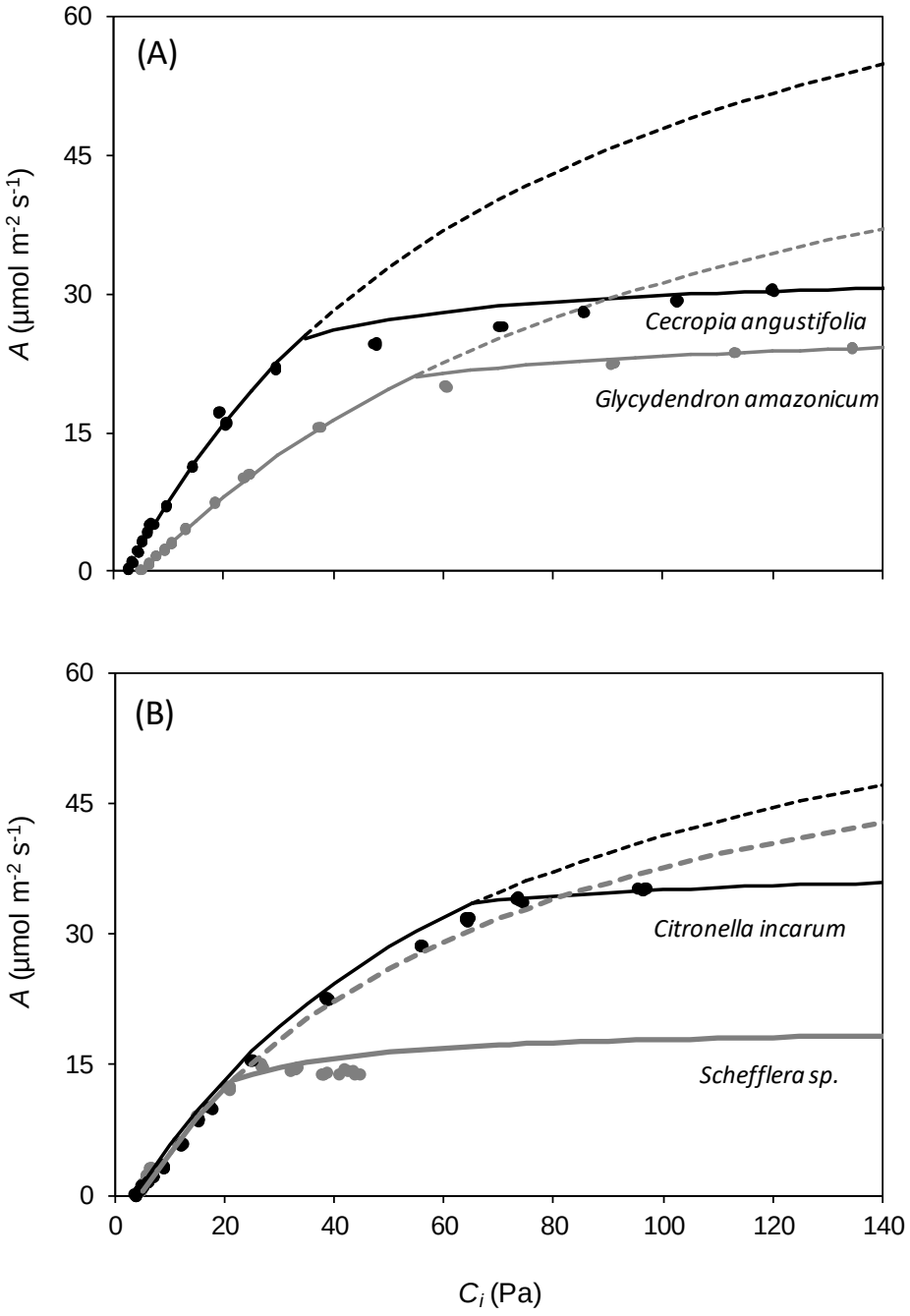

Figure 2.1. Fitted curves of the response of CO_2 assimilation rate, A (area-based) to intercellular CO_2 (C_i) at saturating light for (A) a lowland species *Glycydendron amazonicum* (TAM-09) and an upland species *Cecropia angustifolia* (SPD-01) and (B) two upland species *Citronella incarum* (TRU-03) and *Schefflera* sp. (WAQ-01). Closed circles are the measured rates of assimilation, A. Solid lines correspond to fitted response and dashed lines correspond to estimated response at high C_i. V_{cmax} (maximum Rubisco carboxylation capacity) was calculated from the curvature of dashed line and J_{max} (maximum electron transport rate) were calculated from the points where A saturated. Individual leaf was measured at varying temperature close to growth temperature, therefore V_{cmax} and J_{max} were then normalised to 25°C. CO_2 was not always saturating for most upland measurement due to low partial pressure and/or phosphate limitation.

Finally, rates of *A* obtained at ambient CO_2 concentrations of 400 and 2000 µmol mol^{-1} (A_{400} and A_{2000}, respectively) were extracted from the $A \leftrightarrow C_i$ curves and reported separately.

As atmospheric CO_2 was not always saturating for measurements of upland species (due to low atmospheric partial pressure, resulting in insufficient CO_2-saturated rates of *A* to enable calculate J_{max}), it was likely that J_{max} may have been underestimated in some cases; where this was likely the case (i.e. where there was no clear plateauing of *A* at high C_i values), we excluded the resultant J_{max} values from the Andean data set. With the exception of a few cases (e.g. *Schefflera* sp.; Fig. 2.1), $A \leftrightarrow C_i$ curves typically flattened out at high C_i values (> 90% of curves), with *A* increasing slightly as C_i values increased further (see Fig. 2.1), suggesting that feedback inhibition of *A* through limitations in triose-phosphate utilization (TPU) was unlikely. A check on data quality as used elsewhere (Kattge *et al.*, 2009; Domingues *et al.*, 2010; van de Weg *et al.*, 2012) was applied, where rates of A_N less than 2 µmol CO_2 g N^{-1} s^{-1} were excluded from analysis (52 out of a total of 353 measurements).

2.2.3 Leaf structure and chemistry determination

Leaves were collected immediately following the gas exchange measurements. Initially, the leaf mid rib was removed; thereafter, a digital photograph was taken using a high resolution scanner (CanoScan LiDE 210, Canon, Hanoi, Vietnam) and later analysed for leaf area (Image J, version 1.38x, NIH, USA). Leaves were then placed in an oven at 70 °C for at least two days, the dry mass measured and leaf mass per unit leaf area (M_a) calculated. Total leaf N and P concentrations in dried leaves were extracted using Kjeldahl acid digest method, as detailed in Ayub *et al.* (2011).

2.2.4 Chlorophyll and Rubisco measurements

Leaf discs from mature leaves adjacent to the gas exchange leaf were collected and transferred to -80 °C cryogenic field container for subsequent chlorophyll and Rubisco assays in the laboratory.

Chlorophyll content of each set of leaf discs was determined using a dual-beam scanning UV-VIS spectrometer (Lambda 25, Perkin-Elmer, Shelton, CT, USA) after extraction of chlorophyll pigments from two frozen leaf discs (0.77 cm^2 each) with 100% acetone and $MgCO_3$, as outlined in Asner *et al.* (2014b). Chlorophyll a:b ratios

varied between 2.45 and 2.75, which is consistent with results of past studies on tropical trees in the Peruvian Amazon (Asner & Martin, 2011).

Protein was extracted from frozen leaf discs following the method outlined in Gaspar *et al.* (1997) with slight modifications (see Appendix 1 for details on optimization of protein assays). Frozen samples of 0.50 cm^2 were ground in Eppendorf tubes and washed consecutively in 100% methanol, hexane and acetone. Treated leaf powder was then resuspended in protein extraction buffer (140 mM Tris base, 105 mM Tris–HCl, 0.5 mM ethylenediaminetetraacetic acid, 2% lithium dodecyl sulfate (LDS), 10% glycerol) containing 5 mM DTT and protease inhibitor cocktail (Sigma-Aldrich, Castle Hill, NSW, Australia), heated for 10 min at 100 °C to completely dissolve extracted protein, then clarified by centrifugation (14,000 *x g*; 10 min; room temperature). The supernatant was tested for protein content.

Equivalent volumes of supernatant were diluted in 4 × SDS-PAGE sample buffer (Invitrogen - Life Technologies, Carlsbad, CA, USA) then loaded onto gels. Since we extracted protein from a known amount of leaf area, we were able to analyse our samples on an equivalent leaf area basis. Rubisco purified from tobacco with varying concentrations was also loaded onto gels, serving as a calibration series. Proteins were run on 4-12% NuPAGE Bis-Tris gels (Invitrogen - Life Technologies, Carlsbad, CA, USA) according to the manufacturer's instructions and transferred to Immobilon-P PVDF membranes (Merck Millipore, Kilsyth, Vic., Australia) using an XCell II Blot module (Invitrogen). Membranes were blocked with 5% skim milk powder in Tris-buffered saline containing 0.5% Tween-20 (TBS-T) and an antibody raised in rabbits against tobacco Rubisco (used at 1:5,000) prepared by Spencer Whitney (Research School of Biology, Australian National University, Canberra). Secondary antibody (goat-anti-rabbit-alkaline phosphatase conjugate, Agrisera, Vannas, Sweden) was diluted 1:5,000. Blots were visualized using Attophos AP fluorescent substrate system (Promega, Madison, WI, USA) and imaged using a Versa-Doc (Bio-Rad, Hercules, CA, USA) imaging system. Blots were analysed using Quantity One software (Bio-Rad) and relative band densities of each protein determined from duplicate samples, and data averaged. Rubisco concentration was calculated from the large subunit (molecular mass of 55 kD and 16% N by weight).

2.2.5 Estimation of N allocation in photosynthetic metabolism

N allocation in three major components (pigment-protein complexes, electron transport and Rubisco) for all leaves was estimated from chlorophyll concentration, V_{cmax} and J_{max} respectively. N allocation to pigment-protein complexes (n_P) was calculated by assuming 44 mol N per mol of chlorophyll (Evans, 1989). N allocation to Rubisco (n_R) was estimated from values of V_{cmax} according to Harrison *et al.* (2009), with slight modification [2.33 mol CO_2 (mol Rubisco sites)$^{-1}$ s^{-1} for the catalytic turnover number of Rubisco at 25 °C (Harrison *et al.*, 2009)]. We here assumed all Rubisco was fully activated and mesophyll conductance was infinite. The allocation of N to electron transport components (n_E) was calculated from J_{max} assuming 160 mol electrons (mol cytochrome *f*)$^{-1}$ s^{-1} and 8.85 mol N (mmol cytochrome *f*)$^{-1}$ (Evans & Seemann, 1989). The proportion of total leaf N allocated to each photosynthetic component was calculated by dividing the N investment in each component by the total N content per unit leaf area.

2.2.6 Data analysis

Log_{10} transformations were carried out on leaf trait values when necessary to ensure normality and minimize heterogeneity of residuals. Student *T*-tests (two-tailed) were used to compare overall means of lowland and upland species. Standardized major axis (SMA) estimation was used to describe the best-fit relationship between pairs of variables and to assess whether relationships differed between lowland vs upland elevation classes, using SMATR Version 2.0 software (Falster *et al.*, 2006; Warton *et al.*, 2006). The decision to compare upland and lowland trait relationships reflects the strong elevation contrast in environments, phylogeny, floristic composition and forest structure (Gentry, 1988; van de Weg *et al.*, 2009; Asner *et al.*, 2014b). Significance of SMA regression was tested at $\alpha = 0.05$.

In addition to the above bivariate analyses, we also used a mixed-effects linear model combining fixed and random components (Pinheiro & Bates, 2000) to account for variability in area- and N-based rates of V_{cmax}, and area-based rates of J_{max}. This approach enabled the structured nature of the data set to be recognized, and for interactions between multiple terms to be considered. The model's fixed effect included continuous explanatory variables only: leaf traits (M_a, area-based leaf N and P), and environment variables [soil P and N concentration, mean annual temperature (MAT) and effective cation exchange capacity of soil (ECEC)]. Model specification and

validation was based on the protocols outlined in Zuur *et al*. (2009) and fitted using the *nlme* package (R package ver. 3.1–105, R Foundation for Statistical Computing, Vienna, Austria, R Development Core Team 2011). Phylogeny (family/genus/species) were treated as a nested random effect, placing focus on the variation contained within these terms, rather than mean values for each level. Site variation was captured by soil and environmental factors considered in the model's fixed component; because of this, no site term was included in the random component. Model comparisons and the significance of fixed-effects terms were assessed using Akaike's information criterion (AIC). Unless otherwise stated, statistical analysis was performed using SPSS version 20 (IBM Corporation, Armonk, NY, USA).

2.3 Results

2.3.1 Variations in leaf chemistry and structure

Among lowland sites, there was a six-fold variation in leaf N:P ratios (7.6 - 45.9) but for upland sites, when ranked according to increasing elevation, mean values of leaf N:P were largely consistent across sites of similar elevation (Table 2.1). Across all sites (lowland and upland combined), variations in leaf N:P ratios were predominantly driven by variations in leaf [P] (r^2=0.59, p<0.01; Appendix 2 - Table A2.1) rather than leaf [N]. Variations in area-based leaf [P] (P_a) were positively correlated with soil [P] (r^2=0.37, p<0.01) and elevation (r^2=0.48, p<0.01). Weaker positive associations were observed for area-based leaf [N] (N_a) with total soil [N] (r^2=0.10, p<0.01) and elevation (r^2=0.14, p<0.01).

Leaf mass per unit leaf area (M_a) varied widely, both among and within lowland (54-230 g m^{-2}) and upland (60-249 g m^{-2}) sites (Table 2.1). Although variations in M_a were not correlated with variations in soil [P], there were significant (but weak) correlations between M_a and total soil [N] (r^2=0.04, p<0.01) and elevation (r^2=0.03, p<0.01). Overall means of M_a for the sampled upland species (143±39 g m^{-2}) were significantly higher than that of the lowland species (132±35 g m^{-2}, p<0.05; Table 2.2).

Across all 18 sites, leaf N_a was positively correlated with M_a (p<0.01, r^2=0.12), with the $N_a \leftrightarrow M_a$ relationship being stronger among upland than lowland sites (r^2=0.07 for lowland sites and r^2=0.20 for upland; see Table A2.2 for p-values, slopes and intercepts of each SMA relationship). The slope and intercept of the relationship

differed between the two elevation classes (Fig. 2.2A) - upland species exhibited higher N_a for a given M_a than lowland species, particularly in low M_a species. Across all sites, leaf P_a exhibited a weak, positive correlation with M_a (p<0.01, r^2=0.04). Similarly, a weak positive $P_a \leftrightarrow M_a$ relationship (p=0.003, r^2=0.04) was found among upland species (Fig 2.2B). Although no significant $P_a \leftrightarrow M_a$ relationship was found among lowland species (with leaf P_a varying 20-fold), mean values of P_a at a given M_a were lower than their upland counterparts.

2.3.2 Variations in photosynthetic metabolism

Light-saturated rates of photosynthesis per unit leaf area, measured at the prevailing day-time air temperature (T) at each site and at an atmospheric CO_2 concentration of 400 µmol mol^{-1} ($A_{400,a}$), differed among co-occurring species. However, there was no significant difference between mean values of $A_{400,a}$ from lowland and upland classes (8.2 ± 3.9 and 7.6 ± 3.6 µmol m^{-2} s^{-1}, respectively). This uniformity of $A_{400,a}$ occurred despite significantly lower measuring Ts at the high elevation sites [overall means: lowland 29.4 ± 0.9°C; upland 25.7 ± 2.1°C, p<0.05] and lower intercellular CO_2 partial pressure (C_i) (overall means: lowland 28.4 ± 3.7 Pa; upland 18.8 ± 3.0 Pa, p<0.05). Assessed on a per unit leaf N basis ($A_{400,N}$), average rates were lower at the upland sites compared to their lowland counterparts (3.4 ± 1.7 and 4.3 ± 2.2 µmol CO_2 gN^{-1} s^{-1}, respectively, p<0.05; Table 2.2), reflecting higher leaf N_a for trees at high elevation (Table 2.1). Across sites, mean $A_{400,N}$ decreased with decreasing mean annual temperature (MAT) (Fig. 2.3D). Area-based rates of photosynthesis at elevated CO_2 ($A_{2000,a}$) were higher in upland (17.1-26.5 µmol m^{-2} s^{-1}) than lowland (16.1-22.6 µmol m^{-2} s^{-1}) species (p<0.05). The higher values of $A_{2000,a}$ at the upland sites were achieved despite the colder temperatures. On a per unit leaf N basis ($A_{2000,N}$), average rates were similar for both elevation classifications (Fig. 2.3E).

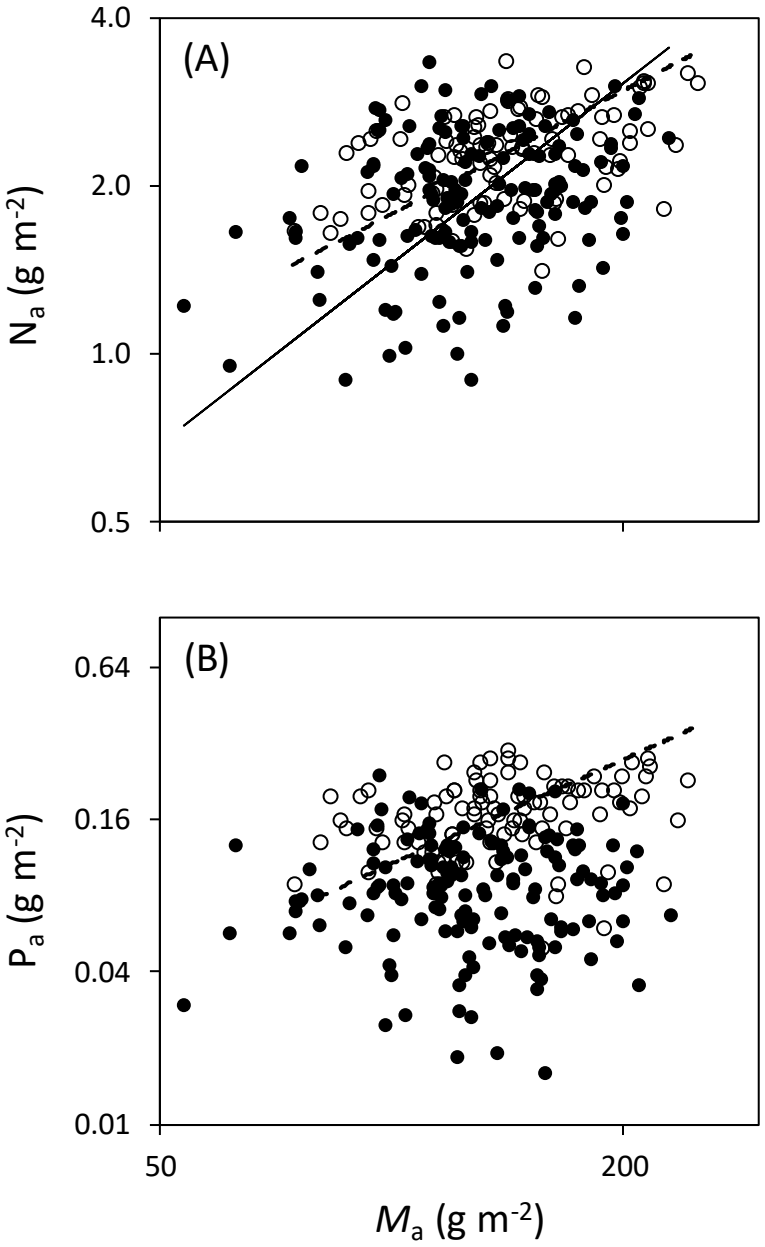

Figure 2.2. Log-log plots of (A) leaf N-area, N_a and (B) leaf P-area, P_a in relation to leaf mass per unit leaf area, M_a. Data points represent individual leaf values (149 lowland species and 97 upland species). Standardized major axis (SMA) tests for common slopes revealed significant differences when comparing $N_a \leftrightarrow M_a$ and $P_a \leftrightarrow M_a$ relationship between lowland and upland species. Symbols: closed symbols, lowland species; open symbols, upland species. SMA regressions: solid line, lowland species; dashed line, upland species. SMA regressions are given only when the relationships are significant ($p<0.05$), refer to Table A2.2.

Table 2.2. Mean values and standard deviation of leaf traits for upland and lowland species.

Leaf Traits	Leaf N_a (g m^{-2})	Leaf P_a (g m^{-2})	Leaf N:P	M_a (g m^{-2})	$A_{400,a}$ (µmol m^{-2} s^{-1})	g_s (mol m^{-2} s^{-1})	$A_{400,N}$ (µmol CO_2 gN^{-1} s^{-1})	$V_{cmax,a}^{25}$ (µmol m^{-2} s^{-1})	$J_{max,a}^{25}$ (µmol m^{-2} s^{-1})	$J_{max,a}^{25}$:$V_{cmax,a}^{25}$	$V_{cmax,N}^{25}$ (µmol CO_2 gN^{-1} s^{-1})
Lowland species	1.96 ± 0.52 [a]	0.09 ± 0.05 [a]	22.2 ± 8.6 [a]	132 ± 35 [a]	8.2 ± 3.9 [a]	0.2 ± 0.1 [a]	4.3 ± 2.2 [a]	35.9 ± 14.6 [a]	66.7 ± 18.6 [a]	1.86 ± 0.40 [a]	18.9 ± 8.1 [a]
Upland species	2.31 ± 0.44 [b]	0.18 ± 0.06 [b]	13.5 ± 3.6 [b]	143 ± 39 [b]	7.6 ± 3.6 [a]	0.1 ± 0.1 [b]	3.4 ± 1.7 [b]	48.8 ± 20.0 [b]	96.9 ± 36.9 [b]	1.92 ± 0.36 [a]	22.5 ± 9.4 [b]

Values expressed on area basis. Abbreviation: leaf N_a = leaf nitrogen, leaf P_a = leaf phosphorus, leaf N:P = leaf nitrogen to phosphorus ratio, M_a = leaf mass per unit leaf area, $A_{400,a}$ = area-based light-saturated net photosynthesis measured at 400 µmol mol^{-1} atmospheric [CO_2], g_s = stomatal conductance to CO_2, $A_{400,N}$ = area-based light-saturated net photosynthesis measured at 400 µmol mol^{-1} atmospheric [CO_2] per unit leaf nitrogen, $V_{cmax,a}^{25}$ = maximum carboxylation velocity of Rubisco normalised to 25°C, $J_{max,a}^{25}$ = maximum rate of electron transport normalised to 25°C, $J_{max,a}^{25}$:$V_{cmax,a}^{25}$ = ratio of maximum Rubisco carboxylation velocity over maximum rate of electron transport, both normalised to 25°C, $V_{cmax,N}^{25}$ = ratio of maximum carboxylation velocity of Rubisco normalised to 25°C per unit leaf nitrogen.

Values are overall mean ± SD of leaf traits for lowland and upland sites. Significantly different means are indicated by different letters (p<0.05).

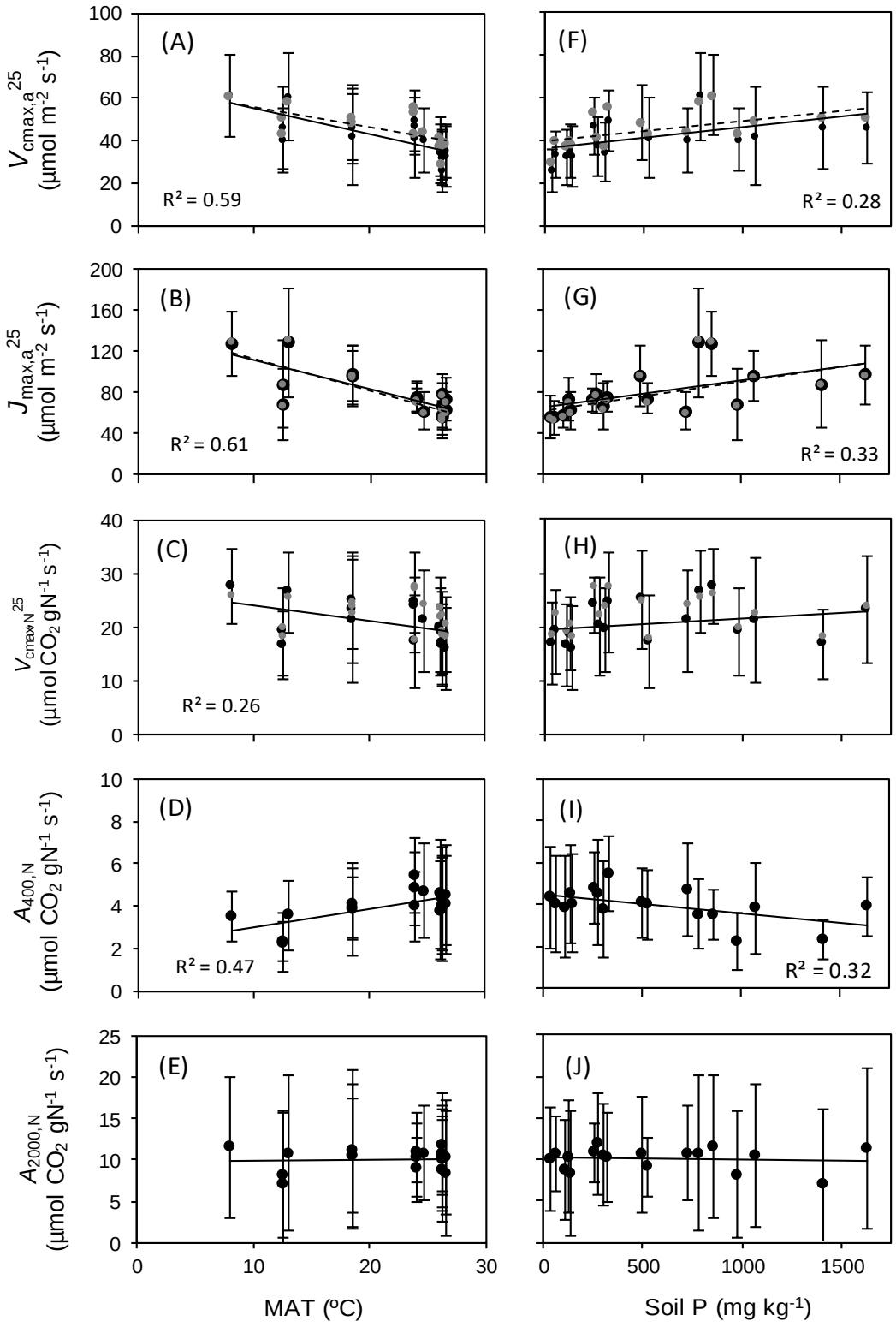

Figure 2.3. Plots of maximum carboxylation velocity of Rubisco normalised to 25°C, $V_{cmax,a}^{25}$ against (A) mean annual temperature (MAT) and (F) soil P concentration; maximum rate of electron transport normalised to 25°C, $J_{max,a}^{25}$ against (B) MAT and (G) soil P; ratio of $V_{cmax,a}^{25}$ over leaf N, $V_{cmax,N}^{25}$ against (C) MAT and (H) soil P; ratio of light-saturated net photosynthesis measured at 400 µmol mol $^{-1}$ atmospheric [CO_2] over leaf N, A_{400}:N against (D) MAT and (I) soil P; and ratio of light-saturated net photosynthesis measured at 2000 µmol mol $^{-1}$ atmospheric [CO_2] over leaf N, A_{2000}:N against (E) MAT and (J) soil P for each site. In (A)-(H), black circles (and solid regression lines) represent photosynthetic parameters calculated using constants of Farquhar *et al.* (1980) and grey circles (and dashed regression lines) represent parameters calculated using Bernacchi *et al.* constants (2002). R^2 values shown are for Farquhar *et al.* (1980) only regressions. Error bars represent standard deviation of mean for each site. Environmental parameters at each site were obtained using site information from Quesada (*et al.* 2010; pers. comm. 2014) and Asner *et al.* (2014a).

To explore differences in rates of the underlying components of net photosynthesis, we compared maximal area-based rates of CO_2 fixation by Rubisco ($V_{cmax,a}$) and photosynthetic electron transport ($J_{max,a}$), using values normalized to a measuring temperature of 25 °C (i.e. $V_{cmax,a}^{25}$ and $J_{max,a}^{25}$). Site mean values of $V_{cmax,a}^{25}$ and $J_{max,a}^{25}$ were significantly higher in the upland class ($V_{cmax,a}^{25}$ and $J_{max,a}^{25}$ were 36 and 45% higher, respectively, in the upland class; Table 2.2; $p<0.05$), reflecting the parameters' negative relationships with MAT (Fig. 2.3A, B). Similarly, the mean $V_{cmax,N}$ at 25 °C ($V_{cmax,N}^{25}$) of the upland group was greater than that of lowland counterparts (Table 2.2; $p<0.05$). Thus, when assessed at a common T and when controlling for elevation differences in C_i (by adopting V_{cmax}), photosynthetic N use efficiency was, on average, greater at high elevations. Importantly, considerable within-site variability was observed for all three parameters ($V_{cmax,a}^{25}$, $J_{max,a}^{25}$, and $V_{cmax,N}^{25}$) (Fig. 2.4), highlighting the heterogeneity of these key photosynthetic traits among trees within each site. Within-site variability was particularly pronounced at the upland sites (Fig. 2.4).

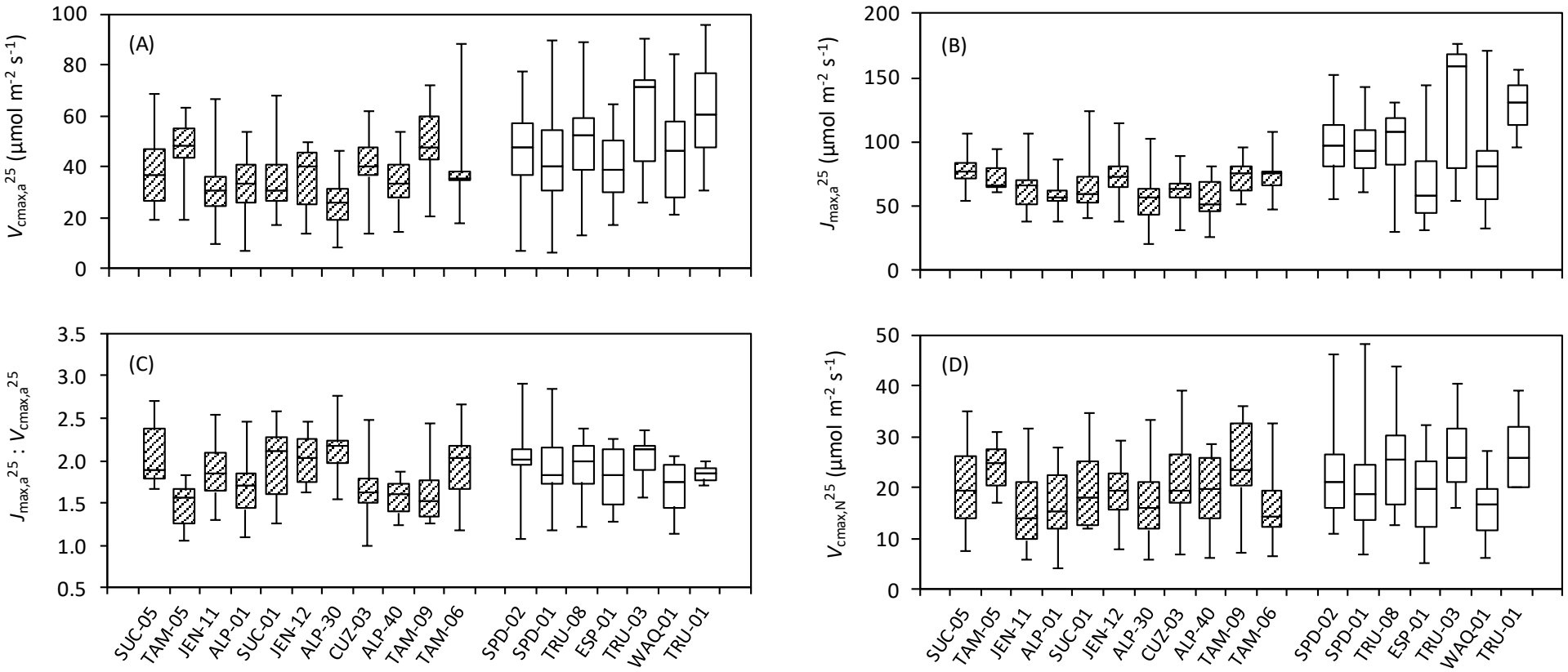

Figure 2.4. Box and whisker plots of (A) maximum carboxylation velocity of Rubisco normalised to 25°C, $V_{cmax,a}^{25}$, (B) maximum rate of electron transport normalised to 25°C, $J_{max,a}^{25}$, (C) $J_{max,25}$:$V_{cmax,25}$ ratio, and (D) ratio of $V_{cmax,a}^{25}$ over leaf N, $V_{cmax,N}^{25}$ for each site. Values expressed on area basis. Sites are arranged according to decreasing leaf N:P for lowland and increasing elevation for upland sites. The upper and the lower edges of each box indicate the 75th and 25th percentiles, respectively. The horizontal line within each box is the median and the vertical bars indicate the 10th to the 90th percentile ranges.

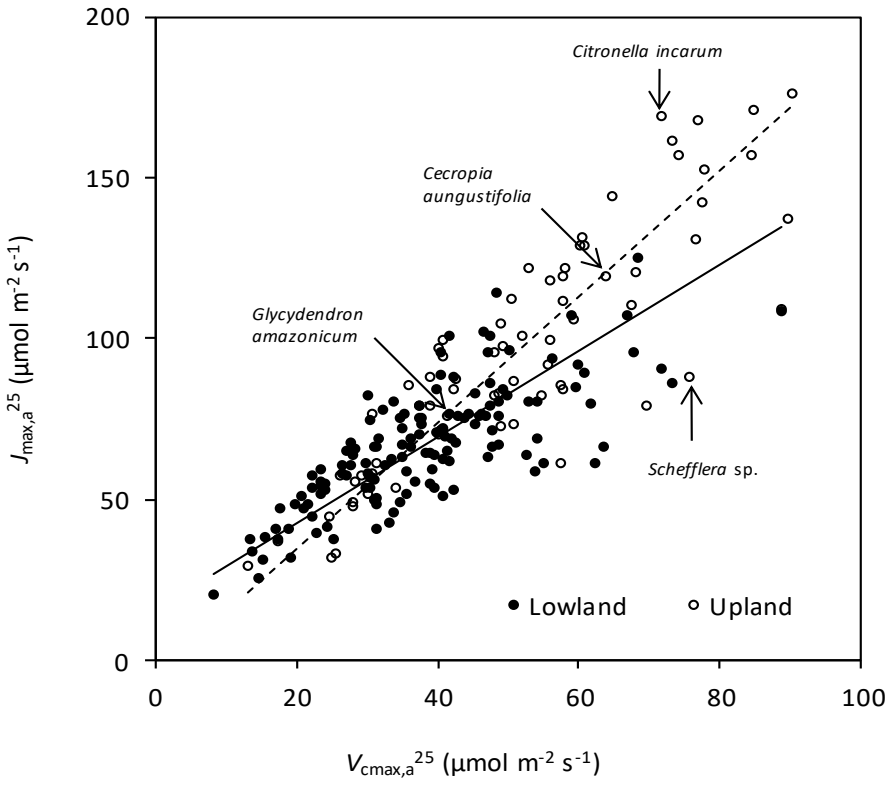

Figure 2.5. Plot of maximum carboxylation velocity of Rubisco normalised to 25°C ($V_{cmax,a}^{25}$) against maximum rate of electron transport normalised to 25°C ($J_{max,a}^{25}$). Data points represent individual leaf values (138 lowland species and 69 upland species). Arrows correspond to the four species depicted in the $A \leftrightarrow C_i$ curves in Fig. 2.1. Symbols: closed symbols, lowland species; open symbols, upland species. Solid line, lowland species; dashed line, upland species.

Variations in $J_{max,a}^{25}$ were strongly correlated with $V_{cmax,a}^{25}$, both for lowland (r^2=0.59) and upland classifications (r^2=0.75) (Fig. 2.5). Overall, the $J_{max,a}^{25} \leftrightarrow V_{cmax,a}^{25}$relationship was similar in the two elevation groups, with mean $J_{max,a}^{25}$:$V_{cmax,a}^{25}$ ratios being statistically equivalent in lowland and upland classes (Table 2.2). Importantly, marked differences in $J_{max,a}^{25}$:$V_{cmax,a}^{25}$ ratios were observed among individuals (Figs 2.4 and 2.5), underpinned by fundamental differences in the CO_2 response of net photosynthesis (e.g. Fig. 2.1B). In most leaves, $J_{max,a}^{25}$ and $V_{cmax,a}^{25}$ co-varied, resulting in relatively constant $J_{max,a}^{25}$:$V_{cmax,25}$ ratios, as illustrated by data from individual plants of *Cecropia angustifolia* and *Glycydendron amazonicum* where the $J_{max,a}^{25}$:$V_{cmax,a}^{25}$ ratio was 1.8 (Fig. 2.1A and Fig. 2.5). However, some leaves exhibited high $V_{cmax,a}^{25}$ but low $J_{max,a}^{25}$ (Fig. 2.1B; individual of *Schefflera* sp., where $J_{max,a}^{25}$: $V_{cmax,a}^{25}$ = 1.1) while other leaves with a similar $V_{cmax,a}^{25}$ had markedly higher $J_{max,a}^{25}$ (e.g. the *Citronella incarum* individual in Fig. 2.1B) leading to a higher $J_{max,a}^{25}$:$V_{cmax,a}^{25}$value (2.4). Such variations in $J_{max,a}^{25}$ and $V_{cmax,a}^{25}$ likely reflect intra- and/or inter-specific variations in relative allocation of N allocation to Rubisco versus electron transport/bioenergetics.

2.3.3 Bivariate relationships

Across all 18 sites, $V_{cmax,a}^{25}$ and $J_{max,a}^{25}$ exhibited positive correlations with soil P, soil N and elevation, and negative correlations with MAT (Table A2.1); the strength of these relationships was greater for $J_{max,a}^{25}$ than $V_{cmax,a}^{25}$. Relationships with MAP were either weak ($J_{max,a}^{25}$) and not significant ($V_{cmax,a}^{25}$) (Table A2.1). Across all sites, variations in $V_{cmax,a}^{25}$ and $J_{max,a}^{25}$ were also correlated with leaf chemical composition traits (Table A2.1), with bivariate relationships being stronger with P_a ($p<0.01$, $r^2= 0.11$ for $V_{cmax,a}^{25}$, $r^2= 0.13$ for $J_{max,a}^{25}$) than N_a ($p<0.01$, $r^2= 0.05$ for both $V_{cmax,a}^{25}$ and $J_{max,a}^{25}$). Leaf N:P ratios exhibited weak, negative correlations with $V_{cmax,a}^{25}$ and $J_{max,a}^{25}$ ($p<0.01$, $r^2= 0.08$ for $V_{cmax,a}^{25}$, $r^2= 0.06$ for $J_{max,a}^{25}$).No significant relationship was found between $V_{cmax,a}^{25}$ and M_a, whereas the $J_{max,a}^{25} \leftrightarrow M_a$ relationship was significant ($p<0.05$, $r^2= 0.04$).

When assessed among upland sites, no significant relationships were found between $V_{cmax,a}^{25}$, M_a, N_a, P_a or N:P ratio (Fig. 2.6A-D). For lowland sites, $V_{cmax,a}^{25}$ was positively related with P_a ($p=0.013$, $r^2= 0.04$) and N_a ($p=0.050$, $r^2=0.02$), but not leaf N:P ratio or M_a (Fig 2.6A-D). The absence of a N:P effect for upland or lowland classes was consistent with SMA analyses comparing the slopes of $V_{cmax,a}^{25} \leftrightarrow N_a$, $V_{cmax,a}^{25} \leftrightarrow P_a$ and $V_{cmax,a}^{25} \leftrightarrow M_a$ for the lowland class, split according to leaf N:P ratios below and above 20 - this ratio generally being thought indicative of the N:P above which physiological processes are more likely to be limited by P as opposed to N (and vice versa) (Güsewell, 2004). No significant difference in slopes of the relationships were found ($p>0.05$, data not shown). Similar patterns were observed for $J_{max,a}^{25}$ (Fig. 2.6E-H), which was positively related with N_a ($p=0.012$, $r^2=0.05$) and P_a ($p=0.002$, $r^2= 0.08$) for the lowland class only.

Investigating whether variations in photosynthetic N use efficiency were related to M_a, both across all sites (Table A2.1) and within each elevation class (Fig. 2.7A), there was no significant $V_{cmax,N}^{25} \leftrightarrow M_a$ relationship across all 18 sites (Table A2.1) or within the upland elevation class (Table A2.2). Nevertheless, for the lowland class, a weak negative $V_{cmax,N}^{25} \leftrightarrow M_a$ relationship was observed ($p=0.01$). On average, $V_{cmax,N}^{25}$ at a given M_a was higher in upland species than their lowland counterparts. With respect to foliar phosphorus, there was no significant relationship between $V_{cmax,N}^{25}$ and leaf P_a or with leaf N:P when considering the elevation classes separately. This conclusion was held for $V_{cmax,N}^{25} \leftrightarrow P_a$ when combining upland and lowland data (Table A2.1).

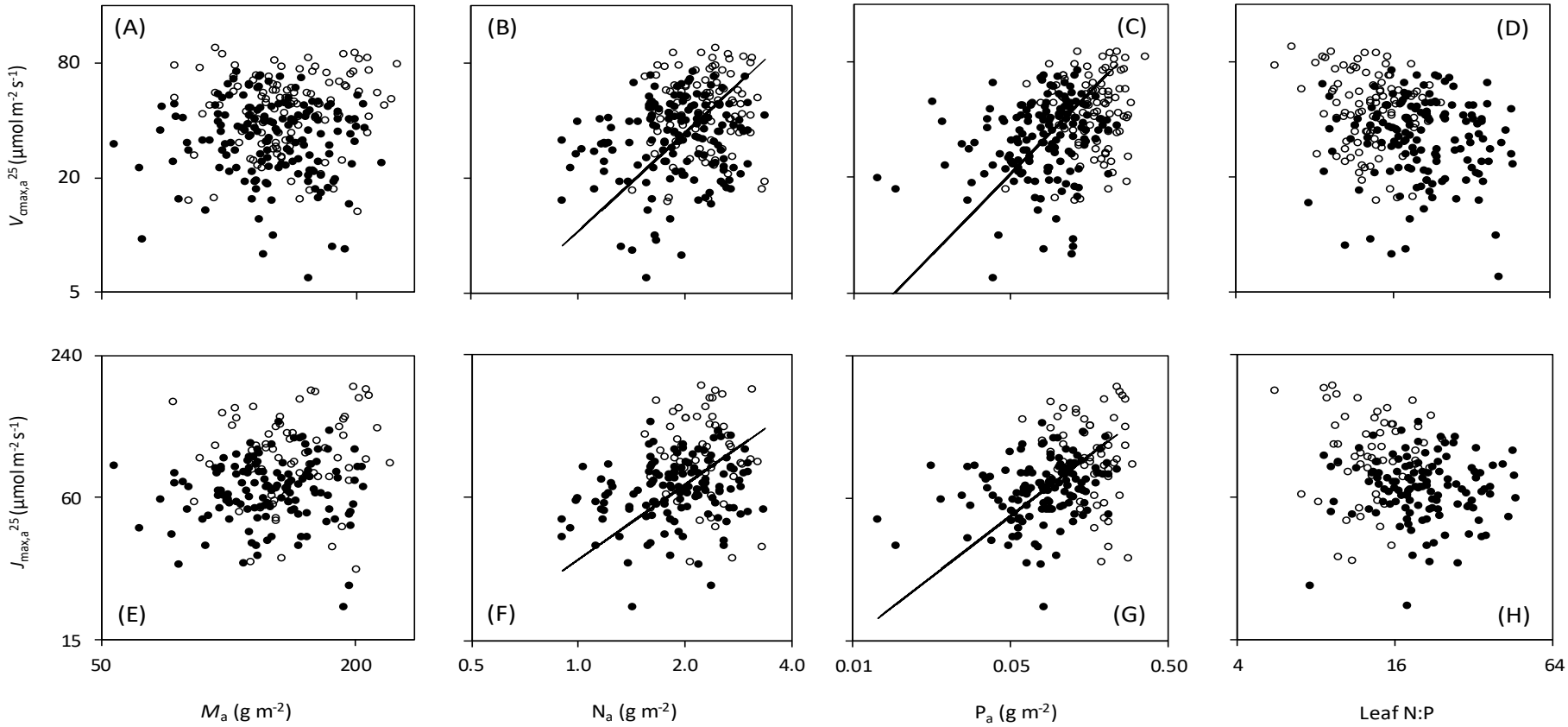

Figure 2.6. Top panel shows log-log plots of maximum carboxylation velocity of Rubisco normalised to 25°C ($V_{cmax,a}^{25}$) in relation to (A) leaf mass per unit leaf area, M_a, (B) leaf N-area, N_a, (C) leaf P-area, P_a and (D) leaf N:P. Data points represent individual leaf values (150 lowland species and 95 upland species). SMA tests for common slopes revealed significant difference when comparing $V_{cmax,a}^{25} \leftrightarrow N_a$, $V_{cmax,a}^{25} \leftrightarrow P_a$ and $V_{cmax,a}^{25} \leftrightarrow$leaf N:P relationships between lowland and upland species, but no significant difference when comparing slopes of $V_{cmax,a}^{25} \leftrightarrow M_a$ relationships between lowland and upland species. Bottom panel shows log-log plots of maximum rate of electron transport normalised to 25°C ($J_{max,a}^{25}$) in relation to (E) leaf mass per unit leaf area, M_a, (F) leaf N-area, N_a, (G) leaf P-area, P_a and (H) leaf N:P. Data points represent individual leaf values (127 lowland species and 58 upland species). SMA tests for common slopes revealed significant difference when comparing $J_{max,a}^{25}$ and leaf traits relationships between lowland and upland species. Symbols: closed symbols, lowland species; open symbols, upland species. SMA regressions are given only when the relationships are significant (p<0.05), refer to Table A2.2.

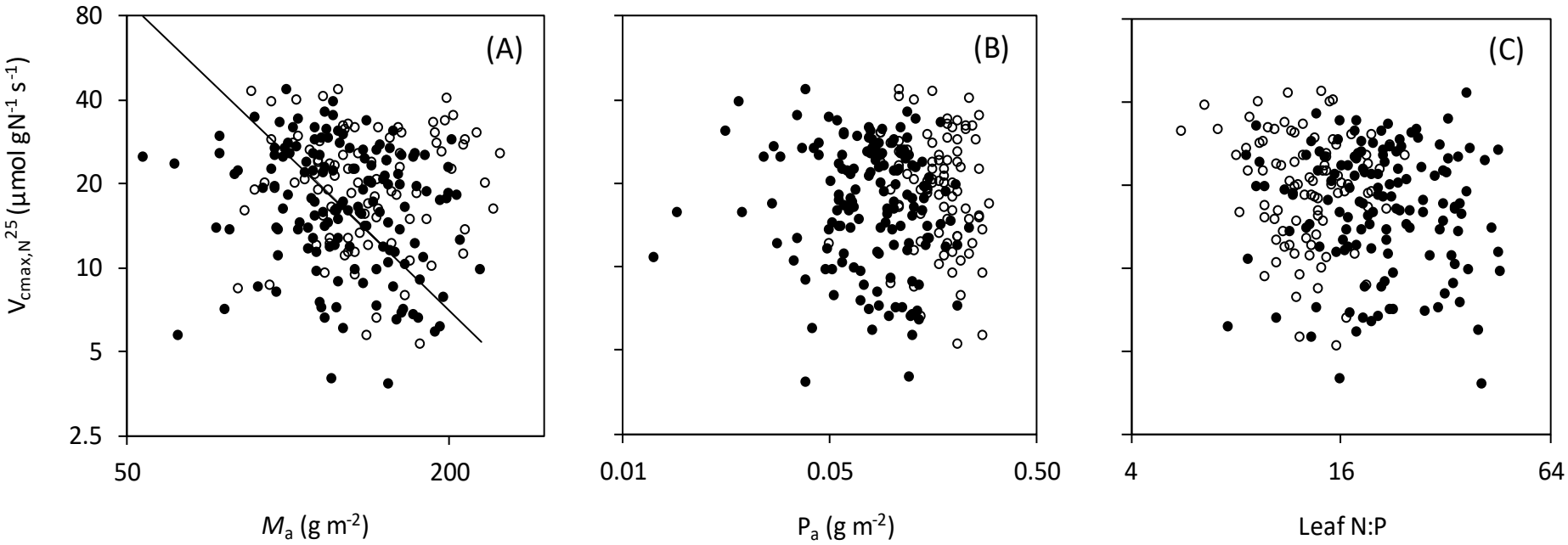

Figure 2.7. Log-log plots of ratio of $V_{cmax,a}^{25}$ to leaf N ($V_{cmax,N}^{25}$) in relation to (A) leaf mass per unit leaf area, M_a, (B) leaf P-area, P_a and (C) leaf N:P. Data points represent individual leaf values (150 lowland species and 95 upland species). SMA tests for common slopes revealed significant difference only when comparing $V_{cmax,N}^{25} \leftrightarrow P_a$ between lowland and upland species. Symbols: closed symbols, lowland species; open symbols, upland species. SMA regressions are given only when the relationships are significant (p<0.05), refer to Table A2.2.

For $V_{cmax,N}^{25} \leftrightarrow$N:P, combining upland and lowland data resulted in a weak significant relationship ($p<0.05$, $r^2 = 0.02$); similarly, relationships between $V_{cmax,N}^{25}$ and soil P, soil N and elevation were relatively weak (Table A2.1). Collectively, these results show that the proportion of the variance in $V_{cmax,N}^{25}$ accounted for by the above soil and leaf level parameters was negligible.

2.3.4 Variation in N-allocation patterns

To further explore what factors might contribute to variations in $V_{cmax,N}^{25}$, we calculated the fraction of leaf N allocated to photosynthesis (n_A); n_A is dependent on the allocation of leaf N to Rubisco (n_R), electron transport (n_E) and pigment-protein complexes (n_P). Figure 2.8 shows that mean values of n_A and its underlying components exhibited relatively little variation across sites. Nevertheless, inter-specific variations were evident at each site, with n_R varying up to seven-fold at some sites (e.g. CUZ-03; 0.03-0.20). A large proportion of N was inferred to be allocated in pigment-protein complexes, with n_P being greater than n_R and n_E combined. The overall mean of n_R for the upland class (0.105) was significantly higher than that for the lowland class (0.090, $p<0.05$). Similarly, n_E was higher for upland (0.034) than for lowland groups (0.028, $p<0.05$). There was no difference between the elevation classes in n_P (~0.23). Overall, n_A was similar in the lowland and upland groupings (0.37-0.38).

There was considerable variability in n_A among lowland and upland species (0.1 to 0.6), with significant negative correlations being found with M_a, N_a and P_a for the lowland group (Fig. 2.9; Table A2.3). Similar significant correlations existed for the upland class but with the important caveat that upland species consistently exhibited higher n_A at a given N_a and P_a (Figs. 2.9 and A2.1; Table A2.3). Thus, while mean values of n_A were similar in upland and lowland species, the fraction of leaf N allocated to photosynthesis was greater in upland plants when comparisons were made at common leaf N_a and P_a values.

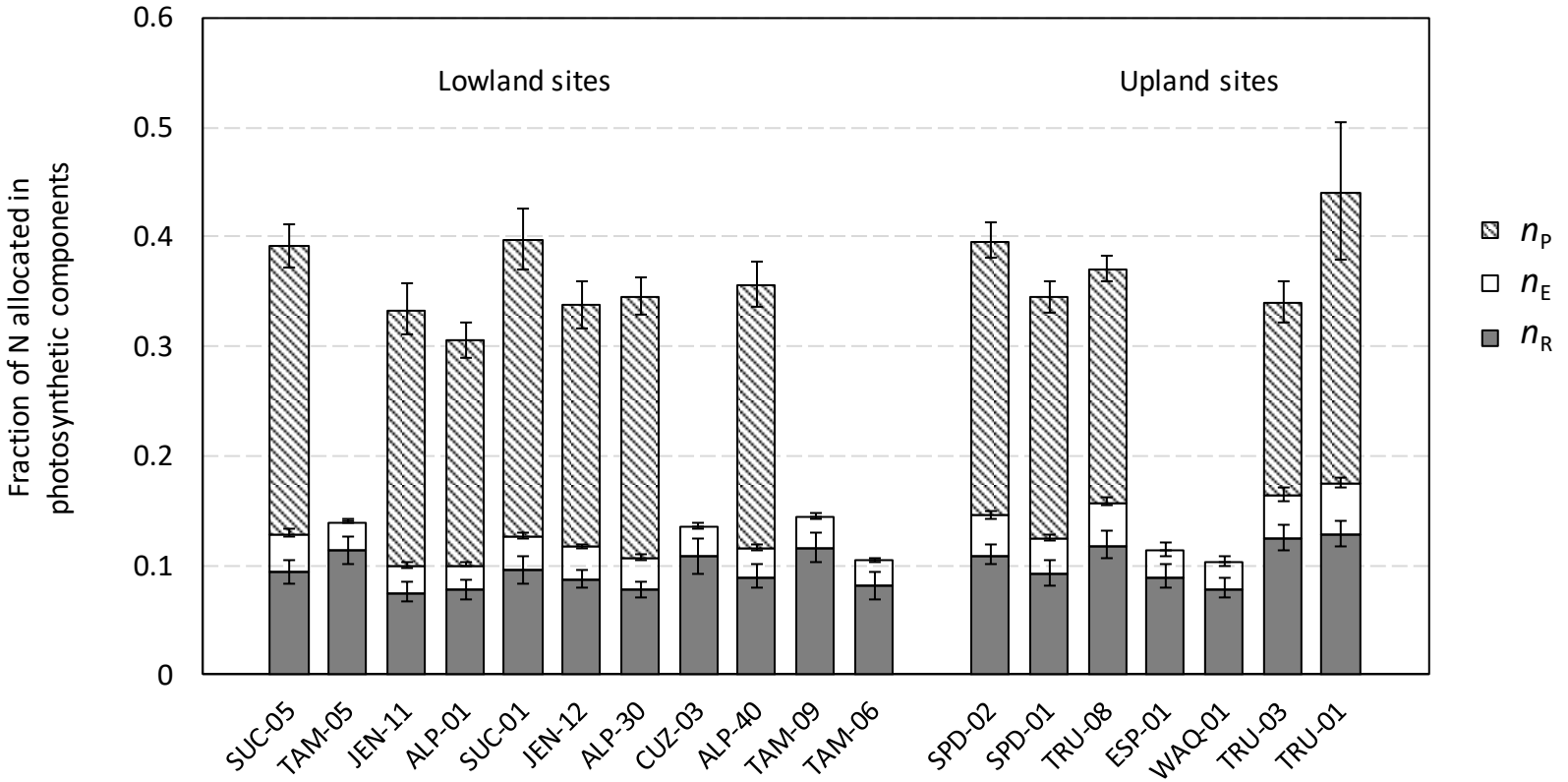

Figure 2.8. Stacked graph shows fraction of leaf N in pigment-protein complexes, n_P; in electron transport, n_E; in Rubisco; n_R, for each sites. n_R was estimated from maximum carboxylation velocity of Rubisco (normalised to 25°C), $V_{cmax,a}^{25}$, n_E estimated from maximum electron transport rate (normalised to 25°C), $J_{max,a}^{25}$; and n_P estimated from chlorophyll concentration. n_P were unavailable for six sites due to thawing of leaf samples. Sites are arranged according to decreasing leaf N:P for lowland and increasing elevation for upland sites. Error bar represent standard error of mean.

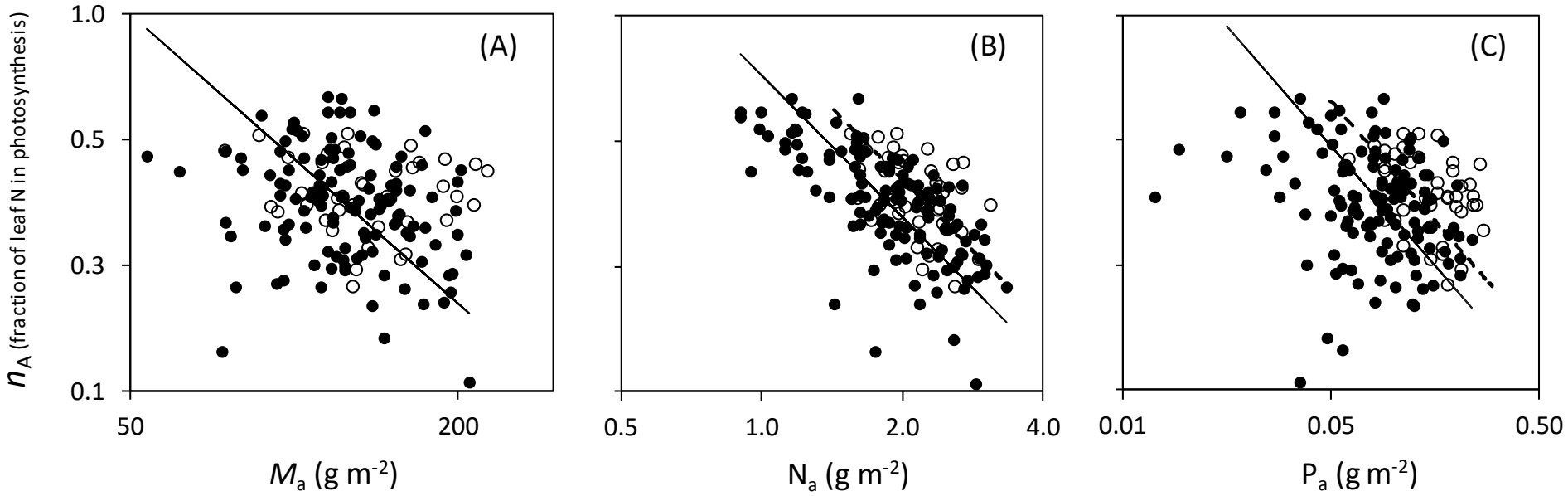

Figure 2.9. Log-log plots of the total fraction of leaf N allocated in photosynthetic metabolism, n_A in relation to (A) leaf mass per unit leaf area, M_a, (B) leaf N-area, N_a, and (C) leaf P-area, P_a. Data points represent individual leaf values (126 lowland species and 40 upland species). SMA tests for common slopes revealed no significant difference when comparing relationships between lowland and upland species, but with the elevation (i.e. y-axis intercept) of the bivariate relationship being higher in upland species than in lowland species. Symbols: closed symbols, lowland species; open symbols, upland species. SMA regressions: solid line, lowland species; dashed line, upland species. SMA regressions are given only when the relationships are significant (p<0.05), refer to Table A2.3.

2.3.5 Validation of Rubisco estimates by in vitro *assays*

We used *in vitro* Rubisco assays on 16 lowland species (Fig. 2.10A) to quantify n_R, thus allowing direct comparison with that of the *in vivo* estimates derived from $V_{cmax,a}^{25}$. Figure 2.10B shows that there was considerable discrepancy between *in vitro* and *in vivo* predicted n_R. If one assumes that the *in vitro* values provide an estimate of potential Rubisco capacity, and that the *in vivo* values are indicative of the realized maximum rate in intact tissues, then it is possible that the *in vivo* approach underestimates the proportion of N allocated in Rubisco. Reliance on the *in vitro* values resulted in marked increases in n_R at a given M_a, albeit with the overall pattern of increasing n_R with decreasing M_a still held (Fig. 2.11A). Considering the overall N investment pattern in photosynthetic metabolism, adopting *in vitro* estimates of n_R resulted in marked increases in the total fraction of N allocated to photosynthesis compared to *in vivo* (Fig. A2.2). Indeed, in some cases *in vitro* estimates of N allocation to Rubisco was similar to, or even higher than, N allocation to pigment protein complexes (Fig. A2.2). Collectively, these results suggest that the answer to the question '*how much leaf N is allocated to photosynthesis'* will depend on whether *in vivo* or *in vitro* estimates of n_R are used in the underlying calculations.

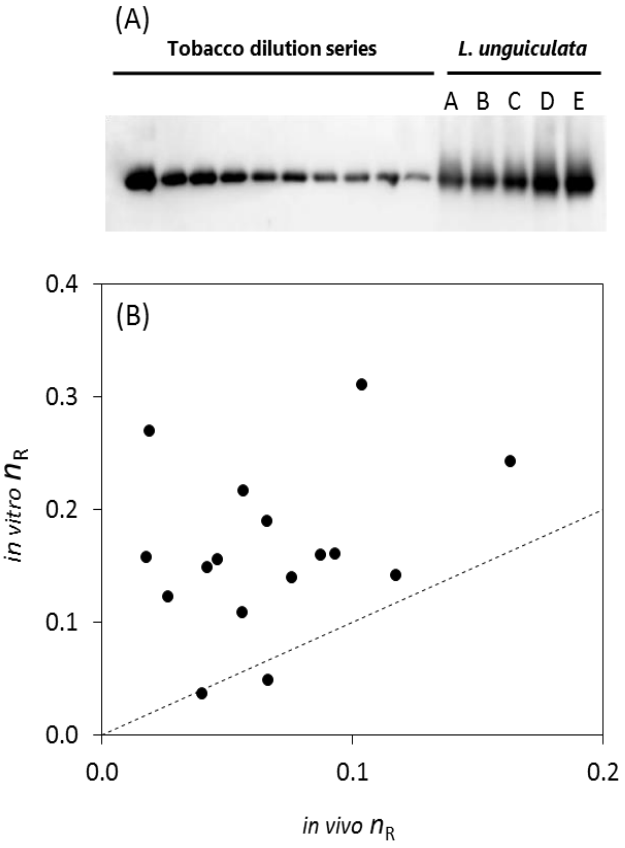

Figure 2.10 (A) SDS-PAGE profile of Rubisco extracted from frozen fresh leaf discs. Individual bands show large subunits of Rubisco. The last five bands on the right side (A-E) correspond to 0.47, 0.54, 0.57, 0.78 and 1.21 g m^{-2} of Rubisco of lowland species (*Licania unguiculata* from *Chrysobalanaceae* family), which then translate to n_R of 0.03, 0.04, 0.04, 0.06, 0.09. In this case, the final value of *in vitro* n_R for *L. unguiculata* was 0.04, as calculated from A - C, since these values fall within the tobacco standard curve. Standard curve was made of a dilution series of tobacco Rubisco. Figure 2.10 (B) *in vitro* n_R estimated from Rubisco western blot assay plotted against *in vivo* n_R derived from maximum carboxylation velocity of Rubisco (normalised to 25°C), $V_{cmax,a}^{25}$. n=16. The dashed line indicates the 1:1 relationship.

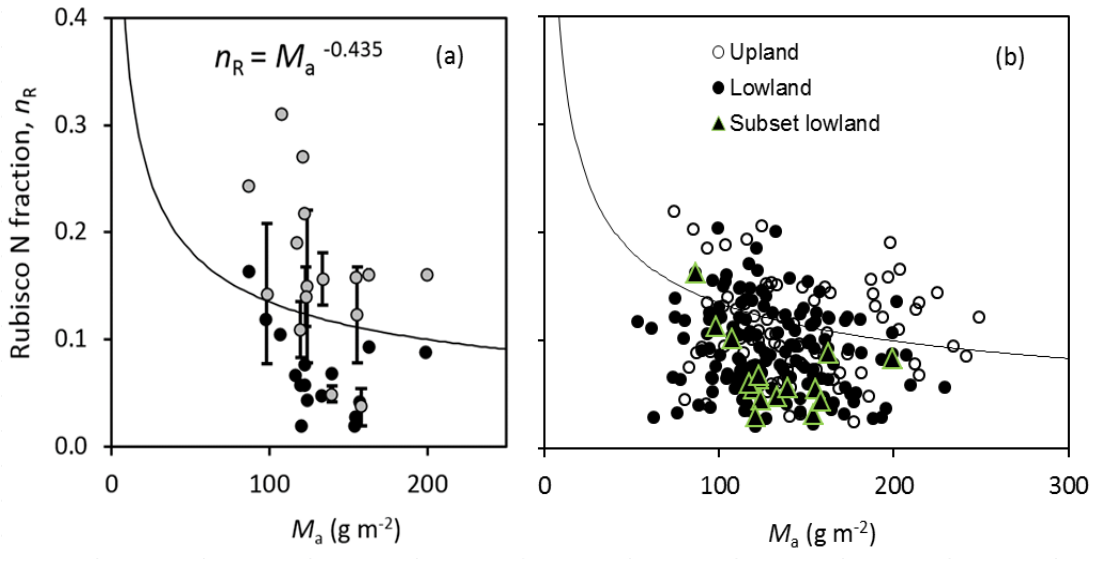

Figure 2.11. Plots of fraction of leaf N allocated in Rubisco, n_R in relation to leaf mass per unit leaf area, M_a, for (A) 16 lowland species for where both *in vivo* and *in vitro* estimates were available; and (B) 150 lowland and 92 upland species for where *in vivo* data was available. Black circles in Fig. 2.11A are *in vivo* n_R derived from maximum carboxylation velocity of Rubisco (normalised to 25°C) (i.e. a subset of those in Fig 2.11B). Grey circles in Fig. 2.11A are *in vitro* n_R derived from Rubisco western blot assay. In both figures, the line shown is inferred from the global relationship between photosynthetic rate per unit leaf N and M_a (Hikosaka, 2004; Wright *et al.*, 2004), the equation $n_R = M_a^{-0.435}$ given in Harrison *et al.* (2009).

2.3.6 Modelling variations in $V_{cmax,a}^{25}$, $J_{max,a}^{25}$ and $V_{cmax,N}^{25}$

We used linear mixed-effects to model variations in $V_{cmax,a}^{25}$, $J_{max,a}^{25}$ and $V_{cmax,N}^{25}$; the starting model included only continuous explanatory terms for leaf traits and environmental variables. Additional details of the model selection procedure are provided in Appendix 2: Table A2.4. When presented with information on soil and leaf P and N as key nutrients driving maximum carboxylation capacity of Rubisco, the final preferred model for $V_{cmax,a}^{25}$ (model 6, Table A2.4) retained P only, suggesting an increase of $V_{cmax,a}^{25}$ as soil and foliar P increase (Table 2.3). A combination of site-level soil P and individual-level foliar P as fixed effects, and family as a random effect, explained 39% of the variation in $V_{cmax,a}^{25}$ (Fig. A2.3). Inclusion of MAT, soil N, leaf N_a, M_a and effective cation exchange capacity of soils as fixed effects did not improve the model performance (Table A2.4). The model's variance components, as defined by the random term, indicated that family accounted for only 2.5% of the unexplained variance (i.e. the response variance not accounted for by the fixed terms) (Table 2.3). Finer phylogenetic detail (genera and species) did not improve the model. A review of diagnostic plots from the final preferred model showed that inclusion of elevation class did not improve model performance, given the prior inclusion of environmental variables that describe the elevation gradient (e.g. soil P, soil N and MAT).

Table 2.3. Output from linear mixed-effects models, with $V_{cmax,a}^{25}$ and $J_{max,a}^{25}$ as the response variables, each showing fixed and random effects.

Final model ($V_{cmax,a}^{25}$)			
Fixed effect	Estimate	S.E	t value
Intercept	41.470	1.578	26.288
log10 (Soil P)	7.909	2.466	3.207
P_a	68.148	22.558	3.021
Random effect		Variance	% of total
Intercept variance: family		45.568	2.49%
Residual error (within family)		1783.626	97.51%
			100.00%
AIC	1645.6		
BIC	1662.0		
-2LL	-817.8		

Final model ($J_{max,a}^{25}$)			
Fixed effect	Estimate	S.E	t value
Intercept	77.217	2.712	28.477
log10 (Soil P)	16.866	4.327	3.898
P_a	94.483	40.245	2.348
Random effect		Variance	% of total
Intercept variance: family		121.3	2.79%
Residual error (within family)		4232.9	97.21%
			100.00%
AIC	1342.4		
BIC	1357.3		
-2LL	-666.2		

$V_{cmax,a}^{25}$= 41.47 + (7.91*log10[SoilP]) + (68.15*P_a)

$J_{max,a}^{25}$ = 77.22 + (16.87*log10[SoilP]) + (94.48*P_a)

Predictive equations for $V_{cmax,a}^{25}$ and $J_{max,a}^{25}$ based on final preferred models are shown at the bottom. For the $V_{cmax,a}^{25}$ and $J_{max,a}^{25}$ model, the fixed component explanatory variables were soil P and leaf P. Parameter estimate, standard error (S.E.) and t-values are given for the explanatory variables. The best predictive models were selected based on a stepwise selection process outlined in Table A2.4. Prior to inclusion in the models, continuous explanatory variables were centred on the population mean. For equations that are not centred on the population mean (i.e. using absolute values), the y-axis intercept values are altered, yielding non-centred equations as follows: $V_{cmax,a}^{25}$= 12.82 + (7.91*log10[SoilP]) + (68.15*P_a); $J_{max,a}^{25}$ = 24.07 + (16.87*log10[SoilP]) + (94.48*P_a).

Similar to $V_{cmax,a}^{25}$, variations in $J_{max,a}^{25}$ were largely accounted for by a combination of site-level soil P and individual-level foliar P, with $J_{max,a}^{25}$ increasing with increasing soil and foliar P (Table 2.3); the final model explained 44% of the variation in $J_{max,a}^{25}$ (Fig. A2.3). The preferred model (determined by assessing the effect of dropping sequentially explanatory variables; Table A2.4) did not retain soil N, leaf N_a, M_a or MAT (Table A2.4). For the random effects, family contributed 2.8% to the unexplained variance (Table 2.3).

For $V_{cmax,N}^{25}$, we attempted to construct a model using combinations of soil and leaf P, soil and leaf N, soil ECEC, and climate (MAT). However, in contrast to $V_{cmax,a}^{25}$ and $J_{max,a}^{25}$, no combination of available explanatory variables produces a model superior to a null construct that merely allowed for variation around the data-set mean value of $V_{cmax,N}^{25}$. This suggests that other factors, such as how leaf N is allocated and/or whether Rubisco is fully active may have played a role.

2.4 Discussion

2.4.1 Regional and inter-biome context

Past studies on forest biomes revealed variability in the slope of $V_{cmax,a}^{25} \leftrightarrow N_a$ relationships, with lower rates of V_{cmax} per unit N in nutrient-poor, lowland tropical forests compared to lowland forests on more fertile soils, upland tropical forests and temperate broadleaf forests (Carswell *et al.*, 2000; Domingues *et al.*, 2007; Meir *et al.*, 2007; Kattge *et al.*, 2009; Domingues *et al.*, 2010; Mercado *et al.*, 2011; van de Weg *et al.*, 2012). Moreover, Reich *et al.* (2009) concluded that the slope of mass-based $A \leftrightarrow N$ relationships is lower in the tropics than in colder arctic and temperate biomes. Our study supports such studies, with $V_{cmax,N}^{25}$ values for our upland and lowland TMFs (22.5 and 18.9 μmol CO_2 g N^{-1} s^{-1}, respectively) being markedly lower than reported for temperate broadleaved trees [34 μmol CO_2 g N^{-1} s^{-1} (Kattge *et al.*, 2009)].

How do our results compare with other analyses of photosynthetic capacity in tropical ecosystems? The range of $V_{cmax,a}^{25}$ (6–96 μmol m^{-2} s^{-1}) and $J_{max,a}^{25}$ (21 –176 μmol m^{-2} s^{-1}) values from our study were wider than those reported for drier tropical sites in West Africa (Domingues *et al.*, 2010), perhaps reflecting environmental differences, or differences in the number of species sampled (210 here versus 39 in the West African study). For our lowland TMFs (which included three low nutrient status white sand sites in Northern Peru), the overall mean $V_{cmax,a}^{25}$ (36±15 μmol m^{-2} s^{-1}) was

lower than previously reported tropical values: Carswell *et al.* (2000): 43 μmol m^{-2} s^{-1}; Domingues *et al.* (2007): 53 μmol m^{-2} s^{-1}; Meir *et al.* (2007): 49-68 μmol m^{-2} s^{-1}; Kattge *et al.* (2009): 41 μmol m^{-2} s^{-1} (non-oxisol); Bloomfield *et al.* (2014a): 63 μmol m^{-2} s^{-1}; Domingues *et al.* (2015): 39-46 μmol m^{-2} s^{-1}. By contrast, our mean $V_{cmax,a}^{25}$ values were higher than the values for lowland TMFs only growing on nutrient-poor, oxisol [29 μmol m^{-2} s^{-1} (Kattge *et al.*, 2009)]. Since $J_{max,a}^{25}$ was tightly correlated with $V_{cmax,a}^{25}$ (Fig. 2.5), our estimates of $J_{max,a}^{25}$ for lowland TMFs were also lower than those reported in above-mentioned studies. Rates of $V_{cmax,a}^{25}$ at our upland sites (49±20 μmol m^{-2} s^{-1}) were similar to those reported by van de Weg *et al.* (2012): 56 μmol m^{-2} s^{-1} for the same Andean region, and fell mid-range of values reported in Dusenge *et al.* (2015) and Vårhammar *et al.* (2015) for high elevation tropical trees of Rwanda.

Taken together, our results support the hypothesis that both $V_{cmax,a}^{25}$ and photosynthetic N efficiency are lower in lowland TMFs than in temperate broadleaved forests. In addition, each parameter is highly variable, both among co-existing tropical species growing at individual sites and between environmentally-contrasting sites.

2.4.2 Phosphorus –does it modulate photosynthetic capacity and/or N-use efficiency?

Our site selection aimed to assess the potential role of phosphorus-limitation on photosynthetic performance across TMFs in western Amazonia and the Andes where substantial variations in soil P occur (lowland sites: 38-727 mg P kg^{-1}; upland sites: 496-1631 mg P kg^{-1}). Low P availability can limit rates of photosynthesis via reduced maximal rates of RuBP regeneration (i.e. J_{max}), with maximal Rubisco activity (i.e. V_{cmax}) also often being reduced (Brooks, 1986; Jacobs & Lawlor, 1992; Loustau *et al.*, 1999). While the mechanisms responsible for reduced V_{cmax} remain uncertain, possible factors include the need to maintain co-limitation by RuBP regeneration and carboxylation, as well as feedback inhibition on Rubisco resulting from inability to export triose phosphates to the cytosol (Wullschleger, 1993; Walker *et al.*, 2014).

The hypothesis that photosynthetic capacity would be positively correlated with soil [P] and leaf P_a was supported by our results – a finding consistent with earlier studies on tropical species in South America, West Africa and Australia (Domingues *et al.*, 2007; Meir *et al.*, 2007; Kattge *et al.*, 2009; Domingues *et al.*, 2010; Bloomfield *et al.*, 2014b). Among lowland sites alone, and the combination of lowland and upland sites together, significant positive relationships were observed between photosynthetic capacity (expressed either as $V_{cmax,a}^{25}$ or $J_{max,a}^{25}$) and foliar P_a, and against soil [P]

(Tables A2.1, A2.2). Across all 18 TMF sites, $V_{cmax,a}^{25}$ and $J_{max,a}^{25}$ also exhibited significant negative relationships with leaf N:P (Table A2.1). Moreover, foliar P_a and soil [P] emerged as significant explanatory variables in linear mixed-effect models of variations in photosynthetic capacity (Table 2.3), accounting for ~40% of the observed variations in $V_{cmax,a}^{25}$ and $J_{max,a}^{25}$. That MAT was not retained in the preferred models suggests that, while growth temperature can affect photosynthetic capacity (Hikosaka *et al.*, 2006; Sage & Kubien, 2007) and patterns of N investment, knowledge of growth temperature along the western Amazon-Andes elevation gradient is not required when data on leaf and soil P are available.

Past studies reported that P-deficiencies also reduce photosynthetic N use efficiency (Reich *et al.*, 2009) and the fraction of leaf N allocated to photosynthesis (Warren & Adams, 2002). While average values $V_{cmax,N}$ and foliar [P] were highest in our upland trees, no significant $V_{cmax,N} \leftrightarrow P_a$ relationships were observed, either across all sites or within each elevation class. Furthermore, we could not identify key factors explaining variation in $V_{cmax,N}$ using linear mixed-effects models; this included models that contained data on soil and foliar [P]. While this does not preclude a role for deficiencies in cytosolic [P] in regulating *in vivo* values of $V_{cmax,N}$, it seems unlikely that either soil or total leaf [P] can be used a predictor of variations in *in vivo* Rubisco capacity per unit leaf N.

2.4.3 Activation state of Rubisco

In vitro quantification in several lowland TMF species revealed that Rubisco content inferred from CO_2 response curves may have substantially underestimated absolute levels of this key protein (Fig. 2.10). When estimating Rubisco abundance from $A \leftrightarrow C_i$ curves, Rubisco is assumed to be fully activated – however, there is growing evidence that Rubisco often operates at less than maximum activity or is in excess of CO_2 fixation requirements (Stitt & Schulze, 1994; Warren *et al.*, 2000). Partial activation could be linked to limitations in sink demand for carbohydrates and/or co-limitation by other rock-derived nutrients such as calcium [e.g. Asner *et al*. (2014b)]. Inactive Rubisco might serve as a temporary N store - as such, Rubisco can act as both a metabolic and non-metabolic protein (Stitt & Schulze, 1994; Warren *et al.*, 2000). Viewed from this perspective, *in vivo* estimates of V_{cmax} provide insights into N investment into the *metabolically active* Rubisco, relevant when modelling gross primary productivity of TMF ecosystems. However, if the objective is to assess how

plants differ in N investment in both active and inactive forms of Rubisco, then n_R estimated from other approaches, such as Western blots (or similar quantitative techniques) might be required.

As noted earlier, the observed values of $V_{cmax,N}^{25}$ were lower than that of trees growing in temperate environments (Kattge *et al.*, 2009). Similarly, when compared at any given M_a, *in vivo* estimates of n_R (i.e. fraction of leaf N allocated to Rubisco estimated from gas exchange) were, on average, lower in our TMF trees compared to the global average (Hikosaka, 2004; Wright *et al.*, 2004) (Fig. 2.11). By contrast, *in vitro* estimates of n_R (i.e. n_R estimated from Western blots) were often higher than the global average (Fig. 2.11). This finding raises the possibility that the efficiency of N investment in Rubisco may not necessarily be lower in TMFs; rather, it may be that the activation state is lower in tropical forests compared with their temperate counterparts. Further work is needed to explore this question; additional work is also needed to determine what role, if any, limitations in mesophyll conductance (g_m) have on estimates of V_{cmax} and the associated values of n_R.

2.4.4 Additional factors influencing V_{cmax} estimates

In our study, we have so far estimated *in vivo* rates of $V_{cmax,a}^{25}$ assuming a common, single set of kinetic constants (K_c and K_o) for Rubisco (von Caemmerer *et al.*, 1994) and associated activation energies (E_a) (Farquhar *et al.*, 1980) as well as infinite g_m. Such assumptions were made necessary in the absence of K_c, K_o, E_a and g_m values for tropical species. Application of different K_c and K_o values, such as those reported by Bernacchi *et al.* (2002), would alter estimates of $V_{cmax,a}^{25}$ for all trees but would not alter relative differences among sites or elevational classes. By contrast, application of Bernacchi *et al.* (2002) E_a values for K_c and K_o (80.99 and 23.72 kJ mol^{-1}, respectively), and V_{cmax} (65.3 kJ mol^{-1}) could potentially relative differences in $V_{cmax,a}^{25}$ between upland and lowland trees, depending on the extent to which leaf temperatures differed among the sites. Similarly, replacement of the Farquhar *et al.* (1980) E_a values of V_{cmax} and J_{max} (of 64.8 and 37.0 kJ mol^{-1}, respectively) with those of Bernacchi *et al.* (2002) (65.3 and 43.9 kJ mol^{-1}, respectively) could alter the relative differences in $V_{cmax,a}^{25}$ and $J_{max,a}^{25}$ between upland and lowland sites. To check whether application of alternative E_a values change our conclusions regarding site-to-site differences, we calculated $V_{cmax,a}^{25}$ and $J_{max,a}^{25}$ using the respective activation energies of Farquhar *et al*. (1980) and Bernacchi *et al.* (2002). Use of the Bernacchi *et al.* (2002) E_a values resulted in an average 10.6%

increase in estimates of V_{cmax25} for lowland trees (Table 2.4), reflecting the fact that lowland leaf temperatures were near 30°C. Upland estimates were less affected (3.5% increase; Table 2.4) as the average leaf temperature of upland group was 25.7˚C. Despite the increased estimates of V_{cmax25} for lowland trees when using E_a values from Bernacchi *et al.* (2002), there remained a significant difference between lowland and upland mean V_{cmax25} values (Table 2.4); the same was true for $J_{max,a}^{25}$ (Table 2.4). As a result, relationships between photosynthetic properties and site MAT and soil P were similar when using Farquhar *et al*. (1980) and Bernacchi *et al.* (2002) E_a values (Fig. 2.3). Thus, irrespective of which E_a values are used [see Medlyn *et al.* (2002) for further discussion the temperature dependence of these constants], we are confident that that mean values of V_{cmax25} and $J_{max,a}^{25}$ are indeed higher in the upland plants growing in the Peruvian Andes.

Table 2.4. Comparison of mean values of V_{cmax} and J_{max} at 25°C values (V_{cmax25} and J_{max25}, respectively) in upland and lowland plants calculated using different activation energies (E_a) for each parameter (i.e. V_{cmax} and J_{max}), and K_c and K_o constants when calculating V_{cmax}. Here, we compare values calculated using E_a values reported by Farquhar *et al.* (1980) and Bernacchi *et al.* (2002). For Farquhar *et al.* (1980), E_a values of K_c and K_o used were 59.4 and 36.0 kJ mol^{-1}, respectively. For Bernacchi *et al*. (2002), the E_a values of K_c and K_o were 80.99 and 23.72 kJ mol^{-1}. For calculations made using Farquhar *et al.* (1980), we used E_a values for V_{cmax} and J_{max} of 64.8 and 37.0 kJ mol^{-1}, respectively; for Bernacchi *et al*. (2002), the E_a values for V_{cmax} and J_{max} were 65.3 and 43.9 kJ mol^{-1}, respectively. Values are overall mean ± SD of leaf traits for lowland and upland sites. Different letters (p<0.05) indicate significantly different means.

Source of constants		$V_{cmax,a}^{25}$ (μmol m^{-2} s^{-1})	$J_{max,a}^{25}$ (μmol m^{-2} s^{-1})
Farquhar *et al*. (1980)	Lowland species	35.9 ± 14.6^a	66.7 ± 18.6^a
	Upland species	48.8 ± 20.0^b	96.9 ± 36.9^b
Bernacchi *et al.* (2002)	Lowland species	39.7 ± 15.6^a	64.7 ± 18.6^a
	Upland species	50.5 ± 18.5^b	96.6 ± 37.3^b

What impact might systematic differences in g_m between upland and lowland TMFs have on our results? If g_m was finite, but similar in upland and lowland TMF environments, then our conclusion that $V_{cmax,a}^{25}$ is higher in upland species would hold (albeit with modified values). However, if g_m was more limiting in lowland TMF trees than their upland counterparts, then calculation of V_{cmax} using $A \leftrightarrow C_c$ curves might fail to differentiate between the upland and lowland groups. A definitive assessment of this issue will require further work assessing g_m in tropical trees (e.g. using concurrent measurements of leaf as exchange and carbon isotope discrimination or chlorophyll fluorescence). Although g_m tends to decrease with increasing M_a (Flexas *et al.*, 2008), the M_a difference between lowland and upland groups was small (Table 2.1). Given the

potential for large variations in g_m among species (at a given M_a), it is unlikely that g_m would have been higher in the selected lowland TMF trees. Irrespective of the effect of elevation on g_m, rates of $A_{40,a}$ and $A_{200,a}$ (measured at prevailing leaf *T*s) were surprisingly high in plants at the cooler, high elevation sites. Given this and our extensive sample size, we feel confident that photosynthetic capacity at a standardised *T* is likely larger in trees growing at high elevations in the Andes compared to those in the lowland regions of Amazonia, as proposed by van de Weg *et al.* (2012; 2014). Enhanced photosynthetic capacity at high altitude could help negate the inhibitory effects of low *T* on leaf-level CO_2 uptake, with the result that gross primary productivity (GPP) would not decline with increasing elevation as much as expected.

Recent modelling of C-exchange processes at a high elevation TMF site (3025 m a.s.l.) in Peru suggested that gross primary productivity (GPP) may be 20-40% lower compared to lowland TMFs (Girardin *et al.*, 2014a; van de Weg *et al.*, 2014); low *T* appeared to be most important factor limiting GPP at high elevations (van de Weg *et al.*, 2014). Our results suggest that the inhibitory effect of low *T* on GPP of upland TMFs would be greater if photosynthetic capacity remained constant across the elevation gradient. Thus, the greater photosynthetic capacity of upland TMFs might contribute to GPP being relatively homeostatic across the Peruvian Amazon-Andes elevation gradient. Further work is needed to explore how elevation-dependent variations in photosynthetic capacity impact on current and future net primary productivity (NPP) of TMFs, when taking into account other NPP components (e.g. leaf area index, biomass allocation, litter fall, autotrophic respiration).

2.4.5 Concluding statements

Our findings reveal greater photosynthetic capacity in Andean forest leaves compared to lowland western Amazonian leaves, underpinned by greater concentrations of leaf N and N-use efficiency per unit leaf area (Table 2.2, Fig. 2.9). Our data also support the hypothesis that variations in leaf and soil P play key role in modulating photosynthetic capacity of TMFs (Fig. 2.6), with the mixed-effects models (Table 2.3) providing the modelling community with predictive equations that will enable model parameterization based on arguably the largest single tropical V_{cmax} datasets available. Finally, our analyses indicate that a substantial fraction of Rubisco is inactive in trees growing in the Peruvian Amazon and suggest that a greater fraction of leaf N may well be invested in photosynthetic machinery than indicated by leaf gas exchange measurements.

Chapter 3: Limitations by mesophyll conductance do not influence estimates of Rubisco capacity obtained from CO_2 response curves of several tropical and temperate moist-forest species

3.1 Introduction

Temperature is one of the key determinants for plant growth and survival, with large effects on physiological activity at all spatial and temporal scales. Plants in warm and cold environments often exhibit adaptive traits which enable them to function and survive under these environments. Globally, plants growing in cold regions typically exhibit higher leaf nitrogen (N) concentrations (Reich & Oleksyn, 2004) and temperature-normalized metabolic rates when compared to plants growing in warmer environments (Kattge *et al.*, 2009; Reich *et al.*, 2009; Atkin *et al.*, 2015). Furthermore, higher rates of light-saturated net photosynthetic assimilation (*A*) per unit leaf N – i.e. photosynthetic N use efficiency (PNUE) - have been reported in plants growing in cold regions (Reich *et al.*, 2009), although this observation is confounded by phosphorus availability. By contrast, other studies have reported similar PNUE in cold and warm-adapted moist-forest species (Xiang *et al.*, 2013), while others have reported lower PNUE in alpine vs lowland species (Westbeek *et al.*, 1999; Hikosaka *et al.*, 2002). In cases where PNUE is higher in cold-adapted plants, it may be that a more N is invested in photosynthetic machinery, particularly CO_2-fixing enzyme Rubisco, to compensate for the low catalysis at low temperatures (Holaday *et al.*, 1992; Sage & Kubien, 2007). Trade-offs associated with leaf longevity (Kikuzawa *et al.*, 2013; Metcalfe *et al.*, 2014) and phosphorus limitation (Jacob & Lawlor, 1992; Loustau *et al.*, 1999; Kattge *et al.*, 2009) might further contribute to lower photosynthetic rate and PNUE of warm-adapted plants.

What factors underpin the difference in photosynthesis and PNUE between warm and cold adapted leaves? Variations in photosynthesis are mostly attributed to biochemical limitations, such as the amount and allocation of N to photosynthetic machinery (e.g. Rubisco, chlorophyll binding proteins, Calvin-cycle enzymes, electron-transport proteins, ATP-synthesising enzymes) as well as to diffusional limitations imposed by stomatal and mesophyll resistances (Evans, 1989; Hikosaka *et al.*, 1998; Evans & Loreto, 2000). Greater N investment in photosynthetic machinery could

explain the higher rates of *A* exhibited by cold-adapted plants compared to their warm-adapted counterparts (Xiang *et al.*, 2013; Scafaro et al. submitted.; Ali *et al.*, 2015; Dusenge *et al.*, 2015; Bahar *et al.*, 2017). What remains unknown, however, is whether higher *A* and PNUE could be attributed to inherently lower limitation to photosynthesis by mesophyll resistance (Lloyd *et al.*, 1992; Warren & Adams, 2006; Flexas *et al.*, 2008). *A* generally correlate with mesophyll conductance, g_m (Evans & Loreto, 2000; Flexas *et al.*, 2008; Tosens *et al.*, 2012); however, there is evidence of greater mesophyll resistance at low rates of *A*, which result in a larger drawdown of CO_2 concentration from sub-stomatal cavities to the site of carboxylation in chloroplasts (Warren & Adams, 2006; Niinemets *et al.*, 2009; Tosens *et al.*, 2012). To our knowledge, the possibility of warm-adapted leaves being more limited by mesophyll resistance than cold-adapted counterparts has yet to be tested.

Many studies exploring *A*-N relationships have focused on Rubisco because it is the largest N sink in the leaves and catalyses a rate-limiting step in photosynthesis (Farquhar *et al.*, 1980; Evans & Seemann, 1989). Although the amount and activity of Rubisco can be measured directly (Vu & Yelenosky, 1988; Lloyd *et al.*, 1992; Hikosaka *et al.*, 1998; Warren *et al.*, 2000), the maximum rate of carboxylation of Rubisco, commonly termed V_{cmax}, are more routinely estimated from gas exchange. The initial slope of the *A* to intercellular CO_2 concentrations (C_i) - from which V_{cmax} is derived - has been shown to correlate strongly with *in vitro* measurements of Rubisco activity (von Caemmerer & Farquhar, 1981). The gas exchange approach is attractive as it provides biochemical parameters using the Farquhar, von Caemmerer & Berry (1980) model, obtained from relatively easy and more readily available technique (Long & Bernacchi, 2003). However, there is a growing concern about the accuracy of the Farquhar *et al.* model in estimating V_{cmax}, owing to its assumption of infinite g_m, which has a consequence of fitting the model on a C_i basis instead of CO_2 partial pressure at the site of carboxylation (C_c) (Farquhar *et al.*, 1980). Estimating V_{cmax} on a C_i basis potentially underestimates the true V_{cmax}, if appropriate kinetic constants are not adjusted (Epron *et al.*, 1995; Manter & Kerrigan, 2004; Warren, 2008; Sun *et al.*, 2014b). Thus, lack of consideration of g_m can result in major discrepancy in estimating key biochemical parameters of photosynthesis.

In Australia, tropical and temperate evergreen moist-forests are distributed along the eastern margin of Australia, being restricted to high annual rainfall (> 1100 mm) habitats (Specht & Specht, 1999). Studies comparing tropical and temperate wet-forest

evergreens are crucial to understanding plant adaptation and acclimation responses to growth temperature (Cunningham, S & Read, J, 2003; Cunningham, SC & Read, J, 2003; Scafaro et al. submitted). Using a range of tropical and temperate moist-forest canopy species, mesophyll conductance was estimated from the difference between C_i and C_c (Evans *et al.*, 1986; Caemmerer & Evans, 1991) via a combination of leaf gas exchange and carbon isotope discrimination measurements described previously (Tazoe *et al.*, 2011; von Caemmerer & Evans, 2015). This study tests the hypothesis that:

(1) The estimates of V_{cmax} are greater when obtained from CO_2 response curves on the basis of C_c compared with that on the basis of C_i.
(2) Greater mesophyll resistance contributes to lower A and V_{cmax} in tropical moist-forest species, in contrast to temperate moist-forest species that are hypothesized to exhibit higher rates of A, V_{cmax} and g_m.

3.2 Material and Methods

3.2.1 Plant material and growth conditions

Seedlings of six tropical species originated from moist-forests of Queensland and five temperate species from cool-temperate moist-forests of Tasmania were sourced from commercial nurseries (see Table 3.1 for details on provenance and climate parameters at each provenance); these species were selected to represent thermally contrasting origins. Seedlings were 4-12 months old and 30 to 70 cm in height at the beginning of experiment. Seedlings were transplanted to 220 mm pots containing organic potting mixture and Osmocote® Exact standard controlled-release fertilizer (Scotts Australia, NSW, Australia) with an N/P/K ratio of 16:3.9:10 and grown in glasshouses in Canberra, Australia. The glasshouse was controlled to achieve 25/20 °C day/night and plants were watered daily to exceed pot capacity. Plants were arranged in four replicate blocks within the glasshouse, with each block containing randomly allocated individual of each species. The experiment took place in June-August 2015 during which time the day length was 10 hours.

Table 3.1. List of tropical and temperate species used in this study. Tropical and temperate seedlings were sourced from Yuruga Native Plants Nursery, Walkamin, Queensland and Habitat Plants, Liffey, Tasmania, respectively. Climate information, according to species provenance, was obtained from *WorldClim* (Hijmans *et al.*, 2005) using the nearest occurrence of each species in the *Atlas of Living Australia* (http://bie.ala.org.au/species/).

					Precipitation (mm)			Temperature (˚C)			
Abbrev.	Family	Species	Provenance	State	Annual	Driest month	Wettest month	Annual mean	Cold month minimum	Warm month maximum	Diurnal range
CA	*Fabaceae*	*Castanospermum australe*	Mareeba	QLD	2166	41	431	22.5	13.6	30.1	9.4
DA	*Monimiaceae*	*Doryphora aromatica*	Walkamin	QLD	1501	34	303	19.6	9.2	28.6	10.9
FB	*Rutaceae*	*Flindersia bourjotiana*	Cape Tribulation	QLD	1860	22	402	24.1	16.2	31.3	9.0
LL	*Lauracea*	*Litsea leefeana*	Cape Tribulation	QLD	1945	29	406	23.0	15.3	30.2	8.8
PE	*Araliaceae*	*Polyscias elegans*	Mt. Molloy	QLD	1469	24	307	19.4	10.3	27.9	10.4
SS	*Myrtaceae*	*Syzygium sayeri*	Tolga	QLD	1688	32	335	20.7	10.9	29.2	10.5
AM	*Monimiaceae*	*Atherosperma moschatum*	Western Tiers	TAS	1181	49	153	8.8	0.0	20.4	10.0
EO	*Myrtaceae*	*Eucalyptus obliqua*	Liffey	TAS	1158	48	150	9.2	0.2	20.8	10.1
EL	*Eucryphiaceae*	*Eucryphia lucida*	Strathgordon	TAS	2288	97	256	10.0	2.7	19.5	8.2
PC	*Phyllocladaceae*	*Phyllocladus aspleniifolius*	Cradle Mt.	TAS	1845	78	239	7.8	0.4	18.1	8.5
PA	*Rhamnaceae*	*Pomaderris apetala*	Liffey	TAS	1161	48	150	9.0	0.2	20.7	10.1

3.2.2 Leaf gas exchange and CO_2 response curve measurements

Leaf gas exchange measurements were made during June to August 2015, using two portable photosynthesis systems (Licor 6400XT infrared gas analyser, Li-Cor BioSciences, Lincoln, NE, USA). Measurements were made on the most recently fully expanded leaves developed in the glasshouse. Initial measurement was made at 400 µmol mol^{-1} of CO_2 concentrations inside the reference chamber, followed by a stepped sequence of 50, 100, 150, 250, 400, 600, 800, 1000, 1200 and finally 1500 µmol mol^{-1} to generate CO_2 response curves. Block temperatures within the chamber were set to 25°C; photosynthetically active radiation (PAR) was 1500 µmol photons m^{-2} s^{-1} and O_2 was that of ambient air (i.e. fixed at 21%). $A \leftrightarrow C_i$ curves (examples shown in Figure 3.1) were fitted following the model described by Farquhar *et al.* (1980) in order to calculate V_{cmax} and J_{max}. V_{cmax} and J_{max} values were determined via minimizing the sum of squares of modelled vs. observed estimates of net CO_2 exchange at given CO_2 partial pressure at the site of the chloroplast (C_c). C_c was calculated from C_i (intercellular CO_2) assuming a constant value of mesophyll conductance, g_m, which was determined for each leaf in 2% O_2 (see the next section).

Rates of A at low CO_2 values were fitted to the Rubisco-limited equation of photosynthesis:

$$A = \left[\frac{V_{cmax}(C_c - \Gamma_*)}{\left(C_c + K_c\left(1 + {}^{O}/_{K_o}\right)\right)}\right] - R_{light} \qquad \text{(Eqn. 3.1)}$$

where R_{light} is respiration in the light, Γ* is the CO_2 compensation point in the absence of photorespiration [36.9 µbar at 25ºC; von Caemmerer *et al.* (1994)] and O is partial pressure of O_2. K_c and K_o are the effective Michaelis-Menten constants for CO_2 and O_2 at 25 °C. If mesophyll conductance is known, C_c can be calculated and the values assumed for K_c and K_o to be 260 µbar and 179 mbar, respectively. When mesophyll conductance was ignored (i.e. g_m assumed to be infinite), Eq 3.1 was fitted to C_i data assuming K_c and K_o to be 404 µbar and 248 mbar, respectively (von Caemmerer *et al.*, 1994). R_{light} was estimated from the CO_2 response curve.

A cross validation between LI-6400XT instruments and 2% versus 21% O_2 measurements on the same leaf was made using Eq 3.1. Having obtained V_{cmax} and R_{light} from the CO_2 response curve measured in 21% O_2, the Rubisco-limited CO_2 assimilation rate in 2% O_2 was calculated using the C_c value measured in 2% O_2.

Values for J_{max} were calculated by fitting the electron-transport-limited equation of CO_2 assimilation to the CO_2 response curve at high CO_2 (generally when C_i > 500 µbar):

$$A = \left[\frac{J_{max}(C_c - \Gamma_*)}{(4C_c + 8\Gamma_*)}\right] - R_{light} \qquad \text{(Eqn. 3.2)}$$

3.2.3 Concurrent gas exchange and carbon isotope discrimination measurements and calculation of mesophyll conductance

Gas exchange and carbon isotope discrimination measurements for the estimation of mesophyll conductance were made as described by Tazoe *et al.* (2011) and Evans & von Caemmerer (2013). A second pair of LI-6400XT gas exchange systems coupled to a tuneable diode laser (TDL; TGA100, Campbell Scientific, Inc., Logan, UT, USA) were used to make a second measurements on the same set of leaves, but in 2% O_2 and 380 µmol mol^{-1} of CO_2 (in leaf chamber). Reference and sample air were sampled via T junctions in the tubing for concurrent measurements of carbon isotope composition, with readings every 4 mins. The flow rate was 200 µmol s^{-1}, irradiance 1500 µmol photons m^{-2} s^{-1} and leaf temperature controlled at 25 °C. Air containing 2% O_2 was made by mixing N_2 and O_2 using mass flow controllers (Omega Engineering Inc., Stamford, CT, USA) and supplied to both the TDL system and the LI-6400 consoles and specified for the LI-6400 calculations. After about one hour of measurement in the light, respiration in the dark (R_{dark}) was measured for each leaf. Mesophyll conductance was calculated from carbon isotope discrimination with equations and fractionation factors described in Evans & von Caemmerer (2013). The ternary effects of transpiration rate on the rate of CO_2 assimilation through stomata were accounted for (Farquhar & Cernusak, 2012). The value of mesophyll conductance at 380 μmol mol^{-1} of CO_2 was used in the estimation on V_{cmax} from CO_2 response curve.

3.2.4 Calculations of the relative limitation of net CO_2 uptake by stomatal and mesophyll resistances to CO_2 diffusion

The limitations imposed by biochemistry, stomatal and mesophyll resistances to CO_2 diffusion on *A* were quantified based on the method published in Grassi and Magnani (2005), which were derived from *A*, stomatal conductance (g_s), g_m and V_{cmax}.

3.2.5 Leaf structural and nutrient measurements

Chlorophyll content was measured using a CCM-300 (Opti Science Inc., Hudson, NH, USA). Leaves were collected immediately after gas exchange and carbon isotope discrimination measurements were completed. Leaf areas were measured with a LI-3100C area meter (LiCor BioSciences, Lincoln, NE, USA) and leaf fresh masses were determined. Leaves were then placed in a drying oven at 60ºC for more than two days and re-weighed to measure dry mass. Total leaf N and P concentrations were measured using Kjeldahl acid digest method, outlined in Ayub *et al.* (2011).

3.2.6 Statistical analysis

Statistical analyses were carried out using SPSS version 20 (IBM Corporation, NY, USA). Two-tailed, equal variance T-tests were used to compare overall means of tropical and temperate species. Comparisons were considered significant if $P < 0.05$. Pearson correlations were used to measure bivariate relationships when tropical and temperate species analysed together. Standardized major axis (SMA) estimation was used to describe the best-fit relationship between pairs of variables and to assess whether relationships differed between tropical and temperate species, using SMATR Version 2.0 software (Falster *et al.*, 2006; Warton *et al.*, 2006).

***note that all V_{cmax} and J_{max} values are expressed at 25ºC, calculated according to similar methodology specified in Chapter 2**

3.3 Results

3.3.1 Cross-checking multiple gas exchange instruments

In our study, leaves were measured using two pairs of LI-6400 instruments. One pair was used to generate CO_2 response curves in 21% oxygen (O_2) while the other pair connected to a tuneable diode laser made measurements in 2% O_2 to suppress photorespiration. CO_2 response curves close to the mean response for tropical and temperate species are shown in Fig. 3.1. In general, photosynthetic rates of tropical and temperate species at ambient CO_2 were Rubisco limited, as illustrated by the arrows. To cross-check the two instruments, a prediction of CO_2 assimilation rate in 2% O_2 with the internal CO_2 observed was made (see dotted lines in Fig. 3.1) from fitting the Farquhar *et al.* (1980) biochemical model to each CO_2 response curve measured in 21% O_2. Measured CO_2 assimilation rate in 2% O_2 (triangles in Fig. 3.1) aligned well with the predicted rates (dotted lines) in both cases. The comparison for all of the leaves is shown in Fig. 3.2. Predicted CO_2 assimilation rate in 2% O_2 correlated strongly with measured rate ($p<0.01$, $r^2=0.95$; Fig. 3.2) and in general was slightly overestimated. The mean ratio of predicted to measured CO_2 assimilation rate in 2% O_2 was 1.11 ± 0.12 and 1.16 ± 0.19 for tropical and temperate trees, respectively, and the ranges of the two groups overlapped. This comparison suggested that there was no bias between the pairs of LI-6400s and that the Farquhar *et al.* (1980) model fitted both tropical and temperate trees**.**

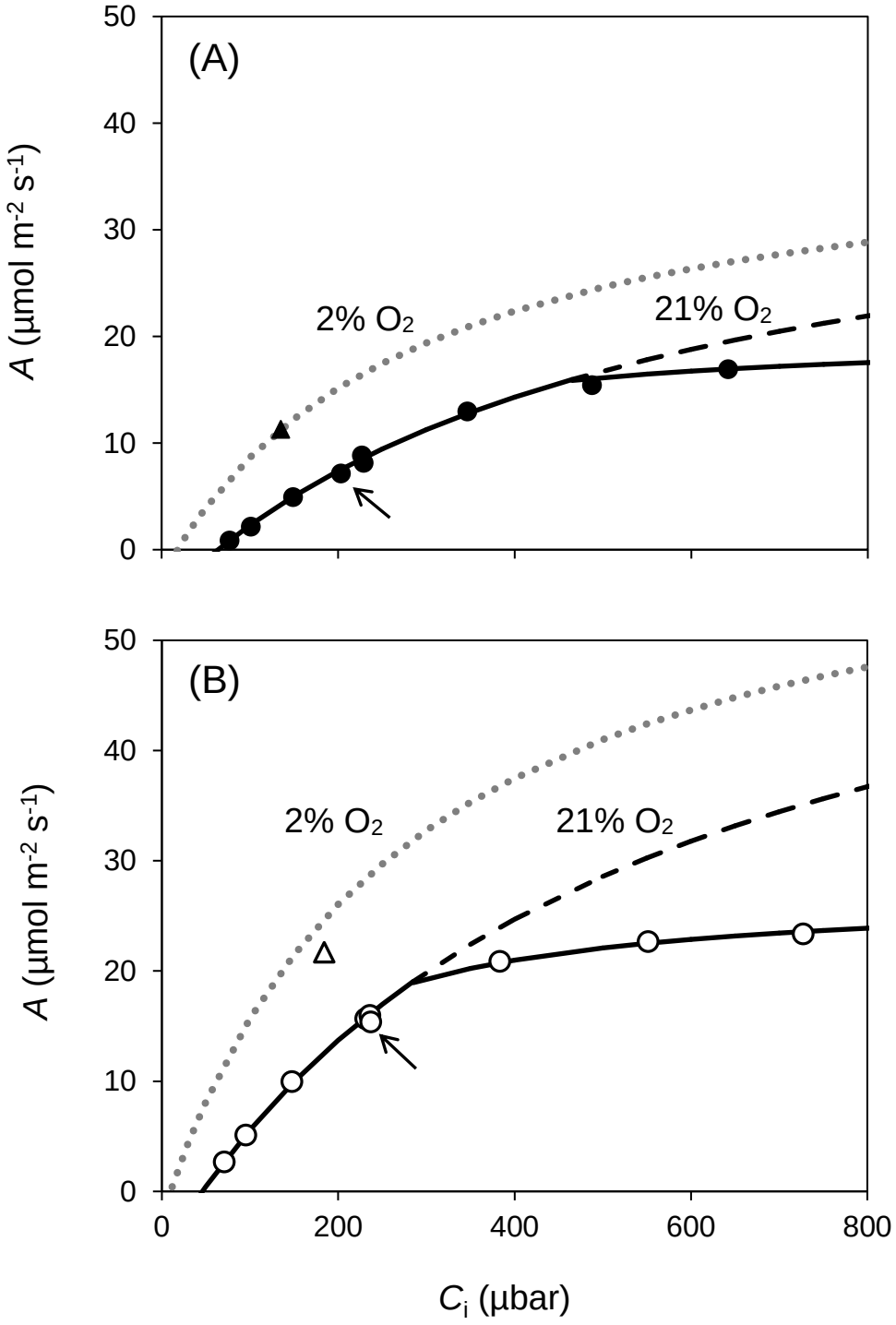

Figure 3.1. Fitted curves of the response of net CO_2 assimilation rate, *A* (area-based) to intercellular CO_2 (C_i) at 1500 µmol quanta m^{-2} s^{-1} for (A) a tropical species *Doryphora aromatica* and (B) a temperate species *Pomaderris apetala*. Arrows point to photosynthetic rates under normal operating conditions at ambient CO_2. Circles are the measured rates of assimilation, *A* under 21% O_2. Dotted lines represent V_{cmax} (maximum Rubisco carboxylation capacity) predicted from Farquhar *et al.* (1980) model under 2% oxygen partial pressure, where triangles correspond to *A* measured in 2% O_2.

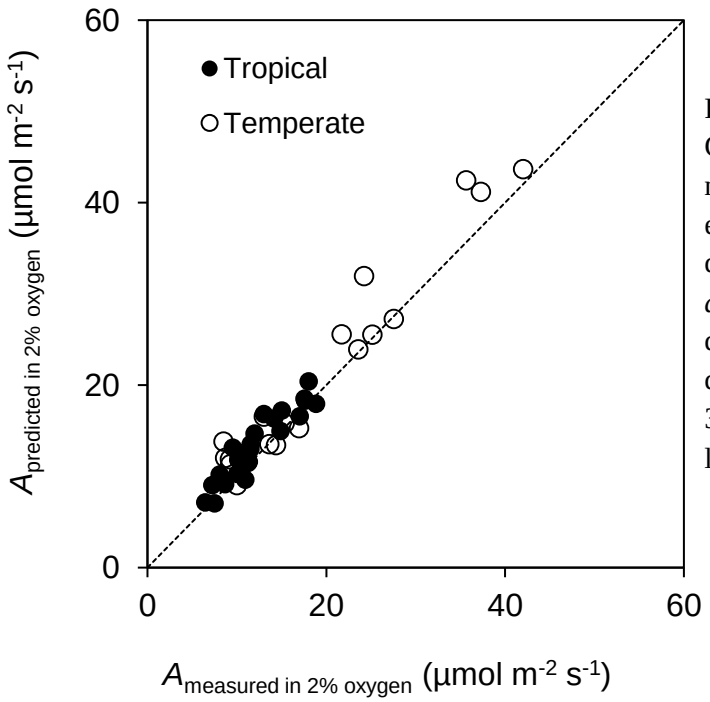

Figure 3.2. Comparison of net CO_2 assimilation rate, *A* directly measured in 2% O_2 against *A* as estimated from V_{cmax} which was derived from fitting Farquhar *et al.* (1980) model in 2% O_2 (see dotted lines in Fig. 3.1). Each data point corresponded to *A* in 380 µmol mol^{-1} CO_2. Dashed line shows the 1:1 relationship.

3.3.2 Assimilation rate, mesophyll conductance and limitation to CO_2 assimilation rate

Strong positive correlations between photosynthetic rate at ambient CO_2 (*A*) and mesophyll conductance (g_m) were observed ($p<0.05$, $r^2 = 0.74$; Figure 3.3A; Table A3.1 in Appendix 3). The tropical and temperate trees shared common *A*-g_m relationships as indicated by no significant difference in slope of the two groups (Table A3.2). The tropical trees occupied low ranges of *A* (4.5-14.3 µmol m^{-2} s^{-1}) and g_m (0.09-0.32 mol m^{-2} s^{-1} bar^{-1}) whereas the temperate trees were spread over larger ranges of *A* (5.4-27.3 µmol m^{-2} s^{-1}) and g_m (0.08-0.47 mol m^{-2} s^{-1} bar^{-1}).

The drawdown of CO_2 from the atmosphere to the sub-stomatal cavity (C_a - C_i) was independent of g_m (Figure 3.3B, mean 103 µbar, $p>0.05$; Table A3.2). No distinct clustering of tropical and temperate trees was observed. At a given g_m, the drawdown of CO_2 in the gaseous phase imposed by stomatal resistance varied three-fold (49-173 µbar, Fig. 3.3B). The magnitude of the CO_2 drawdown from C_i to C_c was also independent of g_m (Fig. 3.3C, mean 55 µbar, $p>0.05$; Table A3.2), again with a three-fold range (30-95 µbar). The CO_2 drawdown from C_i to C_c was generally similar for tropical and temperate trees, overlapping for g_m ranging from 0.1-0.3 mol m^{-2} s^{-1} bar^{-1}. However, two temperate species, *A. moschatum* and *P. aspleniifolius*, exhibited larger drawdowns of CO_2 at low g_m (0.08-0.13 mol m^{-2} s^{-1} bar^{-1}).

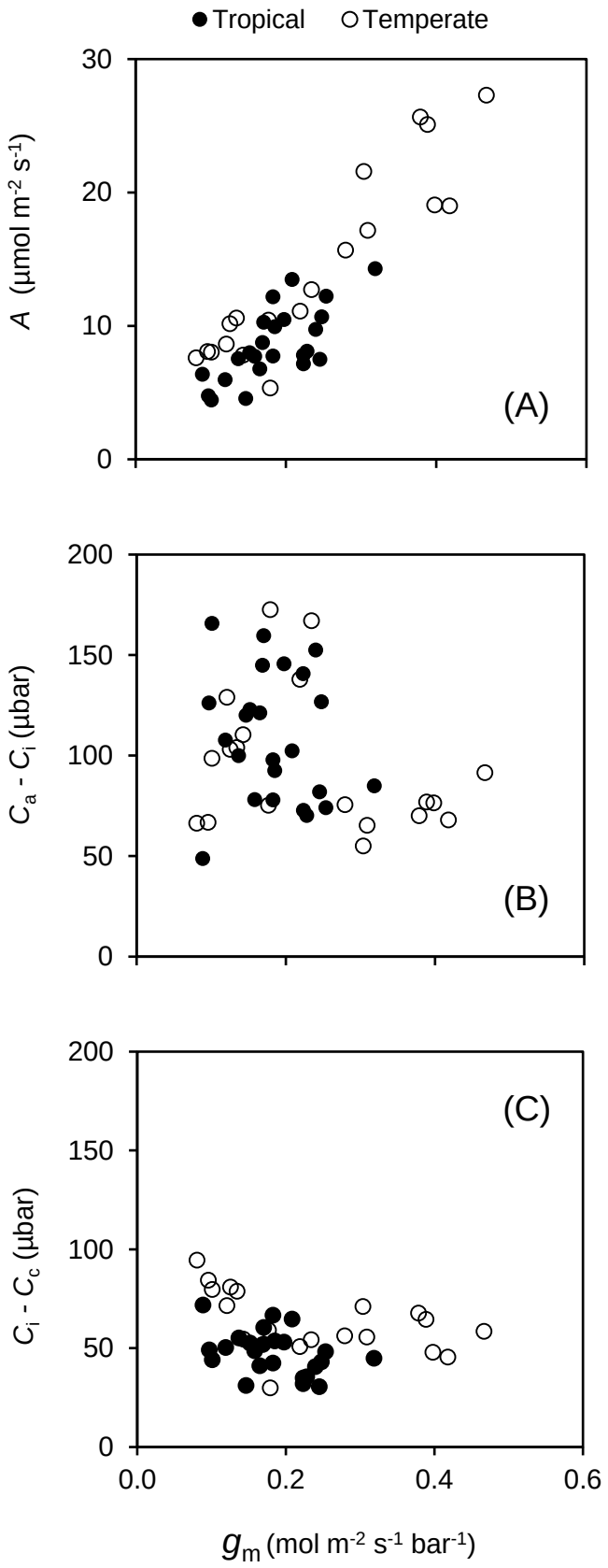

Figure 3.3. Relationships between mesophyll conductance, g_m and **(A)** net CO_2 assimilation rate, A in 400 µmol mol^{-1} CO_2 and 21% O_2, **(B)** draw-down in CO_2 in the gaseous phase and **(C)** draw-down in CO_2 in the liquid phase.

3.3.3 Comparison of V_{cmax} estimated with finite or infinite g_m

By measuring g_m from carbon isotope discrimination for each leaf, it was possible to calculate V_{cmax} on the basis of C_c assuming K_c and K_o values of 260 µbar and 179 mbar, respectively (von Caemmerer *et al.* (1994)]. Secondly, V_{cmax} was calculated on a C_i basis (assuming infinite g_m) using K_c and K_o of 404 µbar and 248 mbar, respectively (von Caemmerer *et al.*, 1994). V_{cmax} values calculated on a C_c basis were positively correlated with g_m ($p<0.05$, $r^2 = 0.59$; Fig. 3.4A). Tropical and temperate trees shared common slopes of A-g_m relationships (Table A3.2), although considerable scatter was observed.

To investigate the consequences of the scatter, the lowest and highest deviation from the average V_{cmax}/g_m ratio (indicated by squares) were analysed by assuming different values of g_m to estimate V_{cmax}. These simulations demonstrated that V_{cmax} decreased curvi-linearly with increasing g_m (solid lines in Fig. 3.4B), declining steeply at the lower range of g_m (generally at 0.1 mol m^{-2} s^{-1} bar^{-1}, depending on species). The estimate of V_{cmax} for *L. leefeana*, a tropical species with the lowest V_{cmax}/g_m ratio (133), was less sensitive to decreasing g_m than *P. aspleniifolius* which had the greatest V_{cmax}/g_m ratio (555). The value of V_{cmax} estimated on the basis of C_i is represented by dashed lines in Figure 3.4B. The greater V_{cmax}/g_m ratio for *P. aspleniifolius* resulted in a steeper increase in V_{cmax} as g_m was reduced below 0.2 mol m^{-2} s^{-1} bar^{-1} compared to *L. leefeana* and meant that V_{cmax} estimated on the basis of C_i would have underestimated the true value of *P. aspleniifolius* by 20% (Figure 3.4B).

A pattern to describe the consequence of variations in V_{cmax}/g_m ratio to estimation of V_{cmax} on C_c and C_i basis was found. For the species reported here, a V_{cmax}/g_m ratio of 218 yielded similar estimates of V_{cmax} on C_c and C_i basis (see dashed line in Fig. 3.4A). For data points distributed close to the dotted line (extrapolated from the lowest point *L. leefeana* illustrated in Fig. 3.4B), V_{cmax}-C_i values exceeded V_{cmax}-C_c values by approximately 3 to 5 %. For data points in proximity to the solid line (extrapolated from the highest point *P. aspleniifolius* illustrated in Fig. 3.4B), V_{cmax}-C_i values were 17% less than V_{cmax}-C_c depicted in Figure 3.5.

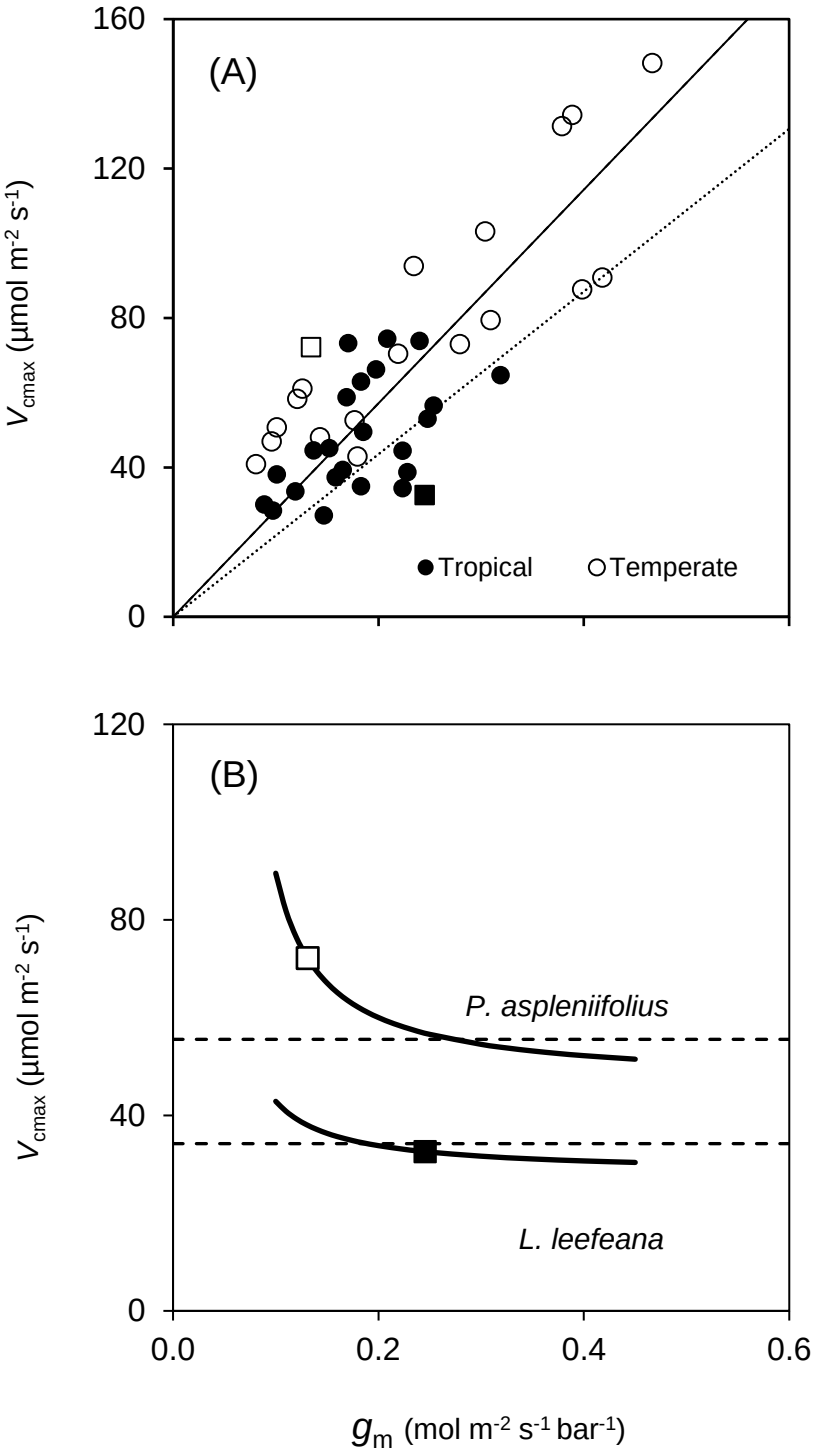

Figure 3.4 **(A)** Relationships between V_{cmax} and g_m for tropical and temperate trees. V_{cmax} was derived from CO_2 response curves (examples shown in Fig. 3.1) in 21% O_2 using finite g_m (i.e. V_{cmax}-C_c). Squares corresponded to V_{cmax} of *Phyllocladus aspleniifolius* and *Litsea leefeana* depicted in Figure 3.4B. The dashed line was extrapolated from the points where V_{cmax}-C_c equals V_{cmax}-C_i, while the dotted line was extrapolated from *L. leefeana* illustrated in Fig. 3.4B and the solid line extrapolated from *P. aspleniifolius* illustrated in Fig. 3.4B.

(B) Simulations of V_{cmax} estimated with different values assumed for g_m for a temperate species *P. aspleniifolius* and a tropical species *L. leefeana* (solid lines). Squares correspond to V_{cmax} estimated using actual g_m calculated on a C_c basis and dashed lines represent V_{cmax} estimated from infinite g_m on a C_i basis.

Despite the variation in V_{cmax}/g_m ratio, V_{cmax} estimated on a C_i basis was generally similar to the actual V_{cmax}-C_c (Fig. 3.5). Although the tropical and temperate trees shared a common slope between V_{cmax}-C_c and V_{cmax}-C_i (Table A3.2), the deviation between V_{cmax}-C_i and V_{cmax}-C_c was slightly greater for temperate trees (Fig. 3.5). Temperate tree averages for V_{cmax}-C_c and V_{cmax}-C_i were 78 ± 32 and 73 ± 29 µmol m^{-2} s^{-1}, respectively; tropical tree averages were 48 ± 15 and 45 ± 13 µmol m^{-2} s^{-1}, respectively. No difference was found in J_{max} estimated on C_c vs. C_i basis (data not shown).

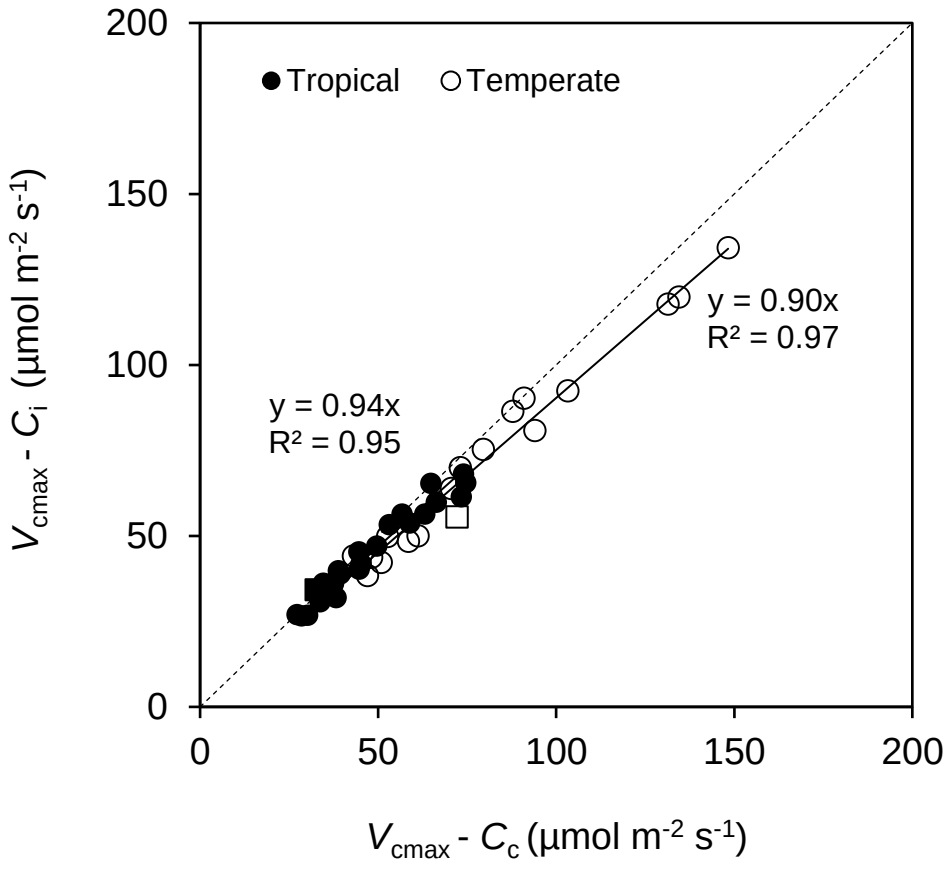

Figure 3.5. Comparison of V_{cmax} (maximum Rubisco carboxylation capacity) estimated using finite mesophyll conductance, g_m (V_{cmax}-C_c) and assumed infinite g_m (V_{cmax}-C_i). V_{cmax} was derived from A↔C_i curves (examples shown in Fig. 3.1) in 21% O_2. Dashed line shows the 1:1 relationship. Squares corresponded to V_{cmax} of *P. aspleniifolius* and *L. leefeana* depicted in Figure 3.4B.

3.3.4 Comparison of tropical and temperate leaf traits

The overall mean value of A in tropical trees (8.6 ± 2.7 μmol m^{-2} s^{-1}) was almost half that of temperate trees (14.3 ± 6.9 μmol m^{-2} s^{-1}; Table 3.2). Lower overall rate of ambient photosynthesis in tropical trees was accompanied by significantly lower stomatal conductance (g_s), as well as lower underpinning biochemical capacities, shown here as V_{cmax} and J_{max} (maximum electron transport rate) in comparison to temperate trees (p<0.05; Table 3.2).

Estimation of the relative limitations imposed by biochemistry, stomatal and mesophyll resistances on A for each species are presented in Figure 3.6. In general, limitations by mesophyll (L_m) contributed to the smallest fraction (approximately a quarter) of total limitations to A. In tropical species, L_m values were relatively constant whilst L_s (stomatal limitations) and L_b (biochemical limitations) were highly variable irrespective of A (Fig. 3.6). In temperate species, L_s and L_m increased with decreasing A, with *E. lucida* showing the highest L_s (Fig. 3.6). L_m and L_s accounted for similar magnitude of the limitations to A in *E. obliqua*, *P. apetala and A. moschatum*. No apparent trend in L_b was observed across tropical and temperate species.

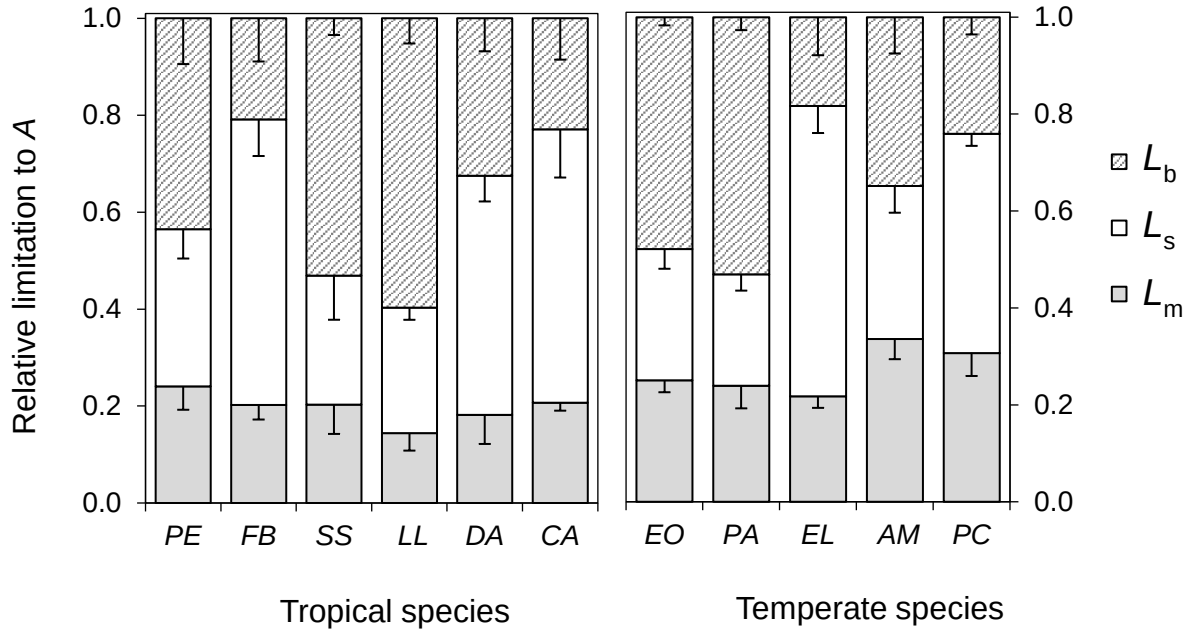

Figure 3.6. Plots of the limitations to A imposed by biochemistry (L_b), stomatal resistance (L_s) and mesophyll resistance (L_m) for tropical and temperate species. Error bars represent std. dev. of mean of each limitation component for each species. Tropical and temperate species was listed according to decreasing A (see Table 3.2). Species abbreviation is provided in Table 3.1.

Table 3.2. Means ± standard deviation of leaf photosynthetic components and chemical and structural traits, expressed on area basis for each species. Tropical and temperate group means are calculated based on the mean of individual species (n=4 within each species). Leaf photosynthetic components were measured at 25 ˚C in 21% oxygen, with exception for g_m at 2% oxygen. Abbreviation: A = light-saturated net photosynthesis measured at 400 µmol mol^{-1} CO_2, g_s = stomatal conductance, g_m = mesophyll conductance, C_i:C_a = ratio of intercellular CO_2 to atmospheric CO_2, V_{cmax} = maximum carboxylation velocity of Rubisco, J_{max} = maximum rate of electron transport, R_{dark} = dark respiration rate, M_a= leaf mass per unit leaf area, LDM:LFM = leaf dry mass to leaf fresh mass ratio, leaf P = leaf phosphorus, leaf N = leaf nitrogen. Species abbreviation is provided in Table 3.1.

Species	A (µmol m^{-2} s^{-1})	g_s (mol m^{-2} s^{-1})	g_m (mol m^{-2} s^{-1} bar^{-1})	C_i:C_a	V_{cmax} (µmol m^{-2} s^{-1})	J_{max} (µmol m^{-2} s^{-1})	R_{dark} (µmol m^{-2} s^{-1})	M_a (g m^{-2})	LDM:LFM	Leaf P area (g m^{-2})	Leaf N area (g m^{-2})	Chlorophyll (g m^{-2})
PE	13.1 ± 1.0	0.28 ± 0.04	0.24 ± 0.06	0.61 ± 0.07	64.7 ± 7.4	109.9 ± 3.4	1.4 ± 0.4	51 ± 8	0.32 ± 0.01	0.08 ± 0.01	1.69 ± 0.25	0.61 ± 0.04
FB	10.3 ± 0.4	0.12 ± 0.02	0.22 ± 0.04	0.52 ± 0.03	66.6 ± 9.7	109.4 ± 13.4	1.2 ± 0.3	74 ± 7	0.28 ± 0.01	0.08 ± 0.03	1.80 ± 0.07	0.66 ± 0.07
SS	8.0 ± 1.8	0.18 ± 0.05	0.15 ± 0.06	0.71 ± 0.05	38.2 ± 10.1	61.7 ± 14.8	1.0 ± 0.1	51 ± 5	0.22 ± 0.02	0.08 ± 0.01	1.15 ± 0.13	0.39 ± 0.01
LL	7.8 ± 0.3	0.19 ± 0.02	0.21 ± 0.04	0.69 ± 0.05	35.8 ± 2.8	70.3 ± 7.7	1.7 ± 0.2	38 ± 4	0.23 ± 0.01	0.09 ± 0.01	1.20 ± 0.97	0.42 ± 0.06
DA	6.8 ± 1.3	0.10 ± 0.02	0.16 ± 0.03	0.57 ± 0.07	40.2 ± 7.6	73.9 ± 16.9	1.3 ± 0.2	53 ± 3	0.21 ± 0.01	0.09 ± 0.01	1.91 ± 0.24	0.47 ± 0.03
CA	6.0 ± 2.0	0.07 ± 0.03	0.12 ± 0.03	0.54 ± 0.07	39.8 ± 13.3	55.8 ± 14.4	1.1 ± 0.2	50 ± 3	0.33 ± 0.01	0.11 ± 0.02	1.50 ± 0.21	0.57 ± 0.16
Tropical mean	8.6 ± 2.7 [a]	0.15 ± 0.08 [a]	0.19 ± 0.06 [a]	0.60 ± 0.09 [a]	47.6 ± 15.3 [a]	80.7 ± 24.6 [a]	1.3 ± 0.3 [a]	53 ± 12 [a]	0.26 ± 0.05 [a]	0.09 ± 0.02 [a]	1.58 ± 0.33 [a]	0.52 ± 0.12 [a]
EO	24.3 ± 3.6	0.62 ± 0.12	0.41 ± 0.04	0.67 ± 0.08	125.5 ± 26.2	186.1 ± 19.1	2.2 ± 0.3	58 ± 8	0.22 ± 0.02	0.10 ± 0.01	2.11 ± 0.15	0.57 ± 0.02
PA	18.4 ± 2.5	0.55 ± 0.18	0.33 ± 0.06	0.71 ± 0.07	86.6 ± 13.3	140.1 ± 19.5	1.1 ± 0.2	41 ± 3	0.28 ± 0.02	0.08 ± 0.02	1.54 ± 0.17	0.53 ± 0.02
EL	9.7 ± 3.9	0.12 ± 0.05	0.21 ± 0.03	0.46 ± 0.05	69.2 ± 25.5	126.3 ± 21.2	1.1 ± 0.4	79 ± 11	0.32 ± 0.02	0.13 ± 0.04	1.85 ± 0.09	0.79 ± 0.05
AM	9.1 ± 1.4	0.20 ± 0.03	0.12 ± 0.04	0.67 ± 0.08	50.4 ± 8.9	92.4 ± 14.0	1.2 ± 0.4	58 ± 3	0.23 ± 0.01	0.11 ± 0.01	1.81 ± 0.21	0.58 ± 0.09
PC	8.8 ± 1.3	0.13 ± 0.02	0.12 ± 0.02	0.57 ± 0.04	57.4 ± 10.8	104.4 ± 22.3	1.7 ± 0.3	97 ± 16	0.28 ± 0.04	0.21 ± 0.04	2.05 ± 0.52	0.47 ± 0.09
Temperate mean	14.3 ± 6.9 [b]	0.33 ± 0.24 [b]	0.23 ± 0.12 [a]	0.62 ± 0.11 [a]	78.3 ± 32.3 [b]	130.1 ± 38.4 [b]	1.5 ± 0.6 [a]	66 ± 22 [b]	0.26 ± 0.04 [a]	0.13 ± 0.05 [b]	1.88 ± 0.33 [b]	0.57 ± 0.12 [a]

As expected, V_{cmax} and J_{max} co-varied on both area and mass bases (Fig. 3.7; Table A3.2). There was a significant difference in the slope of $V_{cmax} \leftrightarrow J_{max}$ relationships between topical and temperate trees on area and mass bases (Table A3.2). However, the overall mean ratio of J_{max} to V_{cmax} was not significantly different between tropical and temperate trees (p>0.05, 1.71 ± 0.24 and 1.74 ± 0.27, respectively).

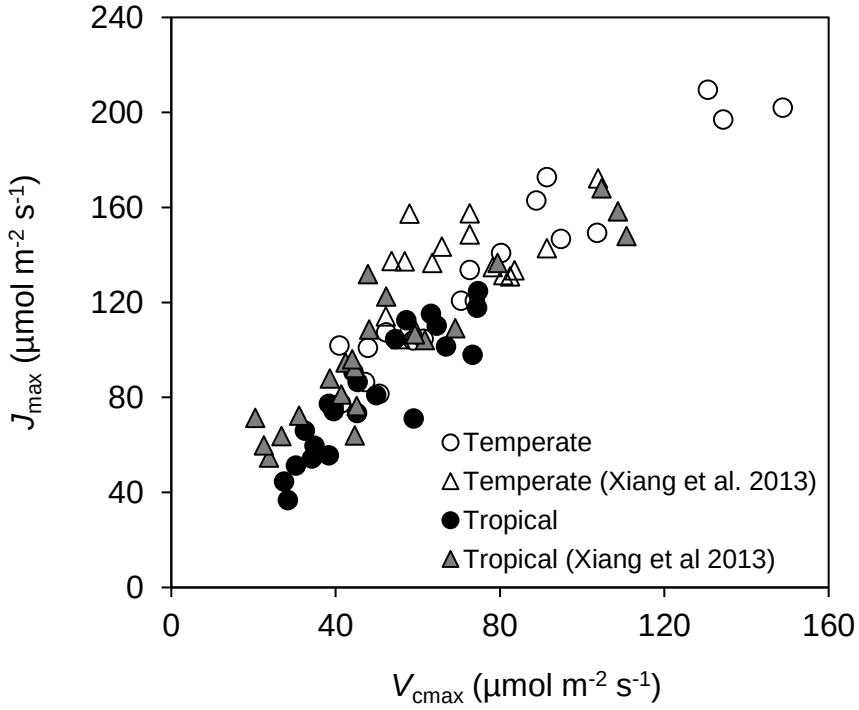

Figure 3.7 Relationships between V_{cmax} (maximum Rubisco carboxylation capacity) and J_{max} (maximum electron transport rate) estimated using finite mesophyll conductance, g_m. V_{cmax} and J_{max} were derived from $A \leftrightarrow C_i$ curve in 21% O_2. Values expressed on area basis. Values of V_{cmax} and J_{max} obtained from Xiang *et al.* (2013) using infinite g_m were plotted on the same scale. Similar patterns were observed when plotting V_{cmax} and J_{max} on a mass basis (data not shown).

In our study, the range of leaf mass per area (M_a) was slightly constrained (32-118 g m^{-2}). A weak negative correlation between V_{cmax} per unit leaf N and M_a was found only for temperate trees (Fig. 3.8; Table A3.2). The tropical trees exhibited lower V_{cmax} per unit leaf N for a given M_a than the temperate trees (Fig. 3.8), with an average of 30.4 ± 7.6 and 42.2 ± 15.8 µmol CO_2 gN^{-1} s^{-1} for tropical and temperate trees, respectively. In addition, tropical leaves contained lower leaf N and leaf phosphorus (P) than temperate leaves (p<0.05; Table 3.2). When placed in the context of the worldwide GLOPNET data (Hikosaka, 2004; Wright *et al.*, 2004), our selected tropical trees were relatively lower, while the selected temperate trees sat above the GLOPNET regression line.

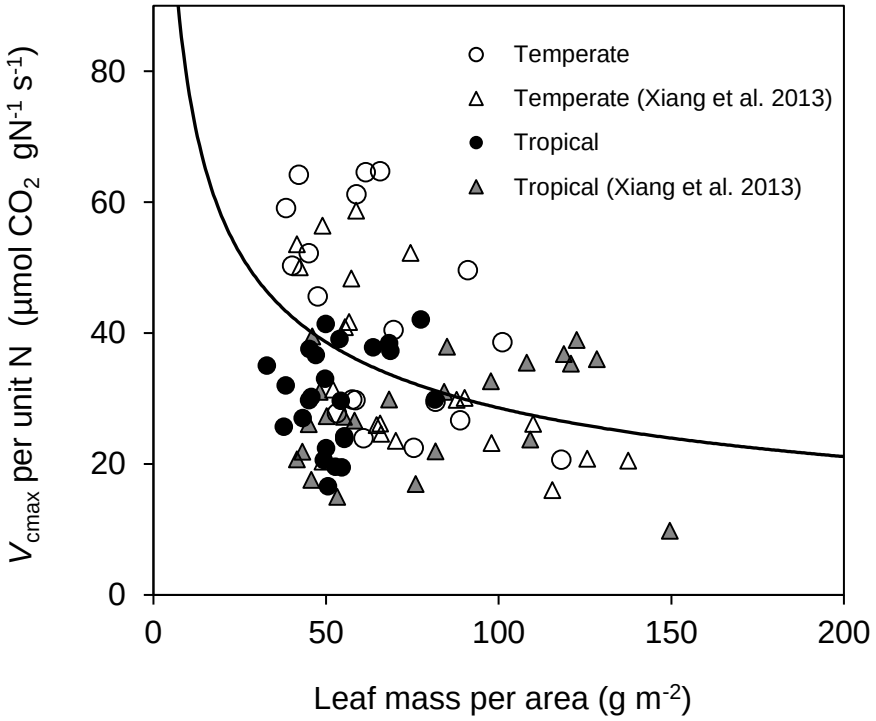

Figure 3.8. Relationships between maximum Rubisco carboxylation capacity, V_{cmax} per unit leaf nitrogen, N on area basis (applying finite g_m) and leaf mass per unit area (M_a). The line shown was inferred from the GLOPNET relationship between V_{cmax} per unit leaf N and M_a (Hikosaka, 2004; Wright *et al.*, 2004). Values of V_{cmax} per leaf N (applying infinite g_m) and M_a obtained from Xiang *et al.* (2013) were plotted on the same scale.

3.4 Discussion

3.4.1 Mesophyll conductance did not affect V_{cmax} estimation from CO_2 response curve

Traditionally, V_{cmax} is calculated from CO_2 response curves on a C_i basis, assuming infinite g_m - i.e. there is no limitation imposed by g_m and thus C_c equals C_i (Farquhar *et al.*, 1980; Long & Bernacchi, 2003). With progress in methods to estimate g_m, we now know that g_m is finite and C_c is significantly less than C_i (Evans *et al.*, 1986; Harley *et al.*, 1992; Lloyd *et al.*, 1992), our tropical and temperate tree species included (Fig. 3.3C). Despite the large influence of g_m in reducing CO_2 partial pressure at the site of carboxylation, the significant drawdown from C_i to C_c did not have impact on estimation of V_{cmax} (Fig. 3.5). Lower chloroplastic CO_2 partial pressure did not necessarily translate into substantial underestimation of V_{cmax} when C_i was used from CO_2 response curve. This observation contrasts studies that reported significant difference between C_c and C_i -based V_{cmax} when using appropriate Michaelis-Menten constants for CO_2 (K_c) and O_2 (K_o) in tobacco, grapevine, cucumber and mountain

beech (Flexas *et al.*, 2006; Flexas *et al.*, 2007; Whitehead *et al.*, 2011). C_i-based V_{cmax} values were 17% less than C_c –based V_{cmax} values in the most extreme cases (Fig. 3.4 and 3.5), which is much lower than 60-75% underestimation of V_{cmax} reported earlier (Warren, 2008; Sun *et al.*, 2014b). Moreover, comparison of our V_{cmax}-C_c values against those calculated by fitting eqn 4 (Sun *et al.*, 2014b), which allows conversion of $A \leftrightarrow C_i$ based parameters to the corresponding $A \leftrightarrow C_c$ based parameters, showed that C_c –based V_{cmax} obtained from direct conversion overestimated C_c –based V_{cmax} by 46%. The use of non-linear conversion equation as per Sun *et al.* (2014b) without adjusting appropriate K_c and K_o could explain the 46% discrepancy.

We show that V_{cmax} estimation on the basis of C_i was equivalent to that on the basis of C_c, when using appropriate K_c and K_o. Crucial to this outcome is the use of appropriate K_c and K_o depending on whether the analysis is based on C_i or C_c (von Caemmerer *et al.*, 1994; Bernacchi *et al.*, 2002). The estimates of K_c and K_o have been shown to depend on the value of g_m chosen for analysis, since g_m is linearly dependent on oxygen and inversely related to K_c; refer to eqn 14 [$K_{o\ (\infty)} = K_c + V_{cmax}/\ g_m$] in von Caemmerer *et al.* (1994). Therefore, apparent K_c will change depending on $V_{cmax}/\ g_m$. When fitting an $A \leftrightarrow C_c$ curve, commonly applied values of K_c are 260 µbar (von Caemmerer *et al.*, 1994), 272.4 µbar (Bernacchi *et al.*, 2001) or 315 µbar (Walker *et al.*, 2013) and K_o are 179 mbar (von Caemmerer *et al.*, 1994), 165.8 mbar (Bernacchi *et al.*, 2001) or 215 mbar (Walker *et al.*, 2013); all values were derived from tobacco. In absence of g_m, C_i-based parameters need to be applied in the Farquhar *et al.* model to account for 'apparent' Rubisco kinetic properties. The appropriate C_i-based values are 404 µbar and 248 mbar for K_c and K_o, respectively (von Caemmerer *et al.*, 1994) or 404.9 µbar and 278.4 mbar for K_c and K_o, respectively (Bernacchi *et al.*, 2002). If the same values were used to fit $A \leftrightarrow C_i$ and $A \leftrightarrow C_c$ curves, then one would obtain significantly lower V_{cmax} on C_i basis than that of C_c basis (Manter & Kerrigan, 2004; Warren, 2008).

The average values of g_m across woody evergreen, deciduous and conifers reported in the literature are close to 0.1 mol m^{-2} s^{-1} (Flexas *et al.*, 2008; Buckley & Warren, 2014) which might indicate that these plant groups are susceptible to significantly different estimates of V_{cmax} on C_c – and C_c –basis when the $V_{cmax}/\ g_m$ ratio is exceptionally large. In addition, a majority of water-stressed plants exhibited large drawdown from C_i to C_c i.e. imbalance V_{cmax}/g_m (Flexas *et al.*, 2006; Warren, 2008; Niinemets *et al.*, 2009). As the values of g_m in our study were larger than 0.1 mol m^{-2} s^{-1}

bar^{-1}, we did not cover the lower bound region where much larger C_i-C_c has been reported (Warren, 2008; Niinemets *et al.*, 2009). A definitive assessment of this issue will require further work focusing on very low range of g_m and validation on the interactive effects of internal and stomatal conductances in influencing water stress responses.

In recent years, V_{cmax} variations across biomes and plant functional types have been more comprehensively characterised and compiled. Majority of V_{cmax} estimations were based on Farquhar et al. (1980) model assuming infinite g_m (Walker *et al.*, 2014; Ali *et al.*, 2015; De Kauwe *et al.*, 2016), because few measurements of g_m were carried out in the field campaigns. More importantly, almost all terrestrial biosphere models use a derivation of Farquhar *et al.* (1980) model and its associated assumptions to estimate gross primary production (Rogers, 2014). Our study provides evidence that – at least for the species used in our study - a valid V_{cmax} estimate can be derived using either C_i or C_c, provided that appropriate Michaelis Menten constants for CO_2 and O_2 are used.

3.4.2 Photosynthetic rate and mesophyll conductance: relationship and limitation

The strong correlations between photosynthetic rate and mesophyll conductance for both tropical and temperate trees (Fig. 3.3A, Table A3.1) are consistent with previous studies on a range of species (Epron *et al.*, 1995; Evans & Loreto, 2000; Flexas *et al.*, 2008; Whitehead *et al.*, 2011; Tosens *et al.*, 2012). Contrary to our expectation, tropical and temperate species fell on a common $A \leftrightarrow g_m$ relationship (Figs 3.3A and 3.4A) and the drawdown of CO_2, C_a - C_i and C_i - C_c were independent of g_m (Figs 3.3B and 3.3C; Table A3.1) for both tropical and temperate species. Moreover, limitations to CO_2 diffusion imposed by mesophyll resistance were relatively constant across tropical and temperate species, irrespective of photosynthetic capacity (Fig. 3.6). Hence, our study showed that tropical trees exhibiting low photosynthetic rates are not penalised by low internal conductance, in contrast with past findings (Niinemets & Sack, 2006; Warren, 2008; Tosens *et al.*, 2012).

Estimation of the relative limitations of A imposed by stomatal and mesophyll resistances revealed that L_s were higher than those by L_m for half of species studied. For the other half of species, L_s were of similar order of magnitude as L_m (Fig. 3.6). This provides evidence that partially supports previous claim of dominant role of mesophyll resistance in limiting A (Epron *et al.*, 1995; Flexas *et al.*, 2008). The L_m values of

tropical and temperate trees (10- 30%) were consistent with those of ash and oak trees (Grassi & Magnani, 2005) but not as high as those reported by other studies on deciduous and evergreen trees (24-50%) (Epron *et al.*, 1995; Miyazawa & Terashima, 2001; Whitehead *et al.*, 2011). The range of L_s values across species, 23 to 60%, was higher than a range of tree species (10-35%) (Epron *et al.*, 1995; Miyazawa & Terashima, 2001; Grassi & Magnani, 2005; Whitehead *et al.*, 2011). Previous studies have shown that L_m and L_s vary seasonally especially in response to water stress and leaf ontogeny (Grassi & Magnani, 2005; Egea *et al.*, 2011; Whitehead *et al.*, 2011); however, we did not explore the influence of season on diffusional limitations.

The drawdown from C_i to C_c varies widely among species. Our average of C_i - C_c, 55 µbar, is consistent with values for tree species measured recently using the same instrument (von Caemmerer & Evans, 2015) but lower than those compiled earlier by Evans and Loreto (2000) and Warren (2008), 83 and 91 µbar, respectively. The range of g_m values, 0.08-0.47 mol m^{-2} s^{-1} bar^{-1}, is comparable to past studies (Pons & Welschen, 2003; Flexas *et al.*, 2008; Whitehead *et al.*, 2011; von Caemmerer & Evans, 2015), but much higher than the range reported in other studies on tropical and temperate trees (Kwesiga *et al.*, 1986; Ramos & Grace, 1990; Riddoch *et al.*, 1991; De Lucia *et al.*, 2003). The drawdown imposed by stomata, C_a - C_i (average of 103 µbar) was double that by the mesophyll. The average of C_a - C_i obtained in our study matches the average of woody evergreen, 109 µbar (Warren, 2008), and values for tree species (von Caemmerer & Evans, 2015). However, both resistances contribute a similar percentage of limitation to CO_2 assimilation rate (Fig. 3.6).

3.4.3 Photosynthetic rate, capacity and efficiency reflect adaptation to thermal environment

Lower rates of A, V_{cmax} and J_{max} (on both C_c and C_i basis) in tropical tree seedlings than their temperate counterparts were observed (Fig. 3.7; Table 3.2), consistent with the pattern reported by Xiang *et al.* (2013) and Scafaro *et al.* (submitted) who assumed infinite g_m. The average g_m of tropical and temperate trees was not statistically different (0.19 ± 0.06 vs. 0.23 ± 0.12 mol m^{-2} s^{-1} bar^{-1}, respectively), although slightly lower g_m was measured in tropical trees. As described in previous section, our result indicates that the lower photosynthetic rates of tropical species are unlikely to be caused by lower g_m (and thus lower concentrations of CO_2 at the site of carboxylation). Rather, the lower photosynthetic rate of tropical species reported here could be ascribed to lower

allocation of leaf N to photosynthetic capacity (resulting in lower PNUE), as well as lower leaf N content (Fig. 3.8; Table 3.2). Our results reinforced past observation of lower nitrogen investment in Rubisco causing lower photosynthetic rates in plants adapted to warm environments (Xiang *et al.*, 2013; Scafaro et al. submitted; Ali *et al.*, 2015; Dusenge *et al.*, 2015; Bahar *et al.*, 2017). The range of leaf mass per area observed here for tropical species overlapped that for temperate species. Consequently, the low PNUE of tropical species cannot simply be attributed to structural reasons (Fig. 3.8) and other explanations for why the efficiency of N use for carbon gain varies are needed.

3.4.4 Concluding statements

Our study showed lower rates of photosynthesis and underpinning biochemistry in tropical tree seedlings than their temperate counterparts (Table 3.2), which were not explained by lower mesophyll conductance. Our study provides evidence that - at least for the species used in our study - a valid V_{cmax} estimate can be derived using either C_i or C_c, provided that appropriate Michaelis Menten constants for CO_2 and O_2 are used.

Chapter 4: Synchronous development of photosynthetic capacity and diffusion conductances in tropical canopy species

4.1 Introduction

Photosynthetic capacity is central to predicting carbon exchange in tropical forests, with carbon uptake by tropical terrestrial ecosystems accounting for one-third of global gross primary productivity (GPP) (Beer *et al.*, 2010; Malhi, 2010). While photosynthesis in mature leaves plays a dominant role in determining tropical forest GPP, the timing and extent of photosynthetic CO_2 uptake during leaf expansion also needs to be considered, as variability in GPP of tropical forests is strongly influenced by changes in canopy phenology and associated physiological processes (Restrepo-Coupe *et al.*, 2013; Lopes *et al.*, 2016; Wu *et al.*, 2016). In vegetation models, changes in photosynthetic parameters during leaf expansion period are parameterised via: 1) partitioning leaves into separate age classes (Wu *et al.*, 2016); 2) leaf age-dependent changes in photosynthesis, such as increasing from a relatively low initial value to a prescribed maximum value (Krinner *et al.*, 2005; De Weirdt *et al.*, 2012); or, 3) application of a leaf flushing model which has a 1-2 months' time-lag component between physical appearance of leaves (greenness) and active photosynthesis (Restrepo-Coupe *et al.*, 2013). While changes in photosynthesis during leaf expansion are increasingly being accounted for in models of tropical ecosystem carbon uptake (De Weirdt *et al.*, 2012; Restrepo-Coupe *et al.*, 2013; Wu *et al.*, 2016), such models are not based on knowledge of mechanisms underpinning photosynthetic development in expanding tropical leaves. Rather, our understanding of photosynthetic development and associated changes in leaf anatomy, chemistry and physiology are derived mainly from temperate trees and crops (Šesták *et al.*, 1985; Niinemets *et al.*, 2012).

For many crop and temperate tree species, photosynthetic rates on area basis reach a maximum either at, or before, full leaf expansion (FLE) (Šesták *et al.*, 1985; Niinemets *et al.*, 2012). Similarly, tropical species show gradual increase in photosynthesis after leaf emergence, reaching maximum rates at FLE or few days thereafter (Kursar, T & Coley, P, 1992; Sobrado, 1994; Woodall *et al.*, 1998; Terwilliger *et al.*, 2001; Cai *et al.*, 2005). Increases in photosynthesis during leaf expansion are related to several factors including the development of internal leaf tissues and stomata (Marchi *et al.*, 2008; Kositsup *et al.*, 2010; England & Attiwill,

2011; Tosens *et al.*, 2012; Wu *et al.*, 2014), synthesis of chlorophyll (Woodall *et al.*, 1998; Gratani & Bonito, 2009; Varone & Gratani, 2009; Moraes *et al.*, 2011) and increases protein and Rubisco activity (Kursar, T & Coley, P, 1992; Eichelmann *et al.*, 2004; Maayan *et al.*, 2008). In most cases, the changes in these processes occur in synchrony with each other (Šesták *et al.*, 1985; Hanba *et al.*, 2001; Miyazawa & Terashima, 2001; Czech *et al.*, 2009; Niinemets *et al.*, 2012), although lags in the development of certain key components in photosynthetic metabolism have been reported (Baker & Hardwick, 1973; Kursar, T & Coley, P, 1992; Miyazawa *et al.*, 2003; Eichelmann *et al.*, 2004).

Photosynthetic capacity has been traditionally analysed in terms of biochemical [e.g. as maximal rates of Rubisco activity (V_{cmax}) and photosynthetic electron transport (J_{max})] and diffusional components, with resistance to CO_2 movement into leaves mainly attributed to stomatal diffusion. However, there is growing evidence of a significant contribution of mesophyll conductance (g_m) in the regulation of photosynthetic capacity (Evans *et al.*, 2009; Flexas *et al.*, 2012). Mesophyll conductance is known to increase together with leaf photosynthetic capacity during early leaf development (Hanba *et al.*, 2001; Miyazawa & Terashima, 2001; Miyazawa *et al.*, 2003; Eichelmann *et al.*, 2004; Marchi *et al.*, 2008); the extent to which g_m changes during development differs, however, among tree species (Miyazawa & Terashima, 2001; Miyazawa *et al.*, 2003; Marchi *et al.*, 2008; Tosens *et al.*, 2012). Although not much is known about changes in leaf anatomy and g_m in tropical tree species, detailed anatomical studies on the diffusion of CO_2 in temperate species have suggested that increases in g_m in expanding leaves could be primarily attributed to increases in chloroplast surface area exposed to intercellular air space (Tosens *et al.*, 2012; Tomás *et al.*, 2013), which enables easier CO_2 diffusion from sub-stomatal intercellular cavities to sites of carboxylation in chloroplasts.

Rates of net CO_2 uptake in leaves not only depend on development of photosynthetic capacity, but also on rates of non-photorespiratory mitochondrial CO_2 release (i.e. leaf respiration - *R*). When measured in darkness, the rate of *R* of young, expanding leaves (when photosynthesis is not fully functional) is greater than fully expanded leaves, reflecting higher demand for energy (e.g. ATP and reducing equivalents) to sustain the construction of leaf tissues and organelles and to support the cost of importing nitrogen and carbon from older leaves (Dickmann, 1971; Azcon-Bieto *et al.*, 1983; Shirke, 2001; Terwilliger *et al.*, 2001; Armstrong *et al.*, 2006; Marra *et al.*,

2009). In the light, mitochondria interact with chloroplasts via metabolite exchange between carbon/nitrogen cycles, by which *R* plays a role in assimilation of inorganic nitrogen (Sawhney *et al.*, 1978). On the one hand, the rates of *R* in light (R_{light}) of expanding leaves are thought to be relatively low due to low demand for the tricarboxylic acid intermediates by inorganic nitrogen assimilation. On the other, R_{light} has been shown to decrease with increasing leaf age (Villar *et al.*, 1995). Positive rates of net CO_2 uptake are only realised when leaves have expanded to the point where respiratory CO_2 release is exceeded gross photosynthesis (Terwilliger *et al.*, 2001; Miyazawa *et al.*, 2003). In many tropical species, positive rates of net CO_2 uptake were achieved at one-third of full leaf expansion (Woodall *et al.*, 1998; Terwilliger *et al.*, 2001; Cai *et al.*, 2005). However, some shade-tolerant tropical species do not exhibit positive net CO_2 uptake until a few weeks after FLE (Baker & Hardwick, 1973; Kursar, T & Coley, P, 1992). Following FLE, respiration reaches a near steady-state rate, with the rate of leaf *R* in mature leaves being dependent on energy demands associated with cellular maintenance, protein turnover and phloem loading (De Vries, 1975; Amthor, 2000).

During leaf formation, how nitrogen (N) is accumulated and allocated in young leaves will be crucial for development of photosynthetic capacity. Most of the N in young leaves is imported as organic N from older leaves (Kursar & Coley, 1991; Wendler *et al.*, 1995; Milla *et al.*, 2005) to support the synthesis of new cells and organelles, photo-protective enzymes and herbivore deterrence compounds (Kursar, T & Coley, P, 1992; Cai *et al.*, 2005; Tellez *et al.*, 2016). As leaves develop, the way in which N is partitioned is expected to change, reflecting changes in the balance between metabolic pathways, protein composition and functions (Niinemets *et al.*, 2012). How leaf N partitioning changes during tropical leaf development and how it influences photosynthetic N-use efficiency are, however, unknown. Most studies of leaf N partitioning tend to focus on fully mature leaves (Miyazawa & Terashima, 2001; Yasumura & Ishida, 2011; Moon *et al.*, 2015). In addition, most photosynthesis-development studies have focused on individual components (e.g. chlorophylls, Rubisco) rather than normalising each component to the overall N pool. While one study showed that the proportion of N allocated to Rubisco increases during leaf development in a Mediterranean shrub (Marchi *et al.*, 2008), it remains unclear whether this pattern holds for tropical moist forest species.

In this study, we explored various leaf traits during leaf development of five canopy species originating from tropical forest of Queensland, Australia. Using plants grown under controlled environment conditions, we monitored changes in leaf area and anatomy, chlorophyll content, photosynthetic rates and capacity, mesophyll and stomatal conductances, and respiratory rates (both in darkness and in the light) at 65 to 100% expansion and few weeks after full leaf expansion. In addition, the changes in the partitioning of leaf N over the course of leaf expansion were monitored. Our study tested the following hypotheses:

(1) As the species in our study are canopy species, all will exhibit gradual, synchronous development of key components of photosynthesis during expansion and reach maximum photosynthesis at full leaf expansion.
(2) Increases in photosynthetic capacity (as quantified by V_{cmax} and J_{max}) and net photosynthetic CO_2 uptake will be associated with increases in stomatal and mesophyll diffusion conductances (underpinned by changes in leaf anatomy) to maintain a balance between CO_2 supply and demand associated with increasing capacity for carbon fixation.
(3) Given that young leaves are likely to rely on organic N import (rather than assimilate inorganic N), we expect rates of leaf *R* in the light (R_{light}) to be relatively low in young leaves and increase as leaves expand. By contrast, rates of leaf R in darkness (R_{dark}) will be highest in young leaves (providing energy for leaf expansion) and decrease as leaves mature.
(4) The fraction of leaf N invested in photosynthetic metabolism will increase as leaves expand, irrespective of developmental changes in overall leaf N content.

4.2 Material and Methods

Seedlings of five tropical canopy species originated from moist-forests of Queensland (see Table 3.1 for details on provenance and climate parameters at each provenance) were grown in glasshouses in Canberra, Australia as described in Chapter 3. The glasshouse was controlled to achieve 30/25 °C day/night and plants were watered daily to exceed pot capacity. The experiment took place in September-October 2015 during which time the day length was 12 hours.

Measurements were performed at four developmental stages of the leaf (I, II, III, and IV), three replicates per developmental stage for each species. Due to constraints of plant number and time, leaves were sampled at different nodal positions down from the plant apex rather than following each given leaf through time. The youngest leaf developmental stage was restricted to expanding leaves that exhibited sufficient flux for carbon isotope discrimination measurements by a tuneable diode laser (TDL; TGA100, Campbell Scientific, Inc., Logan, UT, USA). Leaf traits were measured at four different stages of development; I, II and III, which corresponded to 70, 85, 100% of leaf length and stage IV which corresponded to few weeks after full expansion (i.e. stage III) to confirm whether our species exhibited normal or delayed greening. To provide an estimate of leaf age, leaf length was monitored in individual plants (Fig. 4.1). On average, full leaf expansion was reached in approximately 30 days (Fig. 4.1, Table 4.1).

CO_2 response curve and concurrent gas exchange and carbon isotope discrimination measurements were performed as described in Chapter 3. Similarly, leaf structural traits and nutrient content were measured as outlined in Chapter 3, with an additional measurement of 30 minutes dark-adapted chlorophyll *a* fluorescence ratio using a portable plant efficiency analyser (PEA, Hansatech, Norfolk, UK). The parameter F_v/F_m was taken directly from the output of PEA. Chlorophyll *a* fluorescence was recorded for 5 s following the onset of saturating red light.

4.2.1 Confocal microscopy

Measurements were carried out on leaves at stage I and III. Leaf sections were gently vacuum-infiltrated with water to remove air pockets and improve light transmission in leaf samples (Collings, 2015). The leaf sections were then incubated in 0.01% Tinopal LPW (a cell-wall staining agent; Ciba-Geigy Corp., Greensboro, NC, U.S.A) provided by Adrienne Hardham (RSB, ANU, Canberra) for 15 minutes. Leaf sections were mounted in water on microscope slides, with their transverse section towards the lens. Confocal microscopy was carried out using a Zeiss LSM780 UV-NLO confocal microscope (Zeiss Microscopy, Jena, Germany) with ZEN imaging software, housed within the Centre for Advanced Microscopy, Canberra. A range of dyes, which corresponded to specific range of wavelength settings were used to detect signals from chloroplasts and Tinopal LPW (i.e. cell walls). Laser line of 488 - 561 - 633 nm was chosen to enable detection of chloroplast and cell wall signals simultaneously.

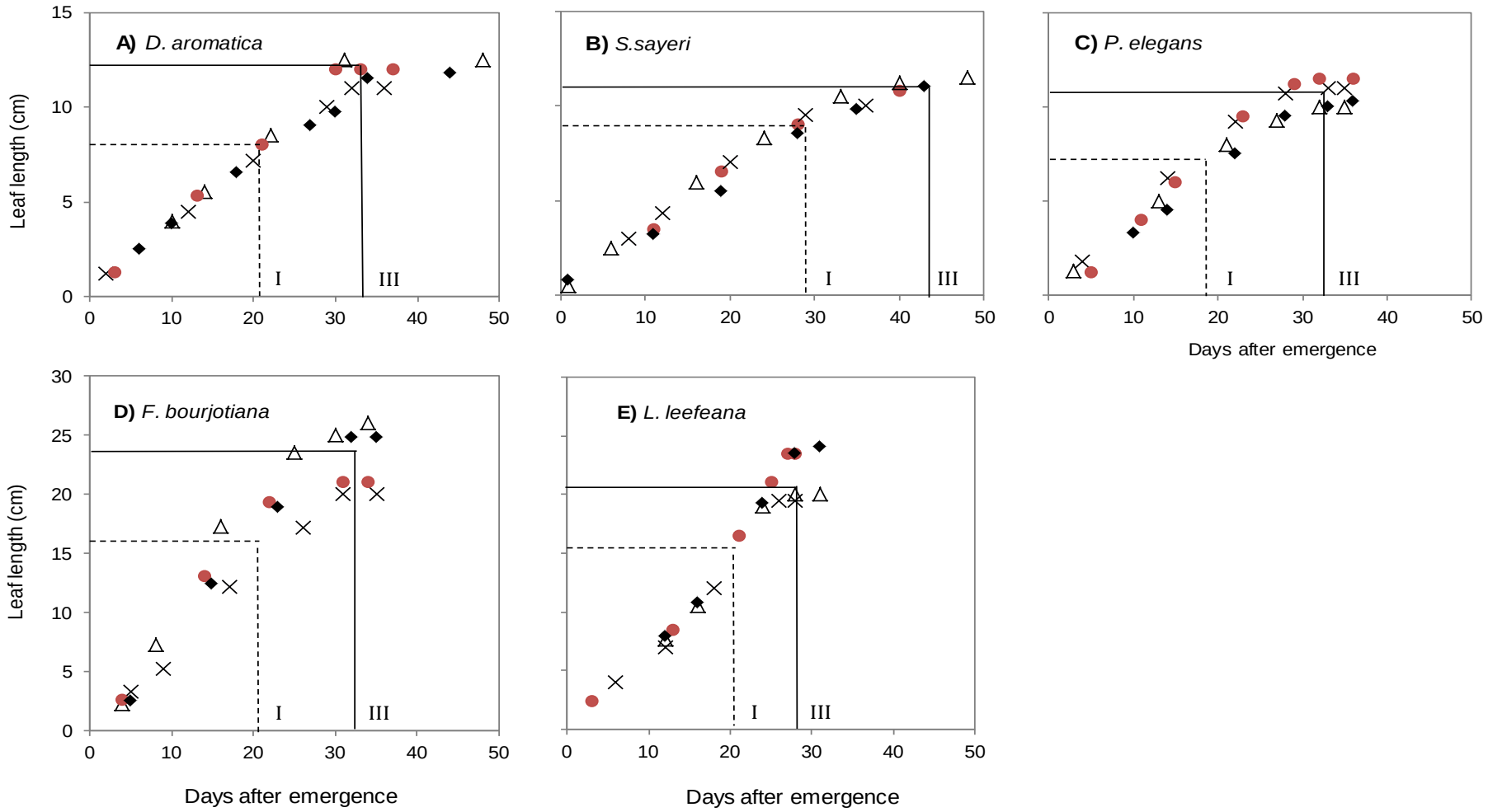

Figure 4.1. Changes in leaf length during leaf development in five tropical canopy species. Each symbol represents an individual plant replicate for each species (n= 4). Lines denote average leaf length for stage I and III, which was extrapolated to estimate days after emergence for each leaf stage.

Table 4.1. Species information. Average leaf length was extrapolated from Fig. 4.1 to estimate days after emergence for each leaf stage.

Abbrev.	Species	Habit	Stage	Estimated days after emergence (±3)	Leaf length (cm)	% leaf length relative to stage III
DA	*Doryphora aromatica*	Canopy tree	I	21	8.0 ± 0.7	0.65
			II	28	9.9 ± 1.1	0.81
			III	33	12.2 ± 1.6	1.00
			IV	43	11.9 ± 0.3	0.98
SS	*Syzygium sayeri*	Canopy tree	I	28	9.1 ± 1.6	0.82
			II	35	10.0 ± 0.9	0.89
			III	43	11.2 ± 0.5	1.00
			IV	55	11.5 ± 1.2	1.02
FB	*Flindersia bourjotiana*	Canopy tree	I	20	16.6 ± 3.4	0.70
			II	28	20.8 ± 1.2	0.88
			III	32	23.8 ± 2.9	1.00
			IV	40	18.3 ± 2.1	0.77
LL	*Litsea leefeana*	Canopy tree	I	21	15.7 ± 2.4	0.74
			II	22	18.1 ± 2.8	0.85
			III	27	21.3 ± 3.3	1.00
			IV	35	26.8 ± 3.6	1.26
PE	*Polyscias elegans*	Canopy tree	I	18	7.3 ± 0.3	0.67
			II	25	9.5 ± 1.4	0.87
			III	32	10.9 ± 1.2	1.00
			IV	40	10.9 ± 1.0	1.00

4.2.2 Statistical analysis

Statistical analyses were carried out using SPSS version 20 (IBM Corporation, NY, USA). Two way analysis of variance (ANOVA) was used to assess difference among developmental stages and interaction with species. The significant level was set at $P< 0.05$. In all traits (leaf chemistry, structure and physiology), there were significant species effect. As this study focuses on the general trend of changes in leaf traits with respect to developmental stages, *P*-values (indicated by different letters) were given only for averages of all species at each developmental stage.

4.3 Results

4.3.1 Leaf anatomy, structure and chemistry

Extensive changes in leaf anatomy were observed as leaves expanded. During the early stage of expansion (stage I), mesophyll cells were relatively small, densely packed, and weakly differentiated (Figs. 4.2A-E). Similarly, chloroplasts (in red in Fig. 4.2) were densely packed within mesophyll cells. Intercellular spaces were narrow. At full leaf expansion (FLE, stage III), the number of mesophyll cells did not appear to change (Figs. 4.2F-J). Mesophyll cells had fully expanded and differentiated into palisade and spongy layers. Chloroplasts were re-distributed across the surface of mesophyll cells, increasing chloroplast surface area exposed to intercellular air space. Intercellular spaces were more apparent.

Figure 4.2. Confocal images of transverse section of tropical leaves at stage I (panels on left) and III (panels on right). Images correspond to leaf section of *D.aromatica* (A, F), *S. sayeri* (B, G), *F. bourjotiana* (C, H), *L. leefeana* (D, I) and *P.elegans* (E, J). Bar = 100 µm. Cell walls were stained with Tinopal and observed by confocal fluorescence microscopy.

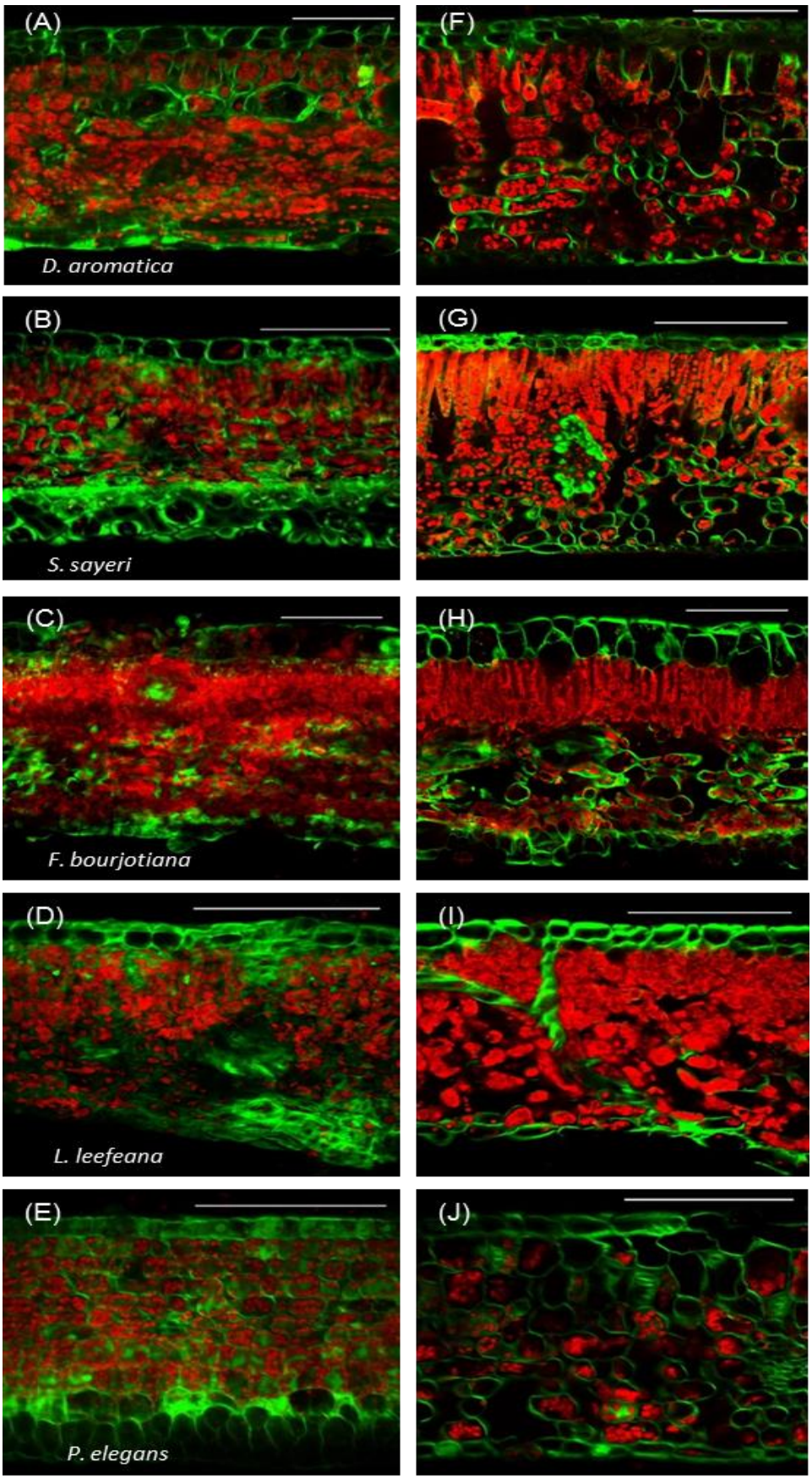

Modest increase in leaf thickness was observed as leaves developed from stage I, II, III to IV (Table 4.2). The qualitative changes in leaf anatomy were reflected in gradual increases in leaf dry and fresh mass per unit area, and leaf dry mass to leaf fresh mass ratio (Table 4.2). Developmental changes in leaf N per unit leaf area varied among species; there were modest increases as leaves expanded in *D. aromatica*, *S. sayeri* and *F. bourjotiana*, no change in *L. leefeana* and a reduction in *P. elegans* (Table 4.2). Hence, averaged across all five species, leaf N (area-based) remained constant from stage I to IV (Table 4.2). Average area-based leaf phosphorus (P) was highest at stage I then stabilised (Table 4.2). Mass-based leaf N and P decreased during leaf expansion (with exception for *S. sayeri* which showed no change in N_{mass} across leaf stages) (Table 4.2).

Chlorophyll content per unit leaf area steadily increased throughout expansion for four species (Table 4.2). By the time leaves were ~85% fully expanded (stage II), average chlorophyll content was around 80% those of fully expanded leaves. By contrast, *P. elegans* exhibited a decline in chlorophyll content per unit area as leaves expanded (Table 4.2). Lowest values of F_v/F_m (dark-adapted chlorophyll *a* fluorescence ratio) was recorded in stage I; F_v/F_m ratio began to increase at stage II, achieving a steady state around 0.83 thereafter (Table 4.3).

Table 4.2. Leaf structural and chemical traits of species studied. Values are mean ± SD (n=3 for each species). Abbreviation: M_a= leaf dry mass per unit leaf area, F_a = leaf fresh mass per unit leaf area, LDM:LFM = leaf dry mass to leaf fresh mass ratio, leaf P = leaf phosphorus, leaf N = leaf nitrogen.

Species	Leaf stage	*M*a ($g\ m^{-2}$)	*F*a ($g\ m^{-2}$)	LDM:LFM	Thickness (mm)	Leaf P ($g\ m^{-2}$)	Leaf P-mass ($mg\ g^{-1}$)	Leaf N-area ($g\ m^{-2}$)	Leaf N-mass ($mg\ g^{-1}$)	Chlorophyll -area ($g\ m^{-2}$)	Chlorophyll-mass ($mg\ g^{-1}$)
D. aromatica	I	30 ± 2	178 ± 13	0.17 ± 0.02	0.17 ± 0.02	0.07 ± 0.01	2.2 ± 0.1	1.36 ± 0.18	46 ± 3	0.40 ± 0.14	13.4 ± 5.0
	II	35 ± 4	179 ± 7	0.20 ± 0.03	0.20 ± 0.02	0.06 ± 0.00	1.7 ± 0.1	1.33 ± 0.19	38 ± 1	0.44 ± 0.11	12.5 ± 1.8
	III	52 ± 9	191 ± 7	0.27 ± 0.05	0.20 ± 0.01	0.08 ± 0.01	1.5 ± 0.3	1.61 ± 0.11	31 ± 4	0.67 ± 0.04	13.2 ± 2.3
	IV	59 ± 3	204 ± 6	0.29 ± 0.01	0.22 ± 0.03	0.09 ± 0.00	1.5 ± 0.1	1.56 ± 0.11	26 ± 1	0.70 ± 0.02	12.0 ± 0.7
S. sayeri	I	35 ± 4	177 ± 37	0.28 ± 0.03	0.20 ± 0.02	0.05 ± 0.00	1.5 ± 0.2	0.68 ± 0.04	20 ± 4	0.21 ± 0.14	6.4 ± 5.2
	II	35 ± 3	180 ± 6	0.27 ± 0.03	0.19 ± 0.01	0.04 ± 0.00	1.2 ± 0.1	0.74 ± 0.06	22 ± 1	0.27 ± 0.04	8.0 ± 1.9
	III	41 ± 8	194 ± 9	0.30 ± 0.05	0.19 ± 0.02	0.05 ± 0.01	1.3 ± 0.2	0.82 ± 0.22	20 ± 2	0.36 ± 0.11	8.8 ± 2.3
	IV	47 ± 7	201 ± 12	0.33 ± 0.03	0.19 ± 0.01	0.06 ± 0.02	1.2 ± 0.3	0.98 ± 0.11	21 ± 1	0.40 ± 0.04	8.6 ± 1.8
F. bourjotiana	I	42 ± 3	177 ± 11	0.24 ± 0.00	0.19 ± 0.02	0.09 ± 0.01	2.1 ± 0.2	1.17 ± 0.12	28 ± 2	0.37 ± 0.02	8.9 ± 0.5
	II	58 ± 16	203 ± 26	0.28 ± 0.04	0.22 ± 0.02	0.06 ± 0.00	1.1 ± 0.4	1.19 ± 0.18	21 ± 4	0.53 ± 0.03	9.4 ± 2.3
	III	72 ± 6	215 ± 9	0.34 ± 0.02	0.23 ± 0.02	0.05 ± 0.01	0.7 ± 0.2	1.35 ± 0.01	19 ± 2	0.63 ± 0.04	8.7 ± 0.1
	IV	70 ± 8	208 ± 11	0.34 ± 0.03	0.23 ± 0.01	0.06 ± 0.01	0.8 ± 0.1	1.32 ± 0.07	19 ± 1	0.61 ± 0.07	8.6 ± 0.0
L. leefeana	I	37 ± 4	121 ± 7	0.30 ± 0.02	0.15 ± 0.02	0.07 ± 0.01	1.9 ± 0.2	1.16 ± 0.18	32 ± 4	0.51 ± 0.12	14.2 ± 5.1
	II	52 ± 8	129 ± 25	0.40 ± 0.03	0.15 ± 0.02	0.07 ± 0.01	1.3 ± 0.1	1.24 ± 0.37	23 ± 3	0.59 ± 0.04	11.5 ± 1.0
	III	53 ± 4	127 ± 4	0.42 ± 0.02	0.15 ± 0.01	0.07 ± 0.01	1.3 ± 0.2	1.20 ± 0.26	23 ± 4	0.64 ± 0.10	12.1 ± 2.3
	IV	51 ± 5	125 ± 10	0.40 ± 0.03	0.14 ± 0.00	0.05 ± 0.01	1.0 ± 0.1	0.94 ± 0.25	18 ± 3	0.59 ± 0.08	11.7 ± 0.8
P. elegans	I	48 ± 1	141 ± 5	0.34 ± 0.01	0.11 ± 0.01	0.08 ± 0.01	1.7 ± 0.2	1.81 ± 0.25	38 ± 5	0.61 ± 0.09	12.7 ± 2.1
	II	49 ± 3	140 ± 7	0.35 ± 0.01	0.13 ± 0.02	0.07 ± 0.00	1.4 ± 0.1	1.41 ± 0.16	29 ± 4	0.68 ± 0.03	13.8 ± 1.5
	III	66 ± 1	157 ± 3	0.42 ± 0.00	0.14 ± 0.02	0.07 ± 0.01	1.0 ± 0.2	1.17 ± 0.15	18 ± 2	0.55 ± 0.06	8.3 ± 0.8
	IV	48 ± 5	136 ± 12	0.36 ± 0.05	0.13 ± 0.01	0.06 ± 0.01	1.2 ± 0.2	0.79 ± 0.07	16 ± 1	0.47 ± 0.07	9.6 ± 0.9
All species average	I	38 ± 7 a	159 ± 29 a, b	0.27 ± 0.06 a	0.16 ± 0.01 a	0.07 ± 0.01 a	1.9 ± 0.3 a	1.2 ± 0.4 a	32 ± 10 a	0.42 ± 0.17 a	11.1 ± 4.6 a
	II	46 ± 12 b	166 ± 32 b	0.30 ± 0.08 b	0.17 ± 0.01 a, b	0.06 ± 0.01 b	1.3 ± 0.3 b	1.2 ± 0.3 a	26 ± 7 b	0.50 ± 0.15 b	11.0 ± 2.6 a
	III	57 ± 13 c	177 ± 33 c	0.35 ± 0.07 c	0.18 ± 0.01 b	0.06 ± 0.01 b	1.2 ± 0.3 c	1.2 ± 0.3 a	22 ± 6 c	0.57 ± 0.13 c	10.2 ± 2.6 a
	IV	55 ± 10 c	175 ± 38 b, c	0.34 ± 0.05 c	0.18 ± 0.01 b	0.06 ± 0.02 b	1.1 ± 0.3 c	1.1 ± 0.3 a	20 ± 4 c	0.55 ± 0.12 b, c	10.1 ± 1.7 a

4.3.2 Development and maturation of photosynthetic capacity and respiration

Net photosynthetic rate (*A*) gradually increased throughout leaf expansion, reaching maximum rates at stage III (5.7 - 13.6 µmol m^{-2} s^{-1}) (Table 4.3, Fig. 4.3A). On average, stage II (~85% of FLE) photosynthetic rates were 80% of those at FLE (Fig. 4.3A). Stomatal conductance (g_s) and mesophyll conductance (g_m) were lowest in recently expanding leaves and gradually increased until FLE (Table 4.3, Fig. 4.3B and C). Photosynthetic electron transport capacity (J_{max}) and maximum Rubisco carboxylation capacity (V_{cmax}) increased in synchrony with *A*, g_s and g_m over the course of leaf expansion (Table 4.3). By the time leaves were 85% fully expanded (stage II), average J_{max} and V_{cmax} were 80% those of fully expanded leaves (Table 4.3). V_{cmax} and J_{max} co-varied positively (r^2 = 0.74, $p<0.05$), with no distinct clustering across different leaf developmental stages (Fig. 4.4A) or species (Fig. 4.4B).

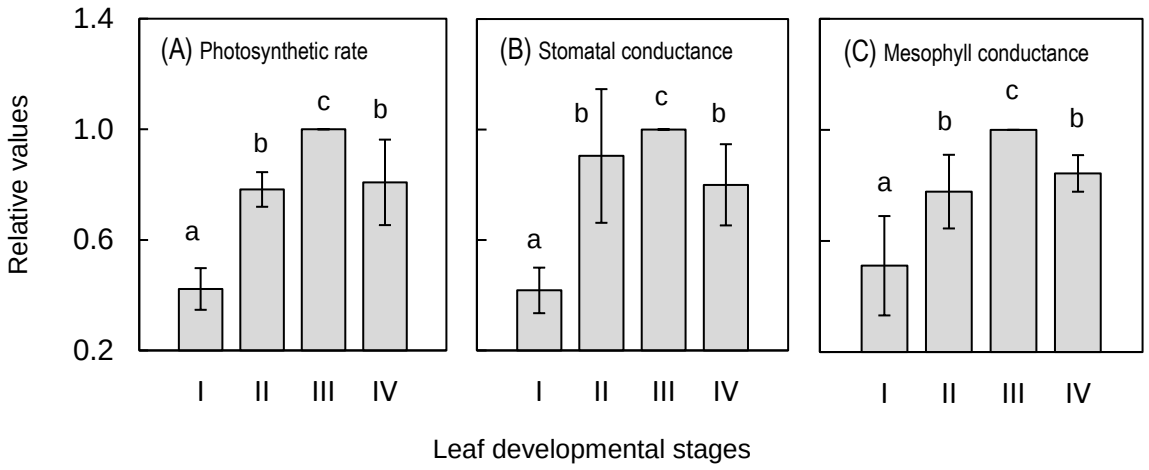

Figure 4.3. Changes in photosynthetic rates and diffusion conductances from leaf stage I to IV, expressed relative to absolute values at stage III. Shown is average of five species ± SD. Different letters indicated significant differences ($p<0.05$).

Changes in CO_2 drawdown from the atmosphere to the sub-stomatal cavity (C_a - C_i i.e. the measure of stomatal limitation) following leaf expansion varied between species (Table 4.3). *D. aromatica* and *F. bourjotiana* exhibited increases in C_a - C_i between stage I and III, no change in *P. elegans* and a decrease in C_a - C_i in *L. leefeana* and *S. sayeri* with leaf expansion (Table 4.3). For all species, no changes in C_a - C_i occurred after FLE. The CO_2 drawdown imposed by g_m, C_i - C_c, did not change much over the course of leaf expansion for four species, except for *P. elegans* which showed reduction in C_i - C_c with leaf expansion (Table 4.3).

Table 4.3. Leaf gas exchange and fluorescence traits of species studied. Values are mean ± SD (n=3 for each species). Abbreviation: A = light-saturated net photosynthesis measured at 400 µmol mol^{-1} CO_2, g_s = stomatal conductance, g_m = mesophyll conductance, R_{dark} = dark respiration rate, R_{light} = light respiration rate, V_{cmax} = maximum carboxylation velocity of Rubisco, J_{max} = maximum rate of electron transport, V_{cmax}:N = maximum carboxylation velocity of Rubisco per unit leaf nitrogen, R_{dark}:V_{cmax} = ratio of R_{dark} to V_{cmax}, C_a - C_i = drawdown of CO_2 from the atmosphere to the substomatal cavity, C_i - C_c = drawdown of CO_2 from the substomatal cavity to chloroplast, F_v : F_m = maximum quantum yield of fluorescence.

Species	Leaf stage	A (µmol m^{-2} s^{-1})	g_s (mol m^{-2} s^{-1})	g_m (mol m^{-2} s^{-1} bar^{-1})	R_{dark} (µmol m^{-2} s^{-1})	R_{light} (µmol m^{-2} s^{-1})	V_{cmax} (µmol m^{-2} s^{-1})	J_{max} (µmol m^{-2} s^{-1})	V_{cmax} : N (µmol CO_2 gN^{-1} s^{-1})	R_{dark}: V_{cmax}	C_a - C_i (µbar)	C_i - C_c (µbar)	F_v : F_m
D. aromatica	I	2.0 ± 0.5	0.03 ± 0.01	0.05 ± 0.02	1.6 ± 0.6	2.0 ± 0.4	17.9 ± 5.7	37.1 ± 6.9	13 ± 4	0.10 ± 0.08	117 ± 35	48 ± 27	0.77 ± 0.03
	II	4.4 ± 0.3	0.08 ± 0.01	0.07 ± 0.01	1.4 ± 0.1	1.9 ± 0.6	27.2 ± 9.9	47.7 ± 5.5	20 ± 6	0.06 ± 0.02	95 ± 13	66 ± 10	0.81 ± 0.00
	III	5.7 ± 1.3	0.07 ± 0.03	0.12 ± 0.04	0.8 ± 0.1	2.0 ± 0.3	39.9 ± 4.2	65.6 ± 4.2	25 ± 1	0.02 ± 0.00	150 ± 29	51 ± 8	0.82 ± 0.01
	IV	5.6 ± 1.6	0.06 ± 0.02	0.11 ± 0.04	0.8 ± 0.2	1.9 ± 0.4	37.9 ± 11.0	59.3 ± 7.6	24 ± 8	0.02 ± 0.01	146 ± 4	54 ± 10	0.81 ± 0.01
S. sayeri	I	4.7 ± 0.6	0.06 ± 0.01	0.12 ± 0.03	1.1 ± 0.2	1.8 ± 0.1	31.3 ± 7.3	53.6 ± 6.0	46 ± 14	0.09 ± 0.01	130 ± 8	42 ± 14	0.81 ± 0.04
	II	7.7 ± 1.4	0.14 ± 0.04	0.15 ± 0.00	0.8 ± 0.1	1.6 ± 0.3	43.1 ± 10.6	62.9 ± 12.7	58 ± 15	0.03 ± 0.01	101 ± 27	52 ± 9	0.82 ± 0.03
	III	9.4 ± 1.9	0.17 ± 0.03	0.16 ± 0.03	0.9 ± 0.1	1.5 ± 0.1	51.1 ± 13.5	76.0 ± 11.0	63 ± 14	0.02 ± 0.01	96 ± 24	58 ± 0	0.81 ± 0.01
	IV	7.9 ± 0.6	0.13 ± 0.01	0.13 ± 0.02	0.8 ± 0.2	1.6 ± 0.3	47.1 ± 9.3	75.3 ± 6.6	48 ± 5	0.01 ± 0.00	104 ± 5	61 ± 12	0.82 ± 0.00
F. bourjotiana	I	3.9 ± 0.5	0.05 ± 0.02	0.12 ± 0.04	2.3 ± 0.4	2.3 ± 0.4	26.5 ± 1.2	61.0 ± 2.7	23 ± 2	0.04 ± 0.02	129 ± 30	36 ± 16	0.71 ± 0.07
	II	8.3 ± 1.2	0.13 ± 0.02	0.18 ± 0.03	1.5 ± 0.5	2.1 ± 0.3	45.1 ± 7.6	81.5 ± 15.3	39 ± 8	0.02 ± 0.01	113 ± 11	46 ± 10	0.75 ± 0.02
	III	10.5 ± 1.4	0.12 ± 0.02	0.25 ± 0.02	0.9 ± 0.3	1.8 ± 0.3	62.1 ± 10.7	98.2 ± 11.4	46 ± 8	0.02 ± 0.01	152 ± 21	42 ± 2	0.82 ± 0.02
	IV	9.6 ± 2.1	0.11 ± 0.03	0.20 ± 0.02	0.7 ± 0.1	2.1 ± 0.3	55.3 ± 7.8	89.4 ± 6.6	42 ± 4	0.02 ± 0.01	149 ± 15	49 ± 11	0.81 ± 0.03
L. leefeana	I	5.6 ± 1.4	0.09 ± 0.03	0.12 ± 0.03	1.5 ± 0.4	2.2 ± 0.5	37.3 ± 6.8	55.0 ± 6.4	33 ± 9	0.06 ± 0.01	117 ± 19	47 ± 8	0.79 ± 0.04
	II	9.4 ± 2.4	0.22 ± 0.08	0.17 ± 0.03	0.9 ± 0.2	1.7 ± 0.1	48.9 ± 4.9	74.8 ± 9.8	41 ± 9	0.03 ± 0.01	80 ± 17	55 ± 3	0.83 ± 0.01
	III	11.1 ± 1.4	0.21 ± 0.04	0.19 ± 0.02	0.8 ± 0.3	1.8 ± 0.1	63.6 ± 7.5	84.4 ± 12.3	54 ± 6	0.01 ± 0.00	93 ± 14	58 ± 4	0.83 ± 0.01
	IV	7.3 ± 0.4	0.15 ± 0.05	0.17 ± 0.03	0.5 ± 0.1	1.2 ± 0.1	37.6 ± 1.9	53.8 ± 5.9	42 ± 8	0.02 ± 0.00	94 ± 28	45 ± 8	0.83 ± 0.00
P. elegans	I	5.2 ± 0.8	0.11 ± 0.02	0.06 ± 0.03	2.0 ± 0.1	1.7 ± 0.3	32.5 ± 3.7	70.3 ± 6.1	18 ± 4	0.04 ± 0.01	85 ± 14	90 ± 22	0.82 ± 0.01
	II	9.3 ± 0.5	0.17 ± 0.05	0.17 ± 0.02	1.3 ± 0.3	1.4 ± 0.2	49.1 ± 6.1	72.9 ± 1.0	35 ± 1	0.02 ± 0.00	99 ± 21	56 ± 5	0.84 ± 0.00
	III	13.6 ± 0.3	0.33 ± 0.04	0.21 ± 0.01	1.0 ± 0.1	1.5 ± 0.1	70.4 ± 5.0	103.7 ± 4.6	60 ± 4	0.01 ± 0.00	77 ± 9	64 ± 3	0.84 ± 0.01
	IV	8.7 ± 1.5	0.22 ± 0.03	0.17 ± 0.02	0.9 ± 0.1	1.3 ± 0.4	39.3 ± 10.6	78.1 ± 10.9	51 ± 18	0.01 ± 0.00	74 ± 4	51 ± 9	0.85 ± 0.00
All species average	I	4.3 ± 1.5 a	0.07 ± 0.03 a	0.09 ± 0.04 a	1.7 ± 0.5 a	2.0 ± 0.4 a	29.2 ± 8.3 a	55.4 ± 12.3 a	27 ± 14 a	0.07 ± 0.04 a	115 ± 26 a	53 ± 25 a	0.78 ± 0.06 a
	II	7.8 ± 2.2 b	0.15 ± 0.06 b	0.15 ± 0.05 b	1.2 ± 0.4 b	1.7 ± 0.4 b	42.8 ± 11.0 b	68.0 ± 14.9 b	39 ± 15 b	0.03 ± 0.02 b	98 ± 19 b	55 ± 9 a	0.81 ± 0.04 b
	III	10.1 ± 2.9c	0.18 ± 0.09 c	0.19 ± 0.05 c	0.9 ± 0.2 c	1.7 ± 0.3 b	57.7 ± 13.6 c	85.6 ± 16.5 c	50 ± 16 c	0.02 ± 0.01 b	114 ± 37 a	55 ± 9 a	0.82 ± 0.02 b
	IV	7.8 ± 1.8 b	0.14 ± 0.06 b	0.16 ± 0.04 b	0.8 ± 0.2 c	1.6 ± 0.4 b	43.8 ± 10.2 b	71.5 ± 15.2 b	41 ± 13 b	0.02 ± 0.01 b	114 ± 33 a	52 ± 10 a	0.82 ± 0.02 b

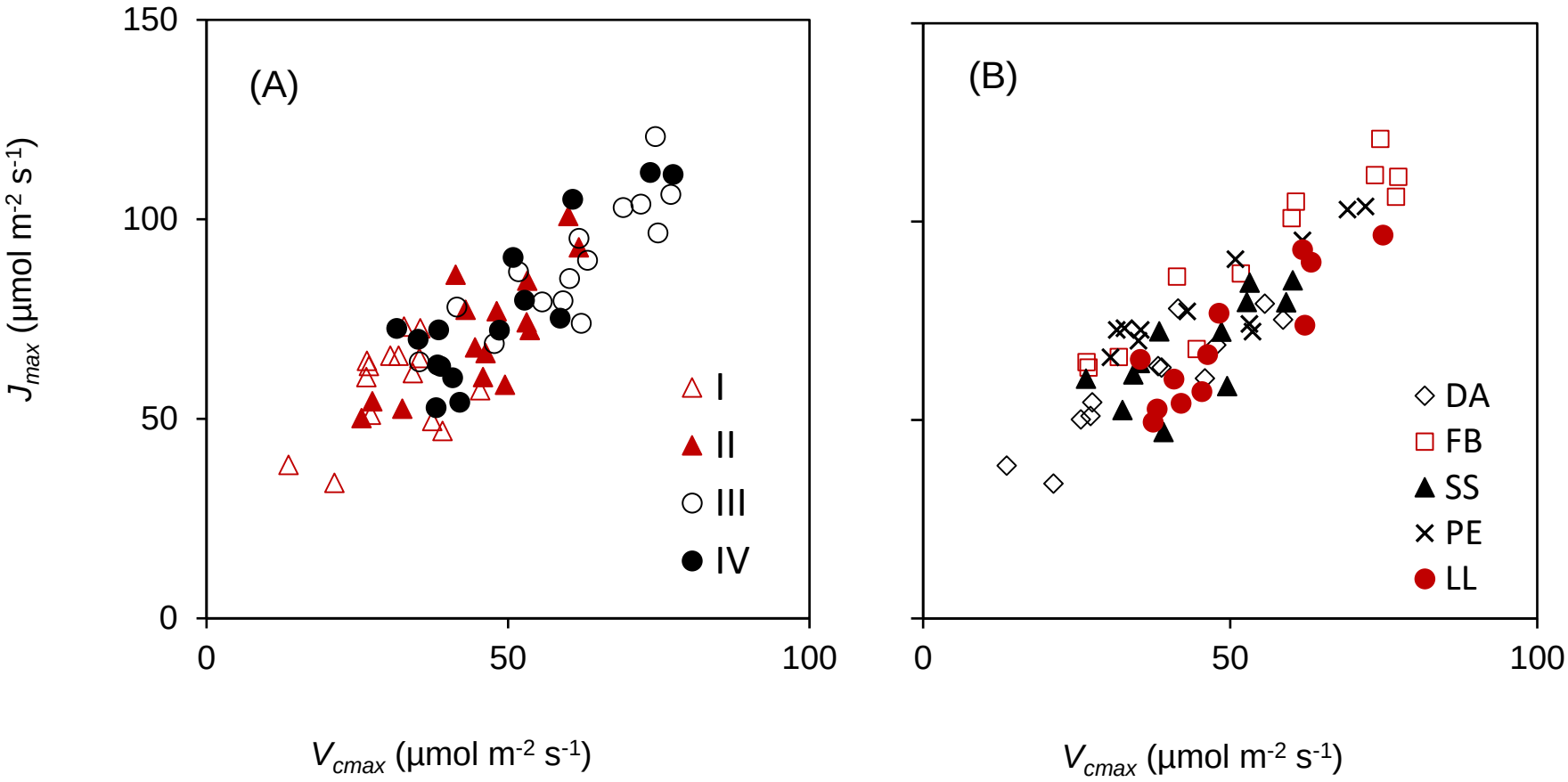

Figure 4.4. Relationships between J_{max} (maximum electron transport rate) and V_{cmax} (maximum Rubisco carboxylation capacity) estimated using finite mesophyll conductance, $g_{m,}$ according to leaf developmental stage (A) and species (B). Values expressed on area basis. Species abbreviation is provided in Table 4.1.

Dark respiration rates (R_{dark}) of expanding leaves were higher than those in fully expanded leaves; the average rates at stage I were double those of stage III (Table 4.3). R_{dark} declined following leaf expansion in all species, reaching a steady state at FLE (Table 4.3). Respiration rates in light (R_{light}) did not change across the different leaf stages of four species except for *L. leefeana*, which showed reduction in R_{light} with leaf expansion (Table 4.3). On average, rates of R_{light} were highest in stage I leaves (Table 4.3). Significant, albeit weak negative relationships were observed between R_{dark} and V_{cmax} ($r^2 = 0.23$, $p<0.05$) (Figs. 4.5A and C). Leaves of stage I occupied the top end of R_{dark} and V_{cmax} relationships (Fig. 4.5A) with average R_{dark} to V_{cmax} to ratio of 0.07 ± 0.04, which was expected given highest R_{dark} and lowest V_{cmax} of this cohort (Table 4.3). Interestingly, there were species-specific clusters along R_{dark} and V_{cmax} relationships (Fig. 4.5C); tall, fast-growing species (*F. bourjotiana*, FB, and *P. elegans*, PE) exhibited higher R_{dark} per given V_{cmax} whilst medium-sized species with moderate growth rate (*D. aromatica*, DA, and *S. sayeri*, SS) showed lower R_{dark} per given V_{cmax}. No significant correlation was found between R_{light} and V_{cmax} ($p>0.05$; Figs. 4.5B and D).

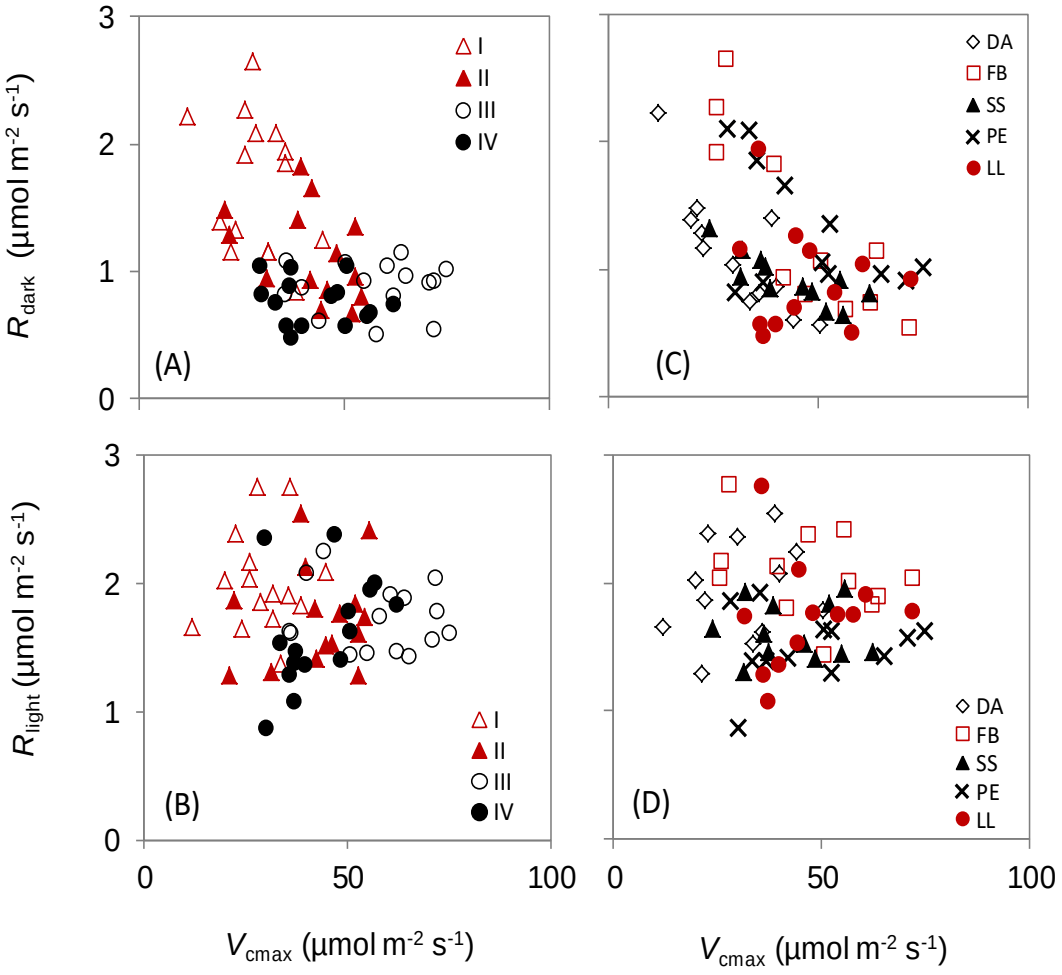

Figure 4.5. Upper panel: Relationships between R_{dark} (respiration rates in dark) and V_{cmax} according to leaf developmental stage (A) and species (C). Lower panel: Relationships between R_{light} (respiration rates in light) and V_{cmax} according to leaf developmental stage (B) and species (D). Values expressed on area basis.

4.3.3 Nitrogen use and partitioning throughout leaf expansion

Photosynthetic N-use efficiency, as calculated by the ratio of V_{cmax} per unit leaf N, was lowest in recently expanding leaves (50% those of fully expanded leaves) (Table 4.3). A significant negative correlation between photosynthetic N-use efficiency and leaf nitrogen (area-basis) was observed (r^2 = 0.41, $p<0.05$) (data not shown), with fully expanded leaves (stage III) and recently expanding leaves (stage I) showed highest and lowest photosynthetic N-use efficiency for a given leaf N, respectively. There was no significant correlation between V_{cmax} and leaf N.

The total fraction on N, n_A, invested in photosynthetic machinery increased gradually following leaf expansion, driven by proportional increase in N allocation to pigment-protein complexes (n_P), electron transport (n_E) and Rubisco (n_R) (Fig. 4.6). N investment in Rubisco doubled from stage I to stage III in *D. aromatica*, *F. bourjotiana* and *P. elegans*; ~ 8-21% of leaf N was allocated to Rubisco at FLE. A large proportion of N was inferred to be allocated in pigment-protein complexes, with n_P being greater than n_R and n_E combined. There were considerable variations in the fraction of total N in photosynthesis among species at FLE (37-57%).

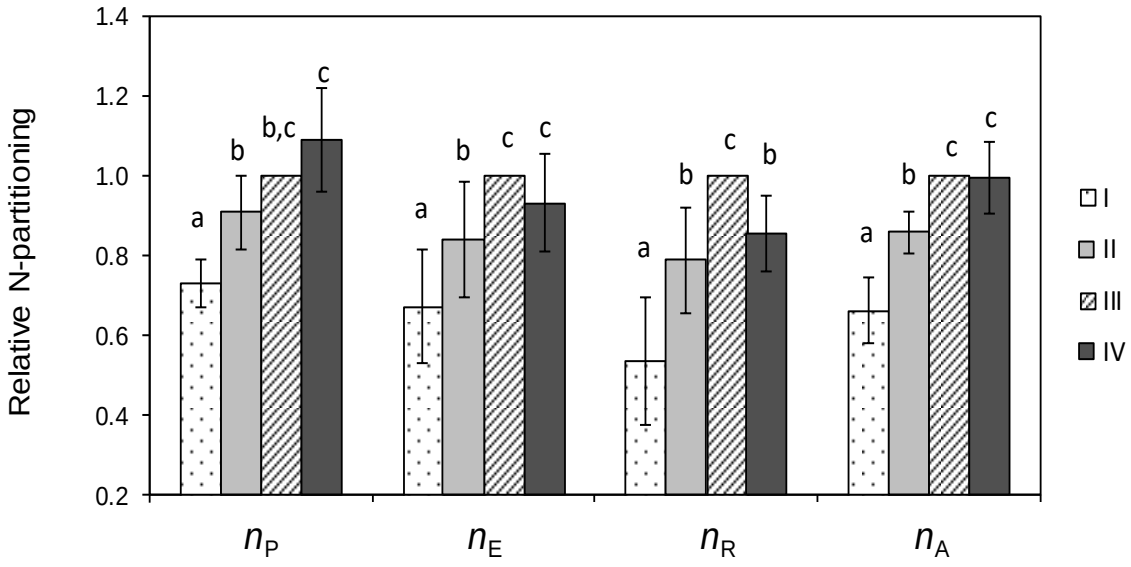

Figure 4.6. Changes in N partitioning to photosynthetic metabolism from leaf stage I to IV, expressed relative to absolute values at stage III. Shown is average of five species ± SD. Different letters indicated significant differences ($p<0.05$). Abbreviations: n_P = fraction of leaf N in pigment-protein complexes, n_E = fraction of leaf N in electron transport, n_R = fraction of leaf N in Rubisco and n_A = total fraction of leaf N allocated in photosynthetic metabolism.

4.4 Discussion

4.4.1 Coordination in photosynthetic maturity during tropical leaf development

In our study, the five tropical canopy species *D. aromatica*, *S. sayeri*, *F. bourjotiana*, *L. leefeana* and *P. elegans* exhibited synchronous increases in photosynthetic capacity, net CO_2 uptake rates, chlorophyll content and diffusion conductances, achieving maximum levels at FLE (Table 4.2 and 4.3, Fig. 4.3). Although we did not quantify changes in protein abundance associated with photosynthetic metabolism, an early study on a tropical light-demanding tree *Annona spraguei* suggested that Rubisco and light-harvesting chlorophyll proteins accumulated in a co-ordinated manner during development, reaching maximum levels at FLE, and then stabilised (Kursar, T & Coley, P, 1992). We found that V_{cmax} and J_{max} co-varied positively across all leaf developmental stages (Fig. 4.4A); this indicates a tight co-regulation between soluble and thylakoid proteins which are involved in the dark and light reactions, even at an early stage of leaf expansion (Wullschleger, 1993; Marchi *et al.*, 2008).

At the early stage of leaf expansion, we found that F_v/F_m values were slightly but significantly lower than was the case in mature leaves (Table 4.3), suggesting that the absorbed light energy was not fully utilised in photochemistry at stage I (Cai *et al.*, 2005; Demmig-Adams & Adams, 2006). Past studies have reported that young tropical leaves exhibit a high degree of reversible photoinhibition to protect photosynthetic apparatus from photo-oxidative damage (Krause *et al.*, 1995; Dodd *et al.*, 1998). In addition, young leaves contain high levels of photoprotective enzymes and pigments (Coley & Aide, 1989; Krause *et al.*, 1995; Woodall *et al.*, 1998; Cai *et al.*, 2005), which might explain the colourful display of red, pink, white and sometimes blue flushes in tropical forest (Dominy *et al.*, 2002). Investment in accessory pigments can reduce F_v/F_m values, while also helping protect leaves from oxidative damage.

As leaves expanded, both the biochemical components that underpin photosynthetic capacity (V_{cmax} and J_{max}) and diffusional components controlling CO_2 movement to the site of carboxylation (g_s and g_m) increased, with chlorophyll also accumulating (Table 4.3). Associated with these changes was the relatively constant drawdown of CO_2 from the atmosphere to the sub-stomatal cavity, and then to the chloroplast (i.e. C_a - C_i and C_i - C_c; Table 4.3). Thus, increases in the demand for CO_2 were matched by increases in CO_2 supply. Past studies have highlighted how

coordination in photosynthetic capacity and diffusion conductance is underpinned by tight co-regulation of primary metabolism (sugars, phosphorylated intermediates, and organic and amino acids) via feedback mechanisms (Paul & Pellny, 2003; Gago *et al.*, 2016). Our study shows that this coordination is not restricted to mature leaves – rather, coordination is maintained throughout leaf development.

4.4.2 Changes in mesophyll conductance reflect changes in leaf anatomy

We found that the increases in mesophyll conductance noted above were paralleled by changes in leaf anatomy (Table 4.3, Fig. 4.2). Initially, young leaves were densely compressed and weakly differentiated; however, later in development (i.e. FLE), mesophyll cells had mostly expanded and their surface area covered by chloroplasts (Fig. 4.2), presumably to increase mesophyll and chloroplast area exposed to intercellular air space (Hanba *et al.*, 2001; Tosens *et al.*, 2012). A considerable fraction of the mesophyll cells were surrounded by intercellular spaces at FLE (Fig. 4.2F-J) as a result of cell separation (Kozela & Regan, 2003). In temperate species, the fraction of mesophyll volume occupied by intercellular air spaces has been shown to increase with leaf expansion and correlate strongly with mesophyll conductance (Marchi *et al.*, 2008); our results suggest that the same is true in the five selected tropical tree species, with leaf expansion being associated with greater distribution of chloroplasts across the surface area of mesophyll cells, combined with increasing carboxylation capacity of Rubisco. Collectively, such changes ensure maximum investment of photosynthetic resources (Marchi *et al.*, 2008; Varone & Gratani, 2009; Tosens *et al.*, 2012) and increase photosynthetic N-use efficiency at FLE (Table 4.3). After FLE, cell walls continue to thicken, thereby reducing conductance to CO_2 diffusion in non-senescent leaves (Niinemets *et al.*, 2005).

The changes in leaf anatomy of our tropical species were consistent with previous studies in developing leaves of temperate evergreen shrubs [*Rhamnus alaternus* (Varone & Gratani, 2009) and *Olea europae* (Marchi *et al.*, 2008)] and deciduous trees [*Prunus persica* (Marchi *et al.*, 2008) and *Populus tremula* (Tosens *et al.*, 2012)]. More importantly, however, our findings provide a mechanistic understanding of factors contributing to physiological development of photosynthetic capacity and net CO_2 uptake during leaf expansion of tropical species. Our results also suggest that the observed time lag between physical appearance of leaves and active

photosynthesis (Restrepo-Coupe *et al.*, 2013) could be explained by a combination of CO_2 diffusional constraints (linked to leaf anatomical traits) and rate-limiting biochemical components of photosynthesis.

4.4.3 Reduction in respiration underpinned by changing demand

Highest respiration rates were observed in the early developmental stage of all five species in our study, with R_{dark} declining following leaf expansion and reaching a steady state at FLE (Table 4.3). Dark respiration rates (R_{dark}) of expanding leaves were higher than those in fully expanded leaves; the average rates at 65% expansion were double those of full leaf expansion (Table 4.3), consistent with past tropical studies showing two-three times higher R_{dark} at 50% expansion (Kursar, T & Coley, P, 1992; Woodall *et al.*, 1998; Cai *et al.*, 2005). Thus, the balance between carbon uptake and release changes dramatically during leaf development. While part of the change is driven by progressive increases in photosynthetic capacity, declines demand for respiratory ATP is also likely to play a role. Demand for respiratory products during early expansion is dominated by biosynthesis of lipid-rich chloroplast membranes and associated photosynthetic enzymes; this coincides with past observation of highest energy content of young leaves compared to mature leaves (Kursar, TA & Coley, PD, 1992). As leaves near FLE, demand for respiratory energy decreases and becomes primarily dominated by maintenance processes (e.g. protein turnover and maintenance of solute gradients) (De Vries, 1975; Kozlowski, 1992; Amthor, 2000).

The negative $R_{dark} \leftrightarrow V_{cmax}$ relationships among four leaf developmental stages were driven by significantly higher R_{dark} to V_{cmax} ratio of leaves at 65-82% expansion (stage I). Interestingly, this pattern is the opposite of that seen in in mature leaves, where $R_{dark} \leftrightarrow V_{cmax}$ relationships across plant functional types are typically positively correlated (Atkin *et al.*, 2015), since high respiratory rates are required to sustain high rates of photosynthesis. Although no significant correlation was found between respiration rate in the light (R_{light}) and V_{cmax} among four developmental stages or tropical leaves (Fig. 4.5B and D), the mean ratio of R_{light} to V_{cmax} of leaves at 65-82% expansion was double those of full leaf expansion (0.08 ± 0.03 vs. 0.03 ± 0.01; all tropical species). Altogether, these results suggested that the ratios of R_{light} to V_{cmax}, R_{dark} to V_{cmax} and R_{light} to R_{dark} were not constant when leaf developmental stages are taken into account. In most modelling exercises that seek to predict rates of leaf R based on

$R \leftrightarrow V_{cmax}$ relationships, an assumption is made that leaf R is the same in darkness as in the light (i.e. $R_{dark} = R_{light}$) and that leaf *R* is a fixed fraction of V_{cmax}. For example, in the JULES model (Cox 2001; Clark et al. 2011), leaf *R* in the light and dark is fixed as 1.5% V_{cmax}, based on previous work by (Collatz *et al.*, 1991) and Farquhar *et al.* (1980). This study shows that this assumption of a constant R/V_{cmax} ratio is unlikely to hold for moist forest species, both in developing and mature leaves, consistent with recent meta-analysis (De Kauwe *et al.*, 2016). Similarly, a comparison of R/V_{cmax} ratios of plants growing in several biomes suggests R/V_{cmax} ratios are consistently higher than 1.5% in mature leaves (Atkin *et al.*, 2015). Thus, to correctly model variation in leaf *R*, account needs to be given to the likelihood that the respiratory 'cost' associated with supporting photosynthesis and other processes is greater than that assumed in current terrestrial biosphere models.

4.4.4. Nitrogen partitioning strategy and potential adaptation to herbivory

Nitrogen partitioning is expected to change following leaf development, reflecting concomitant changes in metabolic rates, protein composition and functions (Niinemets *et al.*, 2012). In our study, partitioning of N to photosynthesis was lowest in the early stages of leaf expansion (Fig. 4.6). Past studies monitoring protein abundance showed that tropical species produce a unique set of proteins during the early stages of expansion, with those proteins being distinct from those after FLE (Kursar, T & Coley, P, 1992). This early, transiently abundant proteins might have a non-developmental function such as herbivore deterrence (Kursar, T & Coley, P, 1992). Such proteins might have a protective role, as in tropical forests, most of the damage to leaves (by herbivores) occurs during the vulnerable period of early leaf expansion (Coley & Kursar, 1996). Young leaves are preferred by herbivores because leaf N (e.g. Table 4.2) and water content are often at their highest levels (Read *et al.*, 2003; Brunt *et al.*, 2006; Silva *et al.*, 2015), with leaves being tender due to lack of lignified cell walls. Toughening of cell walls, despite being a highly effective defence (Choong, 1996; Lucas *et al.*, 2000; Kursar & Coley, 2003), imposes constraint on cell expansion; because of this, expanding leaves rely largely on a variety of chemical defences. Such an approach necessitates N investment in proteins not associated with photosynthesis in young leaves. Indeed, chemical defences (e.g. phenolics, saponins and alkaloids) comprise 10-50% of dry weight of young leaves (Coley & Barone, 1996; Brenes-

Arguedas *et al.*, 2006; Bixenmann *et al.*, 2013; Wiggins *et al.*, 2016); such investments in defence are linked to low rates of herbivory-related leaf damage (less than 20% of the area loss) (Kursar & Coley, 2003). Thus, the lower allocation of leaf N to photosynthesis in young leaves of our tropical trees is likely linked to increased investment in chemical defences.

Importantly, we found that N-partitioning to photosynthetic machinery (pigment complexes, electron transport protein and Rubisco) gradually increased to support increasing rates of photosynthesis as leaves expanded (Fig. 4.6). As described earlier, increases in photosynthesis were associated with expansion of mesophyll cells to increase mesophyll and chloroplast surface areas. At the same time, cell wall thickening also took place, likely underpinned by increased investment in structural proteins (Showalter, 1993). We did not quantify mesophyll cell wall thickness; however with past studies show a 0.1 to 0.3µm increase in cell wall thickness during leaf expansion (Miyazawa & Terashima, 2001; Miyazawa *et al.*, 2003; Tosens *et al.*, 2012). Although thickening of cell walls constrains CO_2 diffusion (Niinemets *et al.*, 2005), thickened, more strongly lignified cell walls reduces palatability and consumption of mature leaves than young leaves (Choong, 1996; Brunt *et al.*, 2006). In addition to increasing N investment in cell walls, N-partitioning within photosynthetic machinery changed after leaves fully expanded which coincided with declines in photosynthesis (Figs. 4.3 and 4.6). This might indicate for acclimation responses to self- and neighbour shading (Ackerly & Bazzaz, 1995; Niinemets *et al.*, 2014). With decreasing irradiance, N was re-distributed from other rate-limiting proteins (Rubisco and electron transport proteins) to light harvesting pigment-protein complexes (Fig. 4.6) (Vapaavuori & Vuorinen, 1989; Evans & Poorter, 2001; Yasumura & Ishida, 2011). Altogether, the N-partitioning reflects dynamic response of leaves to environmental stimulus as well as developmental constraints (Niinemets *et al.*, 2014). Given the importance of leaf N and N-partitioning in estimating photosynthetic capacity and ecosystem carbon flux (Cox, 2001; Kattge *et al.*, 2009; Friend, 2010; Bonan *et al.*, 2011), future study might explore the pattern of N-partitioning to both photosynthetic and non-photosynthetic pools over wider period of leaf lifespan and use this information to model correlation between photosynthetic capacity and N.

4.4.5 Concluding statements

Examination of mechanisms underpinning development of photosynthesis in tropical canopy trees suggested that key components of photosynthesis developed synchronously during expansion; this coordination was not restricted to mature leaves. Mesophyll and stomatal conductances matured almost concurrently, accompanied by development of leaf internal structures. Unlike many shade-tolerant tropical species, no lag in photosynthetic components (e.g. chloroplasts, Rubisco in 'delayed greening' species) was observed. The balance between photosynthetic carbon uptake and respiratory release changed dramatically during leaf development, and our study points toward further investigation on the changing demand for respiratory products and its effect on the balance between respiration in dark and light.

It has been recognised that changes in photosynthetic capacity during leaf expansion need to be considered when modelling carbon uptake. Our study supports the importance of accounting for physiological differences between expanding and mature leaf cohorts, which have direct impact on estimating forest carbon uptake (Wu *et al.*, 2016). With recent advances in digital cameras coupled with flux instrumentation, quantification of new canopy flushes is made possible (Lopes *et al.*, 2016; Wu *et al.*, 2016). Using this method, one could assign specific physiological attributes to young and mature leaves to model canopy phenology and carbon fluxes more accurately.

Chapter 5: General Discussion

5.1 Variation in V_{cmax} between tropical trees

Given the importance of tropical forests in the global C budget and the limited number of species for which there is information relative to the diversity in these biomes, effort was focussed on expanding the number of species for which leaf and photosynthetic characteristics have been described. Key factors influencing variation in V_{cmax} and photosynthetic nitrogen use efficiency for trees characteristic of moist forest biomes were explored. A survey along a 3,300-meter elevation gradient from lowland western Amazon to upland Andes generated detailed photosynthetic attributes for many new species [Chapter 2; Bahar *et al.* (2017)]. Huge variations in V_{cmax} were found within and across the 18 remote field sites. When estimated at a common measuring temperature, the mean V_{cmax} of lowland Amazon trees was significantly lower than that of Andean trees, consistent with past studies (Fig. 5.1, noting that circled numbers indicate the relevant thesis chapters). The difference in V_{cmax} between lowland and upland groups was maintained when calculated using different activation energies values from Farquhar *et al*. (1980) and Bernacchi *et al.* (2002) (Table 2.4, Fig. 2.3). The mean V_{cmax} of upland Andean trees was similar to that reported in past studies (Fig. 5.1), providing further evidence in support of van de Weg *et al.* (2012) recommendation to treat upland tropical trees as a PFT (plant functional type) of their own, or as an intermediate PFT between lowland tropical and temperate trees. Treating upland tropical trees as a unique PFT allows adjustment of parameters specific to upland environments such as low photosynthetic active radiation due to cloud and low leaf area index, which will impact on the estimate of gross primary productivity (GPP) at high elevation tropical forests (Girardin *et al.*, 2014a; van de Weg *et al.*, 2014).

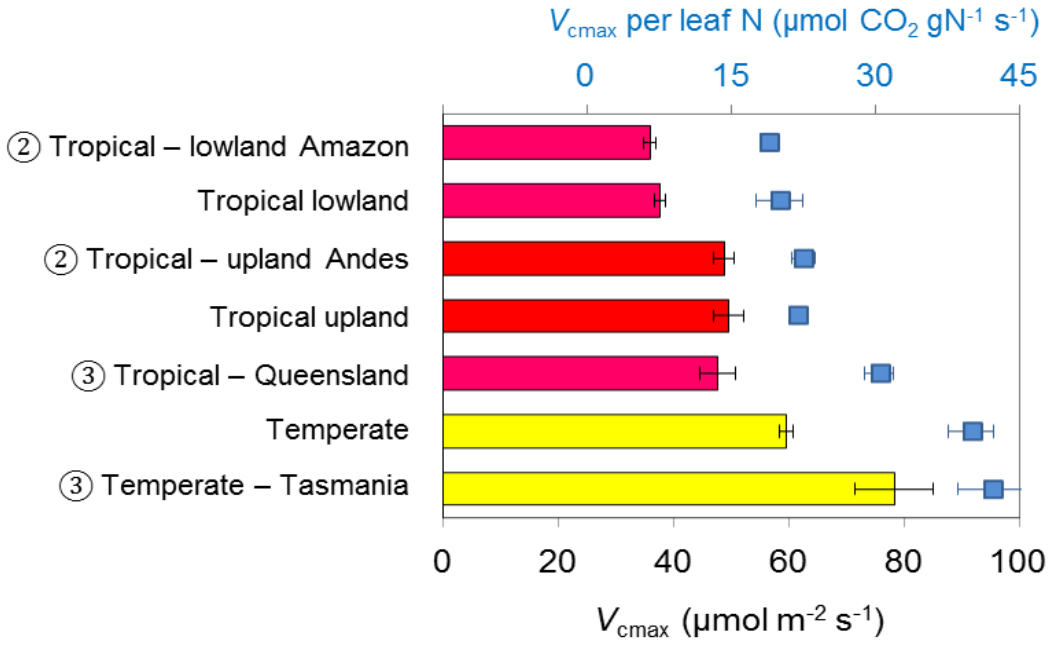

Figure 5.1. Mean values for V_{cmax} at 25 ºC and per unit leaf N (in blue) with S.E. for tropical and temperate tree species. ②: Chapter 2 tropical - lowland Amazon and upland Andes; ③: Chapter 3 glasshouse grown tropical - Queensland and temperate - Tasmania. Mean values for tropical lowland and temperate were obtained from Kattge *et al* (2009) and Ali *et al*. (2015), which compiled individual studies on lowland tropical trees (Carswell *et al.*, 2000; Meir *et al.*, 2002; Coste *et al.*, 2005; Kumagai *et al.*, 2006; Domingues *et al.*, 2007; Domingues *et al.*, 2010) and temperate trees (individual temperate studies are not listed here due to large number of studies). Mean values for tropical upland was sourced from studies on high altitude tropical trees (van de Weg *et al.*, 2012; Dusenge *et al.*, 2015; Vårhammar *et al.*, 2015). Note that V_{cmax} from field surveys were calculated on C_i basis and V_{cmax} from glasshouse study ③ were calculated on C_c basis, with V_{cmax}- C_c being similar to V_{cmax}- C_i when approciate Michaelis-Menten constants for CO_2 and O_2 were applied (see Chapter 3).

The finding of significantly lower V_{cmax} at 25 ºC in lowland Amazonian trees (growing in environments where mean daily temperatures are >28°C) compared to Andean trees growing in colder environments raised the question of whether observed differences are influenced by the process of thermal acclimation and/or inherent differences between Andean vs. Amazonian trees. While few studies have addressed this question, there is some evidence that cold-adapted species can exhibit greater inherent metabolic rates than their warm-adapted counterparts (Chabot & Hicks, 1982; Cunningham, SC & Read, J, 2003; Xiang *et al.*, 2013; Scafaro *et al.*, submitted). The findings in Chapter 3 confirmed that warm-adapted trees from tropical moist forests exhibited significantly lower rates of V_{cmax} (both on a C_c and C_i basis) than their cold-adapted temperate counterparts, when grown in a common environment. The glasshouse study supported field observations of lower V_{cmax} and V_{cmax} per unit leaf N ($V_{cmax,\ N}$) values in tropical trees compared to their temperate counterparts (Fig. 5.1).

5.2 How important is mesophyll conductance when estimating V_{cmax} and $V_{cmax,N}$ of warm-adapted tropical trees?

One factor that has been suggested to contribute towards lower apparent V_{cmax} and $V_{cmax,N}$ is a greater mesophyll resistance (Lloyd *et al.*, 1992; Warren & Adams, 2006; Niinemets *et al.*, 2009; Tosens *et al.*, 2012). By measuring mesophyll conductance, g_m - inverse of mesophyll resistance (Chapters 3 and 4), it was possible to calculate V_{cmax} on the basis of C_c assuming values for the Michaelis-Menten constants for CO_2 (K_c) and O_2 (K_o) of 260 µbar and 179 mbar, respectively (von Caemmerer *et al.* (1994). These estimates could be compared to values of V_{cmax} calculated on a C_i basis (assuming infinite g_m) using values of K_c and K_o of 404 µbar and 248 mbar, respectively (von Caemmerer *et al.*, 1994).

Contrary to my hypothesis, I found no evidence to support greater mesophyll resistance for warm-adapted tropical leaves with lower photosynthetic capacity. As demonstrated in Chapter 3, tropical moist-forest trees are not penalised by low g_m; hence, the lower V_{cmax} of tropical species in my glasshouse study were not caused by lower g_m (and thus lower concentrations of CO_2 at the site of carboxylation). Despite their contrasting thermal origin, all species fell on a common V_{cmax}-g_m and V_{cmax}-g_s (stomatal conductance) relationships (Fig. 5.2), consistent with previous studies on a range of species (Epron *et al.*, 1995; Evans & Loreto, 2000; Flexas *et al.*, 2008; Whitehead *et al.*, 2011; Tosens *et al.*, 2012). To put this observation in field context, the conclusion that V_{cmax} is higher in upland Andean trees would hold (albeit with modified values) if g_m scales with V_{cmax}. However, if g_m was more limiting in lowland Amazon trees than their upland Andes counterparts, then calculation of V_{cmax} on C_c basis might fail to differentiate between the upland and lowland groups. A definitive assessment of this issue will require further work assessing g_m in tropical trees in the field, with particular focus on very low range of g_m (<0.1 mol m^{-2} s^{-1} bar^{-1}) where much larger drawdown from C_i to C_c have been reported. Alternatively, data quality check based on the ratio of V_{cmax} to g_s could be performed as my data showed correlations between V_{cmax}, g_s and g_m (Fig. 5.2); these correlations were maintained under water stress (Niinemets *et al.*, 2009; Cernusak *et al.*, 2011; Cano *et al.*, 2014) thus provide a justification to apply my findings in field settings where water stress is prevalent.

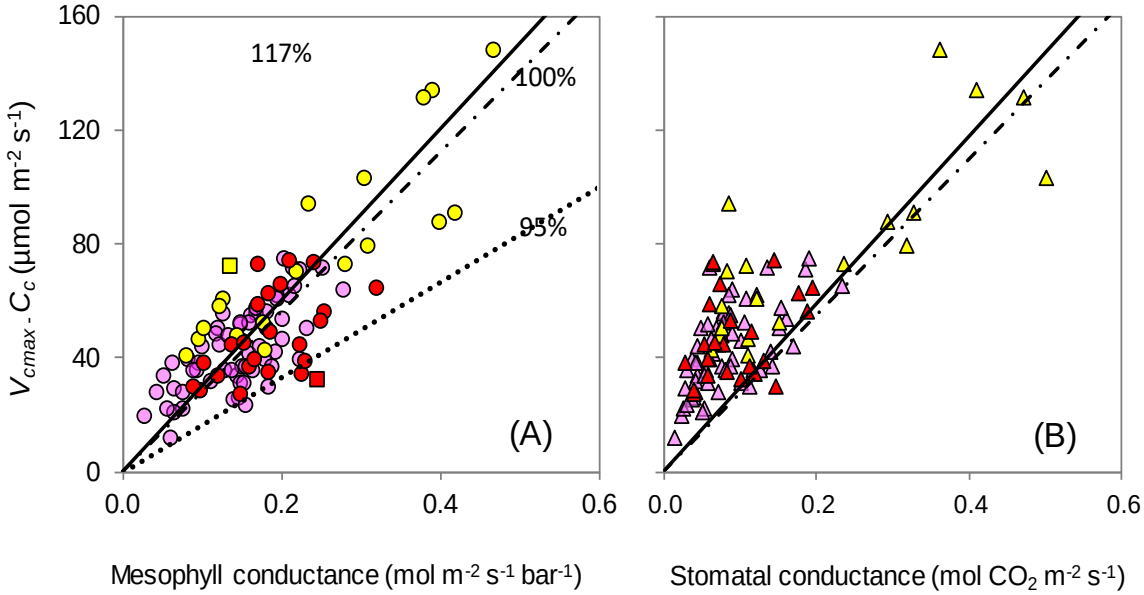

Figure 5.2. Relationships between (A) mesophyll conductance or (B) stomatal conductance and V_{cmax}-C_c respectively, for tropical and temperate trees. Red symbols = tropical trees and yellow symbols = temperate trees (Chapter 3). Pink symbols = tropical trees at four developmental stages (Chapter 4).
The dashed line was extrapolated from the points where V_{cmax}-C_c equals V_{cmax}-C_i. The yellow square denotes a temperate sp. *Phyllocladus aspleniifolius* with the solid line extrapolated from this point along which V_{cmax}-C_c values were 17% more than V_{cmax}-C_i. The red square denotes a tropical sp. *Litsea leefeana* with the dotted line extrapolated from it where V_{cmax}-C_i values exceeded V_{cmax}-C_c values by approximately 3 to 5%.

V_{cmax} estimated on the basis of C_i was equivalent to that on the basis of C_c, when appropriate Michaelis-Menten constants for CO_2 and O_2 were used (Fig. 5.3). Despite the large influence of g_m in reducing CO_2 partial pressure at the site of carboxylation, the significant drawdown from C_i to C_c did not alter estimation of V_{cmax} for leaves from either tropical or temperate trees. This is in marked contrast to previous studies (Epron *et al.*, 1995; Manter & Kerrigan, 2004; Warren, 2008; Sun *et al.*, 2014b). C_i-based V_{cmax} values were 20% less than C_c –based V_{cmax} values in the most extreme cases, which is much lower than 60-75% underestimation of V_{cmax} reported earlier (Fig. 5.3) (Warren, 2008; Sun *et al.*, 2014b). One important issue that emerges from my study is the importance of using appropriate K_c and K_o depending on whether the analysis is based on C_i or C_c (von Caemmerer *et al.*, 1994; Bernacchi *et al.*, 2002). The biochemical model is highly sensitive to kinetic constants hence these constants must be used carefully and consistently (Medlyn *et al.*, 2002; Dietze, 2014); and should be reported in methodology to allow cross comparison and validation of data based on similar denominator.

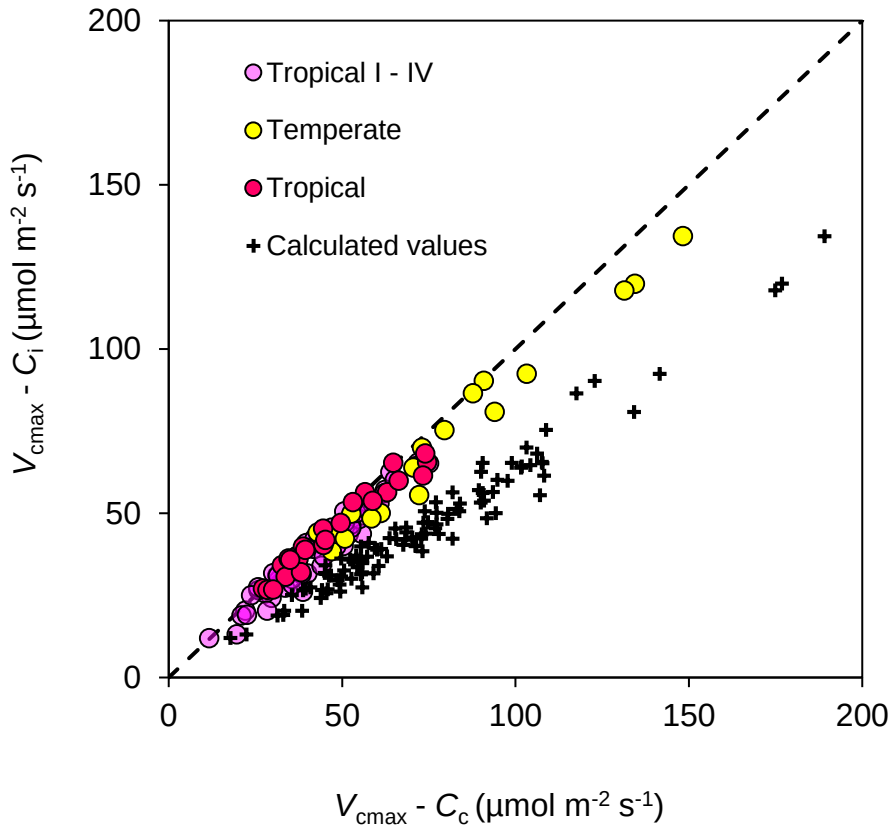

Figure 5.3. Comparison of V_{cmax} estimated using finite g_m (V_{cmax}-C_c) and infinite g_m (V_{cmax}-C_i). Red circles = tropical trees and yellow circles = temperate trees described in Chapter 3. Pink circles = tropical trees at four developmental stages described in Chapter 4. Cross symbols (+) denotes V_{cmax}-C_i of datasets from Chapters 3 and 4 plotted against V_{cmax}-C_c calculated by fitting eqn. 4 (Sun *et al.*, 2014b), which allows conversion of A↔C_i based parameters to the corresponding A↔C_c based parameters. Dashed line shows the 1:1 relationship.

Almost all terrestrial biosphere models assume infinite g_m and calculate V_{cmax} on a C_i basis; however, a recent model demonstrates that accounting for limitations in g_m can yield substantial increases in the modelled cumulative CO_2 fertilization effect on GPP from 915 to 1057 Pg C for the period of 1901 - 2010 (Sun *et al.*, 2014a). It is important to note that this model was parameterised on V_{cmax}-C_c values calculated using a non-linear model that converts A/C_i-based parameters to A/C_c-based values (Sun *et al.*, 2014b), which yielded 46% higher 'calculated' V_{cmax}-C_c values than actual V_{cmax}-C_c values estimated using concurrent gas exchange and carbon isotope discrimination (Fig. 5.3). Hence, overestimation of a cumulative CO_2 fertilization effect on GPP might not be as dramatic as was modelled. It emphasises the need for more empirical assessments of g_m, coupled with correct use of kinetic constants (Medlyn *et al.*, 2002; Dietze, 2014).

5.3. Soil and leaf phosphorus modulate photosynthetic capacity (V_{cmax} and J_{max}), but not N-use efficiency in the Amazon-Andes region

As described in Chapter 2, our field site selection aimed to assess the potential role of P limitation on photosynthetic performance across tropical moist forests in western Amazonia and the Andes where substantial variations in soil P occur (lowland sites: 38-727 mg P kg^{-1}; upland sites: 496-1631 mg P kg^{-1}). The hypothesis that photosynthetic capacity would be positively correlated with soil and leaf P was supported by our results – a finding consistent with earlier studies on tropical species in South America, West Africa and Australia (Domingues *et al.*, 2007; Meir *et al.*, 2007; Kattge *et al.*, 2009; Domingues *et al.*, 2010; Bloomfield *et al.*, 2014b). Significant positive relationships were observed between photosynthetic capacity (expressed either as V_{cmax} or J_{max}) and soil or leaf P (Tables A2.1, A2.2). Moreover, soil and leaf P emerged as significant explanatory variables in linear mixed-effect models of variations in photosynthetic capacity (Table 2.3), accounting for ~40% of the observed variations in V_{cmax} and J_{max}. The following predictive equation will enable model parameterization based on the largest single tropical V_{cmax} datasets available to date (refer to Table 2.3 for details):

$$\boldsymbol{V_{cmax}^{25} = 41.47 + (7.91*\log10[\text{Soil P}]) + (68.15*\text{Leaf P})}$$

where V_{cmax} is expressed on area basis at 25 ºC, (total) soil P on per unit soil dry mass and leaf P on area basis. This finding suggests that P, rather than N, has the dominant role in regulating V_{cmax} and J_{max} in Amazon-Andes regions (Mercado *et al.*, 2011); however, other studies have shown than leaf P and N were best considered in terms of limiting factors (Domingues *et al.*, 2010; Walker *et al.*, 2014), suggesting that either N or P may play a role in different circumstances. Altogether, these observations suggest that leaf P or P-cycle should be included in the latest generation of terrestrial biosphere models (TBMs) (Walker *et al.*, 2014). If we were to account for the effect of P on parameterisation of V_{cmax}↔N in terrestrial biosphere models (TBMs), considerable reduction in the estimate of GPP is anticipated particularly in areas where P-limitation is prevalent i.e. 30% of terrestrial ecosystems (Hedin, 2004; Townsend *et al.*, 2007).

P-deficiencies also reduce photosynthetic N use efficiency (Reich *et al.*, 2009) and the fraction of leaf N allocated to photosynthesis (Warren & Adams, 2002). Analysis of bivariate relationships and linear mixed-effect models (Chapter 2) suggested that soil and leaf level parameters (soil P and N, mean annual temperature, effective cation exchange capacity of soil, leaf N and P and leaf mass per area) did not

explain the variance in $V_{cmax,\ N}$. Hence, it seems unlikely that either soil or total leaf P can be used a predictor of variations in Rubisco capacity per unit leaf N.

5.4 Nitrogen partitioning to photosynthesis per unit leaf N and P might explain species variation in $V_{cmax,N}$

To further explore the influence of N allocation on variations in $V_{cmax,N}$, the total fraction of leaf N allocated to photosynthesis (n_A) was calculated from the sum of leaf N allocation to Rubisco, electron transport and pigment-protein complexes. Overall, mean n_A was similar between the Peruvian lowland and upland groupings and between tropical Queensland and temperate Tasmanian trees (~0.375), although cold-adapted trees exhibited significantly higher leaf N and P (area-based; Tables 2.2 and 3.2). While mean values of n_A were similar, the fraction of leaf N allocated to photosynthesis was greater in upland plants *at a given* leaf nitrogen (Fig. 5.4A) and phosphorus (Fig. 2.9); this trend is also seen when comparing tropical and temperate trees grown in a common temperature (Fig. 5.4B). The higher investment in photosynthesis per unit leaf nutrient could explain higher photosynthetic N use efficiency of cold-adapted species, potentially to compensate for lower catalytic rates at low temperatures (Holaday *et al.*, 1992; Sage & Kubien, 2007) and/or in the case of tropical upland/montane forest species, to compensate for low photosynthetic active radiation due to frequent cloud cover (Letts & Mulligan, 2005). In turn, this implies that a greater fraction of leaf N is allocated to non-photosynthetic components (e.g. cell wall N and/or defence compounds) in warm-adapted species, reflecting trade-offs associated with leaf longevity and herbivory resistance (Kikuzawa *et al.*, 2013; Metcalfe *et al.*, 2014).

Alternatively, there is a possibility that N investment in Rubisco by warm-adapted species may have been underestimated due to significant fraction of inactive Rubisco (Chapter 2), which might weaken V_{cmax}↔N correlations. N is typically not limiting in tropical environments (Martinelli *et al.*, 1999; Townsend *et al.*, 2007) and tropical trees are thought to hold on to N for competitive advantage (Domingues *et al.*, 2010); the N storage in the form of Rubisco could be activated for fast adjustment of photosynthetic machinery under fluctuating light regime (Turnbull *et al.*, 1993; Rozendaal *et al.*, 2006) and/or maintenance of photosynthetic capacity under drought (Rowland *et al.*, 2015). Viewed from this perspective, *in vivo* estimates of V_{cmax} from gas exchange provide insights into N investment into the *metabolically active* Rubisco, relevant when modelling GPP of forest ecosystems. The estimates of N fraction in

Rubisco (n_R) is central to TBMs that set potential rates of carboxylation as a function of leaf N content, assuming PFT-specific n_R (Biome-BGC, 2010; Bonan *et al.*, 2011). Despite being key parameter influencing model output, PFT-specific n_R is arbitrary in some cases, resulting considerable discrepancy between the model representation and observation (Rogers, 2014). In addition, n_R is assumed to be fixed irrespective of changing leaf N content (Cox, 2001; Biome-BGC, 2010), which has been shown to be incorrect (Evans, 1989). Hence, assessing how PFTs differ in N investment in both active and inactive forms of Rubisco and how n_R changes with respect to leaf N might be required (Scafaro *et al.*, submitted) to improve confidence in prescribed n_R values.

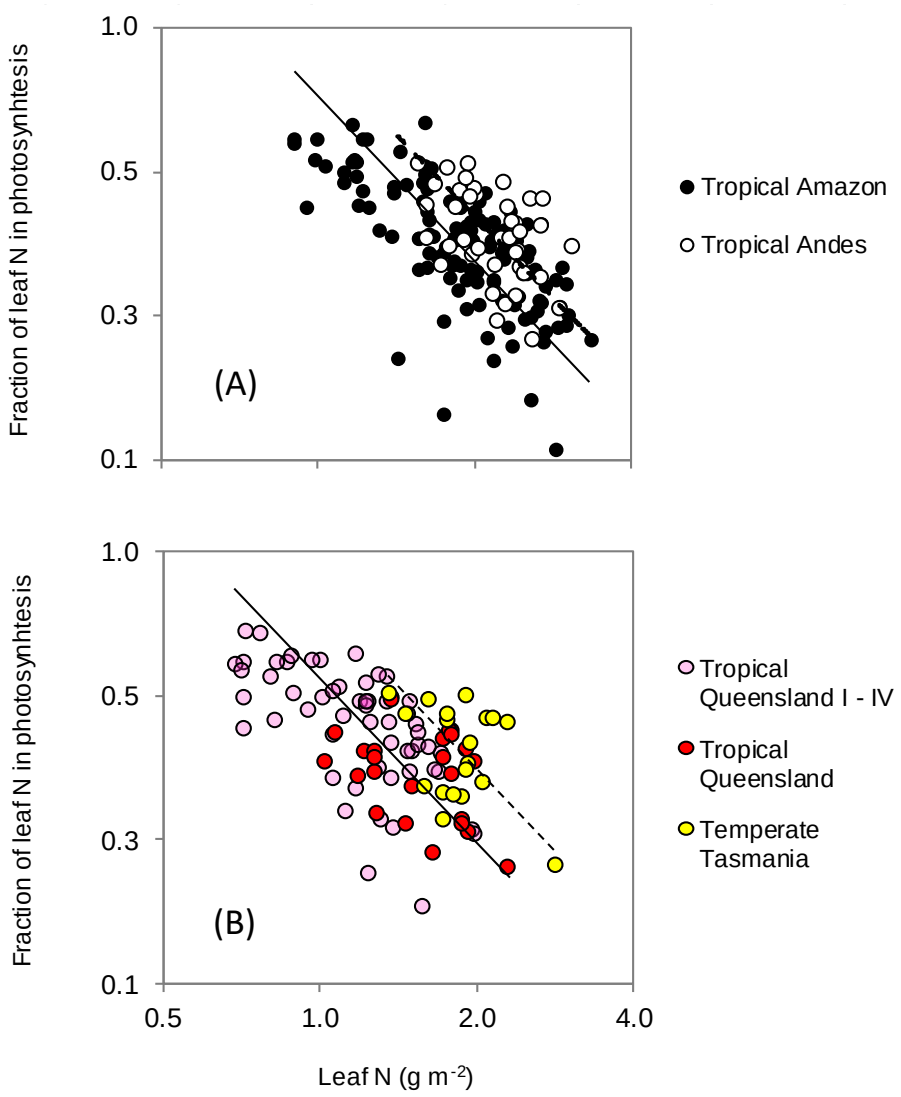

Figure 5.4. Log-log plots of the fraction of leaf N in photosynthetic metabolism in relation to leaf N-area. (A) Closed/black circles = tropical lowland Amazon trees and open circles = tropical upland Andes trees (Chapter 2). (B) Red circles = tropical trees and yellow circles = temperate trees (Chapter 3). Pink circles = tropical trees at four developmental stages (Chapter 4). Dashed and solid lines represent significantly different elevation (i.e. y-axis intercept) of the bivariate relationships between tropical Amazon vs. Andes and between tropical Queensland vs. temperate Tasmania.

5.5 Tropical leaves exhibited synchronous development of photosynthetic capacity at different leaf developmental stages

My thesis has shown that expanding leaves of tropical trees have different photosynthetic and respiratory characteristics than those of mature leaves, as demonstrated in past studies on non-tropical species (Šesták *et al.*, 1985; Niinemets *et al.*, 2012). Not much is known about the mechanisms underpinning photosynthetic development in expanding tropical leaves. Our understanding of photosynthetic development and associated changes in leaf anatomy, chemistry and physiology is derived mainly from temperate trees and crops. To address this gap of knowledge, Chapter 4 monitored changes in photosynthetic capacity, respiratory rates, leaf nutrient and chlorophyll contents, leaf anatomy and partitioning of leaf N as leaves developed on tropical tree seedlings. Key components of photosynthesis developed synchronously during expansion. This coordination was not restricted to mature leaves, as developing leaves fell along similar leaf trait relationships as those of mature leaves (Figs. 5.2 and 5.4). Mesophyll and stomatal conductances matured almost concurrently, as leaf internal structures developed (Chapter 4).

In the ORCHIDEE process-based vegetation model, canopy photosynthesis is calculated at leaf scale following the Farquhar *et al.* model (1980) and V_{cmax} is parameterised as a function of leaf age (Krinner *et al.*, 2005). V_{cmax} increases from a low initial value at leaf flushing to maximum value few weeks after full leaf expansion. The parameterisation of V_{cmax} with leaf age in ORCHIDEE is based on a study on delayed greening tropical species *Dryobalanops aromatica* exhibiting increasing chlorophyll and photosynthesis **after** full expansion (Ishida *et al.*, 1999). This approach has its merit, given the occurrence of delayed greening in tropical forest. However, it is important to note that delayed greening overwhelmingly occurs in shade-tolerant understorey species, which comprise 20-30% of tropical plant communities (Coley & Kursar, 1996; Queenborough *et al.*, 2013). A majority of tropical plants, including Australian canopy species studied in Chapter 4 (*D. aromatica, S. sayeri, F. bourjotiana, L. leefeana* and *P. elegans*) show normal greening behaviour, achieving a net positive carbon assimilation at 5-30% full expansion and near-maximum photosynthesis at full leaf expansion (Kursar, T & Coley, P, 1992; Sobrado, 1994; Woodall *et al.*, 1998; Terwilliger *et al.*, 2001; Cai *et al.*, 2005). My study reveals that canopy species exhibited proportional increase in photosynthetic capacity with leaf expansion i.e. 50% of maximum V_{cmax} at 65-70% FLE and 80% maximum V_{cmax} at 85% FLE (Table 4.3),

suggesting that carbon uptake by expanding leaves is substantial even before full expansion. The canopy species required 30 days after emergence to reach maximum V_{cmax} (Fig. 4.1), whereas delayed greening species usually require 30 days to fully expand plus extra few weeks to achieve maximum photosynthesis (Kursar, T & Coley, P, 1992; Woodall *et al.*, 1998; Cai *et al.*, 2005). Therefore, a model that parameterises V_{cmax} according to greening strategy, potentially by introducing specific time lag between leaf flush and photosynthesis for normal and delayed greening species is recommended to capture variations in the rate of photosynthetic development between canopy vs. understorey tropical communities (Restrepo-Coupe *et al.*, 2013).

Concluding remarks

My PhD thesis addresses some of the gaps in knowledge by: 1) adding new information on V_{cmax} values of tropical moist forests across Amazonian-Andean regions; 2) demonstrating that a valid V_{cmax} estimate can be derived using either C_i- or C_c-based approaches, provided that appropriate Michaelis Menten constants for CO_2 and O_2 are used; 3) identifying the importance of P availability and N partitioning to photosynthesis as key factors influencing V_{cmax} and N use efficiency; and, 4) providing evidence of synchronous photosynthetic and leaf anatomical development in tropical canopy leaves. In addition to future directions proposed earlier and in each main chapter, it is recommended that data should be made available and relevant for photosynthetic model parameterisation and evaluation. The V_{cmax} dataset of Amazonian-Andean regions presented in my thesis is the largest tropical V_{cmax} dataset included in a meta-analysis by de Kauwe *et al.* (2016), with public availability of the dataset helping reducing uncertainties in our prediction of future changes in atmospheric carbon and climate.

List of References

Ackerly DD, Bazzaz FA. 1995. Leaf dynamics, self-shading and carbon gain in seedlings of a tropical pioneer tree. *Oecologia* **101**(3): 289-298.

Aerts R, Chapin FSI. 2000. The mineral nutrition of wild plants revisited : a re-evaluation of processes and patterns. *Advances in Ecological Research* **30**: 1-67.

Ali AA, Xu C, Rogers A, McDowell NG, Medlyn BE, Fisher RA, Wullschleger SD, Reich PB, Vrugt JA, Bauerle WL, et al. 2015. Global-scale environmental control of plant photosynthetic capacity. *Ecological Applications* **25**(8): 2349-2365.

Almeida JP, Montúfar R, Anthelme F. 2012. Patterns and origin of intraspecific functional variability in a tropical alpine species along an altitudinal gradient. *Plant Ecology & Diversity* **6**(3-4): 423-433.

Alton PB. 2011. How useful are plant functional types in global simulations of the carbon, water, and energy cycles? *Journal of Geophysical Research: Biogeosciences* **116**(G1).

Amthor JS. 1994. Scaling CO_2-photosynthesis relationships from the leaf to the canopy. *Photosynthesis Research* **39**(3): 321-350.

Amthor JS. 2000. The McCree–de Wit–Penning de Vries–Thornley respiration paradigms: 30 years later. *Annals of Botany* **86**(1): 1-20.

Anten N, Schieving F, Werger M. 1995. Patterns of light and nitrogen distribution in relation to whole canopy carbon gain in C_3 and C_4 mono-and dicotyledonous species. *Oecologia* **101**(4): 504-513.

Armstrong AF, Logan DC, Atkin OK. 2006. On the developmental dependence of leaf respiration: responses to short- and long-term changes in growth temperature. *American Journal of Botany* **93**(11): 1633-1639.

Asner GP, Anderson CB, Martin RE, Knapp DE, Tupayachi R, Sinca F, Malhi Y. 2014a. Landscape-scale changes in forest structure and functional traits along an Andes-to-Amazon elevation gradient. *Biogeosciences* **11**(3): 843-856.

Asner GP, Knapp DE, Anderson CB, Martin RE, Vaughn N. 2016. Large-scale climatic and geophysical controls on the leaf economics spectrum. *Proceedings of the National Academy of Sciences*.

Asner GP, Martin RE, Tupayachi R, Anderson CB, Sinca F, Carranza-Jiménez L, Martinez P. 2014b. Amazonian functional diversity from forest canopy chemical assembly. *Proceedings of the National Academy of Sciences of the United States of America* **111** (15): 5604-5609.

Atkin OK, Bloomfield KJ, Reich PB, Tjoelker MG, Asner GP, Bonal D, Bönisch G, Bradford MG, Cernusak LA, Cosio EG, et al. 2015. Global variability in leaf respiration in relation to climate, plant functional types and leaf traits. *New Phytologist* **206**(2): 614–636.

Ayub G, Smith RA, Tissue DT, Atkin OK. 2011. Impacts of drought on leaf respiration in darkness and light in *Eucalyptus saligna* exposed to industrial-age atmospheric CO_2 and growth temperature. *New Phytologist* **190**: 1003-1018.

Azcon-Bieto J, Lambers H, Day D. 1983. Respiratory properties of developing bean and pea leaves. *Functional Plant Biology* **10**(3): 237-245.

Bahar NHA, Ishida FY, Weerasinghe LK, Guerrieri R, O'Sullivan OS, Bloomfield KJ, Asner GP, Martin RE, Lloyd J, Malhi Y, et al. 2017. Leaf-level photosynthetic capacity in lowland Amazonian and high-elevation Andean tropical moist forests of Peru. *New Phytologist* **214**(3): 1002–1018.

Baker NR, Hardwick K. 1973. Biochemical and physiological aspects of leaf development in Cocoa (*Theobroma cacao*). I. Development of chlorophyll and photosynthetic activity. *The New Phytologist* **72**(6): 1315-1324.

Bartholomé E, Belward AS. 2005. GLC2000: a new approach to global land cover mapping from Earth observation data. *International Journal of Remote Sensing* **26**(9): 1959-1977.

Beer C, Reichstein M, Tomelleri E, Ciais P, Jung M, Carvalhais N, Rödenbeck C, Arain MA, Baldocchi D, Bonan GB, et al. 2010. Terrestrial gross carbon dioxide uptake: global distribution and covariation with climate. *Science* **329**(5993): 834-838.

Beerling DJ, Quick WP. 1995. A new technique for estimating rates of carboxylation and electron transport in leaves of C_3 plants for use in dynamic global vegetation models. *Global Change Biology* **1**(4): 289-294.

Bernacchi CJ, Portis AR, Nakano H, von Caemmerer S, Long SP. 2002. Temperature response of mesophyll conductance. Implications for the determination of Rubisco enzyme kinetics and for limitations to photosynthesis *in vivo*. *Plant Physiology* **130**(4): 1992-1998.

Bernacchi CJ, Singsaas EL, Pimentel C, Portis Jr AR, Long SP. 2001. Improved temperature response functions for models of Rubisco-limited photosynthesis. *Plant, Cell & Environment* **24**(2): 253-259.

Biome-BGC 2010. Biome BGC version 4.2: Thoeretical framework of BIOME-BGC.

Bixenmann RJ, Coley PD, Kursar TA. 2013. Developmental changes in direct and indirect defenses in the young leaves of the neotropical tree genus *Inga* (*Fabaceae*). *Biotropica* **45**(2): 175-184.

Bloomfield KJ, Domingues TF, Saiz G, Bird MI, Crayn DM, Ford A, Metcalfe D, Farquhar GD, Lloyd J. 2014a. Contrasting photosynthetic characteristics of forest vs. savanna species (far North Queensland, Australia). *Biogeosciences* **11**: 7331-7347.

Bloomfield KJ, Farquhar GD, Lloyd J. 2014b. Photosynthesis–nitrogen relationships in tropical forest tree species as affected by soil phosphorus availability: a controlled environment study. *Functional Plant Biology* **41**(8): 820-832.

Bonan GB. 2008. Forests and climate change: Forcings, feedbacks, and the climate benefits of forests. *Science* **320**(5882): 1444.

Bonan GB, Lawrence PJ, Oleson KW, Levis S, Jung M, Reichstein M, Lawrence DM, Swenson SC. 2011. Improving canopy processes in the Community Land Model version 4 (CLM4) using global flux fields empirically inferred from FLUXNET data. *Journal of Geophysical Research: Biogeosciences* **116**(G2): G02014.

Brenes-Arguedas T, Horton M, Coley P, Lokvam J, Waddell R, Meizoso-O'Meara B, Kursar T. 2006. Contrasting mechanisms of secondary metabolite accumulation during leaf development in two tropical tree species with different leaf expansion strategies. *Oecologia* **149**(1): 91-100.

Brooks A. 1986. Effects of phosphorus nutrition on Ribulose-1,5-Bisphosphate Carboxylase activation, photosynthetic quantum yield and amounts of some Calvin-cycle metabolites in spinach leaves. *Functional Plant Biology* **13**(2): 221-237.

Brooks A, Farquhar G. 1985. Effect of temperature on the CO_2/O_2 specificity of ribulose-1, 5-bisphosphate carboxylase/oxygenase and the rate of respiration in the light. *Planta* **165**(3): 397-406.

Brown C, MacKinnon J, Cockshutt A, Villareal T, Campbell D. 2008. Flux capacities and acclimation costs in *Trichodesmium* from the Gulf of Mexico. *Marine Biology* **154**(3): 413-422.

Bruhn D, Mikkelsen TN, Atkin OK. 2002. Does the direct effect of atmospheric CO_2 concentration on leaf respiration vary with temperature? Responses in two species of Plantago that differ in relative growth rate. *Physiologia Plantarum* **114**(1): 57-64.

Bruijnzeel LA, Scatena FN, Hamilton LS. 2011. *Tropical Montane Cloud Forests: Science for Conservation and Management*: Cambridge University Press.

Bruijnzeel LA, Veneklaas EJ. 1998. Climatic conditions and tropical montane forest productivity: the fog has not lifted yet. *Ecology* **79**(1): 3-9.

Brunt C, Read J, Sanson G. 2006. Changes in resource concentration and defence during leaf development in a tough-leaved (*Nothofagus moorei*) and soft-leaved (*Toona ciliata*) species. *Oecologia* **148**(4): 583-592.

Buckley TN, Warren CR. 2014. The role of mesophyll conductance in the economics of nitrogen and water use in photosynthesis. *Photosynthesis Research* **119**(1-2): 77-88.

Caemmerer S, Evans J. 1991. Determination of the average partial pressure of CO_2 in chloroplasts from leaves of several C_3 plants. *Functional Plant Biology* **18**(3): 287-305.
Cai ZQ, Slot M, Fan ZX. 2005. Leaf development and photosynthetic properties of three tropical tree species with delayed greening. *Photosynthetica* **43**(1): 91-98.
Canadell JG, Le Quere C, Raupach MR, Field CB, Buitenhuis ET, Ciais P, Conway TJ, Gillett NP, Houghton RA, Marland G. 2007. Contributions to accelerating atmospheric CO_2 growth from economic activity, carbon intensity, and efficiency of natural sinks. *Proceedings of the National Academy of Science, USA* **104**(47): 18866-18870.
Cano FJ, LÓPez R, Warren CR. 2014. Implications of the mesophyll conductance to CO_2 for photosynthesis and water-use efficiency during long-term water stress and recovery in two contrasting *Eucalyptus species*. *Plant, Cell & Environment* **37**(11): 2470-2490.
Carswell FE, Meir P, Wandelli EV, Bonates LCM, Kruijt B, Barbosa EM, Nobre AD, Grace J, Jarvis PG. 2000. Photosynthetic capacity in a central Amazonian rain forest. *Tree Physiology* **20**(3): 179-186.
Cernusak LA, Hutley LB, Beringer J, Holtum JAM, Turner BL. 2011. Photosynthetic physiology of eucalypts along a sub-continental rainfall gradient in northern Australia. *Agricultural and Forest Meteorology* **151**(11): 1462-1470.
Chabot BF, Hicks DJ. 1982. The ecology of leaf life spans. *Annual Review of Ecology and Systematics* **13**(1): 229-259.
Choong MF. 1996. What makes a leaf tough and how this affects the pattern of *Castanopsis fissa* leaf consumption by caterpillars. *Functional Ecology* **10**(5): 668-674.
Coley PD, Aide TM. 1989. Red coloration of tropical young leaves: a possible antifungal defence? *Journal of Tropical Ecology* **5**(03): 293-300.
Coley PD, Barone JA. 1996. Herbivory and plant defenses in tropical forests. *Annual Review of Ecology and Systematics* **27**(ArticleType: research-article / Full publication date: 1996 / Copyright © 1996 Annual Reviews): 305-335.
Coley PD, Kursar TA 1996. Anti-herbivore defenses of young tropical leaves: Physiological constraints and ecological trade-offs. In: Mulkey SS, Chazdon RL, Smith AP eds. *Tropical Forest Plant Ecophysiology*: Springer US, 305-335.
Collatz GJ, Ball JT, Grivet C, Berry JA. 1991. Physiological and environmental regulation of stomatal conductance, photosynthesis and transpiration: a model that includes a laminar boundary layer. *Agricultural and Forest Meteorology* **54**(2): 107-136.
Collings DA. 2015. Optimisation approaches for concurrent transmitted light imaging during confocal microscopy. *Plant Methods* **11**(1): 1-11.
Cordell S, Goldstein G, Meinzer FC, Handley LL. 1999. Allocation of nitrogen and carbon in leaves of *Metrosideros polymorpha* regulates carboxylation capacity and $\delta^{13}C$ along an altitudinal gradient. *Functional Ecology* **13**(6): 811-818.
Coste S, Roggy J-C, Imbert P, Born C, Bonal D, Dreyer E. 2005. Leaf photosynthetic traits of 14 tropical rain forest species in relation to leaf nitrogen concentration and shade tolerance. *Tree Physiology* **25**(9): 1127-1137.
Cox PM. 2001. Description of the TRIFFID dynamic global vegetation model: Technical Note 24, Hadley Centre, United Kingdom Meteorological Office, Bracknell, UK.
Cramer W, Kicklighter D, Bondeau A, Iii BM, Churkina G, Nemry B, Ruimy A, Schloss A, Intercomparison T, Model POTPN. 1999. Comparing global models of terrestrial net primary productivity (NPP): overview and key results. *Global Change Biology* **5**(S1): 1-15.
Cunningham S, Read J. 2003. Comparison of temperate and tropical rainforest tree species: growth responses to temperature. *Journal of Biogeography* **30**(1): 143-153.
Cunningham SC, Read J. 2003. Do temperate rainforest trees have a greater ability to acclimate to changing temperatures than tropical rainforest trees? *New Phytologist* **157**(1): 55-64.
Czech AS, Strzałka K, Schurr U, Matsubara S. 2009. Developmental stages of delayed-greening leaves inferred from measurements of chlorophyll content and leaf growth. *Functional Plant Biology* **36**(7): 654-664.

De Kauwe MG, Lin Y-S, Wright IJ, Medlyn BE, Crous KY, Ellsworth DS, Maire V, Prentice IC, Atkin OK, Rogers A, et al. 2016. A test of the 'one-point method' for estimating maximum carboxylation capacity from field-measured, light-saturated photosynthesis. *New Phytologist* **210**(3): 1130-1144.

De Lucia EH, Whitehead D, Clearwater MJ. 2003. The relative limitation of photosynthesis by mesophyll conductance in co-occurring species in a temperate rainforest dominated by the conifer *Dacrydium cupressinum*. *Functional Plant Biology* **30**(12): 1197-1204.

de Pury D, Farquhar G. 1997. Simple scaling of photosynthesis from leaves to canopies without the errors of big-leaf models. *Plant, Cell & Environment* **20**(5): 537-557.

De Vries FWTP. 1975. The cost of maintenance processes in plant cells. *Annals of Botany* **39**(159): 77-92.

De Weirdt M, Verbeeck H, Maignan F, Peylin P, Poulter B, Bonal D, Ciais P, Steppe K. 2012. Seasonal leaf dynamics for tropical evergreen forests in a process-based global ecosystem model. *Geosci. Model Dev.* **5**(5): 1091-1108.

Demmig-Adams B, Adams WW. 2006. Photoprotection in an ecological context: the remarkable complexity of thermal energy dissipation. *New Phytologist* **172**(1): 11-21.

Dickmann DI. 1971. Photosynthesis and respiration by developing leaves of cottonwood (*Populus deltoides* Bartr.). *Botanical Gazette* **132**(4): 253-259.

Dietze MC. 2014. Gaps in knowledge and data driving uncertainty in models of photosynthesis. *Photosynthesis Research* **119**(1): 3-14.

Dodd IC, Critchley C, Woodall GS, Stewart GR. 1998. Photoinhibition in differently coloured juvenile leaves of *Syzygium* species. *Journal of Experimental Botany* **49**(325): 1437-1445.

Domingues TF, Berry JA, Martinelli LA, Ometto JPHB, Ehleringer JR. 2005. Parameterization of canopy structure and leaf-level gas exchange for an eastern Amazonian tropical rain forest (Tapajós National Forest, Pará, Brazil). *Earth Interactions* **9**(17): 1-23.

Domingues TF, Ishida FY, Feldpausch T, Grace J, Meir P, Saiz G, Sene O, Schrodt F, Sonké B, Taedoumg H, et al. 2015. Biome-specific effects of nitrogen and phosphorus on the photosynthetic characteristics of trees at a forest-savanna boundary in Cameroon. *Oecologia* **178**(3): 659-672.

Domingues TF, Martinelli LA, Ehleringer JR. 2007. Ecophysiological traits of plant functional groups in forest and pasture ecosystems from eastern Amazônia, Brazil. *Plant Ecology* **193**(1): 101-112.

Domingues TF, Meir P, Feldpausch TR, Saiz G, Veenendaal EM, Schrodt F, Bird M, Djagbletey G, Hien F, Compaore H, et al. 2010. Co-limitation of photosynthetic capacity by nitrogen and phosphorus in West Africa woodlands. *Plant, Cell & Environment* **33**(6): 959-980.

Dominy NJ, Lucas PW, Ramsden LW, Riba-Hernandez P, Stoner KE, Turner IM. 2002. Why are young leaves red? *Oikos* **98**(1): 163-176.

Dusenge M, Wallin G, Gårdesten J, Niyonzima F, Adolfsson L, Nsabimana D, Uddling J. 2015. Photosynthetic capacity of tropical montane tree species in relation to leaf nutrients, successional strategy and growth temperature. *Oecologia* **177**(4): 1183-1194.

Egea G, Gonzalez-Real MM, Baille A, Nortes PA, Diaz-Espejo A. 2011. Disentangling the contributions of ontogeny and water stress to photosynthetic limitations in almond trees. *Plant, Cell & Environment* **34**(6): 962-979.

Eichelmann H, Oja V, Rasulov B, Padu E, Bichele I, Pettai H, Niinemets ü, Laisk A. 2004. Development of leaf photosynthetic parameters in *Betula pendula* Roth leaves: correlations with photosystem I density. *Plant biology* **6**(3): 307-318.

Ekramoddoullah AKM. 1993. Analysis of needle proteins and N-terminal amino acid sequences of two photosystem II proteins of western white pine (*Pinus monticola* D. Don). *Tree Physiology* **12**(1): 101-106.

England J, Attiwill P. 2011. Changes in stomatal frequency, stomatal conductance and cuticle thickness during leaf expansion in the broad-leaved evergreen species, *Eucalyptus regnans*. *Trees* **25**(6): 987-996.

Epron D, Godard D, Cornic G, Genty B. 1995. Limitation of net CO_2 assimilation rate by internal resistances to CO_2 transfer in the leaves of two tree species (*Fagus sylvatica* L. and *Castanea sativa* Mill.). *Plant, Cell & Environment* **18**(1): 43-51.

Evans J, Sharkey T, Berry J, Farquhar G. 1986. Carbon isotope discrimination measured concurrently with gas exchange to investigate CO_2 diffusion in leaves of higher plants. *Functional Plant Biology* **13**(2): 281-292.

Evans JR. 1989. Photosynthesis and nitrogen relationships in leaves of C_3 plants. *Oecologia* **78**(1): 9-19.

Evans JR, Kaldenhoff R, Genty B, Terashima I. 2009. Resistances along the CO_2 diffusion pathway inside leaves. *Journal of Experimental Botany* **60**(8): 2235-2248.

Evans JR, Loreto F 2000. Acquisition and diffusion of CO_2 in higher plant leaves. In: Leegood RC, Sharkey TD, von Caemmerer S eds. *Photosynthesis: Physiology and Metabolism*. Dordrecht: Springer Netherlands, 321-351.

Evans JR, Poorter H. 2001. Photosynthetic acclimation of plants to growth irradiance: the relative importance of specific leaf area and nitrogen partitioning in maximizing carbon gain. *Plant, Cell & Environment* **24**(8): 755-767.

Evans JR, Seemann JR. 1989. *The allocation of protein nitrogen in the photosynthetic apparatus: costs, consequences, and control.* New York, USA: Alan R. Liss, Inc.

Evans JR, Von Caemmerer S. 2013. Temperature response of carbon isotope discrimination and mesophyll conductance in tobacco. *Plant, Cell & Environment* **36**(4): 745-756.

Falster DS, Warton DI, Wright IJ. 2006. SMATR: Standardised major axis tests and routines, version 2.0. .

Farquhar GD, Caemmerer S, Berry JA. 1980. A biochemical model of photosynthetic CO_2 assimilation in leaves of C_3 species. *Planta* **149**(1): 78-90.

Farquhar GD, Cernusak LA. 2012. Ternary effects on the gas exchange of isotopologues of carbon dioxide. *Plant, Cell & Environment* **35**(7): 1221-1231.

Field C, Mooney HA 1986. The photosynthesis-nitrogen relationship in wild plants. In: Givnish TJ ed. *On the economy of plant form and function: adaptative patterns of energy capture in plants*: Cambridge University Press, 25-56.

Fisher J, Malhi Y, Torres I, Metcalfe D, van de Weg M, Meir P, Silva-Espejo J, Huasco W. 2013. Nutrient limitation in rainforests and cloud forests along a 3,000-m elevation gradient in the Peruvian Andes. *Oecologia* **172**(3): 889-902.

Flexas J, Barbour MM, Brendel O, Cabrera HM, Carriquí M, Díaz-Espejo A, Douthe C, Dreyer E, Ferrio JP, Gago J, et al. 2012. Mesophyll diffusion conductance to CO_2: An unappreciated central player in photosynthesis. *Plant Science* **193–194**(0): 70-84.

Flexas J, Bota J, Galmés J, Medrano H, Ribas-Carbó M. 2006. Keeping a positive carbon balance under adverse conditions: responses of photosynthesis and respiration to water stress. *Physiologia Plantarum* **127**(3): 343-352.

Flexas J, Díaz-Espejo A, Berry J, Cifre J, Galmés J, Kaldenhoff R, Medrano H, Ribas-Carbó M. 2007. Analysis of leakage in IRGA's leaf chambers of open gas exchange systems: quantification and its effects in photosynthesis parameterization. *Journal of Experimental Botany* **58**(6): 1533-1543.

Flexas J, Ribas-Carbó M, Diaz-Espejo A, Galmés J, Medrano H. 2008. Mesophyll conductance to CO_2: current knowledge and future prospects. *Plant, Cell & Environment* **31**(5): 602-621.

Fredeen AL, Rao IM, Terry N. 1989. Influence of phosphorus nutrition on growth and carbon partitioning in *Glycine max*. *Plant Physiology* **89**(1): 225-230.

Friend AD. 2010. Terrestrial plant production and climate change. *Journal of Experimental Botany*.

Fyllas NM, Patiño S, Baker TR, Bielefeld Nardoto G, Martinelli LA, Quesada CA, Paiva R, Schwarz M, Horna V, Mercado LM, et al. 2009. Basin-wide variations in foliar properties of Amazonian forest: phylogeny, soils and climate. *Biogeosciences* **6**(11): 2677-2708.

Gago J, Daloso DdM, Figueroa CM, Flexas J, Fernie AR, Nikoloski Z. 2016. Relationships of leaf net photosynthesis, stomatal conductance, and mesophyll conductance to primary metabolism: A multispecies meta-analysis approach. *Plant Physiology* **171**(1): 265-279.

Gaspar MM, Ferreira RB, Chaves MM, Teixeira AR. 1997. Improved method for the extraction of proteins from *Eucalyptus* leaves. Application in leaf response to temperature. *Phytochemical Analysis* **8**(6): 279-285.

Gentry AH. 1988. Changes in plant community diversity and floristic composition on environmental and geographical gradients. *Annals of the Missouri Botanical Garden* **75**(1): 1-34.

Girardin CAJ, Espejob JES, Doughty CE, Huasco WH, Metcalfe DB, Durand-Baca L, Marthews TR, Aragao LE, Farfán-Rios W, García-Cabrera K. 2014a. Productivity and carbon allocation in a tropical montane cloud forest in the Peruvian Andes. *Plant Ecology & Diversity* **7**(1-2): 107-123.

Girardin CAJ, Farfan-Rios W, Garcia K, Feeley KJ, Jørgensen PM, Murakami AA, Cayola Pérez L, Seidel R, Paniagua N, Fuentes Claros AF, et al. 2014b. Spatial patterns of above-ground structure, biomass and composition in a network of six Andean elevation transects. *Plant Ecology & Diversity* **7**(1-2): 161-171.

Girardin CAJ, Malhi Y, Aragao LEOC, Mamani M, Huaraca Huasco W, Durand L, Feeley KJ, Rapp J, Silva-Espejo JE, Silman M, et al. 2010. Net primary productivity allocation and cycling of carbon along a tropical forest elevational transect in the Peruvian Andes. *Global Change Biology* **16**(12): 3176-3192.

Grace J. 2004. Understanding and managing the global carbon cycle. *Journal of Ecology* **92**(2): 189-202.

Grassi G, Magnani F. 2005. Stomatal, mesophyll conductance and biochemical limitations to photosynthesis as affected by drought and leaf ontogeny in ash and oak trees. *Plant, Cell & Environment* **28**(7): 834-849.

Gratani L, Bonito A. 2009. Leaf traits variation during leaf expansion in *Quercus ilex* L. *Photosynthetica* **47**(3): 323-330.

Grubb PJ. 1977. Control of forest growth and distribution on wet tropical mountains: with special reference to mineral nutrition. *Annual Review of Ecology and Systematics* **8**: 83-107.

Güsewell S. 2004. N : P ratios in terrestrial plants: variation and functional significance. *New Phytologist* **164**(2): 243-266.

Hanba YT, Miyazawa S-I, Kogami H, Terashima I. 2001. Effects of leaf age on internal CO_2 transfer conductance and photosynthesis in tree species having different types of shoot phenology. *Functional Plant Biology* **28**(11): 1075-1084.

Harley PC, Thomas RB, Reynolds JF, Strain BR. 1992. Modelling photosynthesis of cotton grown in elevated CO_2. *Plant, Cell & Environment* **15**(3): 271-282.

Harrison MT, Edwards EJ, Farquhar GD, Nicotra AB, Evans JR. 2009. Nitrogen in cell walls of sclerophyllous leaves accounts for little of the variation in photosynthetic nitrogen-use efficiency. *Plant, Cell & Environment* **32**(3): 259-270.

Haxeltine A, Prentice I. 1996. A general model for the light-use efficiency of primary production. *Functional Ecology*: 551-561.

Hedin LO. 2004. Global organization of terrestrial plant–nutrient interactions. *Proceedings of the National Academy of Sciences of the United States of America* **101**(30): 10849-10850.

Hijmans RJ, Cameron SE, Parra JL, Jones PG, Jarvis A. 2005. Very high resolution interpolated climate surfaces for global land areas. *International journal of climatology* **25**(15): 1965-1978.

Hikosaka K. 2004. Interspecific difference in the photosynthesis–nitrogen relationship: patterns, physiological causes, and ecological importance. *Journal of Plant Research* **117**(6): 481-494.

Hikosaka K, Hanba YT, Hirose T, Terashima I. 1998. Photosynthetic nitrogen-use efficiency in leaves of woody and herbaceous species. *Functional Ecology* **12**(6): 896-905.

Hikosaka K, Ishikawa K, Borjigidai A, Muller O, Onoda Y. 2006. Temperature acclimation of photosynthesis: mechanisms involved in the changes in temperature dependence of photosynthetic rate. *Journal of Experimental Botany* **57**(2): 291-302.

Hikosaka K, Kumagai To, Ito A 2015. Modeling canopy photosynthesis. In: Niinemets Ü, Hikosaka K, Anten NPR eds. *Canopy Photosynthesis: From Basics to Applications*: Springer Netherlands.

Hikosaka K, Nagamatsu D, Ishii HS, Hirose T. 2002. Photosynthesis–nitrogen relationships in species at different altitudes on Mount Kinabalu, Malaysia. *Ecological Research* **17**(3): 305-313.

Hikosaka K, Shigeno A. 2009. The role of Rubisco and cell walls in the interspecific variation in photosynthetic capacity. *Oecologia* **160**(3): 443-451.

Holaday AS, Martindale W, Alred R, Brooks AL, Leegood RC. 1992. Changes in activities of enzymes of carbon metabolism in leaves during exposure of plants to low temperature. *Plant Physiology* **98**(3): 1105-1114.

Houghton RA. 2007. Balancing the global carbon budget. *Annual Review of Earth and Planetary Sciences* **35**(1): 313-347.

IPCC. 2013. *Climate Change 2013: The Physical Science Basis*. Cambridge, UK and New York, USA: Cambridge University Press.

Ishida A, Uemura A, Koike N, Matsumoto Y, Hoe AL. 1999. Interactive effects of leaf age and self-shading on leaf structure, photosynthetic capacity and chlorophyll fluorescence in the rain forest tree, *Dryobalanops aromatica*. *Tree Physiology* **19**(11): 741-747.

Ito A. 2011. A historical meta-analysis of global terrestrial net primary productivity: are estimates converging? *Global Change Biology* **17**(10): 3161-3175.

Ito A, Saigusa N, Murayama S, Yamamoto S. 2005. Modeling of gross and net carbon dioxide exchange over a cool-temperate deciduous broad-leaved forest in Japan: analysis of seasonal and interannual change. *Agricultural and Forest Meteorology* **134**(1): 122-134.

Jacob J, Lawlor DW. 1992. Dependence of photosynthesis of sunflower and maize leaves on phosphate supply, Ribulose-1,5-Bisphosphate Carboxylase/Oxygenase activity, and Ribulose-1,5-Bisphosphate pool size. *Plant Physiology* **98**(3): 801-807.

Jacob J, Lawlor DW. 1993. Extreme phosphate deficiency decreases the *in vivo* CO_2/O_2 specificity factor of Ribulose 1,5-Bisphosphate Carboxylase-Oxygenase in intact leaves of sunflower. *Journal of Experimental Botany* **44**(11): 1635-1641.

Kattge J, Knorr W, Raddatz T, Wirth C. 2009. Quantifying photosynthetic capacity and its relationship to leaf nitrogen content for global-scale terrestrial biosphere models. *Global Change Biology* **15**(4): 976-991.

Kellogg E, Juliano N. 1997. The structure and function of RuBisCO and their implications for systematic studies. *American Journal of Botany* **84**(3): 413-413.

Kikuzawa K, Onoda Y, Wright IJ, Reich PB. 2013. Mechanisms underlying global temperature-related patterns in leaf longevity. *Global Ecology and Biogeography* **22**(8): 982-993.

Kositsup B, Kasemsap P, Thanisawanyangkura S, Chairungsee N, Satakhun D, Teerawatanasuk K, Ameglio T, Thaler P. 2010. Effect of leaf age and position on light-saturated CO_2 assimilation rate, photosynthetic capacity, and stomatal conductance in rubber trees. *Photosynthetica* **48**(1): 67-78.

Kozela C, Regan S. 2003. How plants make tubes. *Trends in Plant Science* **8**(4): 159-164.

Kozlowski TT. 1992. Carbohydrate sources and sinks in woody plants. *Botanical Review* **58**(2): 107-222.

Kraft NJB, Valencia R, Ackerly DD. 2008. Functional traits and niche-based tree community assembly in an Amazonian forest. *Science* **322**(5901): 580-582.

Krause GH, Virgo A, Winter K. 1995. High susceptibility to photoinhibition of young leaves of tropical forest trees. *Planta* **197**(4): 583-591.

Krinner G, Viovy N, de Noblet-Ducoudré N, Ogée J, Polcher J, Friedlingstein P, Ciais P, Sitch S, Prentice IC. 2005. A dynamic global vegetation model for studies of the coupled atmosphere-biosphere system. *Global Biogeochemical Cycles* **19**(1).

Kumagai To, Ichie T, Yoshimura M, Yamashita M, Kenzo T, Saitoh TM, Ohashi M, Suzuki M, Koike T, Komatsu H. 2006. Modeling CO_2 exchange over a Bornean tropical rain forest using measured vertical and horizontal variations in leaf-level physiological parameters and leaf area densities. *Journal of Geophysical Research: Atmospheres* **111**(D10): D10107.

Kursar T, Coley P. 1992. Delayed development of the photosynthetic apparatus in tropical rain forest species. *Functional Ecology*: 411-422.

Kursar TA, Coley PD. 1991. Nitrogen content and expansion rate of young leaves of rain forest species: implications for herbivory. *Biotropica*: 141-150.

Kursar TA, Coley PD. 1992. Delayed greening in tropical leaves: An antiherbivore defense? *Biotropica* **24**(2): 256-262.

Kursar TA, Coley PD. 2003. Convergence in defense syndromes of young leaves in tropical rainforests. *Biochemical Systematics and Ecology* **31**(8): 929-949.

Kwesiga FR, Grace J, Sandford AP. 1986. Some photosynthetic characteristics of tropical timber trees as affected by the light regime during growth. *Annals of Botany* **58**(1): 23-32.

Lauer MJ, Pallardy SG, Blevins DG, Randall DD. 1989. Whole leaf carbon exchange characteristics of phosphate deficient soybeans (*Glycine max L.*). *Plant Physiology* **91**(3): 848-854.

Letts MG, Mulligan M. 2005. The impact of light quality and leaf wetness on photosynthesis in north-west Andean tropical montane cloud forest. *Journal of Tropical Ecology* **21**(05): 549-557.

Lloyd J, Bloomfield K, Domingues TF, Farquhar GD. 2013. Photosynthetically relevant foliar traits correlating better on a mass vs an area basis: of ecophysiological relevance or just a case of mathematical imperatives and statistical quicksand? *New Phytologist* **199**(2): 311-321.

Lloyd J, Grace J, Miranda AC, Meir P, Wong S, Miranda HS, Wright I, Gash J, McIntyre J. 1995. A simple calibrated model of Amazon rainforest productivity based on leaf biochemical properties. *Plant, Cell & Environment* **18**(10): 1129-1145.

Lloyd J, Syvertsen JP, Kriedemann PE, Farquhar GD. 1992. Low conductances for CO_2 diffusion from stomata to the sites of carboxylation in leaves of woody species. *Plant, Cell & Environment* **15**(8): 873-899.

Long SP, Bernacchi CJ. 2003. Gas exchange measurements, what can they tell us about the underlying limitations to photosynthesis? Procedures and sources of error. *Journal of Experimental Botany* **54**(392): 2393-2401.

Lopes AP, Nelson BW, Wu J, Graça PMLdA, Tavares JV, Prohaska N, Martins GA, Saleska SR. 2016. Leaf flush drives dry season green-up of the Central Amazon. *Remote Sensing of Environment* **182**: 90-98.

Loustau D, Brahim MB, Gaudillère J-P, Dreyer E. 1999. Photosynthetic responses to phosphorus nutrition in two-year-old maritime pine seedlings. *Tree Physiology* **19**(11): 707-715.

Lucas PW, Turner IM, Dominy NJ, Yamashita N. 2000. Mechanical defences to herbivory. *Annals of Botany* **86**(5): 913-920.

Luyssaert S, Inglima I, Jung M, Richardson AD, Reichstein M, Papale D, Piao SL, Schulze ED, Wingate L, Matteucci G, et al. 2007. CO_2 balance of boreal, temperate, and tropical forests derived from a global database. *Global Change Biology* **13**(12): 2509-2537.

Maayan I, Shaya F, Ratner K, Mani Y, Lavee S, Avidan B, Shahak Y, Ostersetzer-Biran O. 2008. Photosynthetic activity during olive (*Olea europaea*) leaf development correlates with plastid biogenesis and Rubisco levels. *Physiologia Plantarum* **134**(3): 547-558.

Malhi Y. 2010. The carbon balance of tropical forest regions, 1990–2005. *Current Opinion in Environmental Sustainability* **2**(4): 237-244.

Manter DK, Kerrigan J. 2004. A/C_i curve analysis across a range of woody plant species: influence of regression analysis parameters and mesophyll conductance. *Journal of Experimental Botany* **55**(408): 2581-2588.

Marchi S, Tognetti R, Minnocci A, Borghi M, Sebastiani L. 2008. Variation in mesophyll anatomy and photosynthetic capacity during leaf development in a deciduous mesophyte fruit tree (*Prunus persica*) and an evergreen sclerophyllous Mediterranean shrub (*Olea europaea*). *Trees* **22**(4): 559-571.

Marra FP, Barone E, La Mantia M, Caruso T. 2009. Toward the definition of a carbon budget model: seasonal variation and temperature effect on respiration rate of vegetative and reproductive organs of pistachio trees (*Pistacia vera*). *Tree Physiology*.

Marthews TR, Malhi Y, Girardin CAJ, Silva Espejo JE, Aragão LEOC, Metcalfe DB, Rapp JM, Mercado LM, Fisher RA, Galbraith DR, et al. 2012. Simulating forest productivity along a neotropical elevational transect: temperature variation and carbon use efficiency. *Global Change Biology* **18**(9): 2882-2898.

Martinelli LA, Piccolo MC, Townsend AR, Vitousek PM, Cuevas E, McDowell W, Robertson GP, Santos OC, Treseder K 1999. Nitrogen stable isotopic composition of leaves and soil: Tropical versus temperate forests. In: Townsend A ed. *New Perspectives on Nitrogen Cycling in the Temperate and Tropical Americas*: Springer Netherlands, 45-65.

Medlyn BE, Dreyer E, Ellsworth D, Forstreuter M, Harley PC, Kirschbaum MUF, Le Roux X, Montpied P, Strassemeyer J, Walcroft A, et al. 2002. Temperature response of parameters of a biochemically based model of photosynthesis. II. A review of experimental data. *Plant, Cell & Environment* **25**(9): 1167-1179.

Meir P, Kruijt B, Broadmeadow M, Barbosa E, Kull O, Carswell F, Nobre A, Jarvis PG. 2002. Acclimation of photosynthetic capacity to irradiance in tree canopies in relation to leaf nitrogen concentration and leaf mass per unit area. *Plant, Cell & Environment* **25**(3): 343-357.

Meir P, Levy P, Grace J, Jarvis P. 2007. Photosynthetic parameters from two contrasting woody vegetation types in West Africa. *Plant Ecology* **192**(2): 277-287.

Mercado LM, Patiño S, Domingues TF, Fyllas NM, Weedon GP, Sitch S, Quesada CA, Phillips OL, Aragão LEOC, Malhi Y, et al. 2011. Variations in Amazon forest productivity correlated with foliar nutrients and modelled rates of photosynthetic carbon supply. *Philosophical Transactions of the Royal Society B: Biological Sciences* **366**(1582): 3316-3329.

Metcalfe DB, Asner GP, Martin RE, Silva Espejo JE, Huasco WH, Farfán Amézquita FF, Carranza-Jimenez L, Galiano Cabrera DF, Baca LD, Sinca F, et al. 2014. Herbivory makes major contributions to ecosystem carbon and nutrient cycling in tropical forests. *Ecology Letters* **17**(3): 324-332.

Milla R, Castro-Díez P, Maestro-Martínez M, Montserrat-Martí G. 2005. Relationships between phenology and the remobilization of nitrogen, phosphorus and potassium in branches of eight Mediterranean evergreens. *New Phytologist* **168**(1): 167-178.

Miyazawa SI, Makino A, Terashima I. 2003. Changes in mesophyll anatomy and sink–source relationships during leaf development in *Quercus glauca*, an evergreen tree showing delayed leaf greening. *Plant, Cell & Environment* **26**(5): 745-755.

Miyazawa SI, Terashima I. 2001. Slow development of leaf photosynthesis in an evergreen broad-leaved tree, *Castanopsis sieboldii*: relationships between leaf anatomical characteristics and photosynthetic rate. *Plant, Cell & Environment* **24**(3): 279-291.

Moon M, Kang K-S, Park I-K, Kim T, Kim H. 2015. Effects of leaf nitrogen allocation on the photosynthetic nitrogen-use efficiency of seedlings of three tropical species in Indonesia. *Journal of the Korean Society for Applied Biological Chemistry* **58**(4): 511-519.

Moraes FKC, Castro GLS, Silva Júnior DD, Pinheiro HA, Festucci-Buselli RA. 2011. Chloroplastidic pigments, gas exchange, and carbohydrates changes during *Carapa guianensis* leaflet expansion. *Photosynthetica* **49**(4): 619-626.

Niinemets Ü, Cescatti A, Rodeghiero M, Tosens T. 2005. Leaf internal diffusion conductance limits photosynthesis more strongly in older leaves of Mediterranean evergreen broad-leaved species. *Plant, Cell & Environment* **28**(12): 1552-1566.

Niinemets Ü, Díaz-Espejo A, Flexas J, Galmés J, Warren CR. 2009. Role of mesophyll diffusion conductance in constraining potential photosynthetic productivity in the field. *Journal of Experimental Botany*.

Niinemets U, García-Plazaola JI, Tosens T 2012. Photosynthesis during leaf development and ageing. In: Flexas J, Loreto F, Medrano H eds. *Terrestrial Photosynthesis in a Changing Environment*: Cambridge University Press, 353-372.

Niinemets Ü, Keenan TF, Hallik L. 2014. A worldwide analysis of within-canopy variations in leaf structural, chemical and physiological traits across plant functional types. *New Phytologist* **205**(3): 973-993.

Niinemets Ü, Sack L 2006. Structural determinants of leaf light-harvesting capacity and photosynthetic potentials. In: Esser K, Lüttge U, Beyschlag W, Murata J eds. *Progress in Botany*. Berlin, Heidelberg: Springer Berlin Heidelberg, 385-419.

Niinemets Ü, Tenhunen JD. 1997. A model separating leaf structural and physiological effects on carbon gain along light gradients for the shade-tolerant species *Acer saccharum*. *Plant, Cell & Environment* **20**(7): 845-866.

Pan Y, Birdsey RA, Fang J, Houghton R, Kauppi PE, Kurz WA, Phillips OL, Shvidenko A, Lewis SL, Canadell JG, et al. 2011. A large and persistent carbon sink in the world's forests. *Science* **333**(6045): 988-993.

Paul MJ, Pellny TK. 2003. Carbon metabolite feedback regulation of leaf photosynthesis and development. *Journal of Experimental Botany* **54**(382): 539-547.

Pinheiro J, Bates D. 2000. *Mixed-Effects Models in S and S-PLUS*: Springer New York.

Pons TL, van der Werf A, Lambers H. 1994. *Photosynthetic nitrogen use efficiency of inherently low- and fast-growing species: possible explanations for observed differences.* The Hague, Netherlands: SPB Academic Publishing.

Pons TL, Welschen RAM. 2003. Midday depression of net photosynthesis in the tropical rainforest tree *Eperua grandiflora*: contributions of stomatal and internal conductances, respiration and Rubisco functioning. *Tree Physiology* **23**(14): 937-947.

Poorter H, Evans JR. 1998. Photosynthetic nitrogen-use efficiency of species that differ inherently in specific leaf area. *Oecologia* **116**(1-2): 26-37.

Potter CS, Randerson JT, Field CB, Matson PA, Vitousek PM, Mooney HA, Klooster SA. 1993. Terrestrial ecosystem production: A process model based on global satellite and surface data. *Global Biogeochemical Cycles* **7**(4): 811-841.

Prentice IC, Farquhar GD, Fasham MJR, Goulden ML, Heimann M, Jaramillo VJ, Kheshi HS, Le Quere C, Scholes RJ, Wallace DWR 2001. The carbon cycle and atmospheric carbon dioxide. In: al. JTHe ed. *Contribution of Working Group I to the Third Assessment Report of the Intergovernmental Panel on Climate Change*. Cambridge: Cambridge University Press, 183-237.

Queenborough SA, Metz MR, Valencia R, Wright SJ. 2013. Demographic consequences of chromatic leaf defence in tropical tree communities: do red young leaves increase growth and survival? *Annals of Botany*: mct144.

Quesada CA, Lloyd J, Schwarz M, Patiño S, Baker TR, Czimczik C, Fyllas NM, Martinelli L, Nardoto GB, Schmerler J, et al. 2010. Variations in chemical and physical properties of Amazon forest soils in relation to their genesis. *Biogeosciences* **7**: 1515-1541.

Quesada CA, Phillips OL, Schwarz M, Czimczik CI, Baker TR, Patiño S, Fyllas NM, Hodnett MG, Herrera R, Almeida S, et al. 2012. Basin-wide variations in Amazon forest structure and function are mediated by both soils and climate. *Biogeosciences* **9**(6): 2203-2246.

Quilici A, Medina E. 1998. Photosynthesis-nitrogen relationships in pioneer plants of disturbed tropical montane forest sites. *Photosynthetica* **35**(4): 525-534.

Raaimakers D, Boot RGA, Dijkstra P, Pot S. 1995. Photosynthetic rates in relation to leaf phosphorus content in pioneer versus climax tropical rainforest trees. *Oecologia* **102**(1): 120-125.

Rada F, García-Núñez C, Ataroff M. 2009. Leaf gas exchange in canopy species of a Venezuelan cloud forest. *Biotropica* **41**(6): 659-664.

Ramos J, Grace J. 1990. The effects of shade on the gas exchange of seedlings of four tropical trees from Mexico. *Functional Ecology* **4**(5): 667-677.

Read J, Gras E, Sanson GD, Clissold F, Brunt C. 2003. Does chemical defence decline more in developing leaves that become strong and tough at maturity? *Australian Journal of Botany* **51**(5): 489-496.

Reich P, Oleksyn J, Wright I. 2009. Leaf phosphorus influences the photosynthesis–nitrogen relation: a cross-biome analysis of 314 species. *Oecologia* **160**(2): 207-212.

Reich PB, Oleksyn J. 2004. Global patterns of plant leaf N and P in relation to temperature and latitude. *Proceedings of the National Academy of Sciences of the United States of America* **101**(30): 11001-11006.

Reich PB, Walters MB. 1994. Photosynthesis-nitrogen relations in Amazonian tree species. *Oecologia* **97**(1): 73-81.

Restrepo-Coupe N, da Rocha HR, Hutyra LR, da Araujo AC, Borma LS, Christoffersen B, Cabral OMR, de Camargo PB, Cardoso FL, da Costa ACL, et al. 2013. What drives the seasonality of photosynthesis across the Amazon basin? A cross-site analysis of eddy flux tower measurements from the Brasil flux network. *Agricultural and Forest Meteorology* **182–183**: 128-144.

Riddoch I, Lehto T, Grace J. 1991. Photosynthesis of tropical tree seedlings in relation to light and nutrient supply. *New Phytologist* **119**(1): 137-147.

Rogers A. 2014. The use and misuse of *Vc,max* in Earth System Models. *Photosynthesis Research* **119**(1-2): 15-29.

Rowland L, Lobo-do-Vale RL, Christoffersen BO, Melém EA, Kruijt B, Vasconcelos SS, Domingues T, Binks OJ, Oliveira AAR, Metcalfe D, et al. 2015. After more than a decade of soil moisture deficit, tropical rainforest trees maintain photosynthetic capacity, despite increased leaf respiration. *Global Change Biology* **21**(12): 4662-4672.

Rozendaal DMA, Hurtado VH, Poorter L. 2006. Plasticity in leaf traits of 38 tropical tree species in response to light; relationships with light demand and adult stature. *Functional Ecology* **20**(2): 207-216.

Sage RF, Kubien DS. 2007. The temperature response of C_3 and C_4 photosynthesis. *Plant, Cell & Environment* **30**(9): 1086-1106.

Santiago LS, Mulkey SS. 2003. A test of gas exchange measurements on excised canopy branches of ten tropical tree species. *Photosynthetica* **41**(3): 343-347.

Sawhney SK, Naik MS, Nicholas DJD. 1978. Regulation of nitrate reduction by light, ATP and mitochondrial respiration in wheat leaves. *Nature* **272**(5654): 647-648.

Scafaro AP, Xiang S, Long BM, Bahar NHA, Weerasinghe KWLK, Creek D, Evans JR, Reich PB, Atkin OK. submitted. Strong thermal acclimation of photosynthesis in tropical and temperate wet-forest tree species: the importance of altered Rubisco content.

Schulze E, Kelliher FM, Korner C, Lloyd J, Leuning R. 1994. Relationships among maximum stomatal conductance, ecosystem surface conductance, carbon assimilation rate, and plant nitrogen nutrition: A global ecology scaling exercise. *Annual Review of Ecology and Systematics* **25**(1): 629-662.

Šesták Z, Tichá I, Čatský, F., Solárová J, Pospišilová J, Hodáňová D 1985. Integration of photosynthetic characteristics during leaf development. In: Šestăk Z ed. *Photosynthesis during leaf development*: Springer Netherlands, 263-286.

Sharkey TD, Bernacchi CJ, Farquhar GD, Singsaas EL. 2007. Fitting photosynthetic carbon dioxide response curves for C_3 leaves. *Plant, Cell & Environment* **30**(9): 1035-1040.

Shirke PA. 2001. Leaf photosynthesis, dark respiration and fluorescence as influenced by leaf age in an evergreen tree, *Prosopis juliflora*. *Photosynthetica* **39**(2): 305-311.

Showalter AM. 1993. Structure and function of plant cell wall proteins. *The Plant Cell* **5**(1): 9.

Silman MR. 2014. Functional megadiversity. *Proceedings of the National Academy of Sciences of the United States of America* **111**(16): 5763-5764.

Silva JO, Espírito-Santo MM, Morais HC. 2015. Leaf traits and herbivory on deciduous and evergreen trees in a tropical dry forest. *Basic and Applied Ecology* **16**(3): 210-219.

Sitch S, Smith B, Prentice IC, Arneth A, Bondeau A, Cramer W, Kaplan JO, Levis S, Lucht W, Sykes MT, et al. 2003. Evaluation of ecosystem dynamics, plant geography and terrestrial carbon cycling in the LPJ dynamic global vegetation model. *Global Change Biology* **9**(2): 161-185.

Sobrado MA. 1994. Leaf age effects on photosynthetic rate, transpiration rate and nitrogen content in a tropical dry forest. *Physiologia Plantarum* **90**(1): 210-215.

Specht RL, Specht A. 1999. Australian plant communities: dynamics of structure, growth and biodiversity. *Australian plant communities: dynamics of structure, growth and biodiversity.*

Steffen W, Noble I, Canadell J, Apps M, Schulze ED, Jarvis PG, Baldocchi D, Ciais P, Cramer W, Ehleringer JR. 1998. The terrestrial carbon cycle. *Science* **280**(5368): 1393-1394.

Stitt M, Schulze D. 1994. Does Rubisco control the rate of photosynthesis and plant growth? An exercise in molecular ecophysiology. *Plant, Cell & Environment* **17**(5): 465-487.

Sun Y, Gu L, Dickinson RE, Norby RJ, Pallardy SG, Hoffman FM. 2014a. Impact of mesophyll diffusion on estimated global land CO_2 fertilization. *Proceedings of the National Academy of Sciences* **111**(44): 15774-15779.

Sun Y, Gu L, Dickinson RE, Pallardy SG, Baker J, Cao Y, Damatta FM, Dong X, Ellsworth D, Van Goethem D, et al. 2014b. Asymmetrical effects of mesophyll conductance on fundamental photosynthetic parameters and their relationships estimated from leaf gas exchange measurements. *Plant, Cell & Environment* **37**(4): 978-994.

Takashima T, Hikosaka K, Hirose T. 2004. Photosynthesis or persistence: nitrogen allocation in leaves of evergreen and deciduous *Quercus* species. *Plant, Cell & Environment* **27**(8): 1047-1054.

Tazoe Y, Von Caemmerer S, Estavillo GM, Evans JR. 2011. Using tunable diode laser spectroscopy to measure carbon isotope discrimination and mesophyll conductance to CO_2 diffusion dynamically at different CO_2 concentrations. *Plant, Cell & Environment* **34**(4): 580-591.

Tellez P, Rojas E, Van Bael S. 2016. Red coloration in young tropical leaves associated with reduced fungal pathogen damage. *Biotropica*.

Terashima I, Masuzawa T, Ohba H, Yokoi Y. 1995. Is photosynthesis suppressed at higher elevations due to low CO_2 pressure? *Ecology* **76**(8): 2663-2668.

Terwilliger VJ, Kitajima K, Le Roux-Swarthout DJ, Mulkey S, Wright SJ. 2001. Intrinsic water-use efficiency and heterotrophic investment in tropical leaf growth of two Neotropical pioneer tree species as estimated from $\delta^{13}C$ values. *New Phytologist* **152**(2): 267-281.

Tomás M, Flexas J, Copolovici L, Galmés J, Hallik L, Medrano H, Ribas-Carbó M, Tosens T, Vislap V, Niinemets Ü. 2013. Importance of leaf anatomy in determining mesophyll diffusion conductance to CO_2 across species: quantitative limitations and scaling up by models. *Journal of Experimental Botany* **64**(8): 2269-2281.

Tosens T, Niinemets Ü, Vislap V, Eichelmann H, Castro DÍez P. 2012. Developmental changes in mesophyll diffusion conductance and photosynthetic capacity under different light and water availabilities in *Populus tremula*: how structure constrains function. *Plant, Cell & Environment* **35**(5): 839-856.

Townsend AR, Cleveland CC, Asner GP, Bustamante MMC. 2007. Controls over foliar N:P ratios in tropical rain forests. *Ecology* **88**(1): 107-118.

Turnbull MH, Doley D, Yates DJ. 1993. The dynamics of photosynthetic acclimation to changes in light quanlity and quality in three Australian rainforest tree species. *Oecologia* **94**(2): 218-228.

van de Weg M, Meir P, Grace J, Atkin OK. 2009. Altitudinal variation in leaf mass per unit area, leaf tissue density and foliar nitrogen and phosphorus content along an Amazon-Andes gradient in Peru. *Plant Ecology & Diversity* **2**(3): 243-254.

van de Weg M, Meir P, Grace J, Ramos G. 2012. Photosynthetic parameters, dark respiration and leaf traits in the canopy of a Peruvian tropical montane cloud forest. *Oecologia* **168**(1): 23-34.

van de Weg M, Meir P, Williams M, Girardin C, Malhi Y, Silva-Espejo J, Grace J. 2014. Gross primary productivity of a high elevation tropical montane cloud forest. *Ecosystems* **17**(5): 751-756.

Vapaavuori EM, Vuorinen AH. 1989. Seasonal variation in the photosynthetic capacity of a willow (*Salix cv. Aquatica gigantea*) canopy. 1 Changes in the activity and amount of ribulose 1,5-bisphosphate carboxylase-oxygenase and the content of nitrogen and chlorophyll at different levels in the canopy. *Tree Physiology* **5**(4): 423-444.

Vårhammar A, Wallin G, McLean CM, Dusenge ME, Medlyn BE, Hasper TB, Nsabimana D, Uddling J. 2015. Photosynthetic temperature responses of tree species in Rwanda: evidence of pronounced negative effects of high temperature in montane rainforest climax species. *New Phytologist* **206**(3): 1000-1012.

Varone L, Gratani L. 2009. Leaf expansion in *Rhamnus alaternus* L. by leaf morphological, anatomical and physiological analysis. *Trees* **23**(6): 1255-1262.

Verheijen L, Brovkin V, Aerts R, Bönish G, Cornelissen J, Kattge J, Reich P, Wright I, Van Bodegom P. 2013. Impacts of trait variation through observed trait-climate relationships on performance of a representative Earth System model: a conceptual analysis. *Biogeosciences* **10**: 5497-5515.

Villar R, Held AA, Merino J. 1995. Dark leaf respiration in light and darkness of an evergreen and a deciduous plant species. *Plant Physiology* **107**(2): 421-427.

Vitousek PM. 1984. Litterfall, nutrient cycling, and nutrient limitation in tropical forests *Ecology* **65**: 285-298.

von Caemmerer S, Evans JR. 2015. Temperature responses of mesophyll conductance differ greatly between species. *Plant, Cell & Environment* **38**(4): 629-637.

von Caemmerer S, Evans JR, Hudson GS, Andrews TJ. 1994. The kinetics of ribulose-1, 5-bisphosphate carboxylase/oxygenase *in vivo* inferred from measurements of photosynthesis in leaves of transgenic tobacco. *Planta* **195**(1): 88-97.

von Caemmerer S, Farquhar GD. 1981. Some relationships between the biochemistry of photosynthesis and the gas exchange of leaves. *Planta* **153**(4): 376-387.

Vu JCV, Yelenosky G. 1988. Water deficit and associated changes in some photosynthetic parameters in leaves of `Valencia' orange (*Citrus sinensis* [L.] Osbeck). *Plant Physiology* **88**(2): 375-378.

Walker AP, Beckerman AP, Gu L, Kattge J, Cernusak LA, Domingues TF, Scales JC, Wohlfahrt G, Wullschleger SD, Woodward FI. 2014. The relationship of leaf photosynthetic traits – V_{cmax} and J_{max} – to leaf nitrogen, leaf phosphorus, and specific leaf area: a meta-analysis and modeling study. *Ecology and Evolution* **4**(16): 3218-3235.

Walker B, Ariza LS, Kaines S, Badger MR, Cousins AB. 2013. Temperature response of in vivo Rubisco kinetics and mesophyll conductance in Arabidopsis thaliana: comparisons to Nicotiana tabacum. *Plant, Cell & Environment* **36**(12): 2108-2119.

Warren CR. 2008. Stand aside stomata, another actor deserves centre stage: the forgotten role of the internal conductance to CO_2 transfer. *Journal of Experimental Botany* **59**(7): 1475-1487.

Warren CR, Adams MA. 2001. Distribution of N, Rubisco and photosynthesis in *Pinus pinaster* and acclimation to light. *Plant, Cell & Environment* **24**(6): 597-609.

Warren CR, Adams MA. 2002. Phosphorus affects growth and partitioning of nitrogen to Rubisco in *Pinus pinaster*. *Tree Physiology* **22**(1): 11-19.

Warren CR, Adams MA. 2006. Internal conductance does not scale with photosynthetic capacity: implications for carbon isotope discrimination and the economics of water and nitrogen use in photosynthesis. *Plant, Cell & Environment* **29**(2): 192-201.

Warren CR, Adams MA, Chen Z. 2000. Is photosynthesis related to concentrations of nitrogen and Rubisco in leaves of Australian native plants? *Functional Plant Biology* **27**(5): 407-416.

Warton DI, Wright IJ, Falster DS, Westoby M. 2006. Bivariate line-fitting methods for allometry. *Biological Reviews* **81**: 259-291.

Wendler R, Carvalho P, Pereira J, Millard P. 1995. Role of nitrogen remobilization from old leaves for new leaf growth of *Eucalyptus globulus* seedlings. *Tree Physiology* **15**(10): 679-683.

Westbeek MHM, Pons TL, Cambridge ML, Atkin OK. 1999. Analysis of differences in photosynthetic nitrogen use efficiency of alpine and lowland *Poa* species. *Oecologia* **120**(1): 19-26.

Whitehead D, Barbour MM, Griffin KL, Turnbull MH, Tissue DT. 2011. Effects of leaf age and tree size on stomatal and mesophyll limitations to photosynthesis in mountain beech (*Nothofagus solandrii* var. cliffortiodes). *Tree Physiology* **31**(9): 985-996.

Wiggins NL, Forrister DL, Endara M-J, Coley PD, Kursar TA. 2016. Quantitative and qualitative shifts in defensive metabolites define chemical defense investment during leaf development in *Inga*, a genus of tropical trees. *Ecology and Evolution* **6**(2): 478-492.

Wittich B, Horna V, Homeier J, Leuschner C. 2012. Altitudinal change in the photosynthetic capacity of tropical trees: A case study from Ecuador and a pantropical literature analysis. *Ecosystems* **15**(6): 958-973.

Woodall GS, Dodd IC, Stewart GR. 1998. Contrasting leaf development within the genus *Syzygium*. *Journal of Experimental Botany* **49**(318): 79-87.

Wright IJ, Reich PB, Westoby M, Ackerly DD, Baruch Z, Bongers F, Cavender-Bares J, Chapin T, Cornelissen JHC, Diemer M, et al. 2004. The worldwide leaf economics spectrum. *Nature* **428**(6985): 821-827.

Wu B-J, Chow WS, Liu Y-J, Shi L, Jiang C-D. 2014. Effects of stomatal development on stomatal conductance and on stomatal limitation of photosynthesis in *Syringa oblata* and *Euonymus japonicus* Thunb. *Plant Science* **229**(0): 23-31.

Wu J, Albert LP, Lopes AP, Restrepo-Coupe N, Hayek M, Wiedemann KT, Guan K, Stark SC, Christoffersen B, Prohaska N, et al. 2016. Leaf development and demography explain photosynthetic seasonality in Amazon evergreen forests. *Science* **351**(6276): 972-976.

Wullschleger SD. 1993. Biochemical limitations to carbon assimilation in C_3 plants—A retrospective analysis of the A/C_i Curves from 109 species. *Journal of Experimental Botany* **44**(5): 907-920.

Wullschleger SD, Epstein HE, Box EO, Euskirchen ES, Goswami S, Iversen CM, Kattge J, Norby RJ, van Bodegom PM, Xu X. 2014. Plant functional types in Earth system models: past experiences and future directions for application of dynamic vegetation models in high-latitude ecosystems. *Annals of Botany*.

Xiang S, Reich PB, Sun S, Atkin OK. 2013. Contrasting leaf trait scaling relationships in tropical and temperate wet forest species. *Functional Ecology* **27**(2): 522-534.

Yasumura Y, Ishida A. 2011. Temporal variation in leaf nitrogen partitioning of a broad-leaved evergreen tree, *Quercus myrsinaefolia*. *Journal of Plant Research* **124**(1): 115-123.

Zuur A, Ieno EN, Walker N, Saveliev AA, Smith GM. 2009. *Mixed effects models and extensions in ecology with R*: Springer.

Appendix 1: Optimization of protocols for protein extraction from the leaves of recalcitrant tree species

Trouble-shooting using temperate and tropical evergreen species

The analysis of protein recalcitrant to extraction from some tree species is complicated by the abundance of lipids, tannins, phenols, waxes, oils and other secondary compounds (Ekramoddoullah, 1993; Gaspar *et al.*, 1997). The leaves of many of the species analysed in this study are characteristically aromatic and tough in nature and initial attempts to extract protein resulted in smeared bands on SDS-PAGE gels and highly oxidized extracts in most cases. Invariably, the extraction of proteins in their native confirmation (for example for the analysis of Rubisco active site concentration) was impossible. Moreover, previous attempts to isolate protein and Rubisco from hard-leaved species had been unsuccessful (Harrison *et al.*, 2009, Bloomfield, Long, Evans, unpublished). Using a combination of protein extraction from recalcitrant species (Gaspar *et al.*, 1997) and detergent based-extraction buffer (Brown *et al.*, 2008), we successfully extracted protein from Peruvian tropical leaves and Australian tropical and temperate leaves (Scafaro *et al.* submitted).

The process of extracting protein from the leaves was modified from that described by Gaspar *et al.* (1997) in order to allow the extraction and measurement of chlorophyll prior to protein analysis. Leaves were initially pulverised using a Tissue-Lyser (Qiagen) and were treated with one of the following extraction solvents:

1) Acetic acid, methanol and water (1:10:9) (as per Gaspar *et al.* (1997))
2) 80% (v/v) acetone
3) 100% (v/v) methanol

After initial extraction in these solvents, precipitated protein was further washed in hexane and acetone as described by Gaspar *et al.* (1997) to remove lipids and remaining pigments, leaving a protein pellet. Proteins were dissolved in protein extraction buffer [PEB, (Brown *et al.*, 2008)] containing 140 mM Tris base, 105 mM Tris–HCl, 0.5 mM EDTA (ethylenediaminetetraacetic acid), 2% lithium dodecyl sulfate (LDS), 10% glycerol, 0.1 mg/mL PefaBloc SC (AEBSF) protease inhibitor (Roche) and 5 mM dithiothreitol (DTT) for analysis by SDS-PAGE and Western blotting for Rubisco proteins.

Analysis by SDS-PAGE and Western blotting was performed according to protocols described in *Materials and Methods: Chlorophyll and Rubisco measurements* in Chapter 2. Based on this analysis, extraction with 100% methanol consistently provided the cleanest protein extracts as assessed by SDS-PAGE (lanes 11-15; Fig. A1.1). The smearing of protein on SDS-PAGE gels may reflect either interference by unwanted compounds in the extract (e.g. lipids) or the degradation of Rubisco. Thus, the clean-up and extraction of protein in a way which prevents this interference/degradation is vital for accurate Rubisco estimation. When applied to protein extraction from the leaves of different tree species, each solvent provided similar estimations of leaf Rubisco content (Fig. A1.2).

We estimated Rubisco content using an antibody raised against tobacco Rubisco. An alternative approach using Coomassie staining is a common practice, where the relatively high concentration of Rubisco large and small subunits in the total protein extract makes estimation of their concentration possible. Rubisco concentrations determined from Western blotting were compared with those estimated from Coomassie staining (Fig. A1.3); the Rubisco estimates suggest that estimation of Rubisco from the Western blot were in a similar range to the estimates made by Coomassie staining of gels. Despite the samples being treated differently, both approaches yielded similar estimations of leaf Rubisco content, consistent with the result obtained in Fig. A1.2. Additional tests to check that the primary antibody recognized Rubisco of the study species were performed by spiking temperate evergreen species with Rubisco from tobacco prior to SDS-PAGE analysis. Figure A1.4 shows a comparison of Rubisco concentration of tree species alone versus that spiked with known concentration of tobacco Rubisco (0.5 µg μL^{-1}). The western blot assay estimated 0.31 µg µL-1 Rubisco in the sample and 0.78 µg µL-1 in the spiked sample; a difference closely equivalent to the spike. This suggests that the Western blot antibody assay, typically designed for crop species, is compatible with temperate and tropical evergreen species and that the antibody used can successfully be applied to a variety of land plants (Kellogg & Juliano, 1997). Moreover, this result suggests that possible interference by compounds found in tropical leaves did not affect Rubisco quantification after sample clean-up.

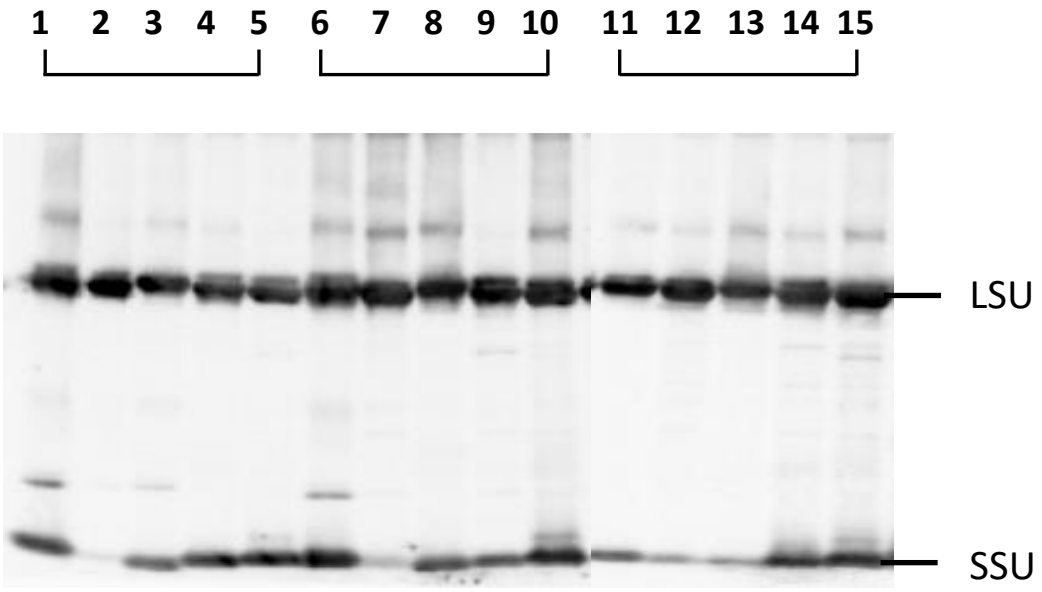

Figure A1.1: **The effect of leaf extraction solvents on Rubisco western blot quality.** Typical western blot profile of Rubisco extracted from five temperate evergreen species after acetic acid, methanol and water (1:10:9) (1-5), 80% (v/v) acetone (6-10) and 100% methanol (11-15) clean-up, prior to washing with hexane and acetone (Gaspar *et al.*, 1997) and dissolution in PEB containing 5 mM DTT (Brown *et al.*, 2008). Individual bands represent Rubisco large subunits (LSU, ~55 kDa) and small subunits (SSU, 15 kDa). Greatest quality blots were consistently observed from 100% methanol-treated leaf samples.

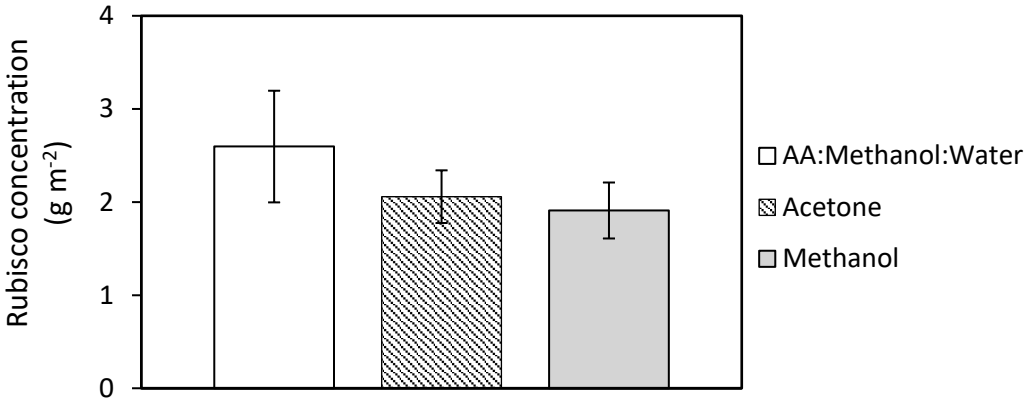

Figure A1.2: **The effect of leaf extraction solvents on estimated Rubisco in protein extracts.** The graph shows estimated Rubisco concentration in leaves of five temperate evergreen species (± S.E.) after acetic acid (AA), methanol and water (1:10:9), 80% acetone and 100% methanol clean-up, prior to washing with hexane and acetone (Gaspar *et al.*, 1997) and dissolution in PEB containing 5 mM DTT (Brown *et al.*, 2008).

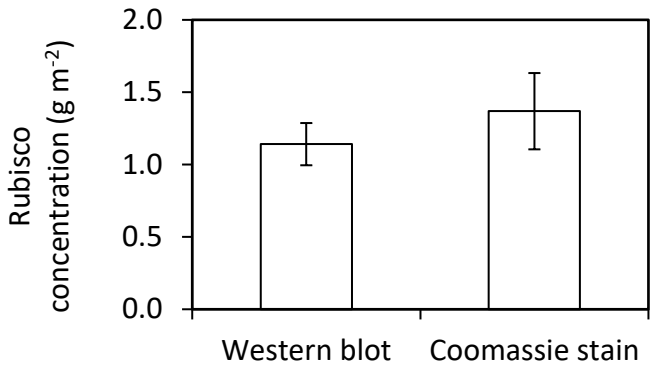

Figure A1.3: **Comparison of western blotting and Coomassie staining for estimation of Rubisco quantities in leaf extracts.** Shown are estimated Rubisco concentrations (± S.E.) of *Atherosperma moschatum* leaves (n=3), determined from Western blot antibody and Coomassie staining. Rubisco estimated from Western blotting was washed with 100% methanol, hexane and acetone, while Rubisco estimated from Coomassie staining was washed with acetic acid, methanol and water (1:10:9), prior to washing with hexane and acetone according to Gaspar *et. al* (1997). Protein was dissolved in PEB containing 5 mM DTT (Brown *et al.*, 2008).

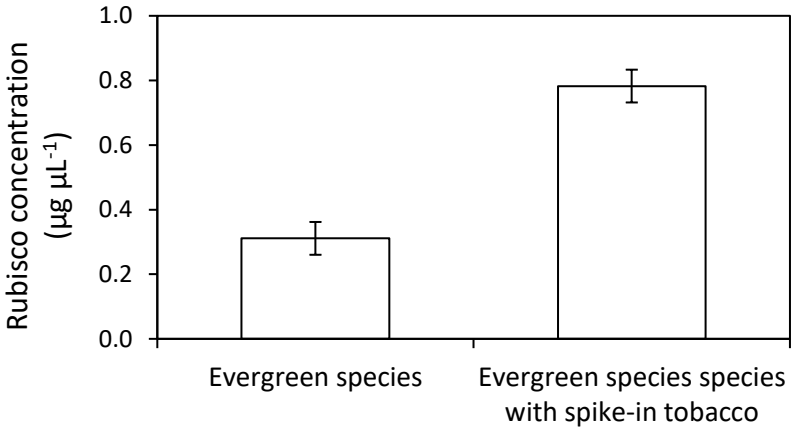

Figure A1.4: **Measurement of Rubisco by western blotting with and without additional Rubisco spike.** Estimated Rubisco concentration of *Atherosperma moschatum* (temperate evergreen) and *Micrandra spruceana* (tropical evergreen) determined from protein extract alone and extract with Rubisco from tobacco spiked into the samples (0.5 µg μL^{-1}). Rubisco from evergreen species was prepared from 100% methanol clean-up, prior to washing with hexane and acetone (Gaspar *et al.*, 1997) and dissolution in PEB containing 5 mM DTT (Brown *et al.*, 2008). Rubisco from tobacco was extracted using extraction buffer (50mM EPPS [4-(2-hydroxyethyl)-1-piperazinepropanesulfonic acid]-NaOH, 1mM EDTA, 1% Polyvinylpolypyrrolidone (PVPP), 10mM DTT, 0.01% Triton, pH 7.8).

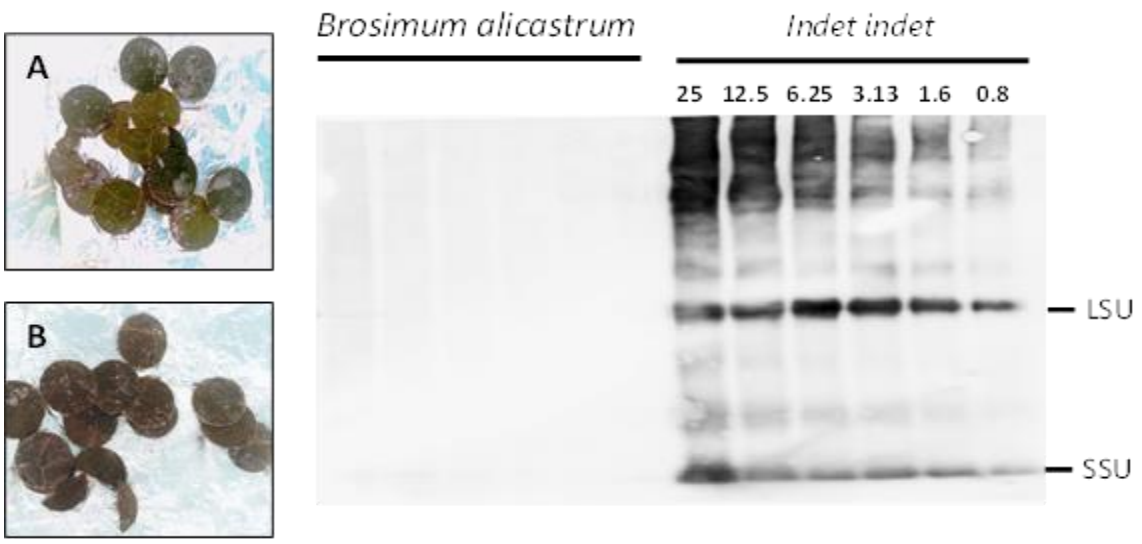

Figure A1.5: **Isolation of Rubisco from tropical leaf samples.** Western blot profile of Rubisco extracted from two lowland species (A) *Indet indet* and (B) *Brosimum alicastrum*. Samples were loaded in a dilution series (25 to 0.8 µg) to estimate the amount of protein to load per lane that yields clear and unsaturated band. No visible bands were seen for *B. alicastrum*, which were consistent with brownish appearance of the leaf discs (A) resulting from thawing during transport. Individual bands represent Rubisco large subunits (LSU, ~55 kDa) and small subunits (SSU, 15 kDa).

Trouble-shooting using Peruvian tropical species

Leaf protein of lowland Peruvian tree species was extracted using a modified protocol as described above. After initial extraction of chlorophyll using 100% methanol, precipitated protein was further washed in hexane and acetone as described by Gaspar *et al.* (1997) and dissolved in PEB containing 5 mM DTT (Brown *et al.*, 2008). This method was compatible with Peruvian tropical species, as protein bands were observed on Western blot (Fig. A1.5). However, some of the leaf discs were degraded due to thawing during shipment from Peru, which resulted in no visible bands on the gel. Approximately less than 1.6 µg sample was required per lane to yield clear, unsaturated band with low background intensity (Fig. A1.5).

Appendix 1 - References

Brown C., MacKinnon J., Cockshutt A., Villareal T. & Campbell D. (2008) Flux capacities and acclimation costs in *Trichodesmium* from the Gulf of Mexico. Marine Biology, 154, 413-422.

Ekramoddoullah A.K.M. (1993) Analysis of needle proteins and N-terminal amino acid sequences of two photosystem II proteins of western white pine (*Pinus monticola* D. Don). Tree Physiology, 12, 101-106.

Gaspar M.M., Ferreira R.B., Chaves M.M. & Teixeira A.R. (1997) Improved method for the extraction of proteins from *Eucalyptus* leaves. Application in leaf response to temperature. Phytochemical Analysis, 8, 279-285.

Harrison M.T., Edwards E.J., Farquhar G.D., Nicotra A.B. & Evans J.R. (2009) Nitrogen in cell walls of sclerophyllous leaves accounts for little of the variation in photosynthetic nitrogen-use efficiency. Plant, Cell & Environment, 32, 259-270.

Hikosaka K. (2004) Interspecific difference in the photosynthesis–nitrogen relationship: patterns, physiological causes, and ecological importance. Journal of Plant Research, 117, 481-494.

Kellogg E. & Juliano N. (1997) The structure and function of RuBisCO and their implications for systematic studies. American Journal of Botany, 84, 413-413.

Quesada C.A., Lloyd J., Schwarz M., Patiño S., Baker T.R., Czimczik C., Fyllas N.M., Martinelli L., Nardoto G.B., Schmerler J., Santos A.J.B., Hodnett M.G., Herrera R., Luizão F.J., Arneth A., Lloyd G., Dezzeo N., Hilke I., Kuhlmann I., Raessler M., Brand W.A., Geilmann H., Moraes Filho J.O., Carvalho F.P., Araujo Filho R.N., Chaves J.E., Cruz Junior O.F., Pimentel T.P. & Paiva R. (2010) Variations in chemical and physical properties of Amazon forest soils in relation to their genesis. Biogeosciences, 7, 1515-1541.

Wright I.J., Reich P.B., Westoby M., Ackerly D.D., Baruch Z., Bongers F., Cavender-Bares J., Chapin T., Cornelissen J.H.C., Diemer M., Flexas J., Garnier E., Groom P.K., Gulias J., Hikosaka K., Lamont B.B., Lee T., Lee W., Lusk C., Midgley J.J., Navas M.-L., Niinemets U., Oleksyn J., Osada N., Poorter H., Poot P., Prior L., Pyankov V.I., Roumet C., Thomas S.C., Tjoelker M.G., Veneklaas E.J. & Villar R. (2004) The worldwide leaf economics spectrum. Nature, 428, 821-827.

Appendix 2: Supplementary Tables and Figures for Chapter 2

Table A2.1 Pearson correlations for bivariate relationships among leaf traits and environmental parameters. Number of replicates is given in bracket.
Abbreviations: N_a = leaf nitrogen, P_a = leaf phosphorus, leaf N:P = leaf nitrogen to phosphorus ratio, M_a = leaf mass per unit leaf area, Chl = chlorophyll a and b content, $V_{cmax,a}^{25}$ = maximum carboxylation velocity of Rubisco normalised to 25°C, $J_{max,a}^{25}$ = maximum rate of electron transport normalised to 25°C, $V_{cmax,N}^{25}$ = ratio of maximum carboxylation velocity of Rubisco normalised to 25°C over leaf nitrogen, Soil P=soil phosphorus, Soil N=soil nitrogen, MAT = mean annual temperature, MAP = mean annual precipitation. Environmental parameters at each site were obtained using site information from Quesada (*et al.* 2010; pers. comm. 2014) and Asner *et al.* (2014a). Note that the coefficient of determination, r^2, equals the square of the Pearson correlation coefficient. **Correlation is significant at p<0.01; *Correlation is significant at p<0.05

	N_a	P_a	Leaf N:P	M_a	Chl	$V_{cmax,a}^{25}$	$J_{max,a}^{25}$	$V_{cmax,N}^{25}$	Soil P	Soil N	Elevation	MAT	MAP
N_a ($g\ m^{-2}$)	1 (248)	0.613** (240)	-0.208** (232)	0.353** (246)	0.370** (171)	0.226** (246)	0.227** (184)	-0.297** (242)	0.356** (248)	0.319** (248)	0.368** (248)	-0.375** (248)	-0.041 (248)
P_a ($g\ m^{-2}$)		1 (248)	-0.769** (227)	0.188** (246)	0.229** (170)	0.331** (241)	0.366** (186)	-0.013 (234)	0.611** (248)	0.623** (248)	0.694** (248)	-0.711** (248)	-0.004 (248)
Leaf N:P			1 (245)	-0.085 (232)	-0.047 (159)	-0.280** (243)	-0.244** (177)	-0.157* (227)	-0.476** (245)	-0.512** (245)	-0.539** (245)	0.551** (245)	-0.020 (245)
M_a ($g\ m^{-2}$)				1 (274)	0.157* (185)	0.077 (272)	0.196** (199)	-0.095 (240)	-0.029 (274)	0.195** (274)	0.194** (274)	-0.162** (274)	-0.111 (274)
Chl ($g\ m^{-2}$)					1 (185)	-0.001 (183)	0.085 (133)	-0.109 (166)	0.285** (185)	0.153* (185)	0.145* (185)	-0.151* (185)	0.239** (185)
$V_{cmax,a}^{25}$ ($\mu mol\ m^{-2}\ s^{-1}$)						1 (283)	0.840** (209)	0.810** (242)	0.287** (290)	0.354** (290)	0.384** (283)	-0.399** (283)	-0.070 (283)
$J_{max,a}^{25}$ ($\mu mol\ m^{-2}\ s^{-1}$)							1 (209)	0.629** (182)	0.373** (209)	0.475** (209)	0.461** (209)	-0.462** (209)	0.152* (209)
$V_{cmax,N}^{25}$ ($\mu mol\ gN^{-1}\ s^{-1}$)								1 (242)	0.143* (242)	0.201** (242)	0.186** (242)	-0.198** (242)	0.028 (242)
Soil P ($mg\ kg^{-1}$)									1 (292)	0.681** (292)	0.716** (292)	-0.720** (292)	0.380** (292)
Soil N ($g\ kg^{-1}$)										1 (292)	0.921** (292)	-0.902** (292)	0.104 (292)
Elevation (m a.s.l.)											1 (292)	-0.992** (292)	-0.068 (292)
MAT (°C)												1 (292)	0.070 (292)
MAP (mm)													1 (292)

Table A2.2 Standardized major axis regression slopes and their confidence intervals for log-log transformed relationships comparing leaf traits of lowland (~173 species) and upland (~120 species) species, depicted in Figures 2.2, 2.5, 2.6 and 2.7 in Chapter 2**.** Analysis undertaken using individual replicates. Coefficients of determination (r^2) and significance values (p) of each bivariate relationship are shown. Significantly different p values are shown in bold. 95% confidence intervals (CI) of SMA slopes and y-axis intercepts are shown in parentheses. Where SMA tests for common slopes revealed no significant differences between the two groups (i.e. $p > 0{\cdot}05$), common slopes were used (with CI of the common slopes provided). Where there was a significant difference in the elevation (i.e. y-axis intercept) of the common-slope SMA regressions, values for the y-axis intercept are provided. Where appropriate, significant shifts along a common slope are indicated.

Bivariate relationship (y- vs. x-axis)	Group	r^2	p	Slope	Slope CI	Intercept	p	Common slope	Common slope CI	p	Common slope y-axis intercept	Shift along a common slope?
N_a vs. M_a	Lowland	0.069	**0.001**	1.027	(0.879, 1.199)	-1.889	0.003					
	Upland	0.198	**<0.001**	0.709	(0.593, 0.848)	-1.165						
P_a vs. M_a	Lowland	<0.001	0.985	-2.096	(-2.463, -1.784)	3.323	0.002					
	Upland	0.038	**0.034**	1.345	(1.104 , 1.639)	-3.661						
$V_{cmax,a}^{25}$ vs. M_a	Lowland	0.003	0.468	-1.753	(-2.054, -1.495)	5.183	0.595	1.705	(1.511, 1.925)	0.010	-2.089	Yes, p < 0.001
	Upland	0.014	0.212	1.642	(1.362, 1.981)	-1.863					-1.999	
$V_{cmax,a}^{25}$ vs. N_a	Lowland	0.024	**0.050**	1.707	(1.454, 2.005)	1.022	0.014					
	Upland	0.003	0.613	2.384	(1.950, 2.914)	0.801						
$V_{cmax,a}^{25}$ vs. P_a	Lowland	0.041	**0.013**	0.841	(0.717, 0.986)	2.417	0.003					
	Upland	0.005	0.502	1.231	(1.003, 1.511)	2.602						
$V_{cmax,a}^{25}$ vs. leaf N:P	Lowland	0.002	0.563	-1.246	(-1.468, -1.057)	3.136	0.028					
	Upland	0.027	0.113	-1.657	(-2.030, -1.353)	3.494						
$J_{max,a}^{25}$ vs. M_a	Lowland	0.004	0.473	1.136	(0.956, 1.349)	-0.577	0.022					
	Upland	0.005	0.552	1.620	(1.268, 2.069)	-1.533						
$J_{max,a}^{25}$ vs. N_a	Lowland	0.050	**0.012**	1.046	(0.881, 1.242)	1.518	0.001					
	Upland	0.001	0.794	-2.224	(-2.897, -1.707)	2.736						
$J_{max,a}^{25}$ vs. P_a	Lowland	0.077	**0.002**	0.5113	(0.432, 0.605)	2.368	0.001					
	Upland	0.029	0.205	-1.101	(-1.432, -0.846)	1.086						
$J_{max,a}^{25}$ vs. leaf N:P	Lowland	<0.001	0.888	-0.813	(-0.974, -0.679)	2.876	0.003					
	Upland	<0.001	0.930	-1.378	(-1.800, -1.055)	3.493						
$V_{cmax,N}^{25}$ vs. M_a	Lowland	0.044	**0.010**	-1.841	(-2.157, -1.570)	5.092	0.789	-1.866	(-1.647, -2.114)	<0.001	5.146	No, P= 0.809
	Upland	0.010	0.327	-1.908	(-2.336, -1.559)	5.385					5.295	
$V_{cmax,N}^{25}$ vs. P_a	Lowland	0.012	0.195	-0.890	(-1.048, -0.756)	0.239	0.004					
	Upland	0.030	0.101	-1.301	(-1.599, -1.059)	0.275						
$V_{cmax,N}^{25}$ vs. leaf N:P	Lowland	0.003	0.536	-1.307	(-1.548, -1.103)	2.945	0.057	-1.455	(-1.455, -1.274)	<0.001	3.141	Yes, p < 0.001
	Upland	0.020	0.185	-1.709	(-2.105, -1.388)	3.185					2.903	
$J_{max,a}^{25}$ vs. $V_{cmax,a}^{25}$	Lowland	0.590	**<0.001**	1.341	(1.204, 1.439)	15.81	0.001					
(not log-transformed)	Upland	0.748	**<0.001**	1.962	(1.736, 2.217)	-4.803						

Table A2.3 Standardized major axis regression slopes and their confidence intervals for relationships comparing leaf traits of lowland (~126 species) and upland (~40 species) species, depicted in Figures 2.9 and A2.1 in the main text. Analysis undertaken using individual replicates. Coefficients of determination (r^2) and significance values (p) of each bivariate relationship are shown. Significantly different p values are shown in bold. 95% confidence intervals (CI) of SMA slopes and y-axis intercepts are shown in parentheses. Where SMA tests for common slopes revealed no significant differences between the two groups (i.e. p>0·05), common slopes were used (with CI of the common slopes provided). Where there was a significant difference in the elevation (i.e. y-axis intercept) of the common-slope SMA regressions, values for the y-axis intercept are provided. Where appropriate, significant shifts along a common slope are indicated.

Bivariate relationship (y- vs. x-axis)	Group	r^2	p	Slope	Slope CI	Intercept	p	Common slope	Common slope CI	p	Common slope y-axis intercept	Shift along a common slope?
n_P vs. M_a	Lowland	0.012	0.258	-0.2421	(-0.292, -0.201)	57.02	0.072	-0.2172	(-0.187, -0.253)	0.698	53.600	No, p = 0.185
	Upland	0.002	0.719	-0.1797	(-0.231, -0.134)	47.64					52.945	
n_R vs. M_a	Lowland	0.042	**0.011**	-0.1217	(-0.143, -0.104)	24.841	0.482	-0.1176	(-0.104, -0.133)	<0.001	24.303	No, p = 0.794
	Upland	0.001	0.809	0.1110	(0.090, 0.137)	-5.861					27.171	
n_E vs. M_a	Lowland	0.023	0.087	-0.0279	(-0.033, -0.023)	6.362	0.249	-0.0296	(-0.026, -0.034)	<0.001	6.579	No, p = 0.227
	Upland	0.001	0.870	-0.0339	(-0.045, -0.026)	8.240					7.605	
n_P vs. N_a	Lowland	0.358	**<0.001**	-16.52	(-19.23, -14.18)	55.21	0.711	-16.76	(-14.73, -19.08)	0.017	55.676	Yes, p <0.001
	Upland	0.001	0.773	-17.43	(-22.36, -13.59)	60.53					59.063	
n_R vs. N_a	Lowland	0.171	**<0.001**	-7.876	(-9.127, -6.797)	24.29	0.101	-8.499	(-7.544, -9.564)	<0.001	25.515	No, p = 0.065
	Upland	0.094	**0.003**	-9.725	(-11.842, -7.987)	32.64					29.802	
n_E vs. N_a	Lowland	0.382	**<0.001**	-1.732	(-1.992, -1.506)	6.156	0.001					
	Upland	0.165	**0.002**	-3.039	(-3.889, -2.374)	10.278						
n_P vs. P_a	Lowland	0.154	**<0.001**	-225.4	(-268.6, -189.2)	42.22	0.002					
	Upland	0.028	0.186	-129.5	(-165.9, -101.1)	43.04						
n_R vs. P_a	Lowland	0.013	0.175	-90.48	(-106. 4, -76.96)	17.23	0.167	-84.48	(-74.36, -96.08)	<0.001	16.677	Yes, p <0.001
	Upland	0.030	0.106	-75.48	(92.97, -61.28)	23.26					24.851	
n_E vs. P_a	Lowland	0.050	**0.013**	-19.99	(-23.79, -16.80)	4.635	0.568	-20.60	-17.84 -23.75	<0.001	4.692	Yes, p = 0.001
	Upland	0.155	**0.003**	-21.89	(-28.19, -16.99)	7.047					6.824	
n_A vs. M_a	Lowland	0.070	**0.003**	-1.2405	(-1.471, -1.046)	2.143	0.085	-1.152	(-0.992, -1.345)	0.025	1.958	No, p = 0.742
(log-transformed)	Upland	0.002	0.794	-0.8934	(-1.233, -0.647)	1.475					2.026	
n_A vs. N_a	Lowland	0.445	**<0.001**	-1.078	(-1.231, -0.945)	-0.159	0.099	-1.129	(-0.999, -1.273)	<0.001	-0.145	No, p = 0.189
(log-transformed)	Upland	0.156	**0.011**	-1.403	(-1.881, -1.046)	0.037					-0.054	
n_A vs. P_a	Lowland	0.056	**0.008**	-0.556	(-0.661, -0.468)	-1.065	0.446	-0.576	(-0.495, -0.670)	<0.001	-1.086	Yes, p <0.001
(log-transformed)	Upland	0.100	**0.047**	-0.640	(-0.869, -0.471)	-0.957					-0.904	

Table A2.4 Stepwise selection process for the fixed component of linear mixed effect models: with $V_{cmax,a}^{25}$ and $J_{max,a}^{25}$ as the response variables. The best predictive models, underlined, were presented in Table 2.3. Continuous explanatory variables are N_a, P_a, M_a, total soil P and N, MAT and effective cation exchange capacity of soil. Given the large number of species in our dataset, we treated phylogeny as a random component within the model construct and so focused on phylogenetic variation rather than individual species mean values. Because of low replication at the species level, a simple random term of Family was found to perform just as well as the fully nested Family/Genus/Species. In choosing explanatory terms for the model's fixed component, we began by adopting a beyond-optimal model including those continuous variables suggested by our starting hypotheses, initial data exploration, and with care to avoid problems of collinearity - a limited number of two-way interactions were included (specifically N:P). A backward, stepwise selection process adopted the Maximum Likelihood method; the model's random component was held constant through these iterations. The effect of dropping sequential terms was tested by comparing the nested model variants. The model's random component was identical in all variants. Test parameters and statistics are DF (degrees of freedom), AIC (Akaike Information Criterion), BIC (Bayesian Information Criterion) and -2LL (-2 restricted Log Likelihood). The effect of dropping sequential terms was tested by comparing the nested model variants. The best predictive model, underlined, was selected based on a combination of low criteria score and simplicity, considering two-way interactions only. Because our final preferred model, arrived at by backward selection, was so parsimonious, we then tested the effect of adding selected terms and interactions not previously included – in no case did those additional terms improve model performance. For the J_{max} model, it was not thought necessary to include site average terms for leaf N and P, since those terms had proved so marginal in the equivalent V_{cmax} model selection steps.

Model	Fixed component	DF	AIC	BIC	-2LL
$\boldsymbol{V_{cmax,a}^{25}}$					
1	log10(Soil P) + N_a + Site.N_a + P_a + Site.P_a + N_a.P_a	9	1663.5	1693.1	-822.7
2	log10(Soil P) + N_a + Site.N_a + P_a + Site.P_a + log10(Soil P).N_a	9	1664.0	1693.7	-823.0
3	log10(Soil P) + N_a + Site.N_a + P_a + Site.P_a	8	1663.2	1689.6	-823.6
4	log10(Soil P) + N_a + Site.N_a + P_a	7	1661.4	1684.4	-823.7
5	log10(Soil P) + N_a + P_a	6	1661.5	1681.3	-824.7
6	**log10(Soil P) + P_a**	5	**1659.7**	**1676.1**	**-824.8**
7	log10(Soil P) + P_a + MAT + P_a:MAT	7	1663.1	1686.1	-824.5
8	log10(Soil P) + P_a + MAT	6	1661.1	1680.9	-824.6
9	log10(Soil P) + P_a + SoilN	6	1658.9	1678.6	-823.4
10	log10(Soil P) + P_a + ECEC	6	1657.5	1677.2	-822.7
11	log10(Soil P) + P_a + M_a	6	1660.8	1680.5	-824.4
$\boldsymbol{J_{max,a}^{25}}$					
1	log10(Soil P) + P_a + N_a + M_a + MAT + N_a.P_a	9	1361.1	1388.0	-671.5
2	log10(Soil P) + P_a + N_a + M_a + MAT + log10(Soil P).N_a	9	1358.7	1385.7	-670.4
3	log10(Soil P) + P_a + N_a + M_a + MAT	8	1360.3	1384.3	-672.2
4	log10(Soil P) + P_a + M_a + MAT	7	1358.3	1379.3	-672.2
5	log10(Soil P) + P_a + M_a	6	1357.3	1375.3	-672.6
6	**log10(Soil P) + P_a**	5	**1359.9**	**1374.9**	**-674.9**
7	log10(Soil P)	4	1363.4	1375.4	-677.7

Abbreviations: N_a = leaf nitrogen, P_a = leaf phosphorus, M_a = leaf mass per unit leaf area, Soil P = soil phosphorus, Soil N = soil nitrogen, MAT = mean annual temperature, ECEC = effective cation exchange capacity of soil. Environmental parameters at each site were obtained using site information from Quesada (*et al.* 2010; pers. comm. 2014), Asner *et al.* (2014a) and Y. Malhi *et al.* (unpublished).

Figure A2.1. Plots of % of leaf N to pigment-protein complexes, n_P, % of leaf N to Rubisco, n_R, and % of leaf N to electron transport, n_E, in relation to (a) leaf mass per unit leaf area, M_a, (b) leaf N-area, N_a, and (c) leaf P-area, P_a. Data points represent individual leaf values (150 lowland species and 92 upland species).
SMA regressions: solid line, lowland species; dashed line, upland species. SMA regressions are given only when the relationships are significant (p<0.05) and when lowland and upland shared similar slopes, refer to Table A2.3. Analyses were performed on percentage instead of fraction of N to meet the requirement of SMA analyses.

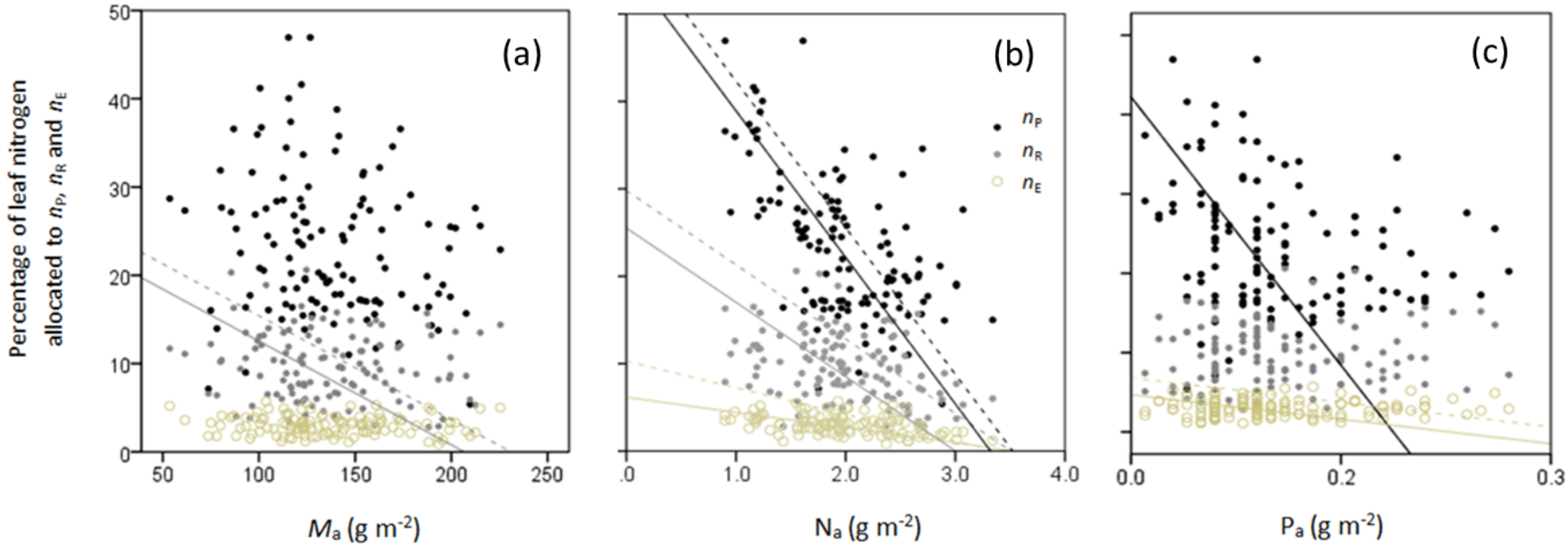

Figure A2.2. Stacked graph shows n_E, n_P and n_R for individual leaves. Individual leaf is arranged first according to sites with increasing soil P (soil P value in mg kg^{-1} depicted underneath site code), then according to decreasing leaf N:P within each site. Leaf N:P for individual leaf is provided on top of the bar. n_E was estimated from maximum electron transport rate (normalised to 25°C), $J_{max,a}^{25}$ and n_P estimated from chlorophyll concentration. Grey panel depicts *in vitro* n_R estimated from Rubisco western blot assay, where black mark within grey panel indicates *in vivo* n_R derived from maximum carboxylation velocity of Rubisco (normalised to 25°C), $V_{cmax,a}^{25}$. Horizontal axis shows family of individual leaf.

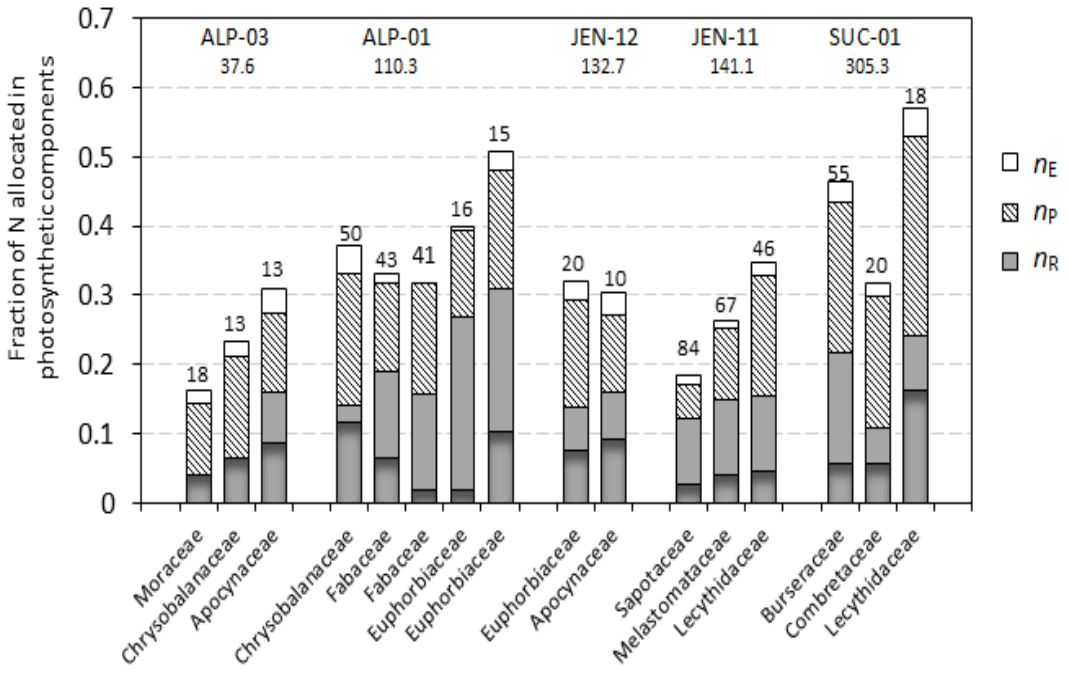

Figure A2.3. Plots for linear mixed-effects model goodness of fits, including fixed and random terms for (A) $V_{cmax,a}^{25}$; and, (B) $J_{max,a}^{25}$. Measured values of $V_{cmax,a}^{25}$ and $J_{max,a}^{25}$ are plotted against model predictions (using the 'best' predictive models detailed in Table 3). For $V_{cmax,a}^{25}$ and $J_{max,a}^{25}$ model, the fixed component explanatory variables were: soil P and leaf P (P_a).

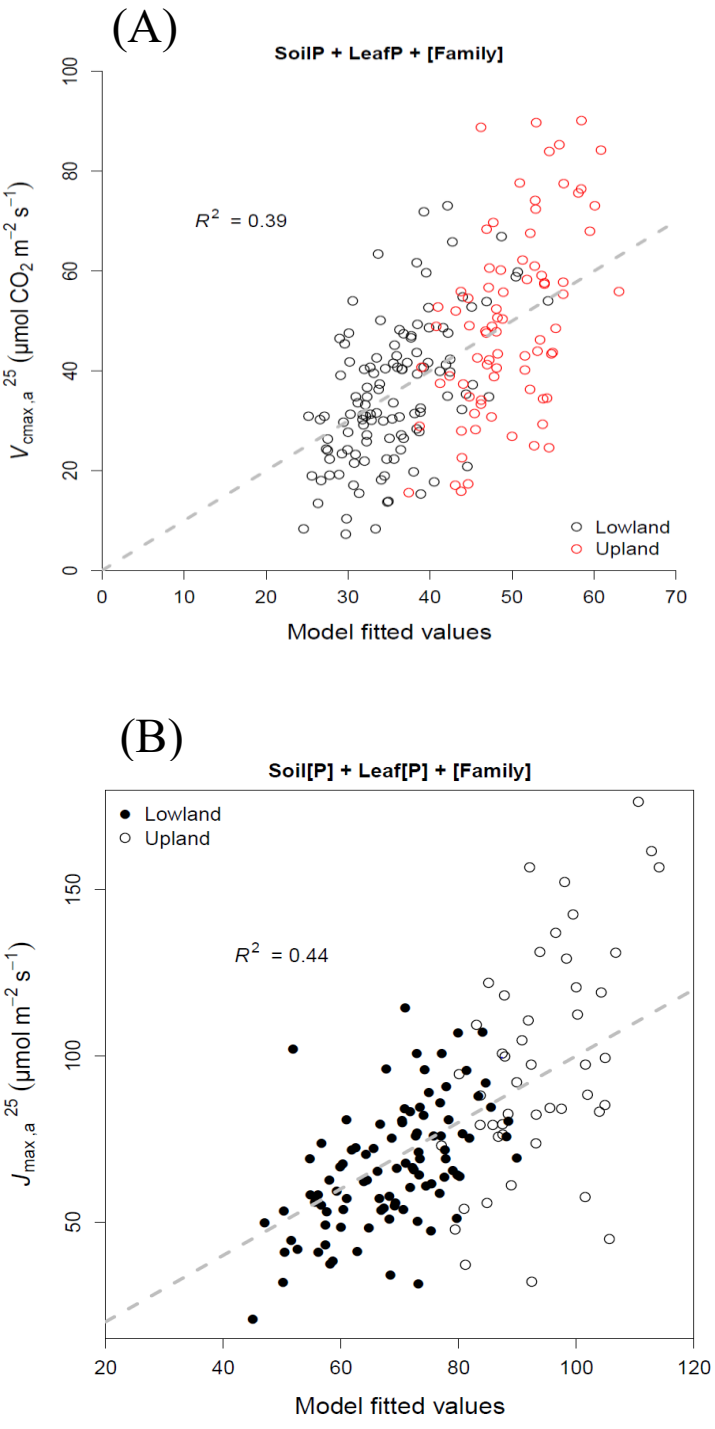

Appendix 3: Supplementary Tables for Chapter 3

Table A3.1. Pearson correlations for bivariate relationships among leaf traits, when tropical and temperate species are analysed together

Abbreviation: A = light-saturated net photosynthesis measured at 400 µmol mol^{-1} CO_2, g_s = stomatal conductance, g_m = mesophyll conductance, C_i:C_a = ratio of intercellular CO_2 to atmospheric CO_2, V_{cmax} = maximum carboxylation velocity of Rubisco, J_{max} = maximum rate of electron transport, R_{dark} = dark respiration rate, LMA= leaf mass per unit leaf area, LDM:LFM = leaf dry mass to leaf fresh mass ratio, leaf P = leaf phosphorus, leaf N = leaf nitrogen.

	g_s	g_m	C_i:C_a	V_{cmax}	J_{max}	R_{dark}	LMA	LDM:LFM	Leaf P	Leaf N	Chlorophyll	V_{cmax} per unit N
A	**0.924****	**0.860****	**0.321***	**0.947****	**0.909****	**0.433****	-0.053	-0.014	-0.159	**0.333***	0.210	**0.916****
g_s		**0.775****	**0.540****	**0.794****	**0.766****	**0.383***	-0.260	-0.130	-0.209	0.131	0.003	**0.855****
g_m			0.182	**0.766****	**0.772****	**0.360***	-0.262	-0.046	**-0.344***	0.165	0.209	0.791**
C_i:C_a				0.111	0.045	0.231	**-0.460****	**-0.410****	-0.299	**-0.381***	**-0.555****	0.299
V_{cmax}					**0.948****	**0.407****	0.172	0.093	-0.061	**0.485****	**0.369***	**0.896****
J_{max}						**0.447****	0.228	0.073	0.029	**0.505****	**0.393***	**0.847****
R_{dark}							0.156	-0.207	0.244	**0.304***	-0.212	0.242
LMA								**0.318***	**0.726****	**0.613****	0.276	-0.091
LDM:LFM									0.190	0.139	**0.524****	0.086
Leaf P										**0.507****	0.024	-0.291
Leaf N											**0.420****	**0.083**
Chlorophyll												**0.237**

** Correlation is significant at $p<0.01$

* Correlation is significant at $p<0.05$

Table A3.2. Standardized major axis regression slopes and their confidence intervals for relationships comparing leaf traits of tropical and temperate species, depicted in figures in the main text. Analysis undertaken using individual replicates. Coefficients of determination (r^2) and significance values (p) of each bivariate relationship are shown. Significantly different p values are shown in bold. 95% confidence intervals (CI) of SMA slopes are shown in parentheses. Where SMA tests for common slopes revealed no significant differences between the two groups (i.e. p>0·05), common slopes were used (with CI of the common slopes provided). Where there was a significant difference in the elevation (i.e. y-axis intercept) of the common-slope SMA regressions, values for the y-axis intercept are provided. Where appropriate, significant shifts along a common slope are indicated.

Bivariate relationship (y- vs. x-axis)	Group	r^2	p	Slope	Slope CI	Intercept	p	Common slope	Common slope CI	p	Common slope y-axis intercept	Shift along a common slope?
A vs. g_m	Tropical	0.501	**<0.001**	47.87	(35.20, 65.11)	-0.2813	0.419	52.87	(44.55, 62.23)	**0.001**	-1.210	Yes, p = 0.001
	Temperate	0.846	**<0.001**	54.96	(45.01, 67.11)	1.0866					1.587	
V_{cmax} vs. g_m	Tropical	0.228	**0.018**	272.4	(186.4, 398.1)	-2.992	0.748	261.4	(212.3, 323.0)	**0.002**	-0.939	Yes, p = 0.005
	Temperate	0.743	**<0.001**	256.9	(198.8, 332.0)	16.607					15.526	
C_a-C_i vs. g_m	Tropical	0.046	0.316	-597.4	(-908.7, -392.7)	236.8	**0.020**					
	Temperate	0.135	0.122	-289.5	(-458.4, -182.8)	181.0						
C_i-C_c vs. g_m	Tropical	0.176	0.051	-249.7	(-369.3, -168.8)	111.3	**0.037**					
	Temperate	0.053	0.341	-129.7	(-209.5, -80.3)	110.3						
V_{cmax}-infinite g_m vs. V_{cmax}-finite g_m	Tropical	0.956	**<0.001**	0.8706	(0.7938, 0.9549)	3.537	0.321	0.9011	(0.8450, 0.9580)	0.197	2.086	Yes, p < 0.001
	Temperate	0.975	**<0.001**	0.9249	(0.8507, 1.0056)	-1.830					0.084	
J_{max} vs. V_{cmax} (mass)	Tropical	0.758	**<0.001**	1.968	(1.586, 2.442)	-231.0	**0.032**					
	Temperate	0.933	**<0.001**	1.497	(1.312, 1.707)	260.7						
J_{max} vs. V_{cmax} (area)	Tropical	0.793	**<0.001**	1.652	(1.353, 2.018)	2.100	**0.041**					
	Temperate	0.917	**<0.001**	1.269	(1.096, 1.470)	33.388						
V_{cmax}/N vs. LMA	Tropical	0.058	0.259	0.6409	(0.4223, 0.9725)	-3.500	0.671	-0.6799	(-0.5042, -0.9141)	**<0.001**	66.388	No, p = 0.671
	Temperate	0.240	**0.033**	-0.7221	(-1.1127, -0.4686)	89.894					87.107	